Investigating the Mechanisms Mediating Circadian Disruption by the Modern Light Environment

Selma Tir
St. Cross College
University of Oxford

A thesis submitted for the degree of
Doctor of Philosophy
Hilary 2025

Acknowledgments

I wish to thank all the people whose assistance has been invaluable in the completion of this thesis. A very special gratitude goes out to my primary supervisor, Prof. Stuart Peirson, for his unwavering support, extensive knowledge of all things vision-related, weekly motivational discussions, and thoughtful guidance. I also wish to thank my secondary supervisor, Prof. Russell Foster, for inspiring me to come to Oxford. I would not be here without both of their help. I wish to thank the members of our lab for their support, from data collection to afternoon teas. With a special mention to Dr. Eric Tam and Dr. Ma'ayan Seemo for their help with experimental procedures, Dr. Carina Pothecary for the development of our "disco" lights, and Dr. Laura Steel, my fellow doctorate with whom I shared it all. I wish to pay special regards to my undergraduate supervisor and mentor, Prof. Mary Harrington, for igniting my passion for research, introducing me to the field of circadian rhythms, and teaching me to lead the way on the SRBR dancefloor. Last but not least, I wish to acknowledge the support from family members, friends and mentors throughout these last 4 years and beyond. To my mother, Imane, who always prioritized me and allowed me to fulfill my dreams of higher education, and to my grandmother, Rahma, who lovingly took care of me during the final push of thesis writing, thank you for being stellar examples of strength and perseverance. As a first-generation college graduate, and soon to be doctor, I couldn't be more proud to be coming from a line of such amazing women. To my hotmamis, Brooke, Elisa, Sophie, Cat, Anna, and most importantly Luna, whom we will always cherish in our thoughts, thank you for keeping me sane through this rollercoaster and for the best memories I could have asked for. To Oxford, thank you for shaping me and allowing me to grow in such a special place. The DPhil has been one of the hardest challenges of my life, and one of the best learning experiences. And finally, to all my mouse babies, thank you for never biting me.

To all my loved ones, merci !

This thesis was conducted with the support of grants from the Seasonal Affective Disorder Association, Biotechnology and Biological Sciences Research Council (BB/X002357/1), and National Centre for the Replacement, Refinement and Reduction of Animals in Research (NC/V000977/1).

The content of the appendix chapter was previously published in Tir et al. (2025) in Scientific Reports. I produced the material and received permission from my co-authors to include it in my thesis.

Table of Contents

Abstract

The circadian system regulates daily rhythms in physiology and behavior, with light as its primary entrainment cue. Modern light environments, characterized by decreased daytime light and increased evening artificial light, have been linked to circadian disruption and various health issues. This thesis investigated the effects of dim light in the evening (DLE) on circadian rhythms in mice. We established that both acute and chronic exposure to DLE (20 lux, ZT12-16) induces consistent phase delays in activity, sleep, and body temperature rhythms. This maintenance of internal synchrony with temporal reorganization suggests a coordinated realignment to the new dark onset. We observed sex-specific differences, with females showing greater vulnerability to metabolic disruptions despite more robust rhythms. To explore underlying mechanisms and discern the contribution of circadian disruption versus changes in sleep state during the dim phase, we combined sleep deprivation during the dim phase with transition to constant darkness. Animals free-ran from a delayed phase regardless of prior sleep during the dim light, demonstrating that DLE directly entrains the circadian clock through photic pathways independent of sleep state and masking effects. We then evaluated interventions to attenuate DLE effects. Neither varying daytime light intensity (20-500 lux) and supplementing violet light to target S-cone activation and melanopsin inhibition showed significant impact. Blue-blocking filters were ineffective at standard illuminance (20 lux), but significantly attenuated phase delays when combined with reduced light intensity (6 lux). These findings establish that the circadian system remains sensitive to modest evening illumination, with effects mediated through direct photic entrainment involving multiple photoreceptor classes. Comprehensive approaches addressing both spectral composition and light intensity may best mitigate the circadian impact of unavoidable evening light exposure. This work contributes to understanding how modern light environments affect biological timing and strategies to support circadian health.

Abbreviations

ALI	Animal Locomotion Index
ALT	Alanine Aminotransferase
AMPA	Amino-Methyl Propionic Acid
ANOVA	Analysis of Variance
AVP	Arginine Vasopressin
BBF	Blue-Blocking Filter
BDNF	Brain-Derived Neurotrophic Factor
BMI	Body Mass Index
CCG	Clock-Controlled Gene
CM / CF	Control Male / Control Female
CRP	C-Reactive Protein
CRY dKO	Cryptochrome double Knock-Out (*Cry1*$^{-/-}$, *Cry2*$^{-/-}$)
CV	Constant Violet
DBP	D-site albumin promoter-Binding Protein
DD	Constant Darkness
DLE	Dim Light in the Evening
DLAN	Dim Light at Night
DVC	Digital Ventilated Cage
E-box	Enhancer box
EDI	Equivalent Daylight Illuminance
EEG	Electroencephalogram
EF / EM	Experimental Female / Experimental Male
EMG	Electromyogram
EPM	Elevated-Plus Maze
GRP	Gastrin-Releasing Peptide
GSK3β	Glycogen Synthase Kinase 3 Beta

IGL	Intergeniculate Leaflet
IL6	Interleukin-6
IL1β	Interleukin-1 Beta
IS	Inter-daily Stability
IV	Intra-daily Variability
IVC	Individual Ventilated Cage
IRS1	Insulin Receptor Substrate 1
KO	Knock-Out
LD	Light-Dark
LED	Light Emitting Diode
LL	Constant Light
LP	Light Pulse
LTC	Light-Tight Chamber
MAC1	Macrophage Marker 1
M/L/S-cone	Medium / Long / Short-wavelength sensitive cones
NF-κB	Nuclear Factor Kappa B
NEFA	Non-Esterified Fatty Acids
NMDA	N-Methyl-D-Aspartate
NMS	Neuromedin S
NPAS2	Neuronal PAS Domain Protein 2
NPY	Neuropeptide Y
OBB-Glucose	O-benzyl-β-D-glucoside
OF	Open Field
OPN	Olivary Pretectal Nucleus
PACAP	Pituitary Adenylate Cyclase-Activating Peptide
PIR	Passive Infrared Sensor
POMC	Pro-opiomelanocortin
pAKT	Phosphorylated AKT

pGSK3β	Phosphorylated GSK3β
pIRS1	Phosphorylated IRS1
pRGC	Photosensitive Retinal Ganglion Cell
RA	Relative Amplitude
REM	Rack Environmental Monitoring
REV-ERB	Reverse Erythroblastosis Virus
RHT	Retinohypothalamic Tract
RI	Recognition Index
ROR	Retinoic Acid Receptor-related Orphan Receptor
ROUT	Robust Regression and Outlier Removal
SCN	Suprachiasmatic Nuclei
SD	Sleep Deprivation
SEM	Standard Error of the Mean
TA	Total Activity
TAG	Triacylglycerol
TNF	Tumor Necrosis Factor
TTFL	Transcription-translation feedback loop
VIP	Vasoactive Intestinal Peptide
VLPO	Ventrolateral Preoptic area
WT	Wildtype
ZT	Zeitgeber Time

List of Figures

Chapter 1

Chapter 2

Chapter 3

List of Supplemental Figures

Chapter 2

Chapter 3

Appendix

List of Tables

Chapter 1

Chapter 2

Appendix

List of Supplemental Tables

Chapter 2

Appendix

Chapter 1. An Introduction to Light and Circadian Rhythms

1.1. The Circadian System

Circadian rhythms (from the Latin "circa-diem", meaning "about a day") are natural 24-hour cycles of physiological and behavioral changes that occur in all living things. Generated by an internal timekeeping system, they keep organisms coordinated to day and night by entraining to environmental cues called zeitgebers (from the German "time-giver") (Roenneberg et al., 2003). From an evolutionary perspective, circadian rhythms represent a critical adaptation to the natural 24-hour rotation of the Earth, which gives rise to the solar day. They provide the ability to anticipate predictable rhythmic environmental changes, rather than merely responding to them, thus conferring a significant selective advantage (Daan & Aschoff, 1982).

The daily fluctuation between light and darkness is the most conspicuous time cue, and in mammals is the dominant zeitgeber. However, other signals such as food availability and external temperature variations also have an influence on the regulation of circadian rhythms (Refinetti, 2010; Tahara et al., 2017). Though the type and strength of zeitgebers vary between organisms, when optimally aligned with the environment, the internal circadian system is in a state of resonance whereby it reflects the world around it (West & Bechtold, 2015). Because the circadian system has a period near, but not exactly 24 hours in most organisms, internal rhythms entrain to the external environment on a regular basis (Duffy & Czeisler, 2009). Without this daily entrainment, the internal clock would slowly drift out of alignment with the external environment. The anticipation of our rhythmically changing world thus regulates every aspect of our physiology and behavior, including sleep/wake cycles, feeding, and hormone release (**Fig. 1.1**).

In humans, circadian rhythms coordinate numerous processes in preparation for expected activities. For example, cortisol levels begin to rise in the early morning hours before awakening, preparing the body for increased metabolic demands during the active phase

(Weitzman et al., 1971). Similarly, body temperature follows a robust circadian pattern, rising during the day and decreasing during the night, with the lowest values occurring approximately two hours before habitual wake time, optimizing energy expenditure (Refinetti & Menaker, 1992). Gastrointestinal functions show circadian variation, with more rapid gastric emptying and higher intestinal blood flow during the day, affecting drug absorption and nutrient processing efficiency (Goo et al., 1987; Konturek et al., 2011). Perhaps most notably, cognitive performance metrics, including reaction time, attention, and working memory, follow circadian patterns that peak between late morning and early afternoon on average (Schmidt et al., 2007). Finally, melatonin secretion, widely used as a circadian marker, begins to rise approximately 2-3 hours before habitual bedtime in properly entrained individuals (Cajochen et al., 2003). These mechanisms illustrate the adaptive value of circadian rhythms in optimizing bodily functions according to the 24-hour day.

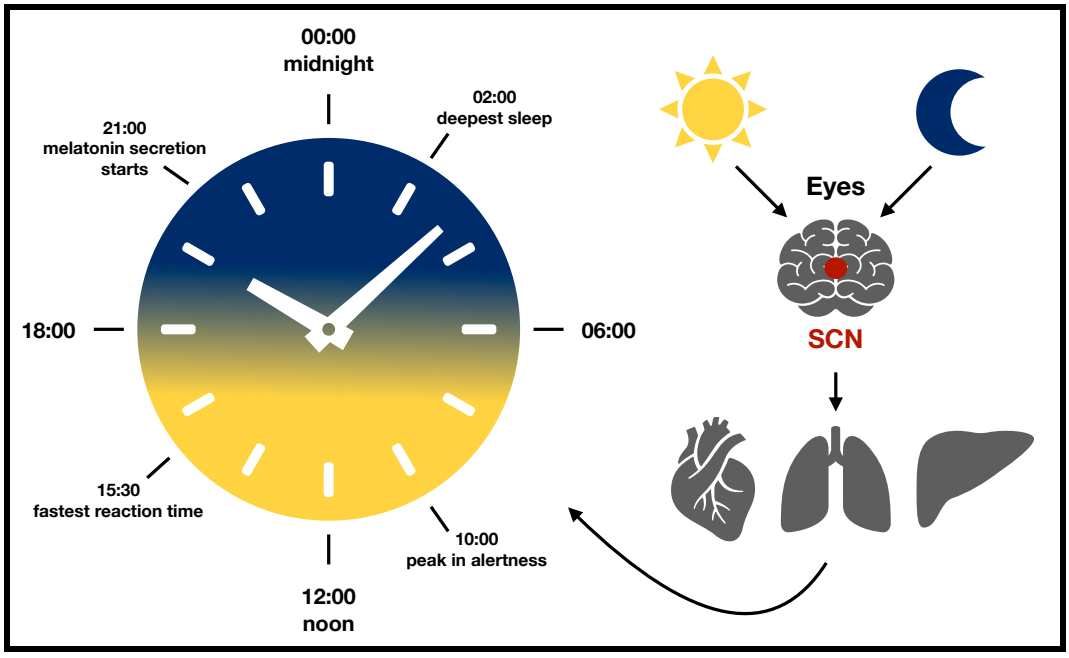

Figure 1.1. Regulation of physiology and behavior by the circadian clock system. Daily fluctuations in the day/night cycle are detected by the eye and transmitted from the suprachiasmatic nuclei (SCN) to peripheral clocks throughout the body. This results in 24-hour oscillations in hormone release, sleep/wake cycles, and metabolic functions among other processes (adapted from Masri & Sassone-Corsi, 2018).

1.1.1. Early Discoveries

The scientific understanding of circadian rhythms has evolved dramatically over time. In 1729, astronomer Jean-Jacques d'Ortous de Mairan observed that mimosa plants maintained their daily leaf movements even when kept in constant darkness, providing the first evidence of an internal timing mechanism. Two centuries later, pioneering research by Curt Richter demonstrated that rats maintained rhythmic feeding and activity patterns even without environmental time cues, leading him to propose the existence of an internal "biological clock" governing these behaviors (Richter, 1922).

In 1938, physiologist Nathaniel Kleitman and his student Bruce Richardson conducted a groundbreaking experiment in Mammoth Cave, Kentucky. They lived in complete isolation from environmental cues for a month, attempting to adopt a 28-hour day. While Richardson successfully adjusted to this longer cycle, Kleitman could not, suggesting individual variability in adaptation. This represented one of the first controlled studies of human circadian rhythms in a natural environment devoid of temporal cues. They also uncovered an association between fluctuations in body temperature and cognitive and physical performance (Hussey, 2023).

Building on this foundation, physician Jürgen Aschoff conducted human isolation studies in the 1960s. Volunteers lived for several weeks in purpose-built underground bunkers without any time cues, revealing the presence of a self-sustained oscillator with a period slightly longer than 24 hours. These experiments established the concept of "free-running" rhythms and led to Aschoff's formulation of fundamental principles of entrainment (Aschoff, 1965). Similarly, in 1962, geologist Michel Siffre conducted a self-experiment by living in isolation in an underground cave for two months without any temporal cues. His observations further revealed that humans maintain a circadian period of approximately 24.5 hours even in the absence of environmental time signals, offering strong evidence for an endogenous biological clock in humans (Hussey, 2023).

The molecular basis of these rhythms began to emerge in the 1970s when Seymour Benzer and Ronald Konopka identified the first clock gene in fruit flies, which they named "period" (Konopka & Benzer, 1971; Panda et al., 2002). They identified three distinct mutations of the period gene that either shortened, lengthened, or abolished circadian rhythmicity in Drosophila, demonstrating for the first time that a single gene could change the properties of circadian rhythms. Concurrently, lesion studies in rats showed that a small paired structure in the hypothalamus, the suprachiasmatic nuclei (SCN), were essential for the entrainment of locomotor activity, drinking, and adrenal corticosterone rhythms to the light-dark cycle (Moore & Eichler, 1972; Richter, 1971; Stephan & Zucker, 1972). As such, the SCN was found to exhibit overarching control over the mammalian circadian system.

1.1.2. The Suprachiasmatic Nuclei

The SCN is recognized as the "master clock" within the brain. It receives direct environmental input from the retina, and coordinates the other clocks found in tissues and organs throughout the body. The peripheral oscillators, such as the heart, liver, and skin, in turn optimize local physiology according to the demands of the day/night cycles. The SCN controls the timing of peripheral clocks to maintain coherence in physiological and behavioral rhythms, which is described as "internal synchronization" (Dibner et al., 2010; Mohawk et al., 2012). In this way, the mammalian circadian system is considered hierarchical, with the SCN acting as a pacemaker (Reppert & Weaver, 2002).

The SCN is referred to as the central pacemaker because its lesion results in the abolition of all circadian rhythms, while transplantation of fetal SCN in arrhythmic animals whose own SCN had been ablated re-establishes circadian rhythms (Lehman et al., 1987). The restored rhythms follow the period of the donor genotype regardless of the host genotype, showing that period is determined by cells in the suprachiasmatic region (Ralph et al., 1990). Additionally, individual SCN neurons cultured in vitro show daily rhythms in electrical activity for several weeks (Buijs

& Kalsbeek, 2001; Welsh et al., 1995). Extensive literature thus supports the central role of the SCN in the mammalian circadian system.

The SCN is located within the anterior hypothalamus, above the optic chiasm. Light is detected in the eye by photosensitive retinal ganglion cells (pRGCs), as well as rods and cones, which convert detected photons into electric signals (Hattar et al., 2002; Hughes et al., 2016). Environmental light information then travels via the retinohypothalamic tract (RHT) and directly stimulates retinorecipient SCN neurons through the neurotransmitters glutamate and pituitary adenylate cyclase-activating peptide (PACAP) (Chen et al., 1999; Ebling, 1996). Glutamate acts via N-methyl-D-aspartate (NMDA) and amino-methyl propionic acid (AMPA) receptors on retinorecipient neurons to trigger calcium influx (Ca^{2+}), which activates intracellular cascades involving calcium/calmodulin-dependent protein kinase (CaMK), extracellular signal-regulated kinase (ERK), and cAMP response element-binding protein (CREB), ultimately inducing expression of the *Per1* and *Per2* clock genes (Colwell, 2011; Impey et al., 1998). PACAP, acting through PAC1 receptors, modulates both calcium and cAMP signaling pathways, influencing the magnitude and temporal gating of the photic response (Hannibal, 2006).

The SCN is organized into functionally distinct subregions characterized by different neuropeptide expression patterns, connectivity, and responses to environmental cues (Abrahamson & Moore, 2001; Herzog et al., 2017; Morin, 2007). The ventrolateral region of the SCN (the “core”) serves as the primary site of light input processing, with neurons predominantly expressing vasoactive intestinal peptide (VIP) and gastrin-releasing peptide (GRP). VIP-expressing neurons are particularly crucial for maintaining SCN function, as genetic deletion of VIP or its receptors (VPAC2) results in disrupted circadian rhythmicity and loss of synchrony between individual SCN cells (Aton et al., 2005; Harmar et al., 2002). In contrast, the dorsomedial region of the SCN (the “shell”) serves as an output generator for the circadian system, with neurons predominantly expressing arginine vasopressin (AVP) and

neuromedin S (NMS) (Lee et al., 2015; Mieda et al., 2015). AVP-expressing neurons receive minimal direct input from the retina, but are strongly influenced by signals from VIP-expressing neurons (Ono et al., 2021). This communication occurs via both GABAergic synaptic connections (which promote rather than inhibit synchronization in the SCN) and gap junction coupling, which together maintain synchrony between SCN cells and coordinate circadian output signals (Choi et al., 2008; Ono et al., 2018). Light-induced *Per* expression thus begins in the core region and then propagates to the shell, creating a spatiotemporal wave of molecular activation that is critical for coherent network oscillations (Hamada et al., 2004; Wen et al., 2020). This well-defined neurochemical organization and the coupling between individual SCN neurons are essential for photic entrainment (Hastings et al., 2018).

1.1.3. The Molecular Circadian Clock

The molecular basis of the circadian system resides in the interaction between genes and proteins. A gene is a sequence of DNA that instructs for the synthesis of proteins. Proteins are polypeptide molecules that serve diverse functions in the body, including structural support, enzymatic catalysis, cell signaling, immune response, and transport. “Core” circadian clock genes are genes essential for the initiation and regulation of circadian rhythms, whose feedback loop is about a 24-hour cycle. Circadian output rhythms in most cells throughout the body depend upon a core and an accessory transcription/translation feedback loop (TTFL), which will here be simplified for clarity purposes (Buhr & Takahashi, 2013; Patke et al., 2020; Reppert & Weaver, 2001).

The core TTFL is composed of the positive transcriptional activator complex formed by CLOCK/BMAL1 heterodimers (proteins that join together to form paired structures), and the negative CRY/PER repressor complex, which interact in a rhythmic manner. CLOCK (Circadian Locomotor Output Cycles Kaput) and BMAL1 (Brain and Muscle ARNT-like 1) heterodimerize and bind to E-box elements in the promoter regions of their target genes, including the cryptochrome (*Cry1* and *Cry2*) and period (*Per1* and *Per2*) genes, thereby

initiating their transcription. CRY and PER proteins accumulate and subsequently form a repressor complex that inhibits CLOCK and BMAL1 transcriptional activity, thus repressing their own transcription (Lowrey & Takahashi, 2011). This negative feedback is thought to allow the CLOCK/BMAL1 activator complex to start a new transcriptional cycle approximately every 24 hours (Eide et al., 2005).

The accessory loop, in which transcription factors bind to clock-controlled genes containing regulatory elements other than the E-box, also contributes to the function of the circadian clock system. The transcription factors REV-ERB (Reverse Erythroblastosis Virus) and ROR (retinoic acid Receptor-related Orphan Receptor) bind to ROREs (ROR Elements) and respectively repress, or activate, BMAL1 expression (Bellet & Sassone-Corsi, 2010). This feedback loop thus has a substantial role in driving the rhythmic expression of *Bmal1*. Moreover, DBP (D site of albumin promoter-Binding Protein) is regulated by the transcriptional activity of the CLOCK/BMAL1 complex, and activates the expression of genes with D-box elements in their promoters. Although there are some tissue-specific differences in this general molecular mechanism, together, these TTFLs regulate circadian rhythms in mammals (**Fig. 1.2**).

It is worth noting that not all cell types possess functional TTFLs. Some cells, such as red blood cells (erythrocytes), lack nuclei and therefore cannot maintain autonomous circadian oscillations through transcriptional mechanisms. Instead, these cells rely on circadian signals from other tissues or exhibit circadian rhythms through post-translational modifications (Henslee et al., 2017; O'Neill & Reddy, 2011).

While mutations in most core clock genes alter period length or amplitude, deletion of *Bmal1* is the only single knockout (KO) that abolishes circadian rhythms in both the SCN and peripheral oscillators (Partch et al., 2014). In contrast, *Clock* KO mice maintain relatively robust circadian rhythmicity due to compensation by its paralog NPAS2 (Neuronal PAS domain protein 2), which can functionally substitute for CLOCK by forming heterodimers with

BMAL1 (Debruyne et al., 2006). *Bmal1*, however, has no functional paralog capable of similar compensation, making its expression essential for generating circadian rhythms throughout the body (Ko & Takahashi, 2006).

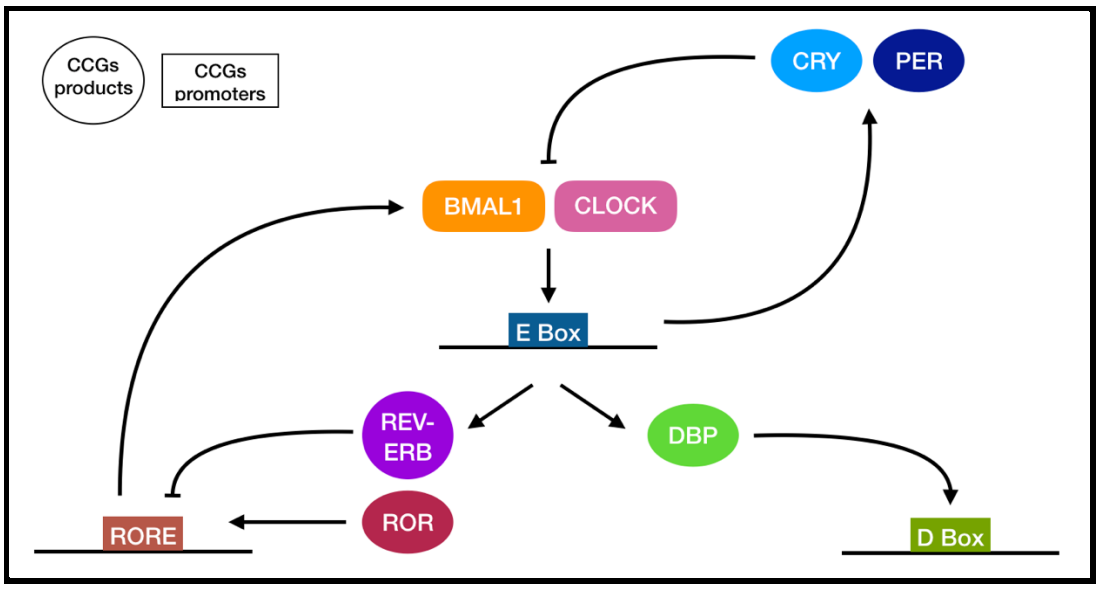

Figure 1.2. Schematic representation of the translation/transcription feedback loops regulating the mammalian circadian system (adapted and simplified from Bellet & Sassone-Corsi, 2010). The positive regulators CLOCK/BMAL1 activate clock-controlled genes (CCGs) with an E-box promoter, including CRY and PER, which act as negative regulators of their own transcription. CLOCK/BMAL1 also activate DBP and ROR, which control the expression of genes with D-box and RORE elements in their promoters.

Clock genes are widely and rhythmically expressed. Research by Zhang and colleagues examined gene expression data in 12 organs throughout the body and found that over 43% of all genes in the mouse genome oscillate with a circadian rhythm, largely in an organ-specific manner (Zhang et al., 2014) (**Fig. 1.3**). This tissue-specificity allows circadian timing to be optimized for the unique functions of each organ, while maintaining overall temporal coordination through the central pacemaker. The clinical relevance of these circadian oscillations becomes evident when considering pharmacological interventions. Many commonly prescribed medications target proteins that exhibit circadian rhythms in their

expression or activity, suggesting potential benefits from timed administration (Dallmann et al., 2014). For instance, allergic symptoms often show variation according to time of day, with many allergy sufferers experiencing heightened symptoms in the morning. This temporal pattern, combined with the sedative properties of certain antihistamines, motivates the administration of such drugs in the evening period (Smolensky et al., 2016). These observations have contributed to growing interest in chronotherapy, the strategic timing of treatments based on the body's internal rhythms, as an approach to optimize drug efficacy.

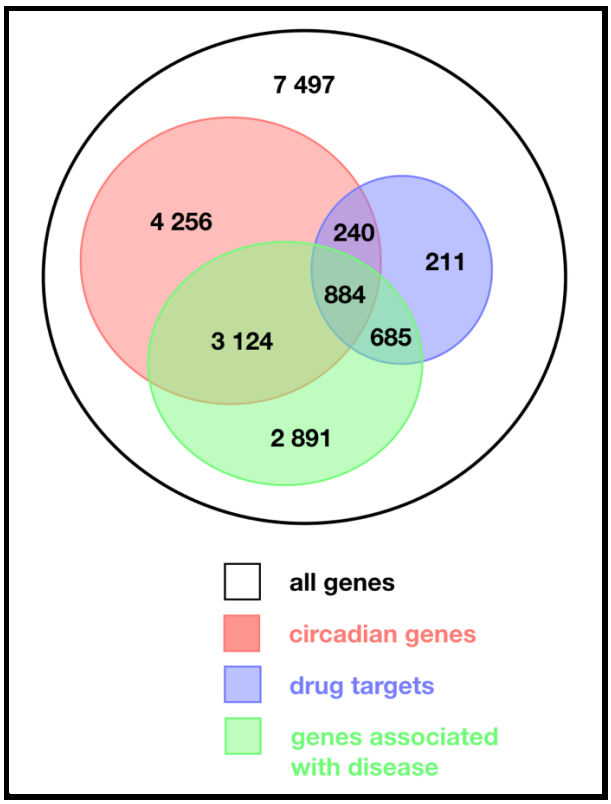

Figure 1.3. Overlap between circadian genes, drug targets and genes associated with diseases in the mouse genome (adapted from Zhang et al., 2014).

1.1.4. Peripheral Oscillators

The widespread distribution of clock gene expression throughout the body highlights the existence of a network of peripheral oscillators that operate outside the SCN. These peripheral clocks, while sharing the same core molecular mechanism, generate tissue-specific rhythms that optimize local physiology (Yamamoto et al., 2004). Unlike the robust and self-sustaining central pacemaker, peripheral clocks require regular synchronization to maintain rhythmicity and proper phase relationships with other clocks, as well as the external environment (Dibner et al., 2010; Mohawk et al., 2012). The SCN coordinates peripheral clocks through multiple pathways, including direct neural connections via the autonomic nervous system and hormonal signals, particularly glucocorticoids (Brown & Azzi, 2013; Buijs & Kalsbeek, 2001; Cailotto et al., 2005; Schibler et al., 2015).

While primarily synchronized by the SCN, peripheral oscillators can also independently entrain to non-photic cues, such as feeding schedules. Time-restricted feeding can uncouple peripheral clocks from the SCN, causing phase shifts in the liver, intestine, and kidney, without affecting SCN rhythmicity (Damiola et al., 2000; Stokkan et al., 2001). This flexibility allows peripheral tissues to adapt to changes in energy availability and metabolic demand independently of the light-dark cycle (Lamia et al., 2008; Saini et al., 2013).

1.1.5. Circadian Responses to Light

The detection of light by the eye serves a dual purpose, not only facilitating vision but also regulating circadian function (Foster & Hankins, 2007). Its impact on the circadian clock varies depending on the timing, intensity, duration, and wavelength of the light exposure. Studies have shown that the timing and intensity of the light stimuli influences the direction and magnitude of the circadian system's response, with maximal sensitivity during the biological night (Duffy & Czeisler, 2009). Depending on the phase in which an animal receives a light pulse, its response varies. Because locomotor activity is thought to be a direct behavioral output of the

central pacemaker, activity is a common assay for the disruption of circadian rhythms at the SCN clock level. Daan & Pittendrigh found that a brief light pulse given early or late in the subjective night causes phase delays or advances in activity, respectively, in multiple rodent models (Pittendrigh & Daan, 1976a). Moreover, animals are insensitive to light pulses during the subjective day, indicating the presence of a "dead zone" for phase shifting. The "phase response curve" demonstrates how light exposure at different times of day affects circadian phase shifts (**Fig. 1.4**).

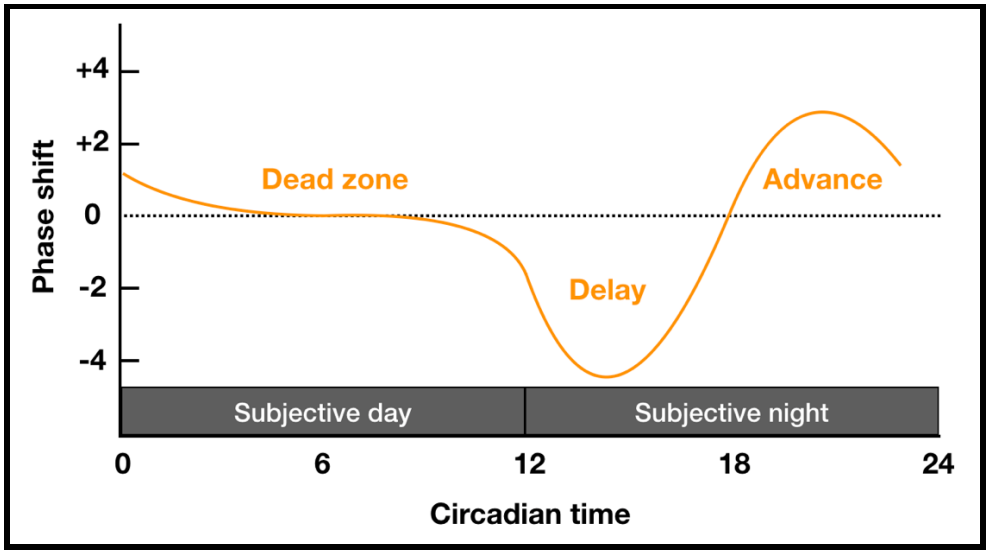

Figure 1.4. Standard phase response curve for mammals (adapted from Kuhlman et al., 2018). Light during the day does not lead to any changes in the circadian response. However, light early or late in the night, respectively delays or advances the phase of circadian rhythms.

Interestingly, all mammals, both diurnal and nocturnal, show a broadly comparable phase response curve with different magnitudes for the advance and delay portions. As such, regardless of whether a subject is active or inactive during the day, light at dusk will have the biggest effect in shifting behavior. Moreover, a study by Rahman and colleagues showed that a single light exposure as short as 15 sec can shift circadian phase in humans (Rahman et al., 2017). Remarkably, work by Heller and colleagues demonstrated that sequences of millisecond

light flashes (as brief as 2 ms) can produce significant phase shifts when delivered at specific intervals in both mice and humans (Van Den Pol et al., 1998; Zeitzer et al., 2014; Zeitzer et al., 2011). These findings collectively highlight the particular temporal sensitivity of the circadian system at night.

The circadian system also responds to light in a dose-dependent manner following a sigmoidal irradiance-response curve (**Fig. 1.5**). Irradiance represents the radiometric measurement of light intensity upon a surface, typically expressed in power e.g. W/m² (Foster et al., 2007b). As irradiance increases, the magnitude of the phase shift increases until reaching saturation (Nelson & Takahashi, 1991). This relationship has been demonstrated across different species, with varying absolute sensitivities. For measurements of brightness relevant to human visual perception, photometric units are commonly employed.

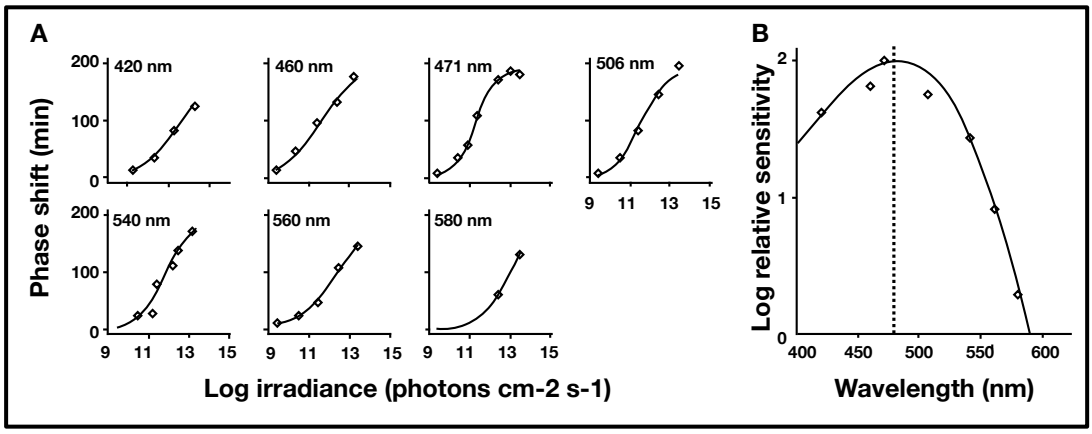

Figure 1.5. Example of irradiance response curves and action spectrum (reproduced from Hattar et al., 2010). **A.** Circadian phase shifting responses in rodless/coneless (*rd/rd*) mice exposed to monochromatic light ranging from 420 to 580 nm, measured through wheel-running behavior. **B.** Corresponding action spectrum for circadian photoentrainment, with a best fit corresponding to the absorption profile of a photopigment peaking at 481 nm (dashed line).

Illuminance, or illumination, represents the amount of light falling on a surface (in power), weighted according to human spectral sensitivity and expressed in photometric lux. This metric differs from irradiance by incorporating human photopic sensitivity peaking at 555 nm (Lucas et al., 2014). Humans show remarkable sensitivity to light, with significant circadian responses occurring at illuminances as low as 10-15 lux of white light, while half-maximal responses occur around 100 lux (Cajochen et al., 2000; Zeitzer et al., 2000). By comparison, mice exhibit even greater sensitivity, detecting and responding to light much dimmer than the human threshold (Foster & Helfrich-Förster, 2001). Studies have shown that mice responses begin at illuminances around 0.1-1 lux, with half-maximal phase shifts occurring at approximately 10-30 lux (Butler & Silver, 2011; Lall et al., 2010).

Additionally, the circadian system can integrate photons over extended periods of time, a mechanism known as temporal integration. Indeed, Nelson and Takahashi demonstrated that hamsters show an equivalent response to a brief, high-intensity light pulse and a longer, lower-intensity exposure, as long as it delivers the same total number of photons (Nelson & Takahashi, 1991).

1.1.6. Photoreceptors

In addition to the timing, duration and intensity of light, the spectral composition of the light is a critical factor in determining its impact on the circadian system. The classical human visual system, mediated primarily through the rods and cones, is most sensitive to red and green light with peak intensity at ~ 555 nm (Dartnall et al., 1983). However, action spectroscopy studies by Takahashi and colleagues, which characterized biological responses to light of varying wavelengths, demonstrated that rodent circadian phase-shifting responses exhibit peak sensitivity in the blue region of the spectrum, between 480 and 500 nm (Takahashi et al., 1984). As this finding was inconsistent with the known spectral sensitivities of rods and cones, it suggested the involvement of a novel photoreceptive mechanism.

In the 1990s, subsequent studies by Foster and colleagues showed that mice with bilateral enucleation (complete removal of the eyes) maintained endogenous circadian rhythms, but were unable to respond to light cues or synchronize to light-dark cycles (Foster et al., 1991). Action spectrum studies using retinally degenerate (*rd/rd*) mice, which have retinal degeneration that eliminates rods and severely reduces cone function, revealed a peak sensitivity for circadian responses around 480-511 nm (Provencio & Foster, 1995; Yoshimura & Ebihara, 1996). These *rd/rd* mice maintained circadian photosensitivity despite their severe visual impairment, providing further evidence for a non-rod, non-cone photoreceptor. This hypothesis was then confirmed in mice with complete elimination of functional rods and cones using cone-specific transgenes (Freedman et al., 1999; Lucas et al., 1999). Studies in humans also showed that individuals with no conscious light perception could still exhibit melatonin suppression and circadian entrainment as long as the eyes remained intact (Czeisler et al., 1995). Together, these results indicated that, while the eyes were critical for photoentrainment, an additional photoreceptor was mediating this response.

The identification of a third class of retinal photoreceptor, comprising a subset of pRGCs expressing the photopigment melanopsin (OPN4), provided the molecular and cellular basis for the circadian system's spectral sensitivity (Hattar et al., 2002; Provencio et al., 2000; Sekaran et al., 2003). Melanopsin-expressing pRGCs constitute approximately 1-2% of the total RGC population and project directly to the SCN via the RHT. Electrophysiological characterization of these cells revealed an intrinsic photosensitivity with maximal response to wavelengths near 480 nm, which corresponds to blue light (Berson et al., 2002; Hattar et al., 2002). The functional significance of melanopsin in circadian photoentrainment was confirmed through genetic ablation studies. While mice lacking either melanopsin or functional rods and cones retained the ability to entrain to light-dark cycles, triple knockout mice deficient in all three photoreceptors failed to exhibit any circadian photosensitivity (Hattar et al., 2003; Panda et al., 2003). These findings established the requirement for photoreceptive input to the circadian system, and identified melanopsin as a key mediator of this function.

While melanopsin-expressing pRGCs serve as the primary photoreceptors for circadian entrainment, the system exhibits greater complexity than initially postulated. These cells also receive synaptic input from rods and cones, creating a network in which all three photoreceptor types contribute to circadian light responses (Dacey et al., 2005; Güler et al., 2008; Wong et al., 2007). The relative contribution of each system is dependent on multiple factors including light intensity, duration, and wavelength (Foster et al., 2020). At very low light levels, rods play a dominant role due to their heightened sensitivity, while cones contribute significantly at intermediate illuminances and more sudden increases in light intensity, such as dawn/dusk transitions (Allen et al., 2014; Lall et al., 2010). Melanopsin becomes more important at higher light intensities and during prolonged light exposure, as it demonstrates increased photochemical stability. Unlike rod and cone opsins, which undergo rapid photochemical deactivation (bleaching) after light absorption and require time-consuming regeneration through the retinoid cycle, melanopsin remains functional during continuous illumination and shows greater adaptation (Emanuel & Do, 2015; Mure et al., 2007; Wong et al., 2005). The different temporal dynamics of these photoreceptors create a complementary network optimized for detecting all the light information relevant to the internal clock (**Fig. 1.6**) (Lucas et al., 2012).

Additionally, recent studies have demonstrated that different subtypes of pRGCs have distinct morphologies, projections, and functional roles, with six identified subtypes in mice, and five in humans (Ecker et al., 2010; Lazzerini Ospri et al., 2017; Sonoda & Schmidt, 2016). While M1 cells provide the primary input to the SCN for circadian entrainment, other subtypes contribute to diverse non-image-forming functions, including the pupillary light reflex, mood regulation, and sleep induction (Chen et al., 2011; Schmidt et al., 2011).

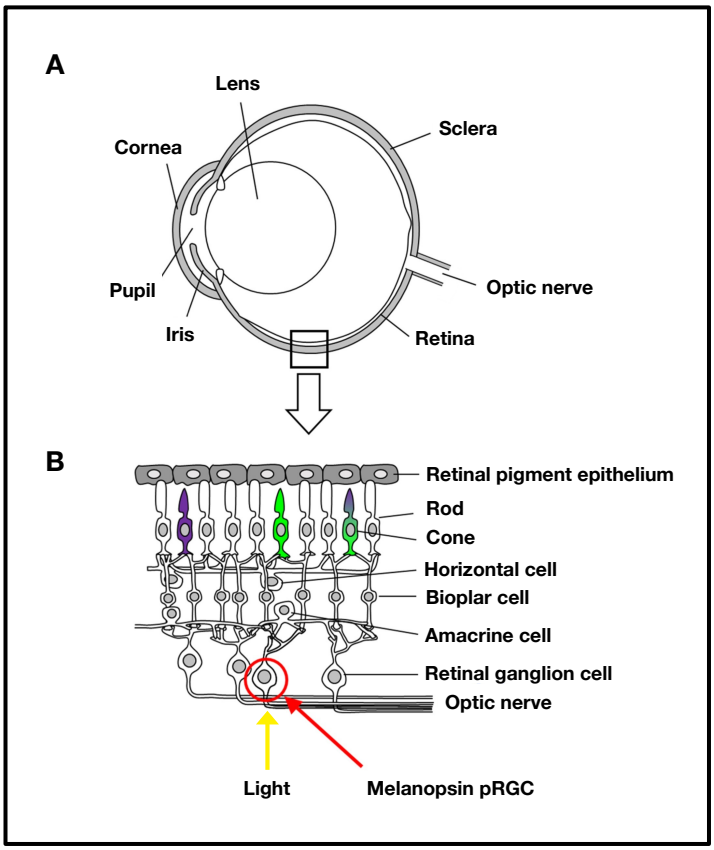

Figure 1.6. Mouse **A.** eye and **B.** retina structure (reproduced from Peirson et al., 2018). Rods support vision in low light, while cones mediate bright light and color vision. Mice express two types of cone opsins, an ultraviolet-sensitive (UVS) opsin and a middle-wavelength-sensitive (MWS) opsin, which are co-expressed in the majority of cones. In addition to rods and cones, a subset of photosensitive retinal ganglion cells (RGCs) expresses melanopsin and supports non-visual responses to light.

1.1.7. Measuring Light

The discovery of melanopsin and its distinct spectral sensitivity has revealed significant limitations in the conventional light measurements used in circadian research. Traditional illuminance metrics, such as lux, fundamentally mischaracterize the impact of light on the circadian system. Indeed, it focuses on the green/yellow wavelengths at ~ 555 nm, and fails to capture melanopsin's blue-shifted sensitivity at ~ 480 nm (Lucas et al., 2014). Consequently, two light sources with identical lux values can produce different effects on the circadian system depending on their spectral composition. For example, a blue-enriched LED light at 100 lux may produce circadian effects equivalent to several hundred lux of warmer incandescent

lighting, despite both being measured as photometrically equal (Cajochen et al., 2005; Santhi et al., 2012). This mismatch between photometric measurement and biological effect has led to considerable inconsistencies in research findings and practical applications (Peirson et al., 2018; Rea et al., 2010).

To address these limitations, Lucas and colleagues suggested a framework for quantifying light based on its effect on each photoreceptor class in the human retina (Lucas et al., 2014). This approach was subsequently formalized by the International Commission on Illumination in 2018 as the α-opic equivalent daylight illuminance (α-EDI) system. It calculates five distinct α-opic metrics corresponding to each photoreceptor: S-cone (cyanopic), M-cone (chloropic), L-cone (erythropic), rod (rhodopic), and melanopsin (melanopic). Among these, the melanopic EDI has emerged as the most relevant metric for quantifying circadian responses to light (Brown et al., 2022). It represents the illuminance of standard daylight (D65) that would produce equivalent melanopsin stimulation as the measured light source, thereby providing a standardized reference for comparing diverse spectral distributions.

Furthermore, standardized methodologies for measuring and reporting light exposure in chronobiology research have been proposed to improve experimental reproducibility. The ENLIGHT consensus checklist provides comprehensive reporting guidelines for laboratory-based studies on non-visual effects of light in humans, emphasizing the necessity of complete spectral characterization of experimental lighting conditions (Spitschan et al., 2023). Similarly, detailed recommendations for measuring and standardizing light for laboratory mammals have been published to enhance reproducibility in animal research, with specific guidance for converting human-relevant metrics to those appropriate for various model organisms (Lucas et al., 2024).

1.1.8. From Mice to Humans

While mice serve as invaluable models in circadian research, their visual system differs from that of humans in ways that can impact the interpretation and translation of experimental findings. Understanding these differences is essential when extrapolating results between species or designing experiments that model human light responses. While mice and humans have a similar proportion of melanopsin-expressing pRGCs, they differ in their cone photoreceptor arrangement. Humans have trichromatic vision with blue-sensitive S-cones (~ 420 nm), green-sensitive M-cones (~ 534 nm), and red-sensitive L-cones (~ 564 nm) (Do, 2019). By contrast, mice only have two cone types: S-cones with peak sensitivity in the ultraviolet range (~ 360 nm), and M-cones sensitive to green light (~ 508 nm) (Applebury et al., 2000). As such, the spectral sensitivity of mice is shifted towards shorter wavelengths of light (**Fig. 1.7**). Moreover, the spatial distribution and relative abundance of rods and cones differ between species. Unlike humans, mice lack a fovea (the cone-rich central region of the retina) and possess a rod-dominated retina, which more closely resembles the human peripheral retina in terms of rod/cone ratios (Carter-Dawson & LaVail, 1979; Curcio et al., 1990).

Despite these differences in spectral sensitivities and photoreceptor arrangement, both species possess functional melanopsin-expressing pRGCs that mediate the circadian responses to light. As such, broad-spectrum white light can effectively activate the circadian system in both species, though at different thresholds (Brown et al., 2022; Lucas et al., 2014). Cross-species comparisons become meaningful when researchers employ photoreceptor-based metrics, such as melanopic EDI, adjusted for each species' sensitivity curve. “Equivalent” light exposures that produce comparable levels of relevant photoreceptor stimulation can then be determined (Lucas et al., 2024). Recent standardized frameworks specifically address these cross-species considerations, providing conversion factors and methodological guidelines for translating findings between mice and humans (Spitschan et al., 2021). Therefore, with proper light

characterization, mice remain valuable models for translating circadian light responses to humans (Tir et al., 2022).

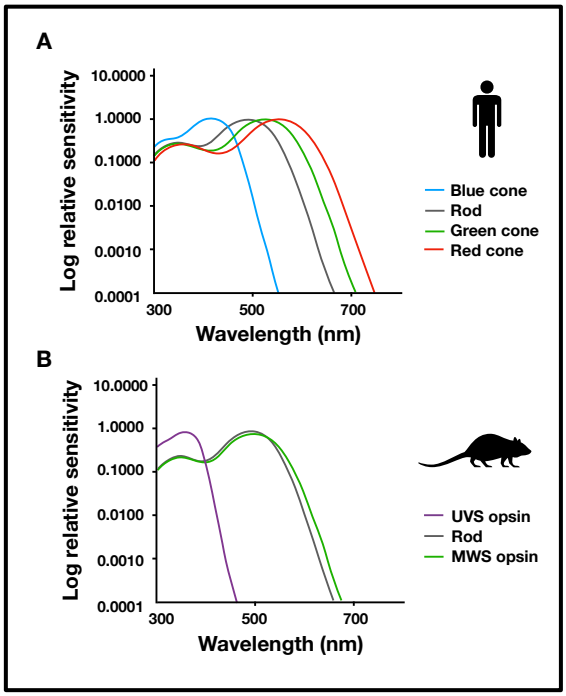

Figure 1.7. Differences in spectral sensitivity between the **A.** human and **B.** mouse visual systems (reproduced from Peirson et al., 2018). The human retina contains rods and three types of cones, maximally sensitive to short (blue S-cone), medium (green M-cone), and long (red L-cone) wavelengths. In contrast, the mouse retina is dominated by rods and contains two types of cones, maximally sensitive to ultraviolet (UVS opsin) and medium (MWS opsin) wavelengths. As such, the spectral sensitivity of the mouse is shifted towards shorter wavelengths of light.

1.2. Circadian Disruption and the Modern Light Environment

Circadian rhythms are remarkably robust and persist even in the absence of periodic external stimuli (Duffy & Czeisler, 2009). In line with natural selection and evolution, the human circadian clock system promotes physical activity and cognition during the day, and sleep at night, with the opposite holding for nocturnal animals. However, inappropriate light exposure, such as receiving too much or not enough light at the wrong time, confuses these internal clocks and disrupts circadian rhythms.

1.2.1. Circadian Misalignment

A clock is of no use unless it is set to the right time. Circadian misalignment occurs when internal biological rhythms are incorrectly phased with regard to the external light-dark cycle (Baron & Reid, 2014). It can manifest as a mismatch between the central pacemaker and peripheral oscillators (internal desynchrony), conflicting timing between critical processes like sleep/wake cycles and feeding-fasting rhythms, or misalignment between biological time and the external world, including social/work schedules. Growing evidence shows that circadian disruption contributes to the pathophysiology of a wide range of deleterious health outcomes, including increased risks of metabolic disease, obesity, depression, and even cancer (Coogan & Wyse, 2008; Sahar & Sassone-Corsi, 2009; Young & Bray, 2007).

The most significant examples of circadian misalignment occur in shift workers. A survey revealed that approximately 27% of male and 16% of female workers in the United States rotate between day and night shifts (Czeisler et al., 1982), requiring constant readjustment of their biological clocks. This circadian disruption carries substantial health consequences, with shift workers showing increased rates of coronary heart disease, impaired glucose tolerance, and mental health challenges amongst many other adverse health effects (Boivin et al., 2022; James et al., 2017; Mosendane et al., 2008). For instance, nurses working night shifts demonstrate significantly higher rates of breast cancer and obesity compared to day-shift counterparts (McGlynn et al., 2015; Schernhammer et al., 2006). As such, the World Health Organization officially defined shift work involving circadian disruption as a potential carcinogen in humans (Straif et al., 2007).

Yet, circadian misalignment extends far beyond shift work. A much larger portion of the population experiences “social jet lag,” a chronic misalignment between biological and social time, which occurs when work and social obligations conflict with one’s innate chronotype (Wittmann et al., 2006). Even modest misalignments of two hours or less are associated with increased BMI, metabolic dysfunction, and elevated cardiometabolic risk factors (Roenneberg

et al., 2012). Individual differences in chronotype, with someone being naturally morning-oriented ("lark") or evening-oriented ("owl"), significantly influence vulnerability to these effects, with evening chronotypes typically experiencing greater misalignment in societies that favor early schedules (Vetter et al., 2015). This widespread tendency to "live against the clock" has been a core focus in the discussion of appropriate work and school start times (Boergers et al., 2014; Díaz-Morales & Escribano, 2015; Morgenthaler et al., 2016; Skeldon et al., 2017).

1.2.2. The Rise of Artificial Light Exposure

Mistimed light exposure, such as light at night, contributes significantly to circadian disruption. For the last century, artificial lighting has enabled the expansion of work and entertainment hours far into the night. As such, this modern light environment differs from the natural one in two critical ways: people are exposed to lower levels of light as they work indoors during the day, and to higher levels of electrical light in their homes at night (**Fig. 1.8**) (Wright et al., 2013). Indeed, satellite data reveals that 80% of the world's population is exposed to artificial nighttime light, rising to 99% in the United States and European Union (Cinzano et al., 2001; Falchi et al., 2016).

Artificial light has become the dominant source of illumination for humans, posing a variety of circadian challenges (de la Iglesia et al., 2015; Lunn et al., 2017; Mason et al., 2018; Stevens & Zhu, 2015). Additionally, nighttime light now emanates not only from room lighting, but increasingly from light-emitting devices, such as phones, computers, and televisions. Recent expert consensus-based recommendations suggest that evening light exposure should remain below 10 lux (melanopic EDI) at eye level for 3 hours prior to habitual bedtime to minimize circadian disruption (Brown et al., 2022). However, typical evening environments in modern homes and workplaces exceed this threshold, with common indoor lighting ranging from 30 to 500 lux (Wright et al., 2013).

The impact of evening light exposure on human physiology has been documented through controlled laboratory studies. Exposure to electrical light in the evening consistently delays the circadian system's phase relationship with the light-dark cycle, pushing biological night to increasingly later hours (Wright et al., 2013). In fact, light exposure > 30 lux for just 2-3 hours before habitual bedtime significantly suppresses melatonin production, delays the phase of dim light melatonin onset (DLMO), and increases alertness. These effects are also accompanied by sleep disruption, including delayed sleep onset, reduced slow-wave sleep, and impaired sleep efficiency, as well as alterations in metabolic function (Cain et al., 2020; Cajochen et al., 2011; Chang et al., 2015; Gooley et al., 2011; Green et al., 2017; Obayashi et al., 2013; Stothard et al., 2017).

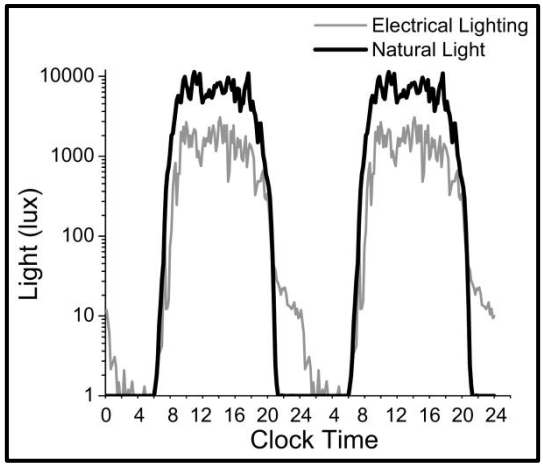

Figure 1.8. Light exposure under artificial and natural conditions (from Wright et al., 2013). Average 24-hour light exposure (in lux, log scale) under electric lighting in a constructed environment and under a natural light-dark cycle while camping. Data are double-plotted.

1.2.3. Dim Light at Night

While the effects of nighttime light exposure are increasingly recognized, the mechanisms by which our bodies are affected by and potentially adapt to this artificial light environment are somewhat debated. Elucidating these processes is crucial for developing strategies to mitigate

circadian disruption and align our bodies with the 21st century light schedule. The first step is thus to measure the effects of such disruptive light.

In rodents, research on artificial light at night has largely focused on continuous dim light throughout the night phase. This paradigm typically exposes animals to low-level illumination (typically ~ 5 lux) across the entire dark period, mimicking conditions experienced by shift workers or those in heavily light-polluted environments. The following section synthesizes the existing literature on the effects of acute and chronic (> 2 weeks) dim light at night (DLAN) exposure in mice, hamsters, and rats, providing a foundation for understanding how even low levels of nighttime light exposure can impact physiology and behavior. This analysis serves as a basis for introducing our experimental paradigm, dim light in the evening, which more accurately models contemporary patterns of circadian light disruption in the general populace. It reveals that DLAN disrupts physiological systems at a multitude of levels, from circadian rhythms and metabolism to mood regulation and immune function.

Circadian Clock Genes. At a molecular level, studies have found significant alterations in the expression of core clock genes under DLAN exposure (**Table 1.1**). In male CD1 mice, chronic DLAN reduced PER1 expression in the SCN (Shuboni & Yan, 2010). Similarly, it attenuated PER1 expression in the SCN, and PER2 expression in the hippocampus of female Siberian hamsters (Bedrosian, Galan, et al., 2013). Effects were also observed in male Swiss Webster mice, with attenuated *Per1/2* in the SCN, and *Per1/2* and *Cry2* in the hypothalamus (Fonken, Aubrecht, et al., 2013). In peripheral tissues, more pronounced and widespread disruptions were observed, with dampened rhythms for *Bmal1*, *Per1*/*2*, and *Rev-Erb* in the liver, and *Rev-Erb* in white adipose tissue (WAT) (Fonken, Aubrecht, et al., 2013). Across studies, these results indicate that all the core clock genes mentioned above are reduced at an oscillator level, but only the *Per* genes are altered in the central pacemaker. One important consideration is that the tissues were collected under dim light rather than darkness for DLAN animals. *Per* expression is known to be light-inducible, whereas *Clock* and *Bmal1* are not directly light-responsive

(Takahashi, 2017). As such, the attenuated *Per* expression in the SCN might reflect a direct response to the constant low-level light input rather than disruptions in the circadian system itself, or a change in light sensitivity to light stimuli.

Table 1.1. Effects of DLAN exposure on circadian clock genes in rodents. The duration of DLAN exposure and the age of the animals are reported in weeks (w). Effects are expressed as a reduction (↓), or no change (Ø).

Species	Night light	Day light	LD cycle	DLAN duration	Sex	Age	Results Circadian Clock Genes	Reference
Swiss Webster mouse	5 lux	150 lux	14:10	4w	♂	8w	↓ Per1/2 and PER1/2 rhythms in SCN ↓ Per1/2 and Cry2 rhythms in hypothalamus Ø hippocampus ↓ Bmal1, Per1/2, Cry1/2 and Reverb rhythms in liver ↓ Reverb rhythms in WAT	Fonken, Aubrecht, et al., 2013
Siberian hamster	5 lux	150 lux	16:8	?	♀	8w	↓ PER1 in SCN ↓ PER2 in hippocampus	Bedrosian, Galan, et al., 2013
CD1 mouse	20 lux	300 lux	12:12	3w	♂	3w	↓ PER1 in SCN ↓ Per1 in SCN after light pulse	Shuboni & Yan, 2010

Activity. The effects of DLAN on the architecture of activity rhythms in rodents have been widely investigated (**Table 1.2**). Studies in Swiss-Webster mice have reported no changes in total wheel-running or locomotor activity under short and long-term DLAN exposure for both sexes (Aubrecht et al., 2015; Borniger et al., 2014; Borniger et al., 2013; Fonken et al., 2014; Fonken et al., 2010). One study noted a weakening of the rhythms, with only half of the animals displaying a 24-hour pattern in wheel-running activity (Fonken et al., 2014). In C57BL/6J mice, no effects were found on the onset and power of wheel-running activity, but a subtle reduction in period length was reported (Cleary-Gaffney & Coogan, 2018). In contrast, the robustness and stability of home-cage locomotor activity rhythms was altered, with increased daytime activity, but no changes in total activity (Delorme et al., 2022). While the total amount of activity was not noted in male CD1 mice, chronic DLAN increased wheel-running activity during the day, altered activity onsets and offsets, and led to a shorter free-running period (Shuboni & Yan, 2010). In female Siberian hamsters, chronic DLAN reduced the strength of locomotor activity rhythms and decreased nighttime activity, but did not affect the onset,

acrophase, or total amount of locomotor activity (Bedrosian, Galan, et al., 2013; Bedrosian, Weil, et al., 2013). Similarly, weakened locomotor activity rhythms were found in young and aged male C57BL/6JOlaHsd mice, with no effect on period (Panagiotou & Deboer, 2020). DLAN attenuated the amplitude of locomotor activity rhythms in Wistar rats, with a decrease in total activity, and redistribution of activity towards the day (Rumanova et al., 2025). No changes were found in the total amount, onset, offset, acrophase, and amplitude of locomotor activity rhythms in diurnal Nile grass rats (Fonken et al., 2012). Additionally, Shuboni and Yan (2010) investigated phase shifting responses under chronic DLAN exposure. Following a LP (30 min, 300 lux) at ZT17.5, DLAN animals showed a reduced phase shift in activity and attenuated *Per1* expression in the SCN, indicating dampened SCN light responses (Shuboni & Yan, 2010). Taken together, these findings demonstrate that DLAN exposure can impact the strength and temporal organization of activity rhythms while preserving its total daily amount. The magnitude and nature of the disruptions vary across species, strains, and measurement methodologies. DLAN also attenuates phase shifting responses to light pulses, suggesting reduced plasticity in the circadian system.

Table 1.2. Effects of DLAN exposure on wheel-running and locomotor activity in rodents. The duration of DLAN exposure and the age of the animals are reported in weeks (w) and months (m). Effects are expressed as an increase (↑), a reduction (↓), or no change (Ø).

Species	Night light	Day light	LD cycle	DLAN duration	Sex	Age	Results Activity	Reference
Swiss Webster mouse	5 lux	150 lux	14:10	2w	♂	8w	Ø total locomotor activity Ø period length Ø acrophase	Borniger et al., 2014
				3w	♂	8w	↓ wheel-running activity rhythms Ø total activity	Fonken et al., 2014
				8w	♂	?	Ø total wheel-running activity	Borniger et al., 2013
			16:8	6w	♀	8w	Ø total locomotor activity	Aubrecht et al., 2015
				8w	♂	8w	Ø total locomotor activity	Fonken et al., 2010
Siberian hamster	5 lux	150 lux	16:8	4w	♀	8w	↓ locomotor activity rhythms ↓ nighttime activity	Bedrosian, Weil et al., 2013
				?	♀	8w	↓ locomotor activity rhythms Ø activity onset, acrophase Ø total activity	Bedrosian, Galan et al., 2013
Nile grass rat (diurnal)	5 lux	150 lux	14:10	3w	♂	10w	Ø total locomotor activity Ø activity onset, offset, acrophase, amplitude	Fonken et al., 2012
Wistar rat	2 lux	150 lux	12:12	2w	♂	?	↓ locomotor activity rhythms	Rumanova et al., 2025
C57BL/6 mouse	5 lux	150 lux	12:12	3w	♀♂	10w	Ø wheel-running activity rhythms Ø activity onset	Cleary-Gaffney & Coogan, 2018
	20 lux	200 lux	12:12	1y	♂	10w	↑ locomotor activity rhythms Ø total activity ↑ daytime activity ↓ interdaily stability Ø intradaily variability	Delorme et al., 2022
C57BL/6J OlaHsd mouse	5 lux	75 lux	12:12	12w	♂	6m, 18m, 24m	↓ locomotor activity rhythms Ø period length	Panagiotou & Deboer, 2020
CD1 mouse	20 lux	300 lux	12:12	3w	♂	3w	↑ daytime wheel-running activity Ø activity onset, offset ↓ free-running period ↓ phase shift after light pulse	Shuboni & Yan, 2010

Table 1.3. Effects of DLAN exposure on sleep in rodents. The duration of DLAN exposure and the age of the animals are reported in weeks (w). Effects are expressed as an increase (↑), a reduction (↓), an alteration (Δ), or no change (Ø).

Species	Night light	Day light	LD cycle	DLAN duration	Sex	Age	Results Sleep	Reference
Swiss Webster mouse	5 lux	150 lux	14:10	3w	♂	3m	↓ nighttime plasma melatonin	Fonken et al., 2013b
				8w	♂	?	Ø total sleep Ø REM, SWS, delta power	Borniger et al., 2013
Wistar rat	2 lux	150 lux	12:12	2w	♂	?	↓ nighttime plasma melatonin	Jerigova et al., 2023
				2w	♂	?	Ø total sleep ↑ daytime wakefulness ↓ REM, NREM, SWA amplitude	Stenvers et al., 2016
				3w	♂	18w	↓ nighttime plasma melatonin	Molcan et al., 2019
	5 lux	250 lux	12:12	5w	♀	7w	↓ nighttime plasma melatonin	Gutiérrez-Pérez et al., 2023
C57BL/6J OlaHsd mouse	5 lux	75 lux	12:12	12w	♂	6m, 18m, 24m	↓ sleep rhythms ↑ daytime wakefulness Δ NREM sleep	Panagiotou & Deboer, 2020

Sleep. Mixed results support the detrimental effects of DLAN on sleep patterns (**Table 1.3**). Borniger and colleagues (2013) initially found no effects on sleep in Swiss-Webster mice, with no differences in the distribution or total amount of wake, rapid eye movement (REM), slow wave sleep (SWS), and delta power, a measure of sleep intensity and pressure (Borniger et al., 2013). The authors suggested that the potential disruptive effects of DLAN are sleep-independent, and that DLAN could serve as a control light paradigm for sleep research. In contrast, significant disturbances in sleep architecture were observed in Wistar rats. While the total amount of sleep was not impacted, chronic DLAN reduced the amplitude of REM sleep, NREM sleep, and slow wave activity (SWA) rhythms. It also disrupted the timing of sleep/wake cycles, with increased wakefulness and decreased sleep during the day, and the opposite pattern at night (Stenvers et al., 2016). Moreover, a decrease in nighttime plasma melatonin levels was consistently observed in animals producing melatonin (Fonken, Weil, et al., 2013b; Gutiérrez-Pérez et al., 2023; Jerigova et al., 2023; Molcan et al., 2019), aligning with the well-documented light-induced suppression of melatonin secretion (Zeitzer et al., 2000). Sleep was further impacted in young and aged C57BL/6JOlaHsd mice, with increased daytime wakefulness and weakened sleep rhythms. Chronic DLAN shifted young mice towards an aged sleep phenotype, while worsening existing sleep disturbances in older mice (Panagiotou & Deboer, 2020). Similar to the pattern observed with activity rhythms, these results suggest that DLAN disrupts sleep regulation, not by altering the total sleep duration, but by modifying its distribution, amplitude, and quality across the 24-hour cycle. According to the two-process model of sleep, the SCN primarily modulates the distribution and amplitude of sleep over the 24-hour cycle rather than the total amount of sleep (Borbély et al., 2016; Dijk & Czeisler, 1995; Mistlberger, 2005). If DLAN reduces the amplitude of circadian rhythms through its effects on the SCN, the observed alterations in sleep architecture likely reflect this dampened circadian drive (process C), while leaving homeostatic sleep pressure (process S) largely intact.

Cardiovascular Function. The impact of DLAN extends to cardiovascular regulation, with significant disruptions observed in key cardiac parameters. In male Wistar rats, 2 weeks of

DLAN attenuated the 24-hour rhythm in heart rate, systolic blood pressure, and spontaneous baroreflex sensitivity, a measure of autonomic cardiovascular control (Molcan et al., 2019). The study also revealed important changes in vascular reactivity, with a reduction in the daily variability in blood pressure response to norepinephrine, indicating altered sympathetic vascular control. At the molecular level, endothelial nitric oxide synthase (eNOS) expression was increased in arterial tissue, suggesting a compensatory vasodilatory mechanism, while endothelin-1 expression (a vasoconstrictor) remained unchanged (Thosar et al., 2018). However, when monitoring continued through 5 weeks of DLAN exposure, some cardiovascular parameters showed partial restoration of rhythmicity. This suggests a potential adaptation of the cardiovascular system to chronic DLAN conditions (Molcan et al., 2024).

Body Temperature. Studies have found that DLAN exposure significantly disrupts body temperature rhythms (**Table 1.4**). DLAN abolished daily rhythms in body temperature and decreased mean body temperature during the night in female Wistar rats (Gutiérrez-Pérez et al., 2023). In male Swiss-Webster mice, DLAN dampened and phase advanced body temperature rhythms, but did not affect the period length (Borniger et al., 2014).

Body Mass. The effects of DLAN exposure on weight gain are perhaps the most investigated, yet variable findings (**Table 1.4**). Multiple studies have reported increased body mass under chronic DLAN in Wistar rats, Swiss-Webster mice, C57BL/6J mice, and a mouse model of type 2 diabetes, with effects observed in both males and females (Aubrecht et al., 2015; Aubrecht et al., 2013; Borniger et al., 2014; Fonken, Aubrecht, et al., 2013; Fonken, Lieberman, et al., 2013; Fonken et al., 2014; Fonken, Weil, et al., 2013a; Fonken et al., 2010; Rumanova et al., 2025; Russart et al., 2019; Sarmiento et al., 2022). This increase was typically accompanied by elevated epididymal fat pad mass, a representative measure of WAT accumulation (Fonken, Lieberman, et al., 2013; Fonken et al., 2014; Fonken, Weil, et al., 2013a; Fonken et al., 2010). Importantly, the DLAN-induced increases in body mass showed both reversibility and preventability. Re-exposure to a standard light-dark (LD) cycle following DLAN reversed the

increases in body mass and fat pad mass (Fonken, Weil, et al., 2013a; Russart et al., 2019), while access to a running-wheel or day-restricted feeding prevented the reported gain (Fonken et al., 2014; Fonken et al., 2010). This suggests that exercise and the timing of food intake could be used as a preventive measure. Indeed, studies providing access to a running-wheel did not observe any weight gain under DLAN conditions (Borniger et al., 2013; Cleary-Gaffney & Coogan, 2018). On the other hand, several studies using similar protocols found no significant DLAN-induced changes in body mass in both young and aged animals across species (Borniger et al., 2013; Cleary-Gaffney & Coogan, 2018; Fonken et al., 2012; Gutiérrez-Pérez et al., 2023; Liu et al., 2022; Okuliarova et al., 2020; Stenvers et al., 2016). While the overall change in body mass was not affected, Gutiérrez-Pérez and colleagues (2023) did find an impaired growth curve in female Wistar rats during the five weeks of DLAN exposure.

Feeding & Drinking Behavior. Similar variability has been reported on the changes in timing and amount of food consumption (**Table 1.4**). While no changes in total caloric intake were observed, Swiss-Webster and C57BL/6J mice exposed to DLAN displayed increased daytime feeding, which is atypical for nocturnal animals (Fonken, Aubrecht, et al., 2013; Fonken, Lieberman, et al., 2013; Fonken et al., 2014; Fonken, Weil, et al., 2013a; Fonken et al., 2010). Interestingly, access to a running-wheel exacerbated food consumption (Fonken et al., 2014). Aubrecht and colleagues (2015) found a decrease in total food intake during weeks 5 and 6 of DLAN exposure. However, these results are ambiguous, as DLAN animals maintained consistent food intake, while controls increased their consumption during this period. The authors did not address potential causes for this shift in control animals (Aubrecht et al., 2015). In Wistar rats, one study observed no changes in food consumption (Okuliarova et al., 2020), while two others found a decrease in total and nighttime food intake (Gutiérrez-Pérez et al., 2023; Stenvers et al., 2016). Rumanova and colleagues (2025) did not observe changes in total food intake, but noted a weakening and temporal redistribution of feeding rhythms following 2 weeks of DLAN exposure. Moreover, drinking rhythms were suppressed and redistributed towards the day, with a reduction in the total water intake for Wistar rats (Rumanova et al.,

2025). These results underline inconsistencies in the impact of DLAN exposure on weight gain and feeding behavior, even within the same rodent species, and regardless of the length of DLAN exposure. Yet, it suggests a temporal shift in feeding and behavior, with a redistribution rather than an increase in overall consumption. The interaction between DLAN and high-fat diet (HFD) has been examined in multiple studies, revealing exacerbated effects on weight gain, metabolic dysfunction, and inflammation (Fonken, Lieberman, et al., 2013; Guan et al., 2024; Liu et al., 2024; Ren et al., 2025; Rumanova et al., 2025; Stenvers et al., 2016).

Indirect Calorimetry. Metabolic effects of DLAN have been further characterized through indirect calorimetry, which measures gas exchange to determine energy expenditure and substrate utilization (Ferrannini, 1988) (**Table 1.4**). In male Swiss-Webster mice, chronic DLAN reduced whole-body energy expenditure during the dim to light transition (around ZT0). It also reduced oxygen consumption and increased the respiratory exchange ratio (RER), indicating a preference for carbohydrate over fat metabolism independent of protein oxidation (Borniger et al., 2014). This alteration in fuel selection is significant because it suggests fundamental changes in metabolic regulation. It could also contribute to the adiposity increase observed in multiple DLAN studies (Eckel-Mahan & Sassone-Corsi, 2013).

Clinical Chemistry. DLAN exposure alters multiple biochemical parameters related to metabolism, with notable species-specific differences in glucose homeostasis (**Table 1.4**). In Swiss-Webster mice, blood glucose rhythms remained unaffected (Fonken, Aubrecht, et al., 2013; Fonken, Lieberman, et al., 2013), but glucose tolerance was impaired, as evidenced by elevated plasma glucose levels during glucose tolerance tests (Fonken, Lieberman, et al., 2013; Fonken, Weil, et al., 2013a; Fonken et al., 2010). Importantly, these alterations showed reversibility, with restoration of glucose tolerance after returning mice from DLAN to a standard LD cycle (Fonken, Weil, et al., 2013a). In contrast, Wistar rats showed a different pattern of glucose dysregulation. While baseline blood glucose concentrations were elevated following DLAN exposure (Gutiérrez-Pérez et al., 2023), glucose tolerance tests revealed no

significant impairment (Stenvers et al., 2016). This could be due to a potential difference in glucose handling between mice and rats under DLAN conditions (Kowalski & Bruce, 2014). Similarly, DLAN-induced alterations in insulin signaling showed species-specific patterns. Swiss-Webster mice exhibited elevated plasma insulin levels (Fonken, Lieberman, et al., 2013), while Wistar rats showed reduced insulin levels (Okuliarova et al., 2020), but impaired insulin tolerance, as evidenced by elevated plasma glucose levels during the insulin tolerance test (Gutiérrez-Pérez et al., 2023). Plasma insulin levels were further reduced in C57BL/6 mice, and negatively associated with learning performance (Liu et al., 2023). Additionally, in a mouse model of type 2 diabetes, DLAN further impaired both glucose and insulin tolerance beyond the diabetic phenotype, but re-exposure to a standard LD cycle abolished these differences (Russart et al., 2019). Clinical chemistry analysis in Wistar rats revealed no changes in overall plasma triacylglycerols (TAG), total cholesterol, low-density lipoprotein (LDL) cholesterol, free fatty acid (FFA), and thyroid hormone levels (Okuliarova et al., 2020). However, DLAN exposure decreased plasma leptin concentrations, nighttime TAG levels, and hepatic TAG content (Gutiérrez-Pérez et al., 2023; Okuliarova et al., 2020).

Table 1.4. Effects of DLAN exposure on metabolism in rodents. The duration of DLAN exposure and the age of the animals are reported in weeks (w). TALLYHO/JngJ mice are a polygenic model of type 2 diabetes mellitus. Effects are expressed as an increase (↑), a reduction (↓), an alteration (Δ), or no change (Ø). TAG = triacylglycerols, LDL = low-density lipoprotein, FFA = free fatty acid.

Species	Night light	Day light	LD cycle	DLAN duration	Sex	Age	Metabolism	Reference
Swiss Webster mouse	5 lux	150 lux	14:10	2w	♂	8w	↑ body mass Ø total food intake ↓ body temperature rhythms Δ body temperature acrophase Ø body temperature period ↓ oxygen consumption ↑ respiratory exchange ratio ↓ energy expenditure	Borniger et al., 2014
				3w	♂	8w	↑ body and epididymal fat pad mass ↑ daytime food intake	Fonken et al., 2014
				4w	♂	8w	↑ body mass Ø total food intake ↑ daytime food intake Ø blood glucose	Fonken, Aubrecht et al., 2023
				4w	♂	8w	↑ body and epididymal fat pad mass Ø total food intake ↑ daytime food intake Ø fasting blood glucose ↓ glucose tolerance ↑ daytime blood insulin	Fonken, Lieberman et al., 2013
				4w	♂	8w	↑ body and epididymal fat pad mass Ø total food intake ↑ daytime food intake ↓ glucose tolerance	Fonken et al., 2013a
				8w	♂	?	Ø body mass	Borniger et al., 2013
				8w	♂	8w	↑ body mass Ø adrenal gland mass	Aubrecht et al., 2013
			16:8	6w	♀	8w	↑ body mass ↓ total food intake	Aubrecht et al., 2015
				8w	♂	8w	↑ body and epididymal fat pad mass Ø total food intake ↑ daytime food intake ↓ glucose tolerance	Fonken et al., 2010
Nile grass rat (diurnal)	5 lux	150 lux	14:10	3w	♂	10w	Ø body mass Ø reproductive tissue mass	Fonken et al., 2012
Wistar rat	2 lux	150 lux	12:12	2w	♂	?	Ø body, WAT, adrenal, thymus mass ↓ total food intake ↓ nighttime food intake ↓ total energy expenditure ↓ nighttime energy expenditure Ø glucose tolerance	Stenvers et al., 2016
				2w	♂	?	↑ body mass Ø fat, lean mass ↓ feeding rhythms ↓ nighttime food intake ↑ daytime food intake ↓ drinking rhythms ↓ total water intake ↓ nighttime water intake ↑ daytime water intake	Rumanova et al., 2025
				5w	♂	18w	Ø body and epididymal fat pad mass Ø visceral fat Ø total food intake Ø blood glucose ↓ blood insulin ↑ liver TAG Ø blood TAG, cholesterol, LDL cholesterol, FFA ↓ blood leptin Ø blood thyroid hormones	Okuliarova et al., 2020
	5 lux	250 lux	12:12	5w	♀	7w	Ø body mass Δ growth curve ↓ total food intake ↓ nighttime food intake ↑ fasting blood glucose ↓ insulin resistance ↑ nighttime blood TAG	Gutiérrez-Pérez et al., 2023
C57BL/6	5 lux	150 lux	12:12	3w	♀♂	10w	Ø body mass	Cleary-Gaffney & Coogan, 2018
				3w	♂	3w	↓ plama insulin	Liu et al., 2023
				1m	♂	3w	↑ body mass	Sarmiento et al., 2022
				24w	♀♂	20w	Ø body mass Ø spleen mass ↑ adrenal gland mass in males	Liu et al., 2022
TALLYHO/ JngJ mouse				8-10w	♂	6w	↑ body mass ↓ glucose tolerance ↓ insulin tolerance	Russart et al., 2019

Learning & Memory. Limited evidence supports the vulnerability of learning and memory functions to DLAN (**Table 1.5**). Spatial learning in the Barnes maze, a hippocampus-dependent cognitive task, was unaffected in C3H/HeNHsd mice (Fonken & Nelson, 2013), but impaired in the diurnal Nile grass rat (Fonken et al., 2012). Similarly, learning and memory impairment in the novel object recognition (NOR) test was observed in C57BL/6J mice (Liu et al., 2023), but not in Swiss-Webster mice (Aubrecht et al., 2013). No changes were found in the Y-maze and passive avoidance tests suggesting that cognitive impact may be task-specific (Aubrecht et al., 2013). These findings indicate that the effects of DLAN on cognitive performance vary by species, with diurnal animals potentially showing greater sensitivity. Additionally, the timing of cognitive testing might be an important factor in the assessment of DLAN-induced changes in learning and memory, though this was not systematically reported.

Mood. The evidence supporting the impact of DLAN exposure on mood is inconsistent within and across species (**Table 1.5**). Stress and anxiety phenotypes were investigated at the physiological and behavioral level. Changes in glucocorticoids varied between studies. In fact, plasma cortisol and corticosterone levels were either not impacted (Aubrecht et al., 2013; Bedrosian et al., 2011; Fonken et al., 2010), reduced (Bedrosian, Galan, et al., 2013), or elevated under DLAN (Fonken et al., 2012). DLAN animals showed either no anxiety phenotype in the EPM, or reduced anxiety in the EPM and in the open field (OF) test. This was evidenced by increased time in the open arms of the EPM, as well as a reduced rearing behavior and increased time spent in the center in the OF (Aubrecht et al., 2013; Bedrosian et al., 2011; Gutiérrez-Pérez et al., 2023; Hogan et al., 2015; Molcan et al., 2019). However, they displayed an anxiety phenotype in the LD box, as indicated by increased latency to enter the light side (Aubrecht et al., 2013). Variation in adrenal gland mass serves as an indicator of stress response activation in rodent models (Herman et al., 2016). Age-dependent differences in adrenal gland mass have been reported, with aged male C57BL/6 mice showing an increase (Liu et al., 2022), while young male Swiss-Webster mice did not exhibit such changes (Aubrecht et al., 2013). Overall, DLAN produced inconsistent effects on anxiety-like behaviors across different assessment

methods and species. The effects of DLAN on depression-like behaviors are more consistent. Depression phenotypes in the forced swim test and sucrose preference test were observed in the majority of studies (Aubrecht et al., 2013; Bedrosian et al., 2011; Bedrosian, Weil, et al., 2013; Fonken et al., 2012; Fonken & Nelson, 2013; Gutiérrez-Pérez et al., 2023; Hogan et al., 2015), but not in others (Cleary-Gaffney & Coogan, 2018; Hogan et al., 2015). Re-exposure to a standard LD cycle following chronic DLAN allowed for the reversal of such phenotype (Bedrosian, Weil, et al., 2013).

Hippocampal Morphology. Neuroinflammation and changes in hippocampal circuitry have been associated with stress and depression (Dantzer et al., 2008) (**Table 1.5**). Though highly variable, changes in hippocampal cell morphology were consistently reported under DLAN conditions. A reduction in the spine densities of CA1 neurons was observed in some studies (Aubrecht et al., 2013; Bedrosian et al., 2011; Bedrosian, Weil, et al., 2013; Hogan et al., 2015; Liu et al., 2023). This reduction was reversible upon return to standard LD conditions (Bedrosian, 2013a). In most studies, no changes in CA1 dendrite length, cell body perimeter, or area were reported (Aubrecht et al., 2013; Bedrosian et al., 2011; Fonken et al., 2012; Hogan et al., 2015), with only one study noting a reduction in basal dendrite length (Fonken et al., 2012), and another in cell body area (Hogan et al., 2015). This suggests that the connectivity of CA1 neurons was primarily impacted, rather than its cell size. A reduction in CA3 and dentate gyrus (DG) neuronal density was observed in mice (Aubrecht et al., 2013; Liu et al., 2023), but not in hamsters (Bedrosian et al., 2011). This was accompanied by an increase in CA3 cell body area (Aubrecht et al., 2013), and a decrease in DG dendrite length (Fonken et al., 2012). Additionally, an acute exposure of only 4 days of DLAN reduced hippocampal vascular density in the CA1, CA3, and DG regions, with sex-specific changes (Bumgarner et al., 2023). This effect was further characterized under chronic DLAN, with reduced levels of hippocampal vascular endothelial growth factor (VEGF) (Aubrecht, 2013). DLAN promoted neuronal apoptosis, as evidenced by elevated *Bax*, *Bcl2*, and *Bcl-xl* hippocampal expression, as well as elevated Caspase-3/p17/p19 levels in the CA3 region (Liu et al., 2023). This was accompanied

by a decrease in NeuN-positive cells, indicating neuronal loss (Liu et al., 2023). Moreover, a decrease in the cell proliferation marker Ki-67 was observed in the DG region (Cleary-Gaffney & Coogan, 2018). While the effects of DLAN exposure on hippocampal cell morphology are highly variable, when observed, studies found positive associations between these changes and depression phenotypes exhibited in the forced swim test and the sucrose preference test (Bedrosian, Weil, et al., 2013; Fonken et al., 2012). Interestingly, administration of a TNF inhibitor, XPro1595, prevented the depression phenotype in the forced swim test, but not changes in hippocampal cell morphology (Bedrosian, Weil, et al., 2013).

Hippocampal Inflammation. Hippocampal proinflammatory cytokines were minimally impacted under DLAN conditions (**Table 1.5**). Tumor necrosis factor (TNF) expression was either increased (Bedrosian, Weil, et al., 2013; Hogan et al., 2015), or unaffected by DLAN (Aubrecht et al., 2013; Fonken & Nelson, 2013). Interleukin-1 beta (IL1β) and interleukin-6 (IL6) gene expression levels were unaltered across studies (Bedrosian, Weil, et al., 2013; Fonken & Nelson, 2013; Hogan et al., 2015). Despite minimal effects on inflammatory markers, brain-derived neurotrophic factor (BDNF) expression was consistently reduced in the hippocampus following DLAN exposure (Bedrosian, Weil, et al., 2013; Fonken & Nelson, 2013). BDNF supports neuronal survival, differentiation, and synaptic plasticity, with important roles in learning, memory, and mood regulation (Bramham & Messaoudi, 2005). Beyond neurotrophic factors, DLAN reduced the hippocampal expression levels of insulin signaling molecules, including phosphorylated AKT (pAKT), phosphorylated GSK3β (pGSK3β), and β-catenin, while phosphorylated IRS1 (pIRS1) remained unaffected (Liu et al., 2023). Complementary in vitro experiments using HT22 hippocampal cells demonstrated that insulin treatment ameliorated DLAN-induced hippocampal neuronal apoptosis via the IR/AKT/pGSK3β/β-catenin pathway, suggesting impaired insulin signaling as another potential mechanism contributing to DLAN's neural effects (Liu et al., 2023). Together, these findings provide some evidence for a broad inflammatory activation and impaired neurogenesis

in response to DLAN exposure. However, it suggests that DLAN may impact neural plasticity independently from hippocampal inflammation (McEwen et al., 2016).

Hypothalamic & Peripheral Inflammation. The effects of DLAN on inflammatory processes outside the hippocampus show a mixed pattern (**Table 1.5**). In the hypothalamus, classical inflammatory cytokines showed no response to DLAN exposure, with no detectable changes in TNF, IL6, or IL1β expression (Fonken, Lieberman, et al., 2013). Similarly, molecular markers of inflammatory signaling pathways remained unchanged, including the macrophage marker MAC1, the NF-κB pathway gene Ikbkb, and the neuropeptide precursor POMC (Fonken, Lieberman, et al., 2013). POMC neurons in the hypothalamus are particularly important for coordinating stress responses and regulating feeding behavior (Krude & Grüters, 2000). Despite the absence of cytokine changes, subtle microglial alterations were observed. While Iba1 immunoreactivity was not impacted, the number of Iba1-positive cells increased (Fonken, Lieberman, et al., 2013). This dissociation between microglial presence and lack of inflammatory cytokine expression suggests that DLAN may alter microglial distribution or proliferation in the hypothalamus without triggering a complete inflammatory response (Wolf et al., 2017). In peripheral tissues, inflammation was observed in WAT. Gene expression analysis revealed elevated MAC1 levels (Fonken, Lieberman, et al., 2013), indicating increased macrophage activation under DLAN conditions. TNF was also elevated in WAT (Fonken, Lieberman, et al., 2013), but not in epididymal fat pad specifically (Fonken, Weil, et al., 2013a), while IL6 remained unchanged in either tissue. No inflammatory changes were observed in the liver (Fonken, Lieberman, et al., 2013). These findings suggest that DLAN induces tissue-specific inflammatory responses.

Table 1.5. Effects of DLAN exposure on learning, mood and immune function in rodents. The duration of DLAN exposure and the age of the animals are reported in weeks (w) and months (m). TALLYHO/JngJ mice are a polygenic model of type 2 diabetes mellitus. Effects are expressed as an increase (↑), a reduction (↓), or no change (Ø). EPM = elevated-plus maze, NOR = novel object recognition, OF = open field.

Species	Night light	Day light	LD cycle	DLAN duration	Sex	Age	Results		Reference
							Mood & Learning	Immune Function	
Swiss Webster	5 lux	150 lux	14:10	4d	♀♂	7w		↓ hippocampal vascular density (CA1, CA3, DG)	Bumgarner et al., 2023
				4w	♂	8w		Ø hypothalamic inflammation () ↑ hypothalamic microglia (Iba1 positive cells) Ø hypothalamic microglial activation (Iba1 immunoreactivity) Ø hepatic inflammation ↑ WAT inflammation (TNF, MAC1)	Fonken, Lieberman, et al., 2013
				4w	♂	8w		↑ epididymal fat inflammation (MAC1) Ø epididymal fat inflammation (TNF,	Fonken, Weil, et al., 2013
				8w	♂	8w	Ø blood corticosterone Ø anxiety (EPM) ↓ anxiety (OF) ↑ anxiety (LD box) ↑ depression (forced swim) Ø learning (NOR, Y-maze,	Ø hippocampal inflammation (TNF) ↓ hippocampal vascular density (VEGF) Ø hippocampal neuronal density (CA1 apical and basilar spine, CA3 apical spine) ↓ hippocampal neuronal density (CA3	Aubrecht et al., 2013
				8w	♂	8w	Ø blood corticosterone		Fonken et al., 2010
Siberian hamster	5 lux	150 lux	16:8	4w	♀	8w	↑ anhedonia ↑ depression (forced swim)	↓ hippocampal neuronal density (CA1 apical spine) ↓ hippocampal BDNF ↑ hippocampal inflammation (TNF)	Bedrosian, Weil, et al., 2013
				?	♀	8w	↓ blood cortisol		Bedrosian, Galan et al., 2013
				8w	♀	8w	Ø plasma cortisol ↓ anxiety (EPM) ↑ anhedonia ↑ depression (forced swim)	↓ hippocampal neuronal density (CA1 apical and basilar spine) Ø CA1 dendrite length, cell body area and perimeter Ø CA3, DG neurons	Bedrosian et al., 2011
Nile grass rat (diurnal)	5 lux	150 lux	14:10	3w	♂	10w	↑ blood corticosterone ↑ anhedonia ↑ depression (forced swim)	Ø hippocampal spine density, cell body area and perimeter ↓ CA1 and DG basilar dendrite length	Fonken *et al.* , 2012
Wistar rat	5 lux	250 lux	12:12	5w	♀	7w	Ø anxiety (EPM) ↓ anxiety (OF) ↑ anhedonia		Gutiérrez-Pérez et al., 2023
C57BL/6 mouse	5 lux	150 lux	12:12	3w	♀♂	10w	Ø anhedonia Ø depression (forced swim, tail suspension) Ø anxiety (EPM)	↓ DG cell proliferation (Ki-67)	Cleary-Gaffney & Coogan, 2018
				3w	♂	3w	↓ learning (NOR)	↓ hippocampal neuronal density (CA1, CA3, DG) ↑ neuronal loss (↓ NeuN-positive cells) ↑ hippocampal apoptosis (Bax, Bcl2, Bcl-xl, Caspase-3/p17/p19) ↓ insulin signaling molecules in hippocampus (pAKT, pGSK3β, β-catenin) Ø insulin signaling molecules in	Liu et al., 2023
C3H/HeNHsd mouse	5 lux	150 lux	14:10	4w	♂	8w	↓ anxiety (OF) Ø anxiety (EPM) ↑ anhedonia Ø depression (forced swim)	↑ hippocampal inflammation (TNF) Ø hippocampal inflammation (IL1β, IL6) ↓ hippocampal neuronal density (CA1 apical and basilar spine) Ø CA1 dendrite length	Hogan et al., 2015
	5 lux	150 lux	16:8	4w	♂	8w	↑ anhedonia ↑ depression (forced swim)	↓ hippocampal BDNF Ø hippocampal inflammation (TNF, IL1β)	Fonken & Nelson, 2013

Recovery & Survival. Multiple studies have examined the impact of DLAN on the recovery and survival of healthy and impaired animals, revealing consistent detrimental effects across different physiological contexts. DLAN exposure impaired dermal wound healing in female C57BL/6 mice, which is likely associated with a disruption in adaptive immune function (Walker et al., 2019). In models of acute injury, DLAN significantly compromised recovery. Animals housed under DLAN after undergoing ischemic stroke showed increased stroke lesion size, elevated pro-inflammatory responses, sensorimotor deficits, and higher mortality (J. Liu et al., 2022; Liu et al., 2024; Weil et al., 2020). Similarly, animals housed under DLAN following an induced cardiac arrest exhibited increased mortality rates, heightened pro-inflammatory responses, hippocampal damage, and weight loss (Fonken et al., 2019). Moreover, chronic DLAN exposure reduced lifespan in aged C57BL/6 females (Liu et al., 2022), and young TALLYHO/JngJ mice, a polygenic model of type 2 diabetes mellitus (Russart et al., 2019). These findings indicate that DLAN exposure can significantly impair physiological resilience and survival.

Reproductive Function. DLAN exposure can disrupt female reproductive physiology. A study in Wistar rats reported significant disruptions in estrous cycling under chronic DLAN, with all studied animals exhibiting irregular cycles with persistent estrus, as indicated by the predominance of cornified cells in vaginal cytology (Gutiérrez-Pérez et al., 2023). Reproductive disruption is particularly significant since the estrous cycle in rodents is regulated by circadian clock genes and is sensitive to disruptions in circadian rhythms (Miller & Takahashi, 2014).

Transgenerational Effects. Emerging evidence suggests that parental exposure to DLAN can have profound and lasting impacts on offspring physiology, extending beyond immediate environmental conditions. Maternal exposure to DLAN during pregnancy disrupted hormonal and metabolic rhythms in rat offspring. Specifically, DLAN altered plasma melatonin rhythms during early postnatal stages, and interfered with the developmental trajectories of

corticosterone, thyroid hormones, glucose, and cholesterol rhythms during early life, suggesting that prenatal DLAN can disturb endocrine and metabolic programming (Dzirbíková et al., 2022). Moreover, a 9-week exposure to DLAN prior to mating impacted the adaptive immunity of Siberian hamster offspring. In fact, DLAN altered offspring splenic melatonin and glucocorticoid receptor expression, and enhanced antibody production to a novel antigen, keyhole limpet hemocyanin (KLH), as a measure of humoral immune response. It also reduced the delayed type hypersensitivity (DTH), characteristic of T-cell mediated immune response (Cissé, Russart, et al., 2017). Interestingly, these effects showed variability not only by offspring sex, but also by whether exposure occurred in the mother, the father, or both parents. These findings suggest that parental DLAN exposure has transgenerational effects on endocrine, metabolic, and immune function. While epigenetic changes have not been investigated, they could provide a molecular basis for how parental DLAN exposure might permanently alter offspring physiology without direct exposure.

Development. Investigations into the development-specific effects of DLAN have revealed significant windows of vulnerability. Juvenile C57BL/6J mice exposed to 2 weeks of DLAN during early life (PND10-24) or adolescence (PND30-44) showed no immediate changes in anxiety or depression phenotypes (Chen et al., 2021). Strikingly, distinct physiological alterations only emerged in adulthood, with adolescent DLAN exposure inducing a modest anxiety phenotype in females, and depression in both sexes, despite returning to standard LD conditions. Females also exhibited an enhanced hippocampal cytokine response (IL1β) following peripheral lipopolysaccharides (Burkhart & Phelps). These findings suggest that animals are particularly susceptible to developmental DLAN disruptions during adolescence, with females displaying heightened vulnerability. Cissé and colleagues (2017) further compared the effects of 4 weeks of DLAN exposure beginning at either 3 weeks (early adolescence) or 5 weeks of age (late adolescence) in adult Swiss-Webster mice. While locomotor activity, fasting glucose, glucose tolerance, and hepatic clock gene expression remained unchanged, age-specific metabolic and behavioral alterations emerged. Mice exposed

to DLAN at 5 weeks exhibited increased body mass (males), and enhanced gonadal fat (both sexes), while those exposed at 3 weeks showed no significant changes. Conversely, exposure beginning at 3 weeks increased daytime feeding in both sexes without altering total intake, whereas exposure from 5 weeks only shifted male feeding patterns (Cissé, Peng, et al., 2017). These findings underscore specific developmental windows of susceptibility to DLAN, with feeding behavior being more vulnerable during early adolescence, and body composition during later adolescence. Epigenetic modifications, such as changes in DNA methylation patterns within the SCN (Azzi, 2014), could explain the observed lasting effects on immune, endocrine, and metabolic function. It is worth noting that the previously cited study by Liu and colleagues (2023) initiated DLAN exposure during adolescence (3 weeks of age) without specifically framing their research as developmental studies (Liu et al., 2023). While they focused on outcomes rather than developmental windows, their findings on hippocampal insulin signaling, apoptosis, and morphology may reflect both the immediate effects of DLAN and the consequences of exposure during a sensitive neurodevelopmental period. However, as described in the previous sections, the outcomes of early life and adolescent DLAN exposure mirror those reported under adulthood exposure.

Conclusion. This is, to date, the most comprehensive review of the effects of DLAN in rodents. It reveals that DLAN produces widespread, yet nuanced effects in various rodent models, both at the molecular, physiological, and behavioral level. The most consistent findings include disruption of molecular circadian rhythms in peripheral tissues, altered temporal distribution of activity, sleep, and feeding rhythms, metabolic dysregulation, increased depression phenotypes, and compromised recovery from injuries or disease challenges. The magnitude and specific manifestations of these effects vary considerably by species, strain, sex, and developmental stage, with certain populations showing heightened vulnerability.

Limitations. Despite the number and range of studies covered in this review, several important limitations should be considered when interpreting these findings. To start, 70% (28/40) of the

reviewed DLAN literature originates from a single research group, introducing potential investigator biases. While the reviewed studies employ diverse rodent models, they possess inherent differences in light sensitivity that should be noted. About half of the studies used albino strains, including Swiss-Webster mice, CD1 mice, and Wistar rats, which lack melanin in the iris and retinal pigment epithelium, and consequently experience greater retinal light exposure than pigmented strains (Peirson et al., 2018). This heightened sensitivity could amplify DLAN effects, and may not accurately represent responses that are generalizable to other species. Moreover, only ~ 30% of the studies employed females, with 7/40 studies looking at both sexes. This lack of inclusion further complicates the interpretation and direct comparison of findings. Finally, substantial variation exists in exposure parameters, including dim light intensity (2-20 lux), daytime light intensity (130-300 lux), the ratio between day and night light, and the duration of exposure (acute vs chronic). Studies also employ different baseline LD cycles (12:12, 14:10, or 16:8), introducing additional variability. The diversity of measures employed further complicates direct comparisons. Specifically, the timing of measurements relative to circadian phase was inconsistently reported, potentially confounding results for parameters with strong daily rhythms.

1.2.4. Dim Light in the Evening

For most individuals, light exposure is concentrated in the evening hours before sleep, rather than continuously throughout the night. As such, the DLAN model may not reflect the most common pattern of light exposure in humans. This suggests that an evening-specific paradigm would be a more translationally relevant model to investigate. To address this limitation, our laboratory developed the dim light in the evening (DLE) paradigm (Tam et al., 2021). The DLE protocol comprises a standard 12-hour light phase at 200 lux, followed by a 4-hour evening light period at 20 lux, and an 8-hour dark phase. It was designed to parallel human studies conducted in non-laboratory settings (Wright et al., 2013), which reported that approximately 3-4 hours of 20-30 lux artificial lighting exposure disrupted sleep and circadian rhythms.

In our initial characterization of DLE effects, we demonstrated that 2 weeks of 4-hour, 20-lux DLE exposure produces a phase delay of approximately 2-3 hours in C57BL/6J mice, comparable to effects reported in humans (Tam et al., 2021). This phase shift was evident in several physiological and behavioral measures, including locomotor activity rhythms, sleep patterns, and molecular clock rhythms in peripheral tissues. Importantly, these phase shifts persisted in constant darkness, confirming that they represent changes in the circadian system rather than masking effects of light. The molecular basis of the DLE effects was investigated through analysis of clock gene expression in the heart, liver, adrenal gland, and dorsal hippocampus. DLE exposure delayed the phase of multiple core clock genes, including *Bmal1*, *Per2*, *Reverb*, *Cry1*, and *Dbp*. Additionally, analysis of brain cFos expression revealed that DLE attenuated the daily rhythm in SCN activity, while simultaneously reversing activity patterns in the medial prefrontal cortex.

Beyond circadian phase shifts, DLE induced notable changes in sleep architecture. While total sleep duration remained unchanged, DLE significantly altered the temporal distribution of sleep, with increased sleep during the dim evening period and decreased sleep in the first hours of the following light phase. These findings mirror human studies showing that evening light exposure can delay sleep onset and increase morning sleepiness (Cain et al., 2020; Chang et al., 2015). DLE also reversed the diurnal pattern of short-term recognition memory performance. Under standard lighting conditions, mice exhibited better object and odor recognition at ZT2 (early in the light phase) compared to ZT14 (early in the dark phase). Following DLE exposure, this pattern was inverted, with improved performance at ZT14 and reduced performance at ZT2. This behavioral change was strongly correlated with preceding sleep history, suggesting that DLE-induced alterations in sleep patterns directly impacted cognitive function.

Mechanistically, the DLE effects appear to involve a coordinated realignment of central and peripheral oscillators. These findings thus establish DLE as a translationally relevant model for studying the effects of evening light exposure on circadian physiology and behavior. However,

further investigation into the acute and chronic consequences of DLE, as well the underlying mechanisms, is needed to comprehensively characterize the extent of its effects.

1.2.5. Long Photoperiod

One may question how exposing mice to DLE differs from a natural summer day. Indeed, summer days typically provide about 16 hours of light exposure, and are associated with a weakening of SCN neuronal synchrony, notably between VIP-expressing core neurons and AVP-expressing shell neurons, and an alteration of phase-resetting responses (Porcu et al., 2018; Ramkisoensing et al., 2014; VanderLeest et al., 2007). This desynchronization is accompanied by changes in clock gene expression patterns, with *Per1* and *Per2* showing altered amplitude and phase across SCN subregions (Johnston et al., 2005; Messager et al., 1999). Living under constant summer days thus has disruptive effects on circadian organization. However, these effects typically differ from the adverse health outcomes linked to evening artificial light exposure. We argue that DLE differs qualitatively from summer evenings or long photoperiods, with important differences in light intensity dynamics, physiological effects, and behavioral outcomes.

The primary distinction between DLE and long photoperiods lies in the amplitude of light fluctuation. As light intensity in the summer can reach over 50,000 lux at midday, long photoperiods are typically reproduced in a laboratory setting using a constant 16-hour bright light. In contrast, our DLE protocol sets daylight at 200 lux, and only decreases it by a 10-fold in the evening. In that way, the absence of high-intensity daylight makes dim evening light much more impactful. Indeed, Wright and colleagues (2013) showed that exposure to a lower amplitude electrical light during the day delays melatonin and sleep phase compared to a natural summer day (Wright et al., 2013).

To directly examine the differences between DLE and long photoperiods, we compared locomotor activity rhythms and sleep patterns under DLE and 16:8 LD (16h 200 lux:8h 0 lux)

conditions (Tam et al., 2021). Our findings revealed substantial differences in circadian entrainment between these lighting protocols. Under 16:8 LD, activity onsets and midpoints were further delayed by ~ 2h and ~ 1h, respectively, relative to DLE. Additionally, sleep patterns showed more pronounced changes under 16:8 LD, with mice sleeping more during ZT8-16 and ZT20-24, but sleeping less during ZT0-4, compared to DLE conditions.

These differences suggest that while DLE and long photoperiods both extend light exposure, long photoperiods appear to induce more substantial phase shifts and alterations in sleep architecture. The distinct effects of DLE highlight the importance of both light intensity and timing in determining circadian responses. Rather than simply extending the photoperiod, DLE represents a unique form of circadian disruption characterized by the absence of bright daylight and an inappropriate light exposure during the evening. As such, DLE appears to represent a more accurate model of contemporary light exposure.

1.3. Aims

This thesis aims to investigate how DLE exposure impacts circadian physiology and behavior in mice. While the disruptive effects of bright light throughout the night have been well documented, the research regarding the consequences of exposure to dim light during the early evening period remains limited. This thesis thus examines the effects, mechanisms, and potential mitigation strategies for DLE exposure (**.. 1.9**).

1.3.1. Characterization of Chronic Dim Light in the Evening Effects

Chapter 2 aims to characterize the chronic effects of DLE on circadian physiology and behavior in mice, building upon our initial findings on acute DLE exposure. Specifically, this chapter addresses the effects of a 12-week DLE exposure on a) activity, b) sleep, c) body temperature, d) clinical blood chemistry, e) stress hormones, f) anxiety behavior, and g) cognitive performance. It investigates potential differences between acute and chronic exposure

to DLE, as well as whether males and females respond differently to this disrupted lighting condition.

1.3.2. Mechanisms of Dim Light in the Evening Effects

Chapter 3 seeks to elucidate the mechanisms through which DLE affects physiology and behavior in mice. This chapter addresses the distinct contribution of circadian disruption and changes in sleep distribution during the dim phase, and investigates whether the phase-delaying effects of DLE represent true entrainment or masking responses that disappear in constant conditions.

1.3.3. Mitigation of Dim Light in the Evening Effects

Finally, **Chapter 4** explores potential strategies to attenuate the effects of DLE on activity rhythms in mice. This chapter examines a) whether increasing daytime light intensity can reduce the phase-delaying effects of DLE by enhancing the contrast between day and evening light levels. It also investigates b) whether filtering short-wavelength light during the evening attenuates DLE effects, and whether this effectiveness depends on the overall light intensity. Additionally, this chapter tests c) whether targeted stimulation of specific photoreceptors through violet light supplementation can counteract the phase-delaying effects of DLE.

Together, these aims provide a comprehensive investigation of DLE, from characterization to mechanisms and intervention, with the overarching goal of understanding how modern artificial light environments affect circadian biology, and identifying potential strategies to mitigate any adverse effects.

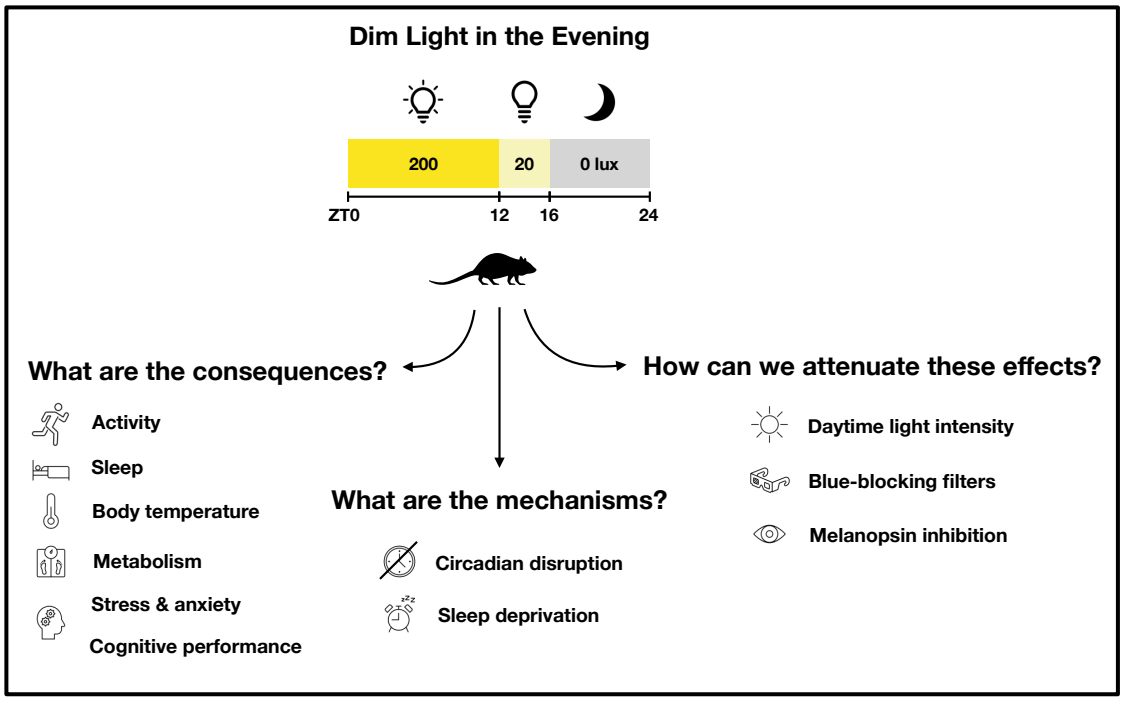

Figure 1.9. Schematic overview of the aims of the thesis. This project investigates the effects of dim light in the evening (DLE; ZT12–ZT16) on circadian rhythms. It addresses 1) the consequences, 2) mechanisms, and 3) potential interventions to attenuate these effects.

Chapter 2. Consequences of Extended Dim Light in the Evening

2.1. Introduction

The preceding chapter established DLE as a translationally relevant model for studying the effects of evening artificial light exposure on circadian physiology and behavior. Our initial characterization demonstrated that a 2-week exposure to DLE produces significant alterations in activity, sleep, and molecular rhythms, and affects cognitive performance (Tam et al., 2021). However, in the modern environment, humans are typically exposed to evening artificial lighting throughout their lives rather than for brief periods. This chronic exposure raises important questions about potential adaptation, accumulation of effects, or emergence of novel physiological consequences that may not be apparent during shorter exposures.

While our initial investigation uncovered the effects of acute exposure, the consequences of extended DLE remain unknown. Chronic circadian disruption has been associated with a wide range of adverse health outcomes, including metabolic dysfunction, cognitive impairment, mood disorders, and compromised immune function (Bass & Takahashi, 2010; Johnston et al., 2016; Marcheva et al., 2013; Panda, 2016; Serin & Acar Tek, 2019). However, most studies have employed more severe disruption paradigms, such as constant light or jet lag. This chapter therefore examines the effects of a 12-week exposure to DLE on circadian rhythms and its associated physiological and behavioral parameters through a comprehensive phenotyping screen.

Home cage activity and sleep are fundamental outputs of the circadian system and serve as key indicators of circadian entrainment and disruption in mice. Locomotor activity exhibits robust 24-hour rhythms with characteristic metrics, including period length, amplitude, phase, power, and stability (Brown et al., 2019). Sleep, while regulated by both circadian and homeostatic processes, shows distinct temporal patterns, with approximately 60-70% occurring during the light phase (Brown et al., 2016). Body temperature follows a robust circadian rhythm that is

closely tied to the sleep/wake cycle. Its daily oscillation, typically ranging 1-2 °C in mice, is orchestrated by the SCN in concert with peripheral clocks throughout the body, and peaks during the night when mice are most active (Refinetti & Menaker, 1992). Measuring activity, sleep, and body temperature rhythms thus provides direct insights into the effects of disruptive light schedules on the circadian system.

These primary circadian outputs are intimately connected with metabolic regulation, with bidirectional interactions that synchronize energy production and utilization with the sleep/wake cycle. The relationship between metabolism and circadian rhythms is further reflected in the daily fluctuations of various metabolites in mice. Glucose, the primary cellular energy source and a key regulator of insulin secretion, exhibits clear diurnal variations (Kalsbeek et al., 2014; Qian & Scheer, 2016). Glucose levels in mice typically peak during the dark phase, coinciding with their active feeding period (la Fleur et al., 2001; Rudic et al., 2004). Lactate, a product of anaerobic glycolysis, fluctuates with activity levels and glucose utilization, peaking during the dark phase (Naylor et al., 2012). Glycerol, a component of triglycerides involved in gluconeogenesis and glycolysis, is a key indicator of lipolysis and an important energy substrate during fasting. Glycerol concentrations generally rise during the light phase when mice are mostly inactive and fasting, peaking near the light-to-dark transition as lipolysis increases to prepare for the active phase (Shostak et al., 2013). Total cholesterol and its high-density lipoprotein (HDL), crucial for cell membrane structure, function, and steroid hormone synthesis, also show circadian patterns (Gooley & Chua, 2014). HDL specifically plays a role in reverse cholesterol transport, removing excess cholesterol from peripheral tissues (Gordon et al., 2015; Lee-Rueckert et al., 2016). Cholesterol synthesis rates, influenced by feeding cycles, are highest during the dark phase, with total and HDL cholesterol levels peaking in the early light phase (He et al., 2021). Similarly, triacylglycerols (TAG), the main form of stored energy in adipose tissue and a transport form of fatty acids, display diurnal variations connected to feeding patterns, with their synthesis mirroring food intake, and highest concentration during the light phase (Adamovich et al., 2014; Pan & Hussain, 2009). These

oscillating metabolic parameters serve as sensitive indicators of potential disruption in peripheral clocks.

Beyond metabolic parameters, circadian disruption can also impact stress responses and anxiety behaviors. To assess these effects, we employed three complementary and widely used behavioral assays for rodents: the elevated-plus maze (EPM), the open field (OF), and the light-dark (LD) box. The EPM is based on rodents' innate fear of open and elevated spaces (Komada et al., 2008; Pellow et al., 1985; Rodgers & Dalvi, 1997; Walf & Frye, 2007). It consists of two open arms and two closed arms arranged in a cross shape and elevated above the floor. Increased time and entries in closed arms indicates higher anxiety behavior. The OF test consists of a large open arena, and is further used as a measure of open space-induced anxiety (Gould et al., 2009; Kraeuter et al., 2019; Seibenhener & Wooten, 2015; Walsh & Cummins, 1976). Decreased overall activity and increased thigmotaxis, or wall-hugging behavior, indicates higher anxiety. On the other hand, the LD box utilizes the natural aversion of mice to brightly illuminated areas to assess anxiety (Bourin & Hascoët, 2003; Crawley & Goodwin, 1980). It consists of two compartments: one lit and one dark area. Increased time spent in the dark area and fewer LD transitions suggest higher anxiety behavior. These tests provide complementary information about an array of anxiety behaviors in rodents, and are typically interpreted in conjunction with other physiological measures, such as plasma corticosterone levels, to provide a comprehensive assessment of stress and anxiety (Bailey & Crawley, 2009).

Furthermore, cognitive function, particularly recognition memory, also demonstrates daily variation. The spontaneous recognition memory task exploits rodents' natural preference for novelty, requiring minimal training while providing robust measures of recognition memory. As such, it was employed as a measure of cognitive performance.

Here, we examine the consequences of a 12-week DLE exposure on circadian physiology, mood, cognitive function, and metabolic regulation. This comprehensive assessment will

provide the first evidence for how prolonged DLE exposure affects mouse circadian biology in ways that may parallel the experiences of humans in modern light environments.

2.2. Methods

Animals and Housing Conditions. Two cohorts, each consisting of 24 animals (1:1 male-female ratio), were used in this study. Wild-type C57BL/6J animals were purchased from Inotiv, Inc. (UK), and were about 9 weeks old at the beginning of the study. Animals were singly housed in large MB1 (NKP Isotec) open top cages (45 L x 28 W x 13 H cm) under a 12:12 LD cycle for a minimum of one week prior to the start of experiments. They had no prior history of regulated procedures. Food (Teklad 2916) and water were provided *ad libitum* throughout the study. The temperature and relative humidity of the animal room were maintained at 20–24°C and 45–65%. Pathogen-free conditions were maintained throughout the study by the animal facility. Serology, bacteriology, and parasitology reports (Surrey Diagnostics Ltd., UK) noted one case of Enteromonas Sp, and one case of Chilomastix Sp, though the animals were not part of this study.

Lighting. Mice were housed in ventilated light-tight chambers (LTC) equipped with multiple cool-white light-emitting diodes (LEDs) (Luxeon Star LEDs, Quadica Developments Inc., Canada). These LEDs provided a light level of 200 photopic lux during the day, giving < 10 S-cone, 130 melanopic, 140 rhodopic and 150 M-cone opic lux. The spectral power distribution featured a higher, narrower peak at ~ 460 nm, and a lower, broader peak at ~ 560 nm (**Supp. Fig. 2.1**; **Supp. Table 2.1**).

Experimental Design. After a one-week baseline period under 12:12 LD, the experimental group received dim light in the evening (DLE) from ZT12 to ZT16 for 12 weeks. Evening light levels were kept at 20 lux, giving < 1 S-cone opic lux, 13 melanopic lux, 14 rhodopic lux and 15 M-cone opic lux (Lucas et al., 2024). Control animals remained under standard LD conditions throughout. Animals were handled periodically to habituate them to experimenter

handling. Following the 12-week period, animals underwent a series of behavioral tests, as well as either terminal tissue collection or blood collection. At the end of the experiment, mice were euthanized by cervical dislocation. The experimental timeline for each cohort of animals is detailed in **Figure 2.1**. Experimenters were not blind to the animals' sex or lighting condition.

Compliance. This study is reported in accordance with the ARRIVE 2.0 guidelines. All experimental procedures were carried out at the University of Oxford, UK, in accordance with the University of Oxford Policy on the Use of Animals in Scientific Research and the United Kingdom Animals (Scientific Procedures) Act 1986, under Project License PP0911346 and Personal License I34186130.

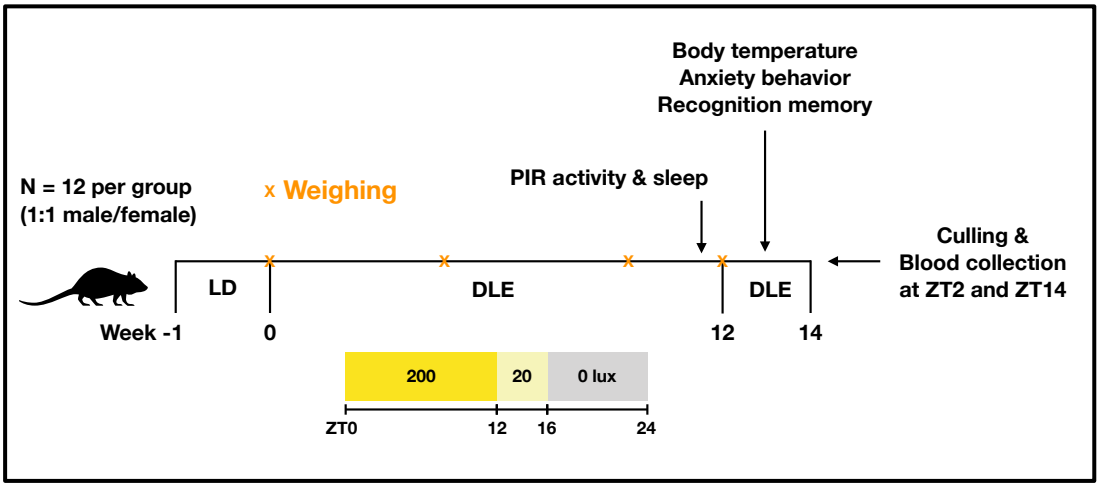

Figure 2.1. Experimental timeline for the investigation of the chronic effects of DLE on physiology and behavior. Animals (N = 12 per group, balanced male/female ratio) were first maintained under baseline LD conditions (12:12, 200/0 lux) for 1 week before transitioning to DLE (12:4:8, 200/20/0 lux) for 12 weeks. Body mass was recorded at baseline and at weeks 5, 10 and 12 of DLE exposure. Home cage locomotor activity was continuously monitored throughout the 12-week period using PIR sensors, with activity analysis performed on the data from the final week. At the conclusion of the 12-week DLE exposure, peripheral body temperature, anxiety behavior, and cognitive performance were assessed, with the test order counterbalanced between groups. Behavioral testing lasted 2 weeks, after which animals were euthanized at either ZT2 or ZT14, with terminal blood samples collected for clinical chemistry analysis and corticosterone measurement.

Home Cage Activity Monitoring. A passive infrared sensor (PIR, Panasonic AMN32111) was positioned above each cage to monitor locomotor activity, following the validated method described by Brown et al. (2016). To optimize tracking accuracy, gaps beneath the food and water hoppers in MB1 cages were sealed using Perspex blocks, and nesting material (paper-based sizzle-nest or cotton fiber nestlets) was provided in a quantity that did not fully obscure the animal from the sensor. Within each LTC, six PIR sensors were connected to an Arduino (Arduino Uno R3) alongside a light-dependent resistor (Farnell, UK) to monitor the light environment. The Arduinos were interfaced with a Raspberry Pi (Raspberry Pi 3 B) and processed using Node-RED. PIR data were recorded at a 10 s temporal resolution. Data from the 12th week of DLE exposure (7 days) were used for the analysis. PIR activity counts were averaged in 1 min bins and in 1 h bins to compute the different activity analyses.

Circadian Disruption Measures. Actograms and Chi-square periodogram were computed in ActogramJ (Schmid et al., 2011). Inter-daily stability, intra-daily variability, relative amplitude, light-phase activity, and total activity were calculated in R. Equations are provided in **Supplemental Figure 2.2** (Brown et al., 2019; Witting et al., 1990).

PIR-Defined Sleep. Brown et al. (2016) have shown that ≥ 40 s of PIR immobility is highly correlated with electroencephalogram (EEG)-defined sleep (Brown et al., 2016). Using this method, we computed PIR-defined sleep for every animal. For each 10 s bin of the recording, mouse activity was scored as "1" if the activity count > 0, and "0" otherwise. A 40 s rolling sum was applied to count the number of consecutive bins of activity. If the sum = 0, then PIR-defined sleep was scored as "1" for asleep. If the sum > 0, then it was scored as "0" for awake. Sleep proportion was defined as the number of bins with a "1" sleep score divided by the total number of bins in that time window.

Body Mass. Animals (Cohort A) were weighed at four time points throughout the study, around ZT10. Initial baseline measurements were taken prior to the start of the DLE protocol.

Subsequent weighings were conducted at week 5 and week 10 of DLE exposure, with a final measurement at the conclusion of the 12-week DLE period.

Body Temperature. Animals (Cohort A) were transferred to small open top cages (48 L x 15 W x 13 H cm) positioned under thermal cameras (Optris PI 160 with standard 61° lens, Optris, Germany). Skin temperature was recorded at a 1 sec temporal resolution for 48 h using the PIX Connect software (Optris, Germany), storing the temperature of the warmest pixel. Nesting material was limited to ensure continuous visibility of the mice. One animal, a control male, was excluded from the analysis due to a system malfunction during the recording. Data from the second day of body temperature recordings were analyzed, eliminating potential disruptions caused by the cage change on the first day. To estimate core body temperature from skin temperature measurements, data were first processed by selecting the maximum value per rolling 60 s intervals. This step accounted for fluctuations in the hotspot location or temporary concealment due to peripheral temperature variations. The values were then averaged into 30 min bins to reduce noise associated with movement (van der Vinne et al., 2020).

Anxiety Testing. Anxiety testing took place over three consecutive days, and only one behavioral test was conducted per day for each animal. For each experiment, mice (Cohort A) were brought into the test room 5 to 10 min prior to the onset of testing. The testing arena was cleaned with 70% ethanol between trials. Illuminance was 200 lux at the base of each apparatus, unless stated otherwise.

Elevated-Plus Maze (EPM). The EPM consisted of a black, wooden, cross-shaped elevated platform (50 cm H), with two closed arms (30 L x 5 W x 20 H cm) and two open arms (30 L x 5 W cm) connected by a central square (5 x 5 cm) (**Fig. 2.7A)**. A USB video camera was placed on a tripod ~ 1 m above the EPM and connected to a desktop. Two "closed" arm regions, two "open" arm regions, and one "center" region, were defined using the ANY-maze software (Stoelting Co, US). EPM tests took place at ZT4. Animals (N = 24) were placed in the center of the apparatus and allowed to explore for 10 min. The key variables extracted were the number

of entries and the time spent in the open-arms, closed-arms, and center zone, as well as the total distance travelled.

Light-Dark Box (LD box). The LD box consisted of one white and one black Perspex acrylic box (20 L x 20 W x 40 H cm), connected by a small opening. The opening allowed animals to move between the two adjacent boxes (**Fig. 2.7E)**. The white box was equipped with an LED light giving a 200 lux light level, while the black one was under constant darkness. Both boxes were equipped with an infra-red USB video camera attached to the boxes' lid. "Light" and "dark" regions were defined using the ANY-maze software (Stoelting Co, US). LD box tests took place at ZT5, and the order of testing between the EPM and the LD box was counterbalanced. Animals (N = 24) were placed in the light section of the apparatus and left to explore for 10 min. The key variables extracted were the number of transitions and the time spent in the light and dark boxes, as well as the total distance travelled.

Open Field (OF). The OF consisted of an open white Perspex acrylic arena (25 x 25 x 25 cm). A USB video camera was placed on a tripod ~ 1 m above the OF and connected to a desktop. Two distinct regions within the OF were defined using ANY-maze (Stoelting Co, US). A "center" region was defined as a 15 cm x 15 cm square at the center of the box, while an "outer" region represented a 5 cm width perimeter outside that square (**Fig. 2.7I)**. Four "corner" regions (5 x 5 cm) were also defined within the outer region, at each corner of the box. OF tests took place at ZT6 and occurred after animals were tested for both the EPM and LD box. Animals (N = 24) were placed at the center of the box and left to explore for 10 min. The key variables extracted were the number of entries and time spent in the center, outer, and corner zones, as well as the average speed and total distance travelled.

Recognition Memory Tasks. Recognition tests were conducted in a square open field arena (25 x 25 x 25 cm) made of opaque white Perspex acrylic. Prior to experimentation, animals (Cohort A) were acclimatized to the arena for 10 min at ZT6 (midday) one day before the first recognition test. The recognition paradigm comprised three phases: training, delay, and test,

and were performed at two time points: ZT2 under 200 lux illumination (day) and ZT14 under dim red light (night). To mitigate potential order effects, animals were counterbalanced for the time point of their initial test and the objects/odors they encountered, as well as their placement, as detailed in **Supplemental Table 2.2**. The study employed three sets of objects and three sets of odors **(Supp. Fig. 2.3).** To eliminate olfactory cues, the arena, objects, and flasks were thoroughly cleaned with 70% ethanol after each phase.

Novel Object Recognition. All animals first underwent the novel object recognition task. During the training phase, animals were placed in an arena for 10 min to explore two identical objects positioned at opposite ends of the box (**Fig. 2.8A**). Subsequently, animals were returned to their home cages for a 3-minute delay phase. The test phase involved reintroducing the animals to the arena for 3 min, where they encountered one "familiar" object and one "novel" object to assess novelty preference.

Novel Odor Recognition. The novel odor recognition task followed an identical protocol on the subsequent day (**Fig. 2.8E**). During the training phase, 1 mL of the same extract was placed in two brown glass vials (1.5 cm base diameter x 2.2 cm height, with a circular opening of 0.7 cm diameter) positioned on each side of the cage. A vial with a different extract was introduced as the "novel" odor during the testing phase.

All sessions were video-recorded with a USB camera mounted ~ 1 m above the arena, and analyzed using ANY-maze tracking software (Stoelting Co, US). The key variables extracted were the number of entries and the time spent within the familiar and novel object/odor zone, as well as the total distance travelled during the testing phase. Investigation was defined as directing the head toward the object or odor at a distance of ≤ 2 cm. Calculations for the recognition index are provided in **Supplemental Figure 2.4**. Results for the 3-minute testing phase were analyzed.

Tissue Collection. Animals (Cohort A) were euthanized by cervical dislocation at ZT2 (N = 12) and ZT14 (N = 12). Samples from the eye, dorsal hippocampus, motor cortex, olfactory bulb, SCN, paraventricular nucleus, heart, liver, lung, kidney, adrenal gland, and white adipose tissue were collected and flash frozen on dry ice before being stored at − 80 °C.

Blood Collection and Analysis. Animals (Cohort B) were euthanized by cervical dislocation at ZT2 (N = 12) and ZT14 (N = 12). Blood was immediately collected via cardiac puncture into polypropylene tubes. Samples were allowed to clot at room temperature for 2 h before being centrifuged at 2000 x g for 20 min. The serum (60-180 µL) was removed, aliquoted and stored at - 80 °C until analysis. Serum samples were processed for corticosterone concentration and clinical chemistry panel.

Corticosterone Concentration. The Parameter™ Corticosterone Assay (Catalog Number KGE009, R&D Systems Inc, US) was used to quantitatively determine corticosterone concentration. Serum samples (5 µL) were diluted by 100 fold using the Calibrator Diluent RD5-43 provided in the kit. Samples were then pre-treated by adding 150 µL of the sample and 150 µL of the Pretreatment E. Reagent preparation and assay procedure were conducted according to the manufacturers‘ instructions. Samples and standards were assayed in triplicate. The absorbance was read using a microplate reader (FLUOstar Omega, BMG Labtech, Germany) set to 450 nm, with a wavelength correction set to 540 nm. Corticosterone concentrations were calculated based on the standard curve (**Supp. Fig. 2.5**), and adjusted for dilution (multiplied by 200).

Clinical Chemistry. Serum samples (50 µL) were diluted in distilled water (1:1) and processed for their concentration of glucose, O-benzyl-β-D-glucoside (OBB-glucose), total cholesterol, glycerol, high-density lipoprotein (HDL) cholesterol, lactate, triacylglycerols (TAG), non-esterified fatty acids (NEFA), alanine aminotransferase (ALT), urea, 3-hydroxybutyrate (3-OHB), and C-reactive protein (CRP). Metabolites were measured via photometric assays on a semi-automatic analyzer (AU480 Chemistry Analyzer, Beckman Coulter, US), following the

manufacturer's instructions. Metabolite concentration was adjusted for dilution (multiplied by 2). Three samples per sex, per time point, and per lighting condition were processed. One sample (female, ZT14, DLE) only yielded results for glucose concentration, likely due to equipment malfunction. Additionally, ALT concentrations were unavailable for four samples (1 male, ZT2, LD; 1 male, ZT14, LD; 1 female, ZT14, LD; 1 female, ZT14, DLE). The reduced sample size, particularly for ALT measurements and the female DLE ZT14 group, lowered statistical power.

Statistical Analyses. Statistical testing and plotting were conducted in Prism 10. Regular and repeated-measures two-way ANOVAs, with a Geisser-Greenhouse correction (for lack of sphericity), and Holm-Šídák's multiple comparisons test were computed. When comparing two groups, unpaired nonparametric Mann-Whitney tests were used, as the distribution of the data was not Gaussian. $\alpha = 0.05$ was adopted in all analyses. Mean ± standard error of the mean (SEM) was used for all plots.

2.3. Results

Locomotor Activity. Home cage locomotor activity was recorded continuously for 12 weeks for animals exposed to 12:12 LD (**Fig. 2.2A**) or DLE (**Fig. 2.2B**). All animals exhibited a circadian period close to 24 h (Mann-Whitney, $U = 68$, $p = 0.8662$; **Fig. 2.2C**). Chi-square periodogram analysis revealed no differences between groups in the distribution of periodogram power (Time x Lighting, $F_{(959, 21098)} = 0.8181$, $p > 0.9999$; **Fig. 2.2D**) or maximum Qp (Mann-Whitney, $U = 52$, $p = 0.2657$; **Fig. 2.2E, Supp. Table 2.3**). This indicates a similar level of robustness for activity rhythms under both LD and DLE.

Averaged daily activity profiles revealed a main effect of Time (Time, $F_{(5.732, 126.1)} = 69.47$, $p < 0.0001$; **Fig. 2.3A**), as expected for mouse activity over the day/night cycle. We also found a Time x Lighting interaction (Time x Lighting, $F_{(23, 506)} = 17.83$, $p < 0.0001$; **Fig. 2.3A**), showing that the timing of activity differed between groups. This was caused by a delay in the peak of

activity rhythms from ZT12 to ZT16 for DLE animals. The distribution of activity also varied, with DLE animals showing higher levels of activity during the day (ZT0-12) and night (ZT16-24) periods, but lower levels of activity during the evening (ZT12-16) relative to controls (Time x Lighting, $F_{(2, 44)} = 38.95$, $p < 0.0001$; **Fig. 2.3B**). Yet, the total activity count per day did not differ between groups (Mann-Whitney, $U = 61$, $p = 0.5512$; **Fig. 2.3C**).

Animals exposed to chronic DLE did not show differences in their inter-daily stability relative to controls, with both groups exhibiting a high level of day-to-day reproducibility (Mann-Whitney, $U = 49$, $p = 0.1978$; **Fig. 2.3D**). DLE animals showed a similar degree of fragmentation, with comparable intra-daily variability measures (Mann-Whitney, $U = 66$, $p = 0.7553$; **Fig. 2.3E)**. However, the distribution of activity bouts slightly differed between groups (Bout length x Lighting, $F_{(7, 154)} = 2.257$, $p = 0.0325$; **Fig. 2.3F**). Post-hoc analysis did not reveal any significant differences. Finally, DLE animals displayed a 4.12% decrease in relative amplitude compared to controls (Mann-Whitney, $U = 23$, $p = 0.0036$; **Fig. 2.3G**).

Data disaggregation by sex revealed differences between the activity rhythms of males and females, regardless of the lighting condition. While there were no sexual differences in circadian period (Sex, $F_{(1, 20)} = 1.762$, $p = 0.1994$; **Supp. Fig. 2.6A**), females exhibited higher maximum periodogram power (Sex, $F_{(1, 20)} = 21.84$, $p = 0.0001$; **Supp. Fig. 2.6B**), higher inter-daily stability (Sex, $F_{(1, 20)} = 15.10$, $p = 0.0009$; **Supp. Fig. 2.6C**), lower intra-daily variability (Sex, $F_{(1, 20)} = 43.17$, $p < 0.0001$; **Supp. Fig. 2.6D**), higher relative amplitude (Sex, $F_{(1, 20)} = 12.21$, $p = 0.0023$; **Supp. Fig. 2.6E**), and higher total activity (Sex, $F_{(1, 20)} = 26.42$, $p < 0.0001$; **Supp. Fig. 2.6F, Supp. Table 2.4**). All representative actograms can be found in **Supplemental Figure 2.7**.

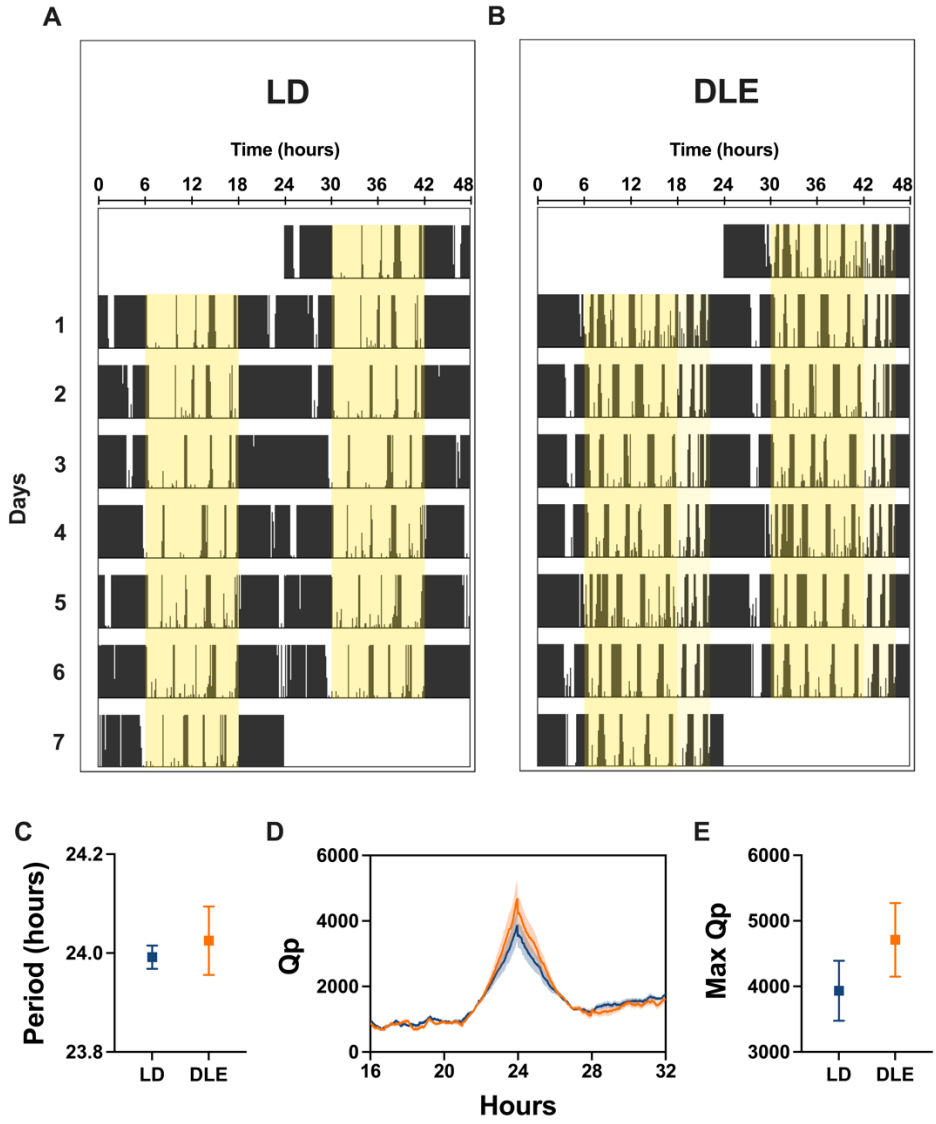

Figure 2.2. Home cage locomotor activity and circadian rhythm measures following 12 weeks of DLE (N = 12 per group). Representative double-plotted actogram of locomotor activity during the 12th week of the experiment for **A.** a control female animal under 12:12 LD, and **B.** a female animal under DLE. Yellow shading indicates light phases. **C.** Period of activity rhythms. **D.** Chi-square periodogram analysis. **E.** Maximum Qp values. Mean +/- SEM.

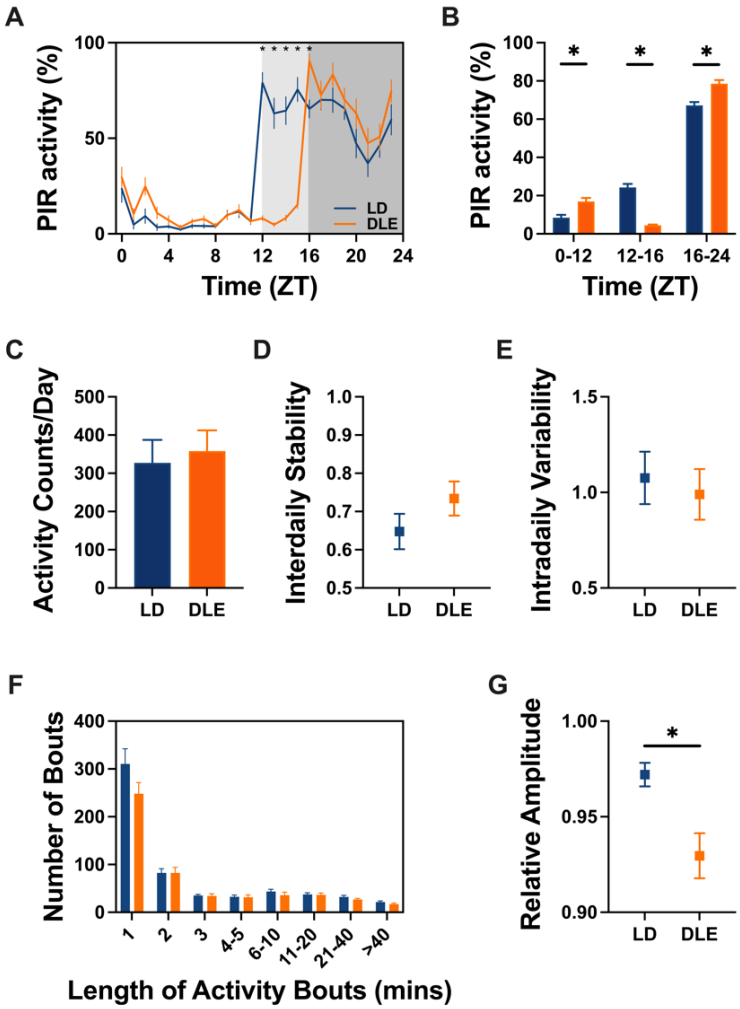

Figure 2.3. Analysis of locomotor activity rhythms following extended DLE exposure (N = 12 per group). **A.** 24-hour activity profile. PIR data were normalized for each animal using min-max scaling. Data are plotted in 1 h bins (Time x Lighting, $F_{(23, 506)} = 17.83$, $p < 0.0001$). **B.** Light-, dim-, and dark-phase activity, as a percentage of total activity per day (Time x Lighting, $F_{(2, 44)} = 38.95$, $p < 0.0001$). **C.** Total activity per day. **D.** Inter-daily stability. **E.** Intra-daily variability. **F.** Distribution of the number and duration of activity bouts (Bout length x Lighting, $F_{(7, 154)} = 2.257$, $p = 0.0325$). **G.** Relative amplitude (Mann-Whitney, $U = 23$, $p = 0.0036$). Mean +/- SEM. Statistically significant post-hoc tests are indicated by an asterisk.

PIR-Defined Sleep. To examine changes in sleep patterns, PIR-defined sleep was computed based on periods of ≥ 40 s of immobility (Brown et al., 2016). Averaged daily sleep profiles revealed a main effect Time (Time, $F_{(4.444, 97.76)} = 66.13$, $p < 0.0001$; **Fig. 2.4A**), as expected for mouse sleep patterns across 24 h. A Time x Lighting interaction was also found (Time x Lighting, $F_{(23, 506)} = 13.12$, $p < 0.0001$; **Fig. 2.4A**), indicating that the timing of sleep differed between DLE animals and controls. DLE animals delayed their activity onset from ZT12 to

ZT16, sleeping more than control animals during the ZT12-16 period. Yet, total sleep proportion per day did not differ between groups (Mann-Whitney, $U = 60$, $p = 0.5137$; **Fig. 2.4B**). There was a main effect of Sex (Sex, $F_{(1, 20)} = 25.70$, $p < 0.0001$), with males sleeping almost 20% more than females, regardless of the lighting condition.

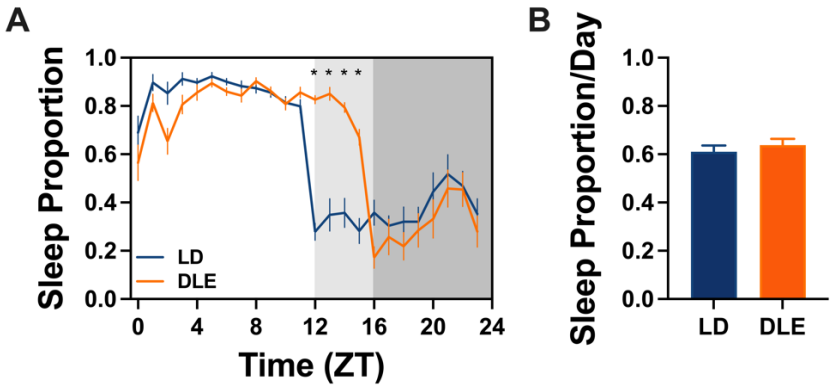

Figure 2.4. PIR-defined sleep following 12 weeks of DLE (N = 12 per group). **A.** Sleep proportion was computed as the number of bins of scored immobility divided by the total number of bins in the time window. Data are plotted in 1 h bins (Time x Lighting, $F_{(23, 506)} = 13.12$, $p < 0.0001$). **B.** Average sleep proportion per day. Mean +/- SEM. Statistically significant post-hoc tests are indicated by an asterisk.

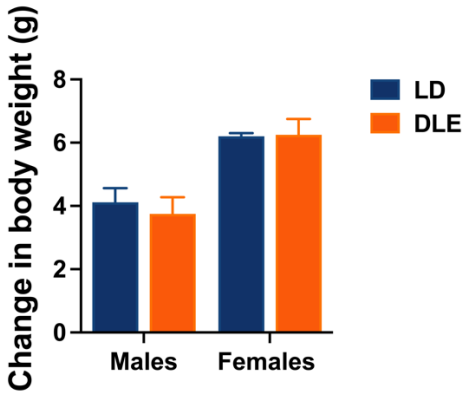

Figure 2.5. Change in body weight following 12 weeks of DLE exposure (N = 6 per group) (Sex, $F_{(1, 20)} = 28.47$, $p < 0.0001$). Mean +/- SEM.

Body Mass. Following the 12-week DLE period, all animals exhibited weight gain. Statistical analysis revealed a significant main effect of Sex (Sex, $F_{(1, 20)} = 28.47$, $p < 0.0001$; **Fig. 2.5**), with females demonstrating greater overall weight gain compared to males, regardless of the lighting condition. Indeed, females gained over 50% more weight than males over 12 weeks. However, Lighting condition did not significantly affect weight gain (Lighting, $F_{(1, 8)} = 0.1359$, $p = 0.7163$; **Fig. 2.5**), indicating no differences in weight gain between DLE-exposed animals and controls. No interaction effect was found (Sex x Lighting, $F_{(1, 20)} = 0.2353$, $p = 0.6329$; **Fig. 2.5**). There were also no differences in growth rates between DLE animals and controls, regardless of sex (Time x Lighting, Males $F_{(3, 30)} = 0.9622$, $p = 0.4233$; Females, $F_{(3, 30)} = 0.4315$, $p = 0.7319$; **Supplemental Figure 2.8**).

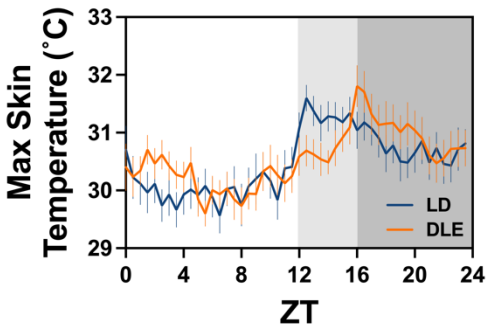

Figure 2.6. Body temperature rhythms following 12 weeks of DLE exposure (N = 11 for LD, N = 12 for DLE; one LD male excluded). To provide an estimate of core body temperature, we computed maximum skin temperature measures over 60 s intervals, and averaged them in 30 min bins. Data are plotted in 30 min windows (Time x Lighting, $F_{(47, 987)} = 2.838$, $p < 0.0001$). Mean +/- SEM.

Body Temperature. Analysis of skin temperature rhythms revealed a significant main effect of Time (Time, $F_{(11.13, 233.7)} = 13.22$, $p < 0.0001$; **Fig. 2.6**). While there was no simple effect of Lighting condition (Lighting, $F_{(1, 21)} = 0.03399$, $p = 0.8555$; **Fig. 2.6**), we found a significant interaction between Time and Lighting condition (Time x Lighting, $F_{(47, 987)} = 2.838$, $p < 0.0001$; **Fig. 2.6**). Animals exposed to chronic DLE showed a delay in the peak timing of temperature

rhythms. Male and female animals both exhibited this delay, with subtle differences in their overall temperature profiles (**Supp. Fig. 2.9**, **Supp. Table 2.5**). Overall, females had a slightly higher, but not statistically significant mean temperature (Sex, $F_{(1, 19)} = 1.767$, $p = 0.1995$; **Supp. Table 2.6**), and a significantly higher range of temperatures compared to males (Sex, $F_{(1, 19)} = 7.889$, $p = 0.0112$; **Supp. Table 2.6**), regardless of lighting condition.

Elevated-Plus Maze. Animals exposed to long-term DLE did not demonstrate signs of increased anxiety in the EPM relative to controls (**Fig. 2.7A**). There were no differences in the total distance travelled (Mann-Whitney, $U = 51$, $p = 0.2415$; **Fig. 2.7B**), the number of entries in each zone (Lighting x Zone, $F_{(2, 66)} = 2.044$, $p = 0.1376$; **Fig. 2.7C**), as well as the time spent in each zone of the EPM (Lighting x Zone, $F_{(2, 66)} = 0.1764$, $p = 0.8387$; **Fig. 2.7D**). Similar results were found for both male and female animals (**Supp. Table 2.7**).

Light-Dark Box. Mice did not exhibit significant anxiety behavior in the LD box following exposure to extended DLE (**Fig. 2.7E**). There were no differences in the total distance travelled (Mann-Whitney, $U = 71$, $p = 0.9774$; **Fig. 2.7F**), number of LD transitions (Mann-Whitney, $U = 51.5$, $p = 0.2458$; **Fig. 2.7G**), or time spent in each box (Mann-Whitney, $U = 65$, $p = 0.7125$; **Fig. 2.7H**), regardless of sex (**Supp. Table 2.8**).

Open Field. DLE animals displayed some signs of heightened anxiety in the OF (**Fig. 2.7I**). There was a significant difference in overall locomotor activity, with a 22.6% increase in the total distance travelled (Mann-Whitney, $U = 34$, $p = 0.0284$; **Fig. 2.7J**), and a 22.2% increase in average speed (Mann-Whitney, $U = 36.5$, $p = 0.0391$; **Fig. 2.7K**) under DLE conditions. Results were consistent across sex (**Supp. Table 2.9**). While there was a significant main effect of Zone, suggesting discrimination between the different areas of the apparatus, DLE animals did not exhibit overall differences in the time spent in each zone of the OF (Lighting x Zone, $F_{(2, 66)} = 2.186$, $p = 0.1204$; **Fig. 2.7L**). However, when disaggregating results by sex, we found a statistically significant interaction for the time spent in each zone of the OF for females only (Lighting x Zone, $F_{(2, 30)} = 5.761$, $p = 0.0076$; **Supp. Table 2.9**). Control females spent 30% of

the test in the center and 70% in the periphery of the OF, compared to 45% in the center and 55% at the periphery for DLE females.

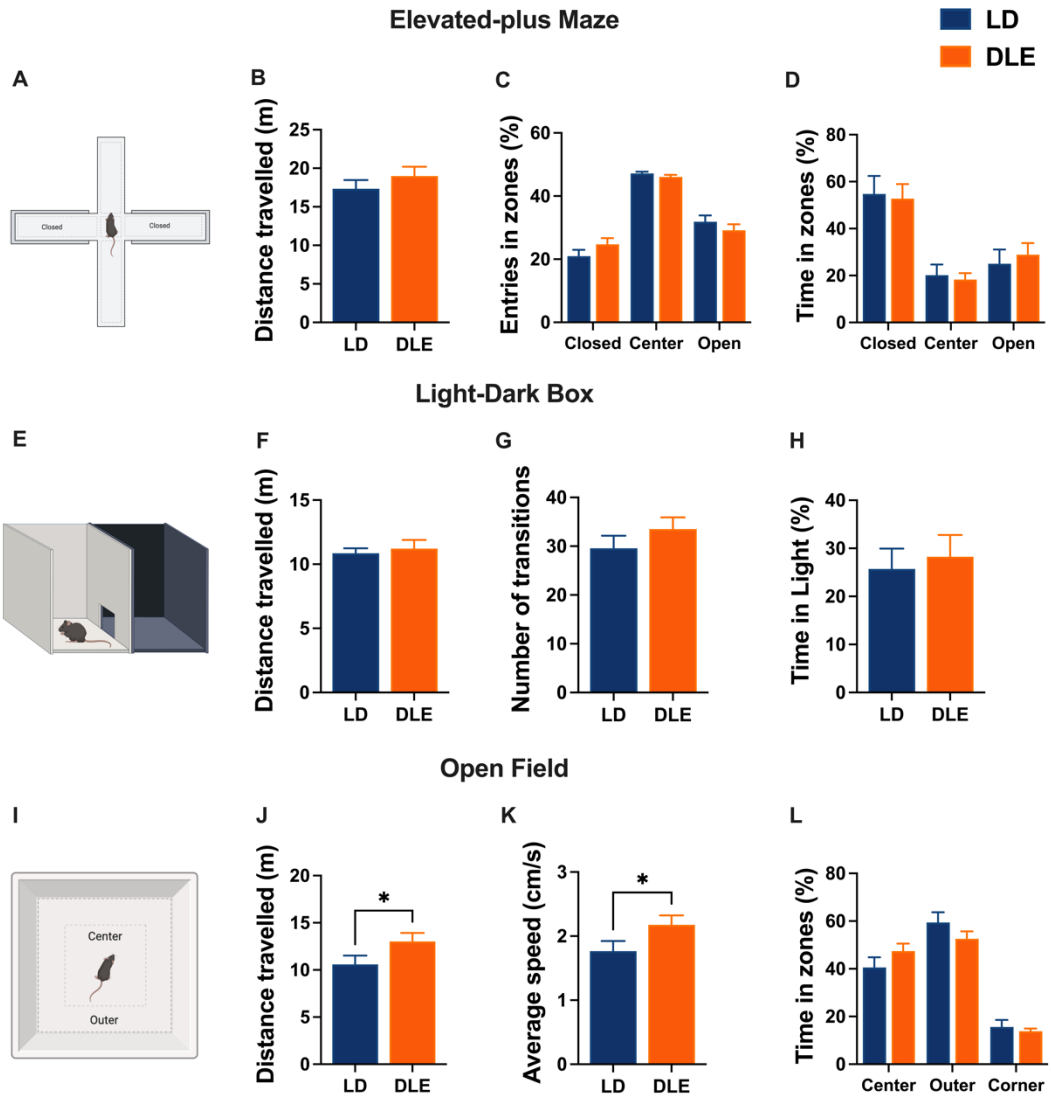

Figure 2.7. Anxiety behavior following 12 weeks of DLE (N = 12 per group). **A.** Schematic of the elevated-plus maze (EPM) apparatus. Mice were tested for 10 min at ZT4. **B.** Total distance travelled (m). **C.** Number of entries in the "closed", "center", and "open" zones of the EPM, as a percentage of the number of entries. **D.** Time spent in each zone of the EPM, as a percentage of the total time spent in the apparatus. **E.** Schematic of the light-dark box (LD box). Mice were tested for 10 min at ZT5. **F**. Total distance travelled (m). **G.** Number of transitions between the light and the dark box. **H.** Time spent in the light box, as a percentage of the total time spent in the apparatus. **I.** Schematic of the open field (OF) apparatus. Mice were tested for 10 min at ZT6. **J.** Total distance travelled (m) (Mann-Whitney, $U = 34$, $p = 0.0284$). **K.** Average speed ($cm.s^{-1}$) (Mann-Whitney, $U = 36.5$, $p = 0.0391$). **L.** Time spent in the "center", "outer", and "corner" zones of the OF, as a percentage of the total time spent in the apparatus. The "corner" zone is a sub-section of the "outer" zone. Mean +/- SEM. Statistically significant Mann-Whitney tests are indicated by an asterisk.

Novel Object Recognition. Animals did not show differences in overall locomotor activity during the novel object recognition task. Indeed, analysis of the total distance traveled by animals during the 3-minute testing phase revealed no significant main effects of Time (Time, $F_{(1, 22)} = 0.2052$, $p = 0.6550$; **Fig. 2.8B**) or Lighting condition (Lighting, $F_{(1, 22)} = 0.2019$, $p = 0.6576$; **Fig. 2.8B**). However, significant Time x Lighting interactions were observed for both the number of investigations (Time x Lighting, $F_{(1, 22)} = 4.928$, $p = 0.0370$; **Fig. 2.8C**), and the time spent investigating the novel object (Time x Lighting, $F_{(1, 22)} = 5.415$, $p = 0.0296$; **Fig. 2.8D**). Notably, DLE animals exhibited an increase in novelty preference from ZT2 to ZT14, whereas control animals showed a decrease over the same period. Data disaggregation by sex (**Supp. Table 2.10**), or by minute of the testing phase (**Supp. Table 2.11**), did not provide more insights into the dynamics at play.

Novel Odor Recognition. The odor recognition test yielded no significant main effects of Time or Lighting condition across all measured parameters (**Fig. 2.8F, Fig. 2.8G, Fig. 2.8H**). It is worth noting that in several instances, the recognition index did not differ from 0, suggesting no discrimination between the odors, and thus potential limitations in the efficacy of this particular test. Moreover, results did not differ between sexes (**Supp. Table 2.12**).

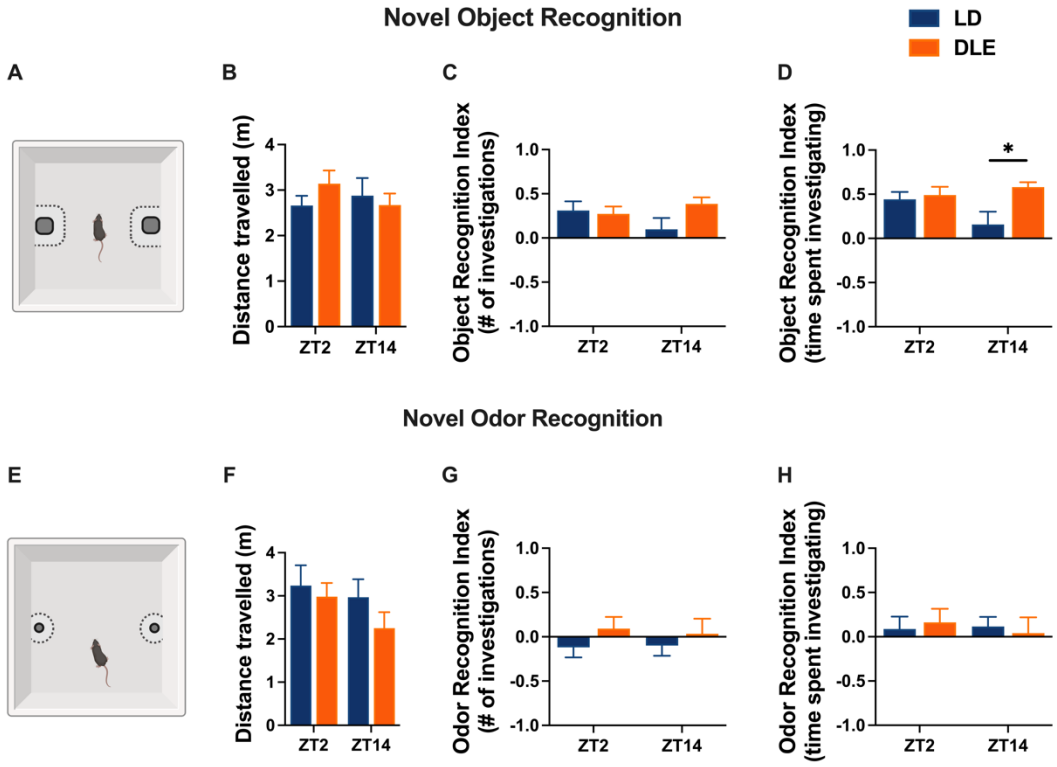

Figure 2.8. Recognition memory performance following 12 weeks of DLE exposure (N = 12 per group). **A.** Schematic of the novel object recognition apparatus. **B.** Total distance travelled (m) during the object testing phase. **C.** Object recognition index based on the number of investigations of the novel and familiar objects (Time x Lighting, $F_{(1, 22)} = 4.928$, $p = 0.0370$). **D.** Object recognition index based on the time spent investigating the novel and familiar objects (Time x Lighting, $F_{(1, 22)} = 5.415$, $p = 0.0296$). **E.** Schematic of the novel odor recognition apparatus. **F.** Total distance travelled (m) during the odor testing phase. **G.** Odor recognition index based on the number of investigations of the novel and familiar odors. **H.** Odor recognition index based on the time spent investigating the novel and familiar odors. A recognition index of 1 indicates novelty preference, while a recognition index of -1 suggests familiar preference. Mean +/- SEM. Statistically significant post-hoc comparisons are indicated by an asterisk.

Blood Corticosterone Concentration. A main effect of Time was found for both males and females (Time, $F_{(1, 8)} = 11.98$, $p = 0.0085$; **Fig. 2.9A**; $F_{(1, 8)} = 5.911$, $p = 0.0411$; **Fig. 2.9B**; respectively), with higher levels of plasma corticosterone at ZT14, as compared to ZT2. Additionally, a main effect of Lighting condition was found for females (Lighting, $F_{(1, 8)} = 8.010$; $p = 0.0221$; **Fig. 2.9B**), with 41.4% higher corticosterone levels at ZT14 for DLE animals relative to controls. No interaction effects were found for either males (Lighting x Time, $F_{(1, 8)}$

= 0.7429, $p = 0.4138$; **Fig. 2.9A**), nor females (Lighting x Time, $F_{(1, 8)} = 2.371$, $p = 0.1621$; **Fig. 2.9B**, **Supp. Table 2.13**).

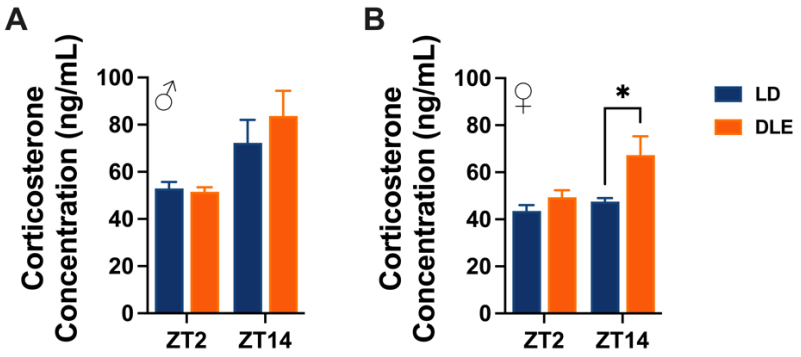

Figure 2.9. Blood corticosterone concentration (ng/mL) following chronic DLE exposure in **A.** males (N = 12 per group), and **B.** females (N = 12) as a measure of stress (Females, Lighting, $F_{(1, 8)} = 8.010$; $p = 0.0221$). Mean +/- SEM. Statistically significant post-hoc comparisons are indicated by an asterisk.

Clinical Blood Chemistry. Preliminary analysis of clinical blood chemistry measures revealed sex-specific effects. In males, no significant main effects of Time or Lighting condition were observed for any of the measured parameters (**Supp. Table 2.14**). In contrast, females exhibited several time-dependent and lighting condition effects. A significant main effect of Time was found for HDL cholesterol (Time, $F_{(1, 8)} = 7.502$, $p = 0.0290$; **Fig. 2.10E**), and lactate (Time, $F_{(1, 8)} = 10.67$, $p = 0.0137$; **Fig. 2.10F**). We also observed a significant main effect of Lighting condition for total cholesterol (Lighting, $F_{(1, 8)} = 9.331$, $p = 0.0185$; **Fig. 2.10C**), glycerol (Lighting, $F_{(1, 8)} = 6.856$, $p = 0.0345$; **Fig. 2.10D**), and TAG (Lighting, $F_{(1, 8)} = 9.136$, $p = 0.0193$; **Fig. 2.10G**). Post-hoc analysis revealed that females exposed to chronic DLE exhibited significantly higher levels of total cholesterol and glycerol at ZT14 compared to controls.

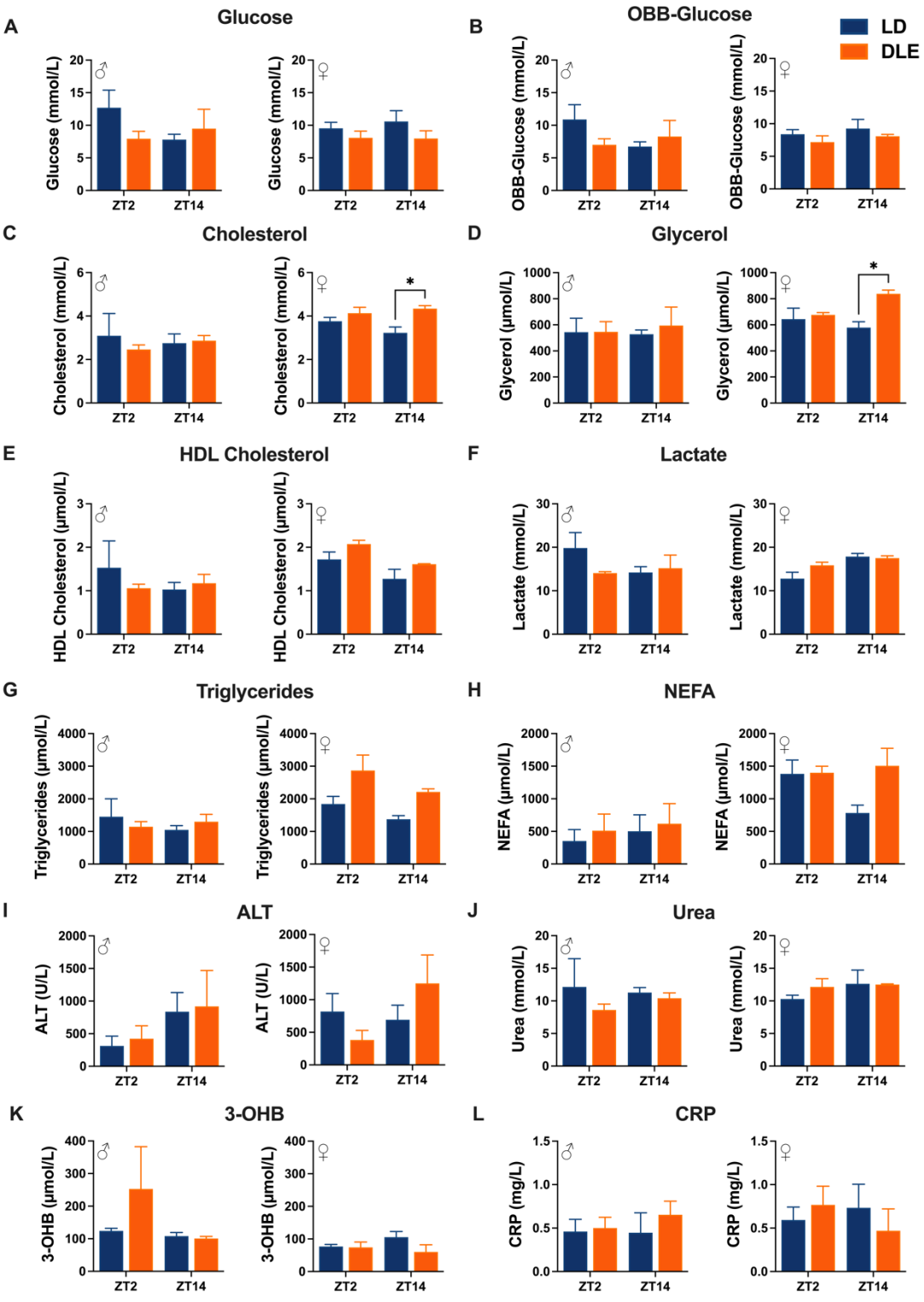

Figure 2.10. Clinical blood chemistry panel following 12 weeks of DLE exposure for males and females (N = 6 per group, exclusions apply, see Methods section). **A.** Glucose. **B.** OBB-Glucose. **C.** Total cholesterol (Females, Lighting, $F_{(1, 8)} = 9.331$, $p = 0.0185$). **D.** Glycerol (Females, Lighting, $F_{(1, 8)} = 6.856$, $p = 0.0345$). **E.** HDL cholesterol. **F.** Lactate. **G.** Triglycerides (Females, Lighting, $F_{(1, 8)} = 9.136$, $p = 0.0193$). **H.** NEFA. **I.** ALT. J. Urea. **K.** 3-OHB. **L.** CRP. Mean +/- SEM. Statistically significant post-hoc comparisons are indicated by an asterisk.

2.4. Discussion

This study investigated the effects of a 12-week exposure to DLE on circadian rhythms and associated physiological and behavioral parameters in mice. Using a comprehensive series of phenotyping measures, including locomotor activity, sleep, body temperature, metabolic parameters, stress hormones, anxiety tests, and recognition memory tasks, we assessed how this environmental perturbation affects temporal biology and downstream physiological processes. Our findings reveal that mice exhibit remarkable adaptability to altered lighting conditions, with coordinated systemic realignment rather than severe circadian disruption, with notable sex-specific consequences (**Table 2.1**).

Chronic DLE exposure led to a temporal compression of activity, expansion of sleep architecture, and reorganization of body temperature rhythms.

We quantified the structure and regularity of locomotor activity rhythms using several metrics. Circadian period did not differ under DLE exposure, maintaining a rhythm close to 24 hours. Similarly, there were no alterations in total daily activity, with females being more active than males in both groups. However, averaged daily activity profiles revealed a significant shift in the timing of activity onsets under DLE conditions, with peak activity delayed from ZT12 to ZT16 (dark onset). This was further accompanied by an increase in daytime activity. This temporal shift is consistent with previous studies showing that two weeks of DLE leads to a realignment between the internal clock and external light cues (Tam et al., 2021). While the total quantity of sleep remained unchanged, the proportion of PIR-defined sleep between ZT12 and ZT16 was higher for DLE animals. This suggests that chronic DLE exposure led to a temporal reorganization, with animals concentrating their activity within the eight hours of darkness, and distributing sleep more extensively throughout the combined 16 hours of bright and dim light. Changes in sleep quality should be further examined using EEG/EMG.

Periodogram power and relative amplitude were used to assess the strength and robustness of the rhythms. The Chi-square periodogram is a statistical method used to analyze the rhythmic patterns of time-series data, determining the distribution of variance at different frequencies (Sokolove & Bushell, 1978). Relative amplitude quantifies the contrast between peak and trough activity levels over a 24-hour period, providing an additional index of the rhythm's strength (Brown et al., 2019). We found high values of periodogram power and relative amplitude for both groups, highlighting the strength and robustness of the activity rhythms. While DLE exposure resulted in a modest but significant 4% decrease in relative amplitude compared to controls, mean amplitude levels remained above 0.9 for both groups. This suggests that, although there were alterations in the amplitude, the robustness of activity remained high, even under DLE conditions.

Inter-daily stability, intra-daily variability and bout length were used to measure the reproducibility and fragmentation of the rhythms. Inter-daily stability assesses the reproducibility of the 24-hour activity pattern across days, indicating the degree to which activity-rest cycles are maintained over time. Intra-daily variability measures the fragmentation of activity rhythms by capturing the frequency and abruptness of transitions between active and rest states within a single day. Activity bouts compute the duration of uninterrupted activity periods. The length and number of activity bouts are further used as a measure of fragmentation (Brown et al., 2019). Here, both groups showed a high level of reproducibility and consolidation based on inter-daily stability and intra-daily variability measures. The statistically significant interaction between time of day and lighting condition for bout length distribution suggests subtle reorganization of activity patterns under DLE conditions. Though post-hoc comparisons did not reveal significant differences at specific bout durations, the overall pattern indicates a tendency toward reduced frequency of short bouts (< 1 min) and increased medium to long bouts (> 5 min) in DLE animals. This redistribution may reflect an adaptation strategy that preserves total activity while accommodating the phase-delayed rhythm.

We examined if there were any changes in skin body temperature using infrared thermography, and used it as an indirect estimate of core body temperature as described in van der Vinne et al. (2020). All animals exhibited clear circadian temperature fluctuations across the 24-hour cycle. DLE-exposed animals showed a delay in the peak timing of temperature rhythms, consistent with the delay in activity rhythms reported above. Previous findings on the effects of two weeks of DLE exposure only found significant effects on the offset of temperature rhythms (Tam et al., 2021). However, it seems to be due to inconclusive analysis rather than a lack of biological effect. We also found that the average and range of body temperatures were consistent between groups.

Together, these findings suggest a coordinated realignment of the circadian system to the new dark onset under DLE conditions. The shift in activity and temperature onsets from ZT12 to ZT16 demonstrates the animals' adaptive response to changing light conditions, and the preservation of the temporal relationship between environmental darkness and activity initiation. This interpretation is supported by the maintenance of the activity rhythms' robustness despite the phase shift. The conservation of total activity and sleep levels, as well as temperature profile, further indicates that animals maintained their overall behavior, while reorganizing its temporal distribution to match the new LD cycle. These results are also comparable to the majority of studies on DLAN exposure in rodents, which reported changes in the temporal organization of activity and sleep patterns.

Sex-specific differences in the stability of activity rhythms were found, regardless of the lighting condition. Indeed, female mice displayed stronger, more robust, reproducible, and consolidated rhythms based on the circadian disruption measures used in this study. Females were also more active, and slept less than males. These findings are consistent with existing literature showing that females are often more active, and exhibit more robust circadian rhythms than males (Bartling et al., 2017; Blattner & Mahoney, 2012; Rosenfeld, 2017). We also attempted to investigate potential estrous cycle influences on female locomotor activity

patterns. While previous studies using running wheels have demonstrated clear 4-5 day modulation of activity (Ogawa et al., 2003), analysis of three consecutive weeks of PIR recordings in our study did not reveal such rhythms. This finding aligns with previous PIR studies, where estrogenic regulation of activity has never been reported. The periodic changes in activity observed with running wheels may thus reflect motivated behavior rather than general home cage locomotion.

Data disaggregation by sex revealed that females had a broader range of skin temperatures compared to males, regardless of the lighting condition. Our results align with previous findings on the sex differences in core body temperature of C57Bl/6J mice (Yang et al., 2007). Elevated core body temperature in females could reflect sex differences in basal metabolic rate, or the influence of sex hormones, which are known to affect thermoregulation (Sanchez-Alavez et al., 2011).

Chronic DLE exposure preserved body weight regulation while inducing sex-specific metabolic changes.

Baseline body mass did not differ between the animals assigned to the control and experimental groups. All animals exhibited weight gain over the 12-week experimental period, which is consistent with normal growth patterns in mice (Gall & Kyle, 1968; Gargiulo et al., 2014). However, a significant sex difference in weight gain was observed, with females showing a 50% greater increase in body weight compared to males, regardless of the lighting condition. This finding is not consistent with previous studies that found that C57Bl/6J males gain more weight, and at a higher rate than females under standard conditions (Medrikova et al., 2012; Stapleton et al., 2024). Sexual dimorphism in body weight gain have been attributed to various factors, including hormones, leptin regulation, and differences in energy metabolism and fat storage (Clegg et al., 2006; Lovejoy & Sainsbury, 2009; Shi et al., 2009). An alternative interpretation is that the greater weight gain observed in females reflects sex differences in

developmental timing. C57BL/6J mice might not reach sexual maturity at the same age. Given that our females began the experiment at 8 weeks of age with relatively low starting weights (approximately 16 g), they may have been at an earlier developmental stage than males, and thus exhibited more pronounced growth during the first weeks of the experiment. This interpretation is supported by the substantial weight gain occurring primarily during the first 5 weeks of the experiment. Future studies might thus consider using older mice (10-16 weeks at the beginning of experiments) to minimize potential confounding effects of developmental differences between sexes.

Chronic DLE exposure did not significantly affect weight gain in either sex. This finding aligns with studies showing that circadian disruptions may not always have a direct impact on overall weight gain, even if other metabolic parameters are significantly altered. This was reported in multiple DLAN studies where body mass was unaffected. Notably, in our study, mice gained the most weight during the first five weeks of the experiment. Investigating growth curves with a higher sampling resolution during this period might shed light on the dynamics at play, and reveal whether more subtle differences emerge from DLE exposure.

The clinical blood chemistry panel revealed sex-specific effects of chronic DLE. While male mice showed no significant changes in response to DLE, females exhibited alterations in several metabolites. However, it is crucial to preface this discussion by acknowledging the significant limitation in our sample size. With some groups having only two samples because of equipment malfunction, our statistical power is limited.

In males, we observed no significant effects of DLE on any of the measured metabolites. We also did not find significant circadian fluctuations between ZT2 and ZT14. However, the absence of detectable effects could be due to insufficient statistical power, rather than a true lack of biological effect, and to the timings of blood collection not capturing the peak and trough metabolite levels. It is also possible that males would show changes in metabolites not measured in this study.

In females, we observed several significant alterations. The main effects of time on HDL cholesterol and lactate levels suggest that these parameters are subject to circadian regulation. The increase in HDL cholesterol at ZT14 (early night) compared to ZT2 (early day) aligns with known circadian rhythms in lipid metabolism (Gooley & Chua, 2014). The parallel increase in lactate levels could reflect circadian variations in glucose metabolism or physical activity patterns. The effects of DLE on total cholesterol, glycerol, and TAG levels in females are particularly notable. The elevated levels of these lipid-related parameters in DLE-exposed females, especially at ZT14, suggest that DLE exposure may disrupt lipid metabolism in a sex-specific manner. This finding is consistent with growing evidence linking circadian disruption to alterations in lipid homeostasis (Bass & Takahashi, 2010). However, we must emphasize that these results, while interesting, are preliminary. The low sample size means that individual variability could have a disproportionate impact on our findings. It warrants further investigation with a larger sample size to reliably confirm these effects.

Together, the sex-specific nature of these effects suggests that females may be more susceptible to metabolic perturbations induced by mild circadian disruptions. This could be due to interactions between the circadian system and sex hormones, differences in the robustness of circadian rhythms between sexes, or sex-specific responses to stress induced by altered light exposure (Bailey & Silver, 2014).

Chronic DLE exposure induced subtle, sex-specific adaptations in stress and anxiety responses, without generalized effects.

We investigated the effects of long-term DLE exposure on anxiety and stress responses in mice. Anxiety behavior was assessed using the EPM, LD box, and OF. These tests exploit the natural tendencies of rodents to avoid open, brightly lit, or elevated spaces, balancing their innate curiosity to explore novel environments against their fear of potential threats. This multi-test approach was employed to obtain a complementary assessment of distinct anxiety responses,

while each test was selected based on its established pharmacological validation and widespread use in circadian research. While variations of the tests we employed exist (e.g., zero maze vs EPM, gradient vs binary LD tests), we employed the standard validated versions that allow for direct comparison with the established literature on circadian disruption and anxiety-like behavior. DLE animals did not show signs of increased anxiety in the EPM. Similarly, the LD box test did not reveal any significant behavioral differences between DLE and control animals. These findings suggest that DLE may not have an impact on risk and light aversion behaviors. However, DLE animals displayed behavioral changes in the OF. They displayed a 20% increase in locomotor activity, as evidenced by greater total distance travelled and higher average speed. This heightened activity could be interpreted as an anxiety response, potentially reflecting increased restlessness or agitation in a novel environment. We note that animals from both groups were sleeping for more than 80% of the 2 hours before the test. As such, differences in activity do not appear to be linked to differences in behavior prior to testing. The lack of overall difference in the time spent in the different zones of the OF between lighting conditions suggests that, while overall activity was increased, spatial preferences typically associated with anxiety were not significantly altered. However, sex-specific analysis revealed an interaction between lighting condition and spatial exploration for females. We found that while control females spent 70% of the test at the periphery of the OF, DLE females showed a lack of spatial preference, spending only 55% of the test time in the periphery. While these specific differences did not reach significance in post-hoc testing, this unexpected reduction in thigmotaxis in DLE females presents an intriguing paradox. Rather than indicating reduced anxiety, the combination of increased locomotion and reduced wall-hugging behavior might indicate an altered risk assessment strategy. This highlights the complexity of interpreting rodent anxiety behaviors and the importance of using multiple behavioral assays (Ramos, 2008).

To complement these results, the presence of DLE-induced stress responses was investigated using blood corticosterone concentration. The assay revealed the expected circadian pattern of blood corticosterone, with higher concentrations at ZT14 compared to ZT2 for both sexes. This

aligns with the well-established circadian rhythm of glucocorticoid secretion in rodents, with a peak at the start of the active phase (Chung et al., 2011; Dickmeis, 2009). This finding suggests that the core circadian regulation of the hypothalamic-pituitary-adrenal (HPA) axis remains intact under chronic DLE. We also found a main effect of lighting condition in females, with DLE animals showing higher corticosterone levels relative to controls. This could indicate that DLE can modulate the stress response system in a sex-specific manner. This finding is particularly noteworthy given the known interactions between the circadian system, stress responses, and sex hormones (Bailey & Silver, 2014). The absence of this effect in males underscores the importance of considering sex as a biological variable in circadian and stress-related research (Krizo & Mintz, 2014).

However, we note that the elevated corticosterone concentration of DLE females at ZT14 may rise from the lack of differences between groups under LD. Indeed, female control animals do not show the clear circadian pattern of corticosterone levels, with similar concentrations at both ZT2 and ZT14. Because corticosterone concentrations peak around dark onset, we expect corticosterone levels to be high at ZT14 for both lighting conditions. Studies have shown that the estrous cycle significantly affects plasma corticosterone levels in female rats, with a maximum concentration at proestrus (Carey et al., 1995). No changes in the acrophase of corticosterone rhythms were reported between males and females, but differences in concentration depending on the stage of the females' cycle were found (Atkinson & Waddell, 1997). This cycle-dependent variation introduces complexity when interpreting female corticosterone data. An important methodological consideration is that our LD and DLE female groups were housed in separate light-tight chambers, which could have resulted in group-specific estrous cycle synchronization. Though the evidence is limited, it has been shown that female rodents housed together often synchronize their estrous cycles through pheromonal communication (McClintock, 1983). While our animals were singly housed, pheromonal communication persists within an LTC. The lack of rhythmicity in our control females may thus reflect natural estrus variability between groups. As such, it is difficult to conclude whether

our results show an impact of DLE exposure on corticosterone concentration in females, or a deviation from baseline from controls.

Follow-up studies would benefit from more frequent sampling of corticosterone across the full 24 hour cycle to better characterize the potential alterations under DLE. Non-terminal blood collection methods, such as ventral tail vein blood collection, would provide greater temporal resolution without requiring additional terminal procedures. Unfortunately, such methods were not possible in this study due to licensing restrictions as well as the sample volume required. An alternative approach would be to monitor estrous cycles through vaginal cytology prior to corticosterone sampling, allowing for stage-matched comparisons between LD and DLE females (Byers et al., 2012). This would minimize confounding effects of hormonal fluctuations. However, the handling and sampling required for estrus determination could itself act as a stressor, potentially confounding the assessment of DLE effects on stress responses (Morgan & Tromborg, 2007). This methodological trade-off highlights the challenge of isolating lighting effects from procedural influences in neuroendocrine studies.

The observed changes in anxiety-like behaviors and stress responses were subtle, exhibiting both context-dependency, with different behavioral tests revealing distinct aspects of anxiety, and sex-specificity, with females showing more pronounced behavioral and hormonal responses to extended DLE exposure. This pattern suggests a nuanced rather than generalized effect of DLE on stress and anxiety.

Chronic DLE exposure shifted the circadian profile of object recognition memory.

This study investigated the effects of long-term DLE exposure on recognition memory in mice, using both novel object and novel odor recognition tasks. In the novel object recognition task, while we observed no significant differences in overall exploratory activity, as measured by total distance traveled, we found a notable interaction between time of day and lighting

condition for both the number of investigations and time spent investigating the novel object. Intriguingly, DLE animals showed an increase in novelty preference from ZT2 to ZT14, whereas control animals exhibited a decrease over the same period. This pattern suggests that chronic DLE exposure may alter the circadian regulation of recognition memory processes. These results are consistent with the reversal of short-term memory performance, as assessed by a spontaneous recognition memory task, following two weeks of DLE (Tam et al., 2021).

The enhanced performance of DLE animals during the evening (ZT14) could be interpreted in several ways. One possibility is that DLE leads to a phase shift in cognitive performance rhythms, resulting in improved recognition memory during the early night. This interpretation aligns with previous studies showing that circadian disruption can affect the timing of peak cognitive performance (Gerstner & Yin, 2010). This is also supported by previous short-term DLE findings, showing that performance is affected by prior sleep (Tam et al., 2021). We have shown that DLE animals sleep more than controls between ZT12 and ZT14. This increase in sleep proportion during the two hours before the evening recognition memory task may thus lead to a better performance. Alternatively, DLE exposure could be associated with chronic stress and might enhance certain aspects of cognitive function, particularly during the animals' active phase. This idea is consistent with research demonstrating that predictable chronic mild stress can sometimes improve cognitive performance (Parihar et al., 2011). However, we have previously shown that DLE animals only exhibited limited signs of stress and anxiety in the various assays used in this study. It thus seems like the increased evening performance displayed by DLE animals is most probably a result of increased sleep prior to the recognition memory task.

In comparison, the novel odor recognition test did not yield significant effects of time or lighting condition. The fact that novelty preference often did not differ from chance suggests that this test may not have been sufficiently sensitive to detect potential differences. This could

be due to various factors, including the choice of odors, their concentration, or the specific timing of the test. Future studies might benefit from optimizing the odor recognition protocol.

Table 2.1. Summary of the observed consequences of extended DLE exposure in mice. Effects are expressed as a reduction (↓), an alteration (Δ), or no change (∅).

Measure	Significant effects of chronic DLE
Locomotor activity	Δ onset and distribution, ↓ relative amplitude
PIR-defined sleep	Δ onset and distribution
Body temperature	Δ phase
Body mass	∅
Clinical blood chemistry	Δ total cholesterol, glycerol and TAG levels in females
Stress responses	Δ nighttime corticosterone levels in females
Anxiety behavior	↑ distance travelled and speed in the OF
Recognition memory	Δ timing of performance (object)

2.5. Conclusion

Our results demonstrate that chronic DLE exposure induces a coordinated realignment of circadian rhythms rather than causing fragmentation or disruption. This raises important questions about how we define "circadian disruption" in experimental contexts. While abrupt phase shifts, constant light, or jet lag models clearly disrupt circadian organization, our DLE protocol reveals a more nuanced response where the circadian system adapts to recognize the new effective dark onset at ZT16. The preservation of rhythm robustness, period, and internal temporal relationships, despite the phase delay, suggests successful system-wide entrainment to DLE conditions rather than disruption per se.

Nevertheless, this temporal reorganization was not without physiological consequences. The sex-specific effects on metabolism and stress responses, with females showing greater vulnerability to lipid disruptions and corticosterone alterations, indicates that adaptation to

altered light environments may carry metabolic costs even when circadian timing mechanisms remain intact.

Our findings have important implications for understanding human responses to modern light environments, where evening light exposure has become increasingly common. The subtle but meaningful physiological changes we observed, particularly in females, suggest that even when circadian rhythms appear robust, altered lighting conditions may still impact downstream metabolic and stress regulatory systems in a sex-dependent manner. These results underscore the importance of considering sex as a biological variable in circadian studies (and in all research), and suggest that even relatively mild alterations in evening light exposure can have measurable physiological impacts.

2.6. Supplemental Material

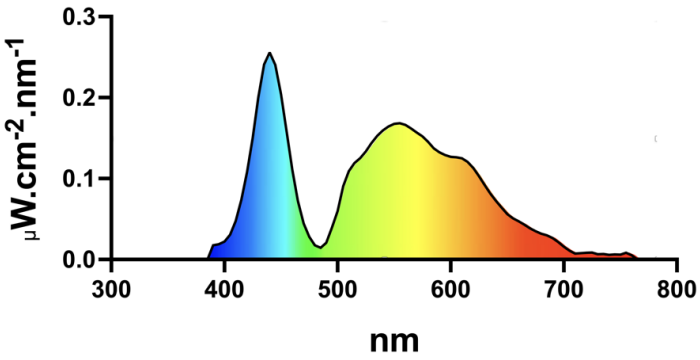

Supplemental Figure 2.1. Spectral power distribution of the DLE lights.

Supplemental Table 2.1. Spectral power distribution of the DLE lights.

nm	µW.cm^{-2}.s^{-1}	nm	µW.cm^{-2}.s^{-1}
300	0	545	0.164316618
305	0	550	0.167658232
310	0	555	0.168416402
315	0	560	0.166216938
320	0	565	0.16183962
325	0	570	0.156844078
330	0	575	0.152198671
335	0	580	0.145527025
340	0	585	0.137408206
345	0	590	0.132347966
350	0	595	0.129034248
355	0	600	0.126804138
360	0	605	0.126383689
365	0	610	0.125083679
370	0	615	0.120684475
375	0	620	0.11292367
380	0	625	0.102859281
385	0	630	0.09221481
390	0.017611299	635	0.081418228
395	0.01887492	640	0.072442635
400	0.022292794	645	0.064297172
405	0.030660634	650	0.05599426
410	0.047488229	655	0.050940238
415	0.073464049	660	0.047309051
420	0.108219057	665	0.043217326
425	0.150183652	670	0.038561346
430	0.20019029	675	0.034924975
435	0.240916939	680	0.031974054
440	0.2558743	685	0.029786514
445	0.240298235	690	0.026649843
450	0.203693402	695	0.02157545
455	0.157514252	700	0.015703372
460	0.111142137	705	0.010781252
465	0.072532035	710	0.007299052
470	0.044431723	715	0.007726199
475	0.028032026	720	0.008271367
480	0.017592049	725	0.008592281
485	0.01442389	730	0.006463777
490	0.020667521	735	0.006715113
495	0.039107497	740	0.00567436
500	0.059783884	745	0.006250914
505	0.090536232	750	0.006033707
510	0.109157816	755	0.008335726
515	0.11919911	760	0.00521248
520	0.125368111	765	0
525	0.133374633	770	0
530	0.143622208	775	0
535	0.152595807	780	0
540	0.159331365		

A. $$IS = \frac{N \sum_{h=1}^{p} (\bar{X}_h - \bar{X})^2}{p \sum_{h=1}^{N} (\bar{X}_i - \bar{X})^2}$$

B. $$IV = \frac{N \sum_{i=2}^{N} (X_i - X_{i-1})^2}{(N-1) \sum_{i=1}^{N} (\bar{X} - X_i)^2}$$

C. $$RA = \frac{M10 - L5}{M10 + L5}$$

D. $$TA = \frac{\sum_{i=1}^{N} X_i}{D}$$

E. $$LPA = \frac{TA_l}{TA_l + TA_d}$$

Supplemental Figure 2.2. Calculation of circadian disruption measures. **A.** Inter-daily stability (IS), where N is the number of data points, p is the number of data points per day, $\bar{X}$ is the mean of all data, $\bar{X}_h$ are the hourly means, and X_i are the individual data points. **B.** Intra-daily variability (IV), where N is the total number of data points, $\bar{X}$ is the mean of all data, and X_i are the individual data points. **C.** Relative amplitude (RA), where $M10$ is the most active 10 h period, and $L5$ is the least active 5 h period over the average 24 h. **D.** Total activity (TA) per day, where N is the number of data points, X_i are the individual data points, and D is the number of days. **E.** Light-phase activity (van der Vinne et al.) as a percentage of total daily activity, where TA_l is the total activity per day in the light phase, and TA_d is the total activity per day in the dark phase.

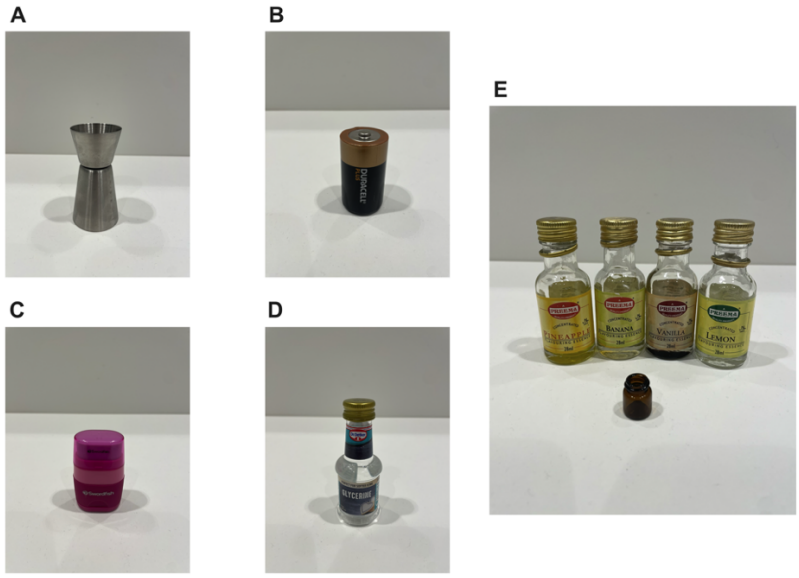

Supplemental Figure 2.3. Objects and odors used for the recognition memory tasks. Objects included **A.** stainless steel jigger (4.5 D x 8.5 H cm), **B.** D battery (3 D x 6 H cm, Duracell), **C.** pink rubber eraser (3.5 L x 2.5 W x 6 H cm, Swordfish), and **D.** icing glycerin plastic bottle (3.5 D x 9 H cm, Dr. Oetker). Odors included **E.** lemon, banana, pineapple, and vanilla concentrated flavoring essences (Preema) in small brown glass vials (1.5 D x 2.2 H cm, with a circular opening of 0.7 D cm).

Supplemental Table 2.2. Experimental design for the novel object and odor recognition tests. Animals went through two trials of novel object recognition tasks, followed by two trials of novel odor recognition tasks. The order of trials was counter-balanced by the time of day and objects/odors. Stimulus pairs of familiar/new objects were as follows: **A**. battery/jigger, **B**. jigger/battery, **C**. bottle/eraser, **D**. eraser/bottle. Stimulus pairs of familiar/new odors were as follows: **E**. banana/pineapple, **F**. pineapple/banana, **G**. lemon/vanilla, **H**. vanilla/lemon. CM = control male, CF = control female, EM = experimental male, EF = experimental female.

Animal ID	Condition	Sex	ZT	Stimulus	ZT	Stimulus	ZT	Stimulus	ZT	Stimulus
CM1	LD	M	14	C	2	B	14	E	2	H
CM2	LD	M	14	C	2	A	14	E	2	H
CM3	LD	M	14	D	2	A	14	E	2	H
CM4	LD	M	2	A	14	D	2	G	14	F
CM5	LD	M	2	B	14	D	2	G	14	F
CM6	LD	M	2	B	14	C	2	G	14	F
EM1	DLE	M	14	D	2	A	14	F	2	G
EM2	DLE	M	14	D	2	B	14	F	2	G
EM3	DLE	M	14	C	2	B	14	F	2	G
EM4	DLE	M	2	B	14	D	2	H	14	E
EM5	DLE	M	2	A	14	D	2	H	14	E
EM6	DLE	M	2	A	14	C	2	H	14	E
CF1	LD	F	14	C	2	A	14	E	2	H
CF2	LD	F	14	C	2	A	14	E	2	H
CF3	LD	F	14	D	2	B	14	E	2	H
CF4	LD	F	2	B	14	D	2	G	14	F
CF5	LD	F	2	B	14	D	2	G	14	F
CF6	LD	F	2	A	14	C	2	G	14	F
EF1	DLE	F	14	D	2	B	14	F	2	G
EF2	DLE	F	14	D	2	B	14	F	2	G
EF3	DLE	F	14	C	2	A	14	F	2	G
EF4	DLE	F	2	A	14	C	2	H	14	E
EF5	DLE	F	2	A	14	C	2	H	14	E
EF6	DLE	F	2	B	14	D	2	H	14	E

A. $RI\ (\#\ of\ investigations) = \frac{\#\ of\ new\ investigations - \#\ of\ familiar\ investigations}{total\ \#\ of\ investigations}$

B. $RI\ (time\ investigating) = \frac{time\ investigating\ new - time\ investigating\ familiar}{total\ time\ investigating}$

Supplemental Figure 2.4. Calculation of the recognition index (RI). **A.** Recognition index for the number (#) of investigations of the objects or odors. **B.** Recognition index for the time spent investigating the objects or odors. A positive recognition index indicates a preference for the novel object or odor, while a negative one shows a preference for the familiar object or odor.

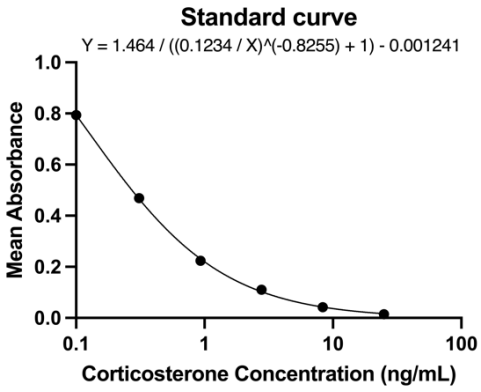

Supplemental Figure 2.5. Calculating corticosterone concentrations from the standard curve. The standard curve was created by plotting the mean absorbance for each standard (except B_0) on a linear y-axis against the concentration on a logarithmic x-axis. The best fit curve was drawn through the points on the graph. As samples were diluted, the concentration read from the standard curve was multiplied by the dilution factor.

Supplemental Table 2.3. Statistical testing of PIR activity for 24 wildtype (WT) C57BL/6J animals (1:1 male-female ratio) following 12 weeks of DLE exposure. Unpaired nonparametric Mann-Whitney tests (LD vs DLE), and two-way repeated-measures ANOVAs, with Time and Lighting condition as variables. Statistical significant tests are highlighted.

Circadian period	
Mann-Whitney	$U = 68$, $p = 0.8662$
Periodogram power	
Time x Lighting Interaction	$F_{(959, 21098)} = 0.8181$, $p > 0.9999$
Main effect of Time	$F_{(1.097, 24.12)} = 44.31$, $p < 0.0001$
Main effect of Lighting	$F_{(1, 22)} = 0.9705$, $p = 0.3353$
Max Qp	
Mann-Whitney	$U = 52$, $p = 0.2657$
Normalized daily activity	
Time x Lighting Interaction	$F_{(23, 506)} = 17.83$, $p < 0.0001$
Main effect of Time	$F_{(5.732, 126.1)} = 69.47$, $p < 0.0001$
Main effect of Lighting	$F_{(1, 22)} = 3.923$, $p = 0.0603$
Light phase activity	
Time x Lighting Interaction	$F_{(2, 44)} = 38.95$, $p < 0.0001$
Main effect of Time	$F_{(1.801, 39.62)} = 614.5$, $p < 0.0001$
Total activity	
Mann-Whitney	$U = 61$, $p = 0.5512$
Inter-daily stability	
Mann-Whitney	$U = 49$, $p = 0.1978$
Intra-daily variability	
Mann-Whitney	$U = 66$, $p = 0.7553$
Activity bouts	
Bout x Lighting Interaction	$F_{(7, 154)} = 2.257$, $p = 0.0325$
Main effect of Bout length	$F_{(1.269, 27.91)} = 153.2$, $p < 0.0001$
Main effect of Lighting	$F_{(1, 22)} = 1.492$, $p = 0.2348$
Relative amplitude	
Mann-Whitney	$U = 23$, $p = 0.0036$

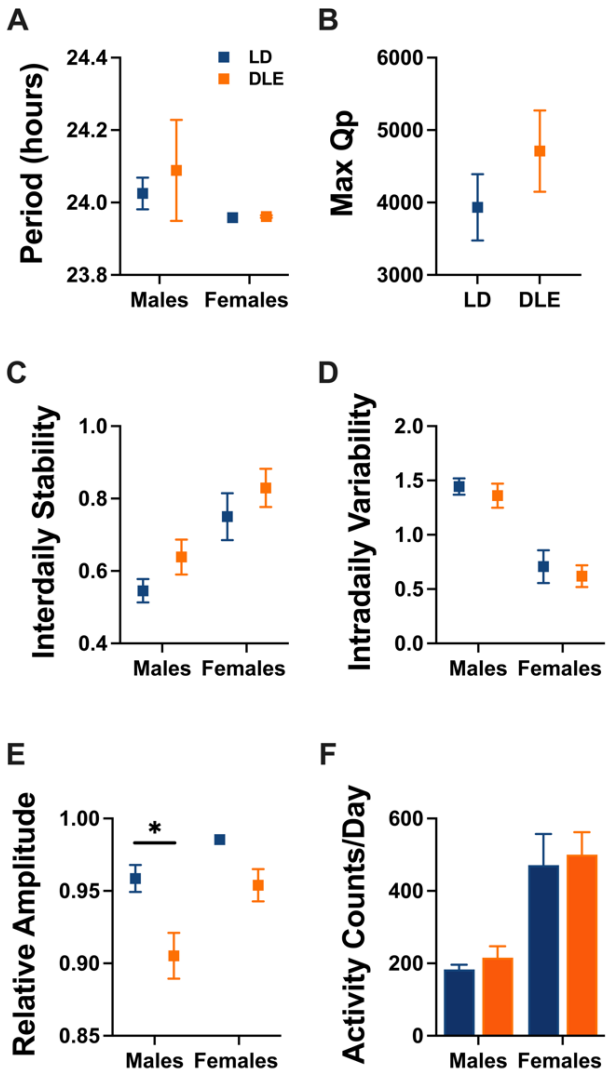

Supplemental Figure 2.6. Analysis of locomotor activity rhythms by sex following extended DLE exposure (N = 6 per group). **A.** Circadian period of activity rhythms. **B.** Maximum Qp values computed using the Chi-square periodogram (Sex, $F_{(1, 20)} = 21.84$, $p = 0.0001$). **C.** Inter-daily stability (Sex, $F_{(1, 20)} = 15.10$, $p = 0.0009$). **D.** Intra-daily variability (Sex, $F_{(1, 20)} = 43.17$, $p < 0.0001$). **E.** Relative amplitude (Sex, $F_{(1, 20)} = 12.21$, $p = 0.0023$). **F.** Total activity per day (Sex, $F_{(1, 20)} = 26.42$, $p < 0.0001$). Mean +/- SEM. Statistically significant post-hoc tests are indicated by an asterisk.

Supplemental Table 2.4. Statistical testing of PIR activity by sex for 24 WT C57BL/6J animals (1:1 male-female ratio) following 12 weeks of DLE exposure. Two way repeated-measures ANOVAs, with Sex and Lighting condition as variables. Statistical significant tests are highlighted.

Circadian period	
Sex x Lighting Interaction	$F_{(1, 20)} = 0.1740$, $p = 0.6810$
Main effect of Sex	$F_{(1, 20)} = 1.762$, $p = 0.1994$
Main effect of Lighting	$F_{(1, 20)} = 0.1740$, $p = 0.6540$
Max Qp	
Sex x Lighting Interaction	$F_{(1, 20)} = 0.4309$, $p = 0.5190$
Main effect of Sex	$F_{(1, 20)} = 21.84$, $p = 0.0001$
Main effect of Lighting	$F_{(1, 20)} = 2.216$, $p = 0.1522$
Inter-daily stability	
Sex x Lighting Interaction	$F_{(1, 20)} = 0.01783$, $p = 0.8951$
Main effect of Sex	$F_{(1, 20)} = 15.10$, $p = 0.0009$
Main effect of Lighting	$F_{(1, 20)} = 2.870$, $p = 0.1058$
Intra-daily variability	
Sex x Lighting Interaction	$F_{(1, 20)} = 0.0003037$, $p = 0.9863$
Main effect of Sex	$F_{(1, 20)} = 43.17$, $p < 0.0001$
Main effect of Lighting	$F_{(1, 20)} = 0.5826$, $p = 0.4542$
Relative amplitude	
Sex x Lighting Interaction	$F_{(1, 20)} = 1.018$, $p = 0.3250$
Main effect of Sex	$F_{(1, 20)} = 12.21$, $p = 0.0023$
Main effect of Lighting	$F_{(1, 20)} = 15.38$, $p = 0.0008$
Total activity	
Sex x Lighting Interaction	$F_{(1, 20)} = 0.0001073$, $p = 0.9752$
Main effect of Sex	$F_{(1, 20)} = 26.42$, $p < 0.0001$
Main effect of Lighting	$F_{(1, 20)} = 0.3029$, $p = 0.5882$

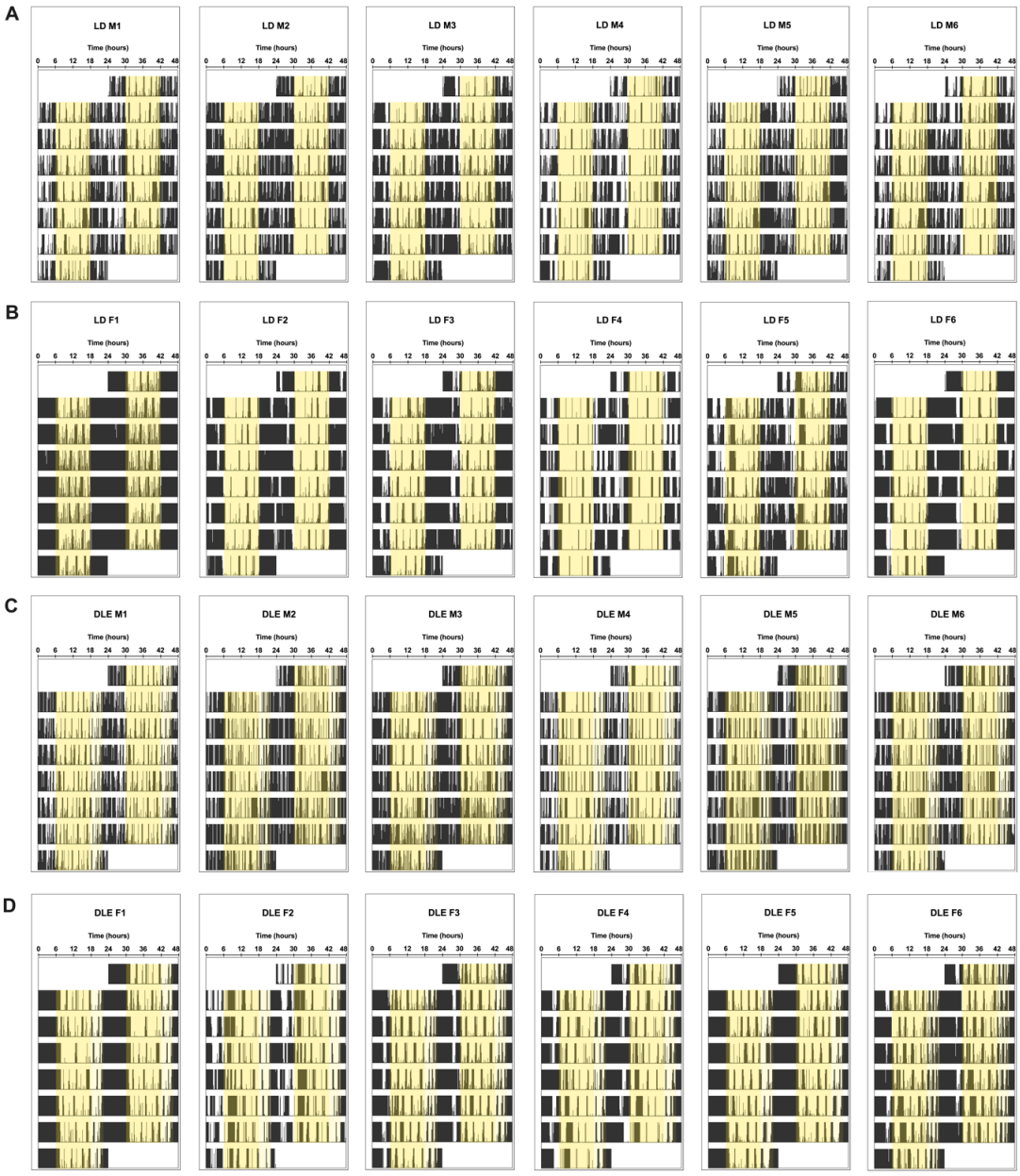

Supplemental Figure 2.7. Representative double-plotted actogram of locomotor activity during the 12th week of the experiment for **A.** 6 males and **B.** 6 females under 12:12 LD; and **C.** 6 males and **D.** 6 females under DLE. Yellow shading indicates light phases**.**

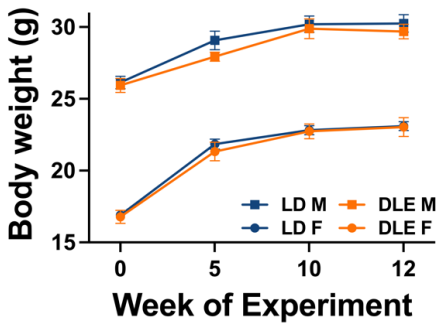

Supplemental Figure 2.8. Body weight measurements at baseline, and after 5 weeks, 10 weeks, and 12 weeks of DLE exposure in males (N = 12) and females (N = 12). Mean +/- SEM.

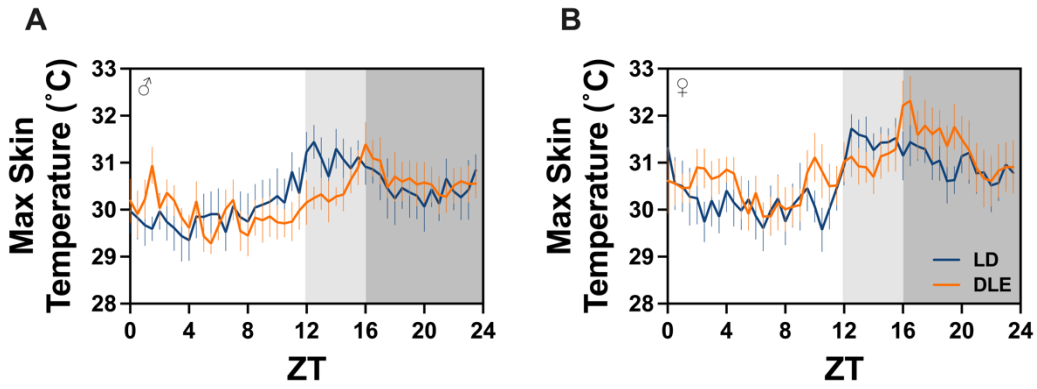

Supplemental Figure 2.9. Body temperature rhythms following 12 weeks of DLE exposure in **A.** Males (N = 11, one LD male excluded) (Time x Lighting, $F_{(47, 423)} = 2.863$, $p < 0.0001$), and **B.** Females (N = 12) (Time x Lighting, $F_{(47, 470)} = 1.665$, $p = 0.0049$). To provide an estimate of core body temperature, we computed maximum skin temperature measures over 60 s intervals, and averaged them in 30 min bins. Mean +/- SEM.

Supplemental Table 2.5. Statistical testing of maximum skin temperature rhythms for N = 11 male and N = 12 female WT C57BL/6J animals (one LD male excluded) following 12 weeks of DLE exposure. Two-way repeated-measures ANOVA, with Time (ZT2 vs ZT14) and Lighting condition (LD vs DLE) as variables with two levels. Statistical significant tests are highlighted.

Body Temperature	**Sex**		**Pooled**
	Males	**Females**	**Males & Females**
Time x Lighting Interaction	$F_{(47, 423)} = 2.86$, $p < 0.0001$	$F_{(47, 470)} = 1.67$, $p = 0.0049$	$F_{(47, 987)} = 2.84$, $p < 0.001$
Main effect of Time	$F_{(6.662, 59.95)} = 7.65$, $p < 0.0001$	$F_{(6.692, 66.92)} = 7.52$, $p < 0.0001$	$F_{(11.13, 233.7)} = 13.0$, $p < 0.0001$
Main effect of Lighting	$F_{(1, 9)} = 0.015$, $p = 0.9049$	$F_{(1, 10)} = 0.19$, $p = 0.6727$	$F_{(1, 21)} = 0.03$, $p = 0.8555$

Supplemental Table 2.6. Descriptive statistics of maximum skin temperature rhythms for N = 11 male and N = 12 female WT C57BL/6J animals (one LD male excluded) following 12 weeks of DLE exposure.

Body Temperature	Males		Females	
	LD	DLE	LD	DLE
Minimum	29.35	29.28	29.57	29.86
Maximum	31.44	31.39	31.73	32.32
Range	2.089	2.110	2.155	2.464
Mean	30.29	30.23	30.64	30.86
Std. Error of Mean	0.076	0.068	0.087	0.084
Lower 95% CI of mean	30.14	30.10	30.46	30.70
Upper 95% CI of mean	30.45	30.37	30.81	31.03

Supplemental Table 2.7. Statistical testing of anxiety behavior from the EPM for N = 24 WT C57BL/6J animals (1:1 male-female ratio) following 12 weeks of DLE exposure. Unpaired nonparametric Mann-Whitney tests (LD vs DLE), and two-way ANOVAs, with Lighting condition (LD vs DLE) and Zones (Closed vs Center vs Open) as variables. Statistical significant tests are highlighted.

EPM	Sex Males	Females	Pooled Males & Females
Total distance			
Mann-Whitney	$U = 11$, $p = 0.3095$	$U = 16$, $p = 0.8182$	$U = 51$, $p = 0.2415$
Entries in zones			
Zone x Lighting Interaction	$F_{(2, 30)} = 0.7312$, $p = 0.4897$	$F_{(2, 30)} = 1.616$, $p = 0.2155$	$F_{(2, 66)} = 2.044$, $p = 0.1376$
Main effect of Zone	$F_{(2, 30)} = 56.74$, $p < 0.0001$	$F_{(2, 30)} = 66.57$, $p < 0.0001$	$F_{(2, 66)} = 108.0$, $p < 0.0001$
Main effect of Lighting	$F_{(1, 30)} = 7.83e^{-017}$, $p > 0.9999$	$F_{(1, 30)} = 0.000$, $p > 0.9999$	$F_{(1, 66)} = 3.81e^{-017}$, $p > 0.9999$
Time spent in zones			
Zone x Lighting Interaction	$F_{(2, 30)} = 0.3161$, $p = 0.7314$	$F_{(2, 30)} = 0.0779$, $p = 0.9253$	$F_{(2, 66)} = 0.1764$, $p = 0.8387$
Main effect of Zone	$F_{(2, 30)} = 22.32$, $p < 0.0001$	$F_{(2, 30)} = 7.398$, $p = 0.0024$	$F_{(2, 66)} = 21.17$, $p < 0.0001$
Main effect of Lighting	$F_{(1, 30)} = 1.92e^{-019}$, $p > 0.9999$	$F_{(1, 30)} = 1.57e^{-018}$, $p > 0.9999$	$F_{(1, 66)} = 1.65e^{-018}$, $p > 0.9999$

Supplemental Table 2.8. Statistical testing of anxiety behavior from the LD box for N = 24 WT C57BL/6J animals (1:1 male-female ratio) following 12 weeks of DLE exposure. Unpaired nonparametric Mann-Whitney tests (LD vs DLE). There were no statistically significant tests.

LD box	Sex		Pooled
	Males	Females	Males & Females
Total distance	$U = 13$, $p = 0.4848$	$U = 13$, $p = 0.4848$	$U = 71$, $p = 0.9774$
# of transitions	$U = 13$, $p = 0.4860$	$U = 15$, $p = 0.6688$	$U = 51.5$, $p = 0.2458$
% in Light	$U = 10$, $p = 0.2403$	$U = 14$, $p = 0.5887$	$U = 65$, $p = 0.7125$

Supplemental Table 2.9. Statistical testing of anxiety behavior from the Open Field for 24 WT C57BL/6J animals (1:1 male-female ratio) following 12 weeks of DLE exposure. Unpaired nonparametric Mann-Whitney tests (LD vs DLE), and two-way repeated-measures ANOVAs, with Lighting condition (LD vs DLE) and Zones (Center vs Outer vs Corner) as variables. Statistical significant tests are highlighted.

Open Field	**Sex** **Males**	**Females**	**Pooled** **Males & Females**
Total distance			
Mann-Whitney	$U = 10$, $p = 0.2403$	$U = 7$, $p = 0.0931$	$U = 34$, $p = 0.0284$
Average speed			
Mann-Whitney	$U = 10.5$, $p = 0.2597$	$U = 7.5$, $p = 0.1039$	$U = 36.5$, $p = 0.0391$
Time spent in zones			
Zone x Lighting Interaction	$F_{(2, 30)} = 0.8668$, $p = 0.4305$	$F_{(2, 30)} = 5.761$, $p = 0.0076$	$F_{(2, 66)} = 2.186$, $p = 0.1204$
Main effect of Zone	$F_{(2, 30)} = 141.9$, $p < 0.0001$	$F_{(2, 30)} = 45.28$, $p < 0.0001$	$F_{(2, 66)} = 81.84$, $p < 0.0001$
Main effect of Lighting	$F_{(1, 30)} = 0.5851$, $p = 0.4503$	$F_{(1, 30)} = 0.5089$, $p = 0.4811$	$F_{(1, 66)} = 0.05021$, $p = 0.8234$

Supplemental Table 2.10. Statistical testing of the Novel Object Recognition test for 24 WT C57BL/6J animals (1:1 male-female ratio) following 12 weeks of DLE exposure. Two-way repeated-measures ANOVAs, with Time (ZT2 vs ZT14) and Lighting condition (LD vs DLE) as variables with two levels. Statistical significant tests are highlighted.

Novel Object Recognition	Sex		Pooled
	Males	Females	Males & Females
Total distance			
Time x Lighting Interaction	$F_{(1,10)} = 0.0009$, $p = 0.9759$	$F_{(1,10)} = 2.819$, $p = 0.1241$	$F_{(1, 22)} = 1.541$, $p = 0.2276$
Main effect of Time	$F_{(1, 10)} = 1.660$, $p = 0.2266$	$F_{(1, 10)} = 2.337$, $p = 0.1573$	$F_{(1, 22)} = 0.2052$, $p = 0.6550$
Main effect of Lighting	$F_{(1,10)} = 1.481$, $p = 0.2516$	$F_{(1,10)} = 0.0239$, $p = 0.8801$	$F_{(1, 22)} = 0.2019$, $p = 0.6576$
# of investigations			
Time x Lighting Interaction	$F_{(1,10)} = 11.09$, $p = 0.0076$	$F_{(1,10)} = 0.0471$, $p = 0.8326$	$F_{(1, 22)} = 4.928$, $p = 0.0370$
Main effect of Time	$F_{(1, 10)} = 3.105$, $p = 0.1085$	$F_{(1, 10)} = 0.4309$, $p = 0.5264$	$F_{(1, 22)} = 0.4678$, $p = 0.5011$
Main effect of Lighting	$F_{(1,10)} = 1.616$, $p = 0.2324$	$F_{(1,10)} = 0.0316$, $p = 0.8625$	$F_{(1, 22)} = 1.085$, p =0.3090
Time spent in zones			
Time x Lighting Interaction	$F_{(1,10)} = 3.330$, $p = 0.0980$	$F_{(1,10)} = 3.045$, $p = 0.1116$	$F_{(1,22)} = 5.415$, $p = 0.0296$
Main effect of Time	$F_{(1, 10)} = 3.271$, $p = 0.1006$	$F_{(1, 10)} = 0.439$, $p = 0.5224$	$F_{(1, 22)} = 1.452$, $p = 0.2409$
Main effect of Lighting	$F_{(1,10)} = 6.041$, $p = 0.0338$	$F_{(1,10)} = 0.531$, $p = 0.4829$	$F_{(1,22)} = 4.093$, $p = 0.0554$

Supplemental Table 2.11. Mean recognition index scores for the Novel Object Recognition test, disaggregated by minute, and pooled across the 3 min testing phase, expressed as the time spent investigating the objects. Two-way repeated-measures ANOVAs, with Time (ZT2 vs ZT14) and Lighting condition (LD vs DLE) as variables with two levels. Statistical significant tests are highlighted.

Time spent investigating	Lighting Condition	Minute of testing phase			Pooled
		0-60 s	60-120 s	120-180 s	0-180 s
ZT2	LD	0.251 ± 0.098	0.482 ± 0.139	0.497 ± 0.153	0.442 ± 0.085
	DLE	0.592 ± 0.098	0.287 ± 0.198	0.455 ± 0.130	0.490 ± 0.146
ZT14	LD	0.135 ± 0.166	0.179 ± 0.181	0.160 ± 0.197	0.157 ± 0.146
	DLE	0.637 ± 0.105	0.584 ± 0.121	0.386 ± 0.178	0.581 ± 0.054
Time x Lighting Interac.		$F_{1, 22)} = 0.605$, $p = 0.445$	$F_{1, 22)} = 5.47$, $p = 0.029$	$F_{1, 22)} = 1.65$, $p = 0.213$	$F_{1, 22)} = 5.42$, $p = 0.029$
Main effect of Time		$F_{1, 22)} = 0.120$, $p = 0.732$	$F_{1, 22)} = 0.0007$, $p = 0.98$	$F_{1, 22)} = 1.29$, $p = 0.268$	$F_{1, 22)} = 1.45$, $p = 0.241$
Main effect of Lighting		$F_{1, 22)} = 9.806$, $p = 0.005$	$F_{1, 22)} = 0.30$, $p = 0.589$	$F_{1, 22)} = 0.01$, $p = 0.933$	$F_{1, 22)} = 4.09$, $p = 0.055$

Supplemental Table 2.12. Statistical testing of the Novel Odor Recognition test for 24 WT C57BL/6J animals (1:1 male-female ratio) following 12 weeks of DLE exposure. Two-way repeated-measures ANOVAs, with Time (ZT2 vs ZT14) and Lighting condition (LD vs DLE) as variables with two levels. There were no statistically significant results.

Novel Object Recognition	Sex Males	Females	Pooled Males & Females
Total distance			
Time x Lighting Interaction	$F_{(1,10)} = 0.074$, $p = 0.7912$	$F_{(1,10)} = 0.5885$, $p = 0.4607$	$F_{(1, 22)} = 0.5380$, $p = 0.4710$
Main effect of Time	$F_{(1, 10)} = 3.395$, $p = 0.0952$	$F_{(1, 10)} = 1.1095$, $p = 0.7476$	$F_{(1, 22)} = 2.543$, $p = 0.1250$
Main effect of Lighting	$F_{(1,10)} = 1.344$, $p = 0.2733$	$F_{(1,10)} = 0.1444$, $p = 0.7119$	$F_{(1, 22)} = 1.088$, $p = 0.3082$
# of investigations			
Time x Lighting Interaction	$F_{(1,10)} = 0.1403$, $p = 0.7158$	$F_{(1,10)} = 0.0049$, $p = 0.9457$	$F_{(1, 22)} = 0.09535$, $p = 0.7604$
Main effect of Time	$F_{(1, 10)} = 0.3256$, $p = 0.5808$	$F_{(1, 10)} = 0.0914$, $p = 0.7687$	$F_{(1, 22)} = 0.02214$, $p = 0.8831$
Main effect of Lighting	$F_{(1,10)} = 0.4952$, $p = 0.4977$	$F_{(1,10)} = 1.002$, $p = 0.3404$	$F_{(1, 22)} = 1.490$, $p =0.2352$
Time spent in zones			
Time x Lighting Interaction	$F_{(1,10)} = 0.0166$, $p = 0.9001$	$F_{(1,10)} = 0.2720$, $p = 0.6133$	$F_{(1, 22)} = 0.2445$, $p = 0.6259$
Main effect of Time	$F_{(1, 10)} = 0.4087$, $p = 0.5370$	$F_{(1, 10)} = 0.0279$, $p = 0.8705$	$F_{(1, 22)} = 0.09588$, $p = 0.7597$
Main effect of Lighting	$F_{(1,10)} = 0.2171$, $p = 0.6513$	$F_{(1,10)} = 0.4474$, $p = 0.5187$	$F_{(1, 22)} = 1.181e^{-6}$, $p = 0.9991$

Supplemental Table 2.13. Statistical testing of corticosterone concentration for 24 WT C57BL/6J animals (1:1 male-female ratio) following 12 weeks of DLE exposure. Two-way ANOVA, with Time (ZT2 vs ZT14) and Lighting condition (LD vs DLE) as variables with two levels. Statistical significant tests are highlighted.

Corticosterone Concentration	Sex		Pooled
	Males	Females	Males & Females
Time x Lighting Interaction	$F_{(1, 8)} = 0.7429$, $p = 0.4138$	$F_{(1, 8)} = 2.371$, $p = 0.1621$	$F_{(1, 20)} = 1.636$, $p = 0.2155$
Main effect of Time	$F_{(1, 8)} = 11.98$, $p = 0.0085$	$F_{(1, 8)} = 5.911$, $p = 0.0411$	$F_{(1, 20)} = 12.36$, $p = 0.0022$
Main effect of Lighting	$F_{(1, 8)} = 0.4553$, $p = 0.5189$	$F_{(1, 8)} = 8.010$, $p = 0.0221$	$F_{(1, 20)} = 2.901$, $p = 0.1040$

Supplemental Table 2.14. Statistical testing of the clinical blood chemistry panel for 24 WT C57BL/6J animals (1:1 male-female ratio) following 12 weeks of DLE exposure. Two-way ANOVA and Holm-Šídák's multiple comparisons, with Time (ZT2 vs ZT14) and Lighting condition (LD vs DLE) as variables with two levels. One sample (female, ZT14, DLE) only yielded results for glucose concentration. ALT concentrations were unavailable for four samples (1 male, ZT2, LD; 1 male, ZT14, LD; 1 female, ZT14, LD; 1 female, ZT14, DLE). Statistical significant tests are highlighted.

Clinical Blood Chemistry		Interaction	Main effects	
		Time x Lighting	Time	Lighting
Glucose	♂	$F_{(1, 8)} = 2.281$, $p = 0.1694$	$F_{(1, 8)} = 0.6148$, $p = 0.4556$	$F_{(1, 8)} = 0.5161$, $p = 0.4930$
	♀	$F_{(1, 8)} = 0.2145$, $p = 0.6556$	$F_{(1, 8)} = 0.1500$, $p = 0.7086$	$F_{(1, 8)} = 2.738$, $p = 0.1366$
	♂♀	$F_{(1, 20)} = 1.200$, $p = 0.2864$	$F_{(1, 20)} = 0.2439$, $p = 0.6268$	$F_{(1, 20)} = 2.179$, $p = 0.1555$
OBB-Glucose	♂	$F_{(1, 8)} = 2.314$, $p = 0.1667$	$F_{(1, 8)} = 0.6549$, $p = 0.4418$	$F_{(1, 8)} = 0.4447$, $p = 0.5236$
	♀	$F_{(1, 7)} = 0.000492$, $p = 0.9829$	$F_{(1, 7)} = 0.7161$, $p = 0.4254$	$F_{(1, 7)} = 1.295$, $p = 0.2029$
	♂♀	$F_{(1, 19)} = 1.774$, $p = 0.1986$	$F_{(1, 19)} = 0.06630$, $p = 0.7996$	$F_{(1, 19)} = 1.313$, $p = 0.2660$
Cholesterol	♂	$F_{(1, 8)} = 0.4191$, $p = 0.5355$	$F_{(1, 8)} = 0.003341$, $p = 0.9553$	$F_{(1, 8)} = 0.2032$, $p = 0.6641$
	♀	$F_{(1, 7)} = 2.312$, $p = 0.1722$	$F_{(1, 7)} = 0.4505$, $p = 0.5236$	$F_{(1, 7)} = 9.331$, $p = 0.0185$
	♂♀	$F_{(1, 19)} = 0.5707$, $p = 0.4593$	$F_{(1, 19)} = 0.1236$, $p = 0.7291$	$F_{(1, 19)} = 0.1814$, $p = 0.6750$
Glycerol	♂	$F_{(1, 8)} = 0.1062$, $p = 0.7529$	$F_{(1, 8)} = 0.0288$, $p = 0.8695$	$F_{(1, 8)} = 0.1246$, $p = 0.7332$
	♀	$F_{(1, 7)} = 4.088$, $p = 0.0829$	$F_{(1, 7)} = 0.7479$, $p = 0.4158$	$F_{(1, 7)} = 6.856$, $p = 0.0345$
	♂♀	$F_{(1, 19)} = 0.9751$, $p = 0.3358$	$F_{(1, 19)} = 0.1107$, $p = 0.7429$	$F_{(1, 19)} = 1.644$, $p = 0.2152$
HDL Cholesterol	♂	$F_{(1, 8)} = 0.8245$, $p = 0.3904$	$F_{(1, 8)} = 0.3277$, $p = 0.5828$	$F_{(1, 8)} = 0.2244$, $p = 0.6483$
	♀	$F_{(1, 7)} = 0.002516$, $p = 0.9614$	$F_{(1, 7)} = 7.502$, $p = 0.0290$	$F_{(1, 7)} = 4.313$, $p = 0.0764$
	♂♀	$F_{(1, 19)} = 0.3406$, $p = 0.5664$	$F_{(1, 19)} = 2.514$, $p = 0.1293$	$F_{(1, 19)} = 0.1049$, $p = 0.7496$
Lactate	♂	$F_{(1, 8)} = 1.959$, $p = 0.1991$	$F_{(1, 8)} = 0.8640$, $p = 0.3798$	$F_{(1, 8)} = 0.9747$, $p = 0.3524$
	♀	$F_{(1, 7)} = 2.807$, $p = 0.1378$	$F_{(1, 7)} = 10.67$, $p = 0.0137$	$F_{(1, 7)} = 1.738$, $p = 0.2289$
	♂♀	$F_{(1, 19)} = 0.2120$, $p = 0.6505$	$F_{(1, 19)} = 0.07702$, $p = 0.7844$	$F_{(1, 19)} = 0.1641$, $p = 0.6899$
Triglycerides	♂	$F_{(1, 8)} = 0.7872$, $p = 0.4008$	$F_{(1, 8)} = 0.1597$, $p = 0.6999$	$F_{(1, 8)} = 0.0089$, $p = 0.9272$
	♀	$F_{(1, 7)} = 0.09463$, $p = 0.7673$	$F_{(1, 7)} = 3.317$, $p = 0.1113$	$F_{(1, 7)} = 9.136$, $p = 0.0193$
	♂♀	$F_{(1, 19)} = 0.02340$, $p = 0.8800$	$F_{(1, 19)} = 1.647$, $p = 0.2148$	$F_{(1, 19)} = 1.786$, $p = 0.1972$
NEFA	♂	$F_{(1, 8)} = 0.007351$, $p = 0.9338$	$F_{(1, 8)} = 0.2585$, $p = 0.6249$	$F_{(1, 8)} = 0.2925$, $p = 0.6033$
	♀	$F_{(1, 7)} = 4.171$, $p = 0.0804$	$F_{(1, 7)} = 2.025$, $p = 0.1977$	$F_{(1, 7)} = 4.556$, $p = 0.0702$
	♂♀	$F_{(1, 19)} = 0.2712$, $p = 0.6086$	$F_{(1, 19)} = 0.1966$, $p = 0.6625$	$F_{(1, 19)} = 0.7978$, $p = 0.3829$
ALT	♂	$F_{(1, 6)} = 0.001400$, $p = 0.9714$	$F_{(1, 6)} = 1.650$, $p = 0.2463$	$F_{(1, 6)} = 0.0588$, $p = 0.8164$
	♀	$F_{(1, 6)} = 3.357$, $p = 0.1166$	$F_{(1, 6)} = 1.864$, $p = 0.2212$	$F_{(1, 6)} = 0.04917$, $p = 0.8319$
	♂♀	$F_{(1, 16)} = 1.293$, $p = 0.2722$	$F_{(1, 16)} = 3.279$, $p = 0.0890$	$F_{(1, 16)} = 0.02730$, $p = 0.8708$
Urea	♂	$F_{(1, 8)} = 0.3400$, $p = 0.5759$	$F_{(1, 8)} = 0.04165$, $p = 0.8434$	$F_{(1, 8)} = 0.9256$, $p = 0.3642$
	♀	$F_{(1, 7)} = 0.4691$, $p = 0.5154$	$F_{(1, 7)} = 0.8842$, $p = 0.3783$	$F_{(1, 7)} = 0.3786$, $p = 0.5578$
	♂♀	$F_{(1, 19)} = 0.002716$, $p = 0.9590$	$F_{(1, 19)} = 0.3577$, $p = 0.5568$	$F_{(1, 19)} = 0.3230$, $p = 0.5765$
3-OHB	♂	$F_{(1, 8)} = 1.085$, $p = 0.3281$	$F_{(1, 8)} = 1.655$, $p = 0.2342$	$F_{(1, 8)} = 0.8634$, $p = 0.3800$
	♀	$F_{(1, 7)} = 1.816$, $p = 0.2197$	$F_{(1, 7)} = 0.2146$, $p = 0.6572$	$F_{(1, 7)} = 2.299$, $p = 0.1733$
	♂♀	$F_{(1, 19)} = 1.232$, $p = 0.2809$	$F_{(1, 19)} = 0.8929$, $p = 0.3565$	$F_{(1, 19)} = 0.2811$, $p = 0.6021$
CRP	♂	$F_{(1, 8)} = 0.2478$, $p = 0.6320$	$F_{(1, 8)} = 0.1749$, $p = 0.6868$	$F_{(1, 8)} = 0.5428$, $p = 0.4823$
	♀	$F_{(1, 7)} = 0.9123$, $p = 0.3713$	$F_{(1, 7)} = 0.1174$, $p = 0.7419$	$F_{(1, 7)} = 0.03875$, $p = 0.8495$
	♂♀	$F_{(1, 19)} = 0.1900$, $p = 0.6679$	$F_{(1, 19)} = 0.001396$, $p = 0.9706$	$F_{(1, 19)} = 0.1304$, $p = 0.7220$

Chapter 3. Circadian and Sleep Mechanisms Underlying the Effects of Dim Light in the Evening

3.1. Introduction

In our previously published data and in Chapter 2, we established both short and long-term consequences of DLE exposure in mice. We found that the acute effects of DLE persisted under chronic exposure, and further characterized disruptions in various physiological and behavioral parameters. Yet, the mechanisms underlying these disruptions remain somewhat unclear, particularly regarding the relative contributions of sleep alterations versus circadian rhythm disruption.

Based on activity patterns, the effects of DLE have been linked to disruptions of the circadian clock. However, changes in activity patterns could also result from masking, a phenomenon where light directly suppresses or enhances activity independent of the circadian clock (Mrosovsky, 1999). This raises an important consideration regarding the mechanisms underlying the observed activity delays under DLE conditions. The delay in activity onset could represent either true circadian entrainment with a phase shift of the clock, or masking effects where light suppresses activity during the dim phase without affecting the endogenous clock.

The regulation of sleep adds further complexity to this question. According to the two-process model of sleep regulation, sleep timing and quality are governed by the interaction between Process C (circadian) and Process S (homeostatic) (**Fig. 3.1**). Process C is controlled by the circadian clock and determines the timing of sleep propensity across the 24-hour day, while Process S represents homeostatic sleep pressure that builds during wakefulness and dissipates during sleep (Borbély et al., 2016). Under DLE conditions, we observed increased sleep during the dim phase, which could be due to either direct effects of light on Process C, or a masking effect of light on behavior that subsequently affects Process S.

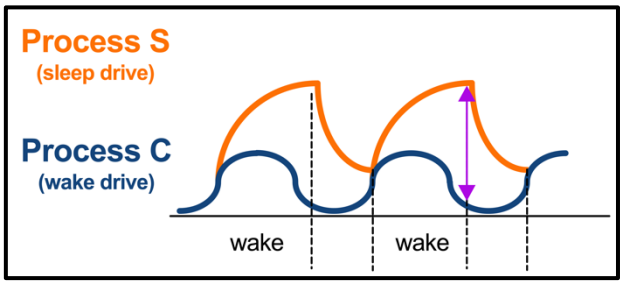

Figure 3.1. Schematic representation of the two-process model of sleep regulation. Sleep is primarily regulated by two processes: the homeostatic sleep drive (Process S) and the circadian wake drive (Process C). In this model, the greatest urge to sleep occurs when the distance between the two processes is the greatest, as shown by the purple arrow.

The distinct neural pathways that mediate masking versus circadian entrainment provide additional insight into the potential mechanisms underlying DLE effects. Masking is primarily mediated through retinal pathways projecting to non-SCN retinorecipient areas, such as the intergeniculate leaflet (IGL) and the olivary pretectal nucleus (OPN), which modulate behavior independently of the SCN (Harrington, 1997; Mrosovsky, 1999; Redlin, 2001). In contrast, true circadian entrainment occurs through the RHT, where intrinsic pRGCs transmit photic input directly to the SCN (Hattar et al., 2002). If sleep regulation is playing a role, then other brain regions involved in sleep/wake control, such as the ventrolateral preoptic area (VLPO), could also mediate the DLE effects (Saper et al., 2005). Recent work has identified adenosine-based regulatory mechanisms that allow sleep and circadian processes to interact, where adenosine encodes sleep history and modulates circadian entrainment by light (Jagannath et al., 2021).

We determined that a one-week DLE exposure would be sufficient for this mechanistic investigation, as our previous work demonstrated similar shifts in activity onset and behavioral patterns between 2-week and 12-week DLE exposures, suggesting that the core entrainment effects establish relatively quickly. Here, we designed an experiment to assess whether 4 hours of 20 lux evening light directly impacts the circadian system, or if the observed effects are mediated through altered sleep architecture. We combined sleep deprivation with transitions to constant darkness (DD) to separate these mechanisms. We hypothesized that if DLE effects

result from masking rather than true circadian entrainment, animals would immediately revert to initiating activity at the former LD transition (ZT12) upon release into DD. Conversely, if animals truly entrain to DLE, activity onsets in DD should persist from the delayed phase established under DLE conditions. Furthermore, by sleep depriving one group of animals during the final dim phase before transition to DD, we could determine whether increased sleep during this period is necessary for the physiological and behavioral effects observed under DLE.

3.2. Methods

Animals and Housing Conditions. 12 animals (1:1 male-female ratio) were used in this study. Wild-type C57BL/6J animals were purchased from Inotiv, Inc. (UK), and were about 8 weeks old at the beginning of the study. Animals were singly housed in large MB1 (NKP Isotec) open top cages (45 L x 28 W x 13 H cm) under a 12:12 LD cycle for a minimum of one week prior to the start of experiments. They had no prior history of regulated procedures. Food (Teklad 2916) and water were provided *ad libitum* throughout the study. The temperature and relative humidity of the animal room were maintained at 20–24°C and 45–65%. Pathogen-free conditions were maintained throughout the study by the animal facility. Serology, bacteriology, and parasitology reports (Surrey Diagnostics Ltd., UK) did not note any positive cases.

Lighting. Mice were housed in ventilated LTCs equipped with multiple cool-white LEDs (Luxeon Star LEDs, Quadica Developments Inc., Canada). These LEDs provided a light level of 200 photopic lux during the day, giving < 10 S-cone, 130 melanopic, 140 rhodopic and 150 M-cone opic lux. The spectral power distribution featured a higher, narrower peak at ~ 460 nm, and a lower, broader peak at ~ 560 nm (See **Chapter 2**, **Supp. Fig. 2.1**, **Supp. Table 2.1**).

Experimental Design. After a one-week baseline period under 12:12 LD, animals received DLE from ZT12 to ZT16 for 1 week. Evening light levels were kept at 20 lux, giving < 1 S-cone opic lux, 13 melanopic lux, 14 rhodopic lux and 15 M-cone opic lux (Lucas et al., 2024).

On the 8th day, animals were randomly assigned to receive regular DLE (N = 6, “DLE”), or sleep deprivation during ZT12-16 (N = 6, “DLE/SD”). Sleep deprivation was conducted using gentle handling and introduction of novel objects when animals displayed sleep-like behavior, without invoking stress responses. Both groups were then transferred to DD for 10 days. At the end of the experiment, mice were euthanized by cervical dislocation. Experimenters were not blind to the animals’ sex or lighting condition.

Compliance. This study is reported in accordance with the ARRIVE 2.0 guidelines. All experimental procedures were carried out at the University of Oxford, UK, in accordance with the University of Oxford Policy on the Use of Animals in Scientific Research and the United Kingdom Animals (Scientific Procedures) Act 1986, under Project License PP0911346 and Personal License I34186130.

Home Cage Activity Monitoring. A passive infrared sensor (PIR, Panasonic AMN32111) was positioned above each cage to monitor locomotor activity, following the validated method described by Brown et al. (2016). To optimize tracking accuracy, gaps beneath the food and water hoppers in MB1 cages were sealed using Perspex blocks, and nesting material (paper-based sizzle-nest or cotton fiber nestlets) was provided in a quantity that did not fully obscure the animal from the sensor. Within each LTC, six PIR sensors were connected to an Arduino (Arduino Uno R3) alongside a light-dependent resistor (Farnell, UK) to monitor the light environment. The Arduinos were interfaced with a Raspberry Pi (Raspberry Pi 3 B) and processed using Node-RED. PIR data were recorded at a 10 s temporal resolution. Data from the last 4 days of DLE exposure were used for the DLE analysis. All 10 days were used for the analysis of free-running behavior. PIR activity counts were averaged in 1 min bins and in 1 h bins to compute the different activity analyses.

Circadian Disruption Measures. Actograms and Chi-square periodogram were computed in ActogramJ (Schmid et al., 2011). Activity onsets were calculated using the median function (without zero activity) and a smoothing gaussian standard deviation of 5 min. Inter-daily

stability, intra-daily variability, relative amplitude, light-phase activity, and total activity were calculated in R (Brown et al., 2019; Witting et al., 1990). See equations in **Chapter 2**, **Supplemental Figure 2.2**. For activity period in DLE, we identified one definite outlier through the robust regression and outlier removal (ROUT) method using Q = 0.1% (one female with a period of 24.9 hours). As such this data point was removed from the analysis of DLE period. This outlier likely resulted from technical issues with activity detection rather than a true biological variation, as the value deviated substantially from the known circadian range for C57BL/6J mice.

Statistical Analyses. Statistical testing and plotting were conducted in Prism 10. Regular and repeated-measures two-way ANOVAs, with a Geisser-Greenhouse correction (for lack of sphericity), and Holm-Šídák's multiple comparisons test were computed. When comparing two groups, unpaired nonparametric Mann-Whitney tests were used, as the distribution of the data was not Gaussian. $\alpha = 0.05$ was adopted in all analyses. Mean ± SEM was used for all plots.

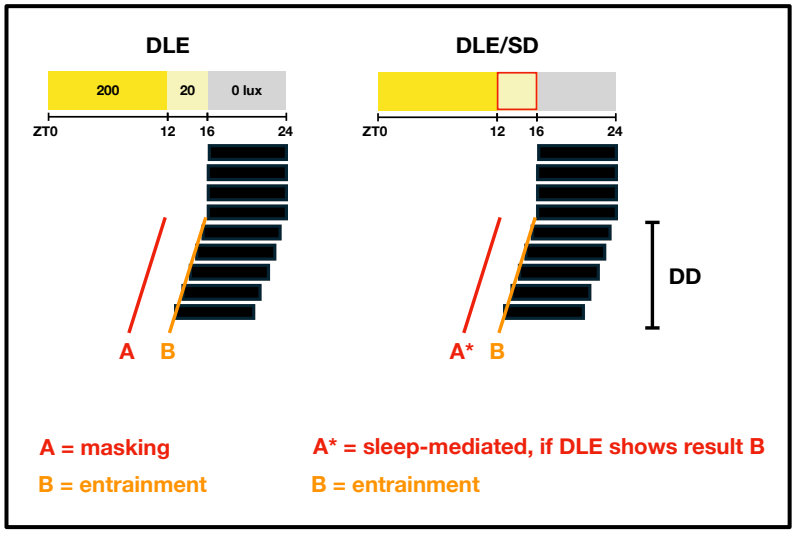

Figure 3.2. Experimental design to uncover the mechanisms mediating DLE effects. Following transition to DD, the onset of free-running behavior will reveal whether the delayed-effects of DLE are a result of negative masking or entrainment. If both the DLE and DLE/SD groups free-run from a delayed phase, then it will reveal true entrainment independent of sleep state during the dim phase. If the DLE/SD group begins to free-run from an earlier phase than the DLE group, then the phase delaying effects of DLE are sleep-mediated.

3.3. Results

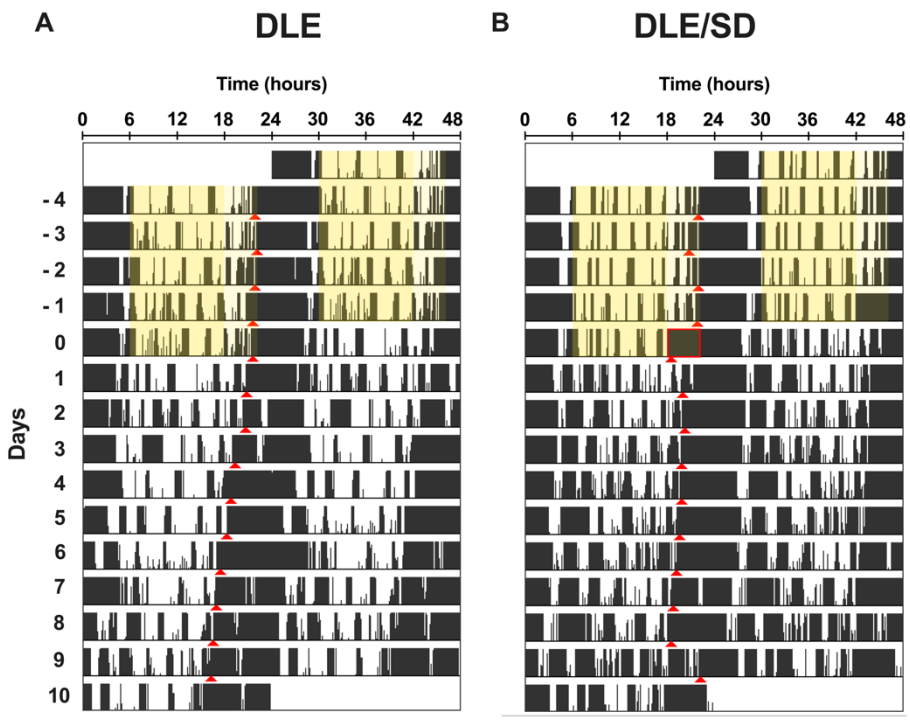

Figure 3.3. Representative double-plotted actogram of locomotor activity during 5 days of DLE (final days of a 1-week exposure) and 10 days of DD for **A.** one animal without sleep deprivation, and **B.** one animal experiencing sleep deprivation during ZT12-16 on the final day of DLE exposure. Yellow shading and red arrows indicate light phases and activity onsets, respectively**.** Sleep deprivation is marked by a red square.

Activity Onsets. All animals were exposed to 1 week of DLE exposure before being transferred into DD (**Fig. 3.3A**), with the DLE/SD group experiencing sleep deprivation (ZT12-16) on the final day of DLE exposure (**Fig. 3.3B**). Analysis of activity onsets revealed no differences between groups (Mean = 15.21 ± 0.12 ZT; Group, $F_{(1, 10)} = 2.981$, $p = 0.1150$; **Fig. 3.4**), with an average onset of activity between ZT15 and ZT15.5 under DLE. On the final day of DLE (day 0 in **Figure 3.4**), sleep deprivation was confirmed by a significant post-hoc difference in activity onset corresponding to ZT12 for the DLE/SD group. In DD, animals free-ran, as evidenced by an advance in the activity onsets throughout the 10 days (Time, $F_{(3.004, 30.04)} = 26.17$, $p < 0.0001$; **Fig. 3.4**). All actograms can be found in **Supplemental Figure 3.1**.

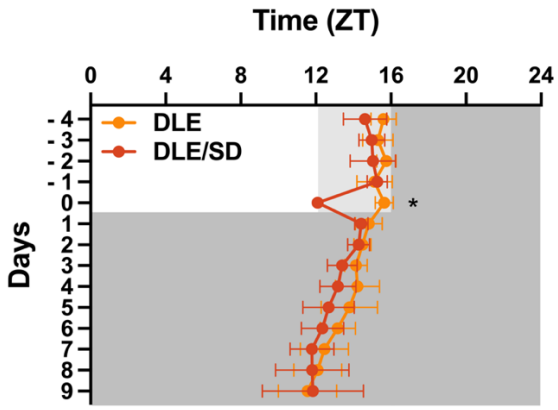

Figure 3.4. Activity onsets under DLE and DD (N = 6 per group). Data for 5 days of DLE (final days of a 1-week exposure) and 10 days of DD are represented. The DLE/SD group experienced sleep deprivation during ZT12-16 on the final day of DLE exposure (Day 0). Dark shading indicates dim/dark phases. Mean +/- SEM. Statistically significant multiple comparisons are indicated by an asterisk.

Locomotor Activity under DLE. Home cage locomotor activity rhythms were examined under DLE to confirm that both groups of animals had a comparable baseline pattern of activity. Under acute exposure to DLE, all animals exhibited a circadian period close to 24 hours (Mean = 23.99 ± 0.02 h; Mann-Whitney, $U = 14.5$, $p = 0.9675$; **Fig. 3.5A**). Chi-square periodogram analysis revealed no differences between groups in the distribution of periodogram power (Group, $F_{(1, 10)} = 2.661$, $p = 0.1339$; **Fig. 3.5B**), or maximum Qp (Mann-Whitney, $U = 13$, $p = 0.4848$; **Fig. 3.5C**). Averaged daily activity profiles revealed a main effect of Time (Time, $F_{(4.175, 41.75)} = 61.34$, $p < 0.0001$; **Supp. Fig. 3.2A**), but no main effect of Group (Group, $F_{(1, 10)} = 0.1864$, $p = 0.6751$; **Supp. Fig. 3.2A**), or interaction (Time x Group, $F_{(23, 230)} = 0.5583$, $p = 0.9507$; **Supp. Fig. 3.2A**). Similarly, the distribution of activity between the light, dim, and dark phases showed a main effect of Time (Time, $F_{(1.371, 13.71)} = 337.2$, $p < 0.0001$; **Supp. Fig. 3.2B**), but no main effect of Group (Group, $F_{(1, 10)} = 0.0625$, $p = 0.8076$; **Supp. Fig. 3.2B**), or interaction (Time x Group, $F_{(2, 20)} = 0.3526$, $p = 0.7072$; **Supp. Fig. 3.2B**). Additionally, there were no statistical differences in total daily activity (Mann-Whitney, $U = 12$, $p = 0.3939$; **Supp. Fig. 3.2C**), inter-daily stability (Mann-Whitney, $U = 11$, $p = 0.3090$; **Supp. Fig. 3.2D**), intra-daily variability (Mann-Whitney, $U = 17$, $p = 0.9372$; **Supp. Fig. 3.2E**), number and

distribution of activity bouts (Group, $F_{(1, 10)} = 0.5033$, $p = 0.4943$; **Supp. Fig. 3.2F**), or relative amplitude (Mann-Whitney, $U = 10$, $p = 0.2403$; **Supp. Fig. 3.2G**) between groups.

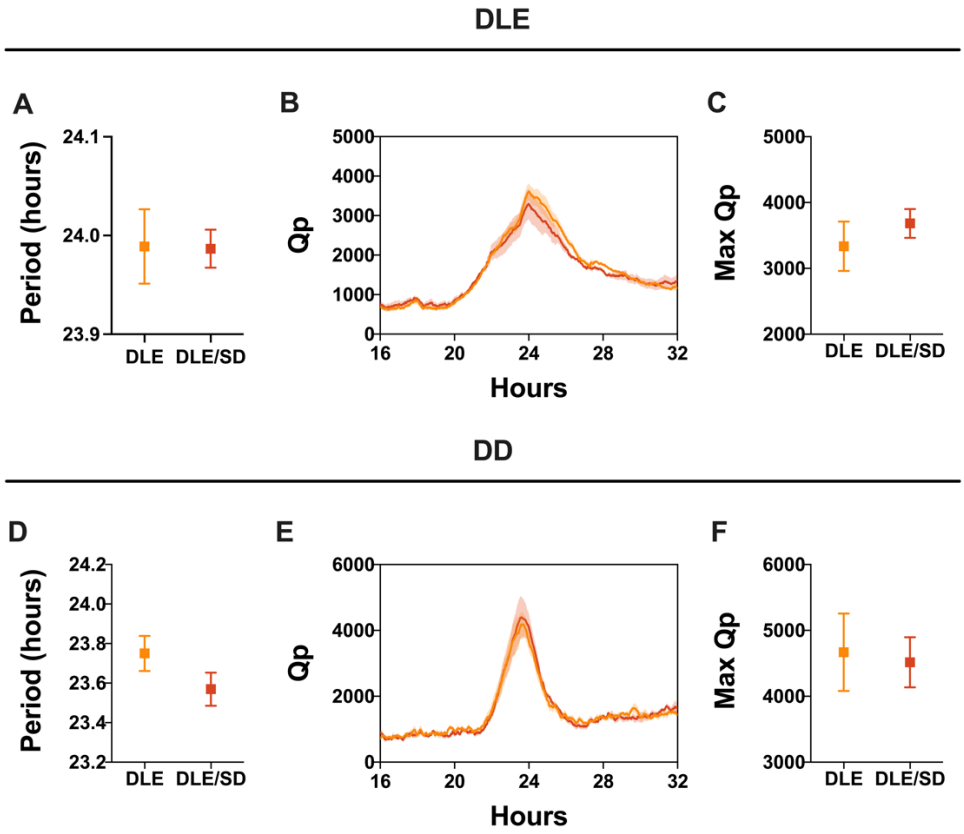

Figure 3.5. Chi-square periodogram analysis of locomotor activity rhythms under DLE and DD (N = 6 per group). **A.** Period of activity rhythms, **B.** Chi-square periodogram analysis, and **C.** Maximum Qp values for the control DLE group. **D.** Period of activity rhythms, **E.** Chi-square periodogram analysis, and **F.** Maximum Qp values for the control DLE/SD group, which was sleep deprived during the final dim phase (ZT12-16) before going into DD. Mean +/- SEM.

Free-Running Locomotor Activity in DD. Home cage locomotor activity rhythms were examined under DD to compare free-running behaviors between groups. Under DD, all animals exhibited a circadian period of about 23.7 hours (Mean = 23.66 ± 0.06 h; Mann-Whitney, $U = 8.5$, $p = 0.1429$; **Fig. 3.5D**). Chi-square periodogram analysis revealed no differences between groups in the distribution of periodogram power (Group, $F_{(1, 10)} = 0.1150$, $p = 0.7415$; **Fig. 3.5E**), or maximum Qp (Mann-Whitney, $U = 17$, $p = 0.9372$; **Fig. 3.5F**). Additionally, there were no statistical differences in total daily activity (Mann-Whitney, $U = 16$, $p = 0.8182$; **Supp.**

Fig. 3.3A), inter-daily stability (Mann-Whitney, $U = 10$, $p = 0.2403$; **Supp. Fig. 3.3B**), intra-daily variability (Mann-Whitney, $U = 13$, $p = 0.4848$; **Supp. Fig. 3.3C**), number and distribution of activity bouts (Group, $F_{(1, 10)} = 0.3469$, $p = 0.5690$; **Supp. Fig. 3.3D**), or relative amplitude (Mann-Whitney, $U = 11$, $p = 0.3095$; **Supp. Fig. 3.3E**) between groups.

Sex Differences. Data disaggregation by sex revealed distinct differences between the activity rhythms of males and females under both DLE conditions and during the transition to DD. Under 1 week of DLE, both sexes displayed similar profiles of daily activity (Sex, $F_{(1, 10)} = 0.5378$, $p = 0.4802$; **Supp. Fig. 3.4A**) and distribution between the light, dim, and dark phases (Sex, $F_{(1, 10)} = 0.0625$, $p = 0.8076$; **Supp. Fig. 3.4B**). However, females were significantly more active, as evidenced by higher total daily activity (Mann-Whitney, $U = 0$, $p = 0.0022$; **Supp. Fig. 3.4C**). Females also showed stronger rhythms with higher periodogram power (Sex, $F_{(1, 10)} = 22.54$, $p = 0.0008$; **Supp. Fig. 3.4D**) and maximum Qp values (Mann-Whitney, $U = 1$, $p = 0.0043$; **Supp. Fig. 3.4E**), though there were no differences in the activity period between sexes (Mann-Whitney, $U = 12.5$, $p = 0.6905$; **Supp. Fig. 3.4F**). Moreover, females exhibited more stable and consolidated rhythms, with higher inter-daily stability (Mann-Whitney, $U = 5$, $p = 0.0411$; **Supp. Fig. 3.4G**), and lower intra-daily variability (Mann-Whitney, $U = 0$, $p = 0.0022$; **Supp. Fig. 3.4H**). Analysis of activity bout distribution revealed a main effect of sex (Sex, $F_{(1, 10)} = 9.655$, $p = 0.0111$; **Supp. Fig. 3.4I**), and an interaction effect for the number and distribution of activity bouts (Bout length x Sex, $F_{(7, 70)} = 6.414$, $p < 0.0001$; **Supp. Fig. 3.4I**). Post-hoc testing showed that females had significantly fewer bouts of activity < 3 min compared to males. There were no differences in relative amplitude (Mann-Whitney, $U = 8$, $p = 0.1320$; **Supp. Fig. 3.4J**).

Following the transition to DD, sex differences in free-running behavior became further apparent. While there were no differences in overall periodogram power (Sex, $F_{(1, 10)} = 1.631$, $p = 0.2304$; **Supp. Fig. 3.5A**), females maintained higher maximum Qp values (Mann-Whitney, $U = 0$, $p = 0.0022$; **Supp. Fig. 3.5B**), and tended towards a shorter free-running period, though

this did not reach statistical significance (Mann-Whitney, $U = 6$, $p = 0.0584$; **Supp. Fig. 3.5C**). Females continued to be more active, as evidenced by increased total daily activity as compared to males (Mann-Whitney, $U = 0$, $p = 0.0022$; **Supp. Fig. 3.5D**). While inter-daily stability did not differ between sexes (Mann-Whitney, $U = 17$, $p = 0.9372$; **Supp. Fig. 3.5E**), females maintained lower intra-daily variability (Mann-Whitney, $U = 0$, $p = 0.0022$; **Supp. Fig. 3.5F**). Activity bout analysis showed a main effect of sex (Sex, $F_{(1, 10)} = 14.58$, $p = 0.0034$; **Supp. Fig. 3.5G**), and an interaction effect (Bout length x Sex, $F_{(7, 70)} = 10.54$, $p < 0.0001$; **Supp. Fig. 3.5G**), with post-hoc testing revealing that females had significantly fewer short activity bouts < 3 min compared to males. There were no differences in relative amplitude (Mann-Whitney, $U = 17$, $p = 0.9372$; **Supp. Fig. 3.5H**).

3.4. Discussion

In this study, we investigated the mechanisms underlying physiological and behavioral changes observed during acute DLE exposure. Specifically, we examined whether increased sleep during the dim phase plays a crucial role in the entrainment to this lighting condition. Our experimental design compared two groups of mice: one exposed to standard DLE followed by DD, and another that experienced sleep deprivation during the final dim phase (ZT12-16) before transitioning to DD. This approach allowed us to disentangle the direct effects of DLE on the circadian system from potential sleep-dependent mechanisms. Our results show that despite confirmed sleep deprivation during the dim phase, both groups exhibited remarkably similar free-running behavior upon release into DD.

Activity onset under acute DLE exposure was consistent across all animals, occurring around ZT15.2. This ~ 3.2 hour delay from the standard ZT12 onset aligns with our previous findings showing that both a 2-week and 12-week DLE exposure shifts activity onset by approximately 3-4 hours (Tam et al., 2021). Prior to sleep deprivation and transition to DD, we confirmed that there were no differences in the period, amplitude, strength, or stability of baseline activity rhythms between groups, ensuring both cohorts had entrained similarly to the DLE conditions.

Upon transition to DD, both groups demonstrated similar free-running behavior with a shortening of activity period to ~ 23.7 hours, consistent with the typical endogenous period of C57BL/6J mice (Schwartz & Zimmerman, 1990). Critically, all animals began free-running from ~ ZT14.6, and not from ZT12, demonstrating that the delay in activity onset represents true entrainment rather than a masking effect that would disappear under DD conditions. The preservation of this delayed phase in DD indicates that DLE directly impacts the circadian clock at the SCN level. Moreover, the absence of differences in activity onsets, periodogram power, total activity, rhythm stability, or fragmentation between sleep-deprived and control animals suggests that sleep during the dim phase is not necessary for entrainment to DLE conditions. The pronounced sex differences observed in our study reinforce our findings from the previous chapter, with females consistently exhibiting more robust, consolidated, and stable activity rhythms under both DLE and DD conditions relative to males.

One limitation of our experimental design is the single-day sleep deprivation protocol before transitioning to DD. It remains possible that altered sleep patterns during the preceding days of DLE exposure had already established lasting impacts on the circadian system that a single day of sleep deprivation could not reverse. A more comprehensive approach would involve sleep deprivation throughout the entire DLE exposure to fully rule out sleep-dependent mechanisms. On the other hand, sleep deprivation itself can influence the circadian system independently of sleep loss per se. Prior studies have shown that sleep deprivation can modulate phase shifting to light, either advancing or delaying circadian rhythms depending on timing, possibly through adenosine accumulation, which alters SCN light responsiveness (Burgess, 2010; Challet et al., 2001; Jagannath et al., 2021; Mistlberger et al., 1997). In our paradigm, this raises the possibility that the similar free-running behavior observed between groups could therefore reflect either independence of DLE entrainment from sleep state, or sleep deprivation-induced alterations in circadian timing that interact with the established DLE entrainment. Nevertheless, the consistent delay in free-running activity onset across both groups provides strong evidence for direct circadian entrainment to the dim evening light stimulus.

Our finding that sleep during the dim phase is not necessary for circadian entrainment to DLE has several parallels in human research. Multiple studies have demonstrated that the human circadian system remains responsive to light during sleep. Zeitzer and colleagues (2014) showed that millisecond flashes of light delivered during sleep were capable of phase-delaying the circadian clock, despite subjects remaining asleep throughout the light exposure (Zeitzer et al., 2014). Similarly, Figueiro and colleagues (2013) demonstrated that light pulses delivered through closed eyelids during sleep could suppress melatonin and phase-shift circadian rhythms, providing a mechanism for how light might affect circadian timing during sleep (Figueiro et al., 2013). This aligns with anatomical evidence that human eyelids transmit approximately 0.3-10% of environmental light depending on wavelength (Bierman et al., 2011). Therefore, these human studies support our finding that DLE exposure, independent of sleep state, can directly affect mouse circadian physiology and behavior.

3.5. Conclusion

Our results demonstrate that the phase-delaying effects of DLE appear to occur through direct photic entrainment rather than through sleep-dependent mechanisms. This finding has important implications for understanding how modern light environments affect circadian biology. Even passive exposure to dim light, regardless of whether an individual is awake or asleep during this exposure, may directly impact physiology and behavior through photic pathways. The understanding of these mechanisms will further inform recommendations for optimizing light environments to support healthy circadian rhythms in modern societies.

3.6. Supplemental Material

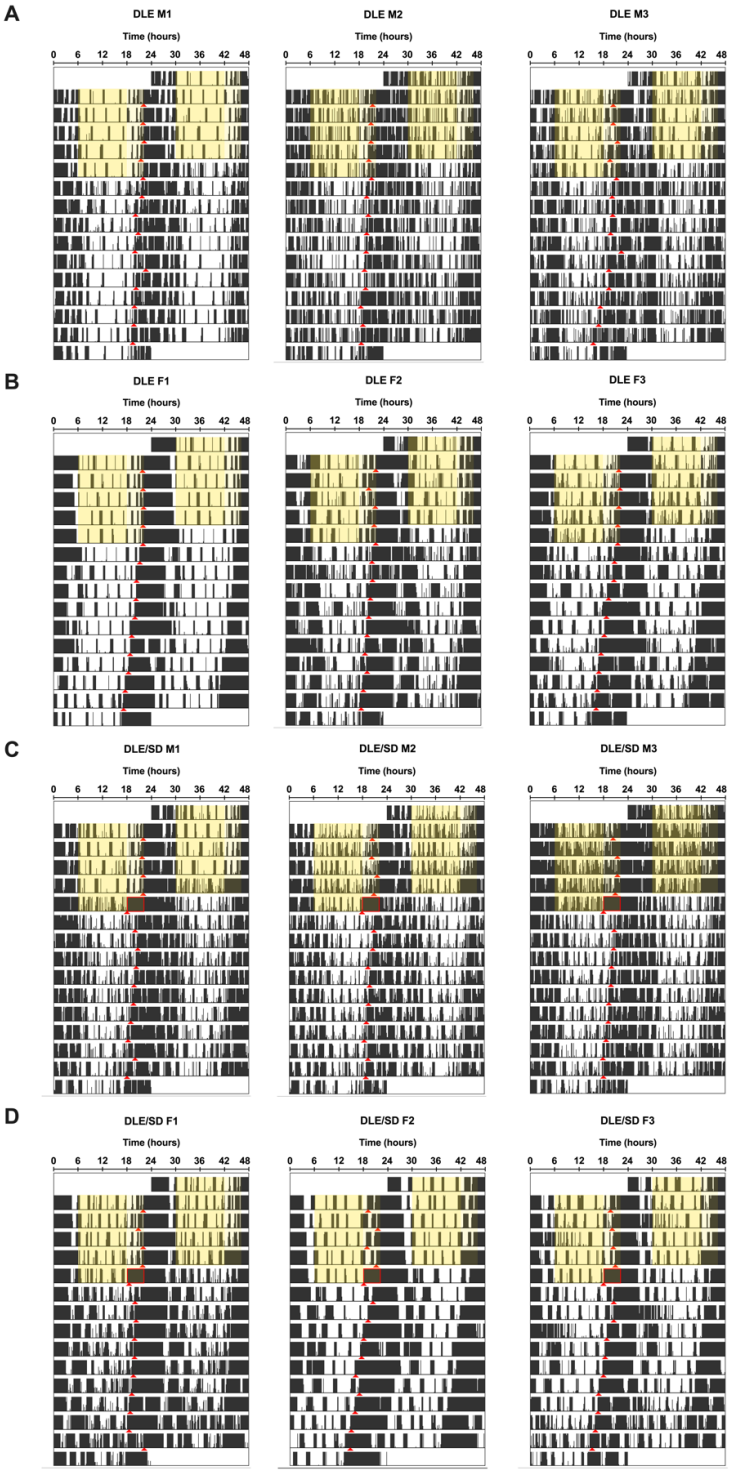

Supplemental Figure 3.1. Representative double-plotted actogram of locomotor activity during 5 days of DLE (final days of a 1-week exposure) and 10 days of DD for **A.** females and **B.** males in the control DLE group, and **C.** females and **D.** males in the DLE/SD group which experienced sleep deprivation during ZT12-16 on the final day of DLE exposure. Yellow shading and red arrows indicate light phases and activity onsets, respectively**.** Sleep deprivation is marked by a red square.

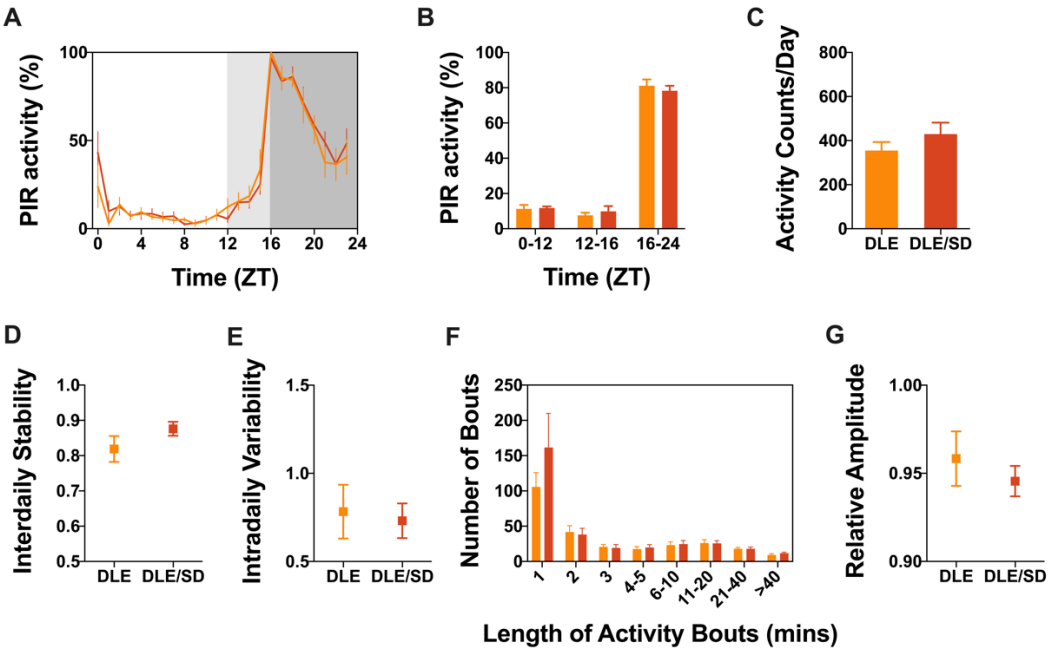

Supplemental Figure 3.2. Analysis of baseline locomotor activity rhythms under acute DLE exposure (N = 6 per group). Both groups were housed in the same conditions, with the DLE/SD group randomly selected for sleep deprivation (ZT12-16) at the conclusion of the 1 week of DLE exposure. **A.** 24-hour activity profile. PIR data were normalized for each animal using min-max scaling. **B.** Light, dim, and dark-phase activity, as a percentage of total activity per day. **C.** Total activity per day. **D.** Inter-daily stability. **E.** Intra-daily variability. **F.** Distribution of the number and duration of activity bouts. **G.** Relative amplitude. Mean +/- SEM.

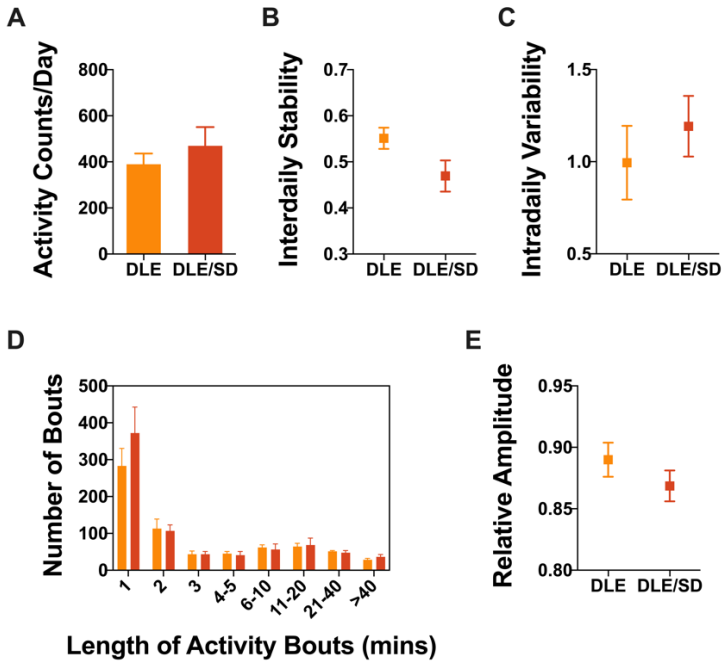

Supplemental Figure 3.3. Analysis of free-running locomotor activity rhythms under DD following acute DLE exposure (N = 6 per group). The DLE/SD group was sleep deprived during the final dim phase (ZT12-16) before going into DD. **A.** Total activity per day. **B.** Inter-daily stability. **C.** Intra-daily variability. **D.** Distribution of the number and duration of activity bouts. **E.** Relative amplitude. Mean +/- SEM.

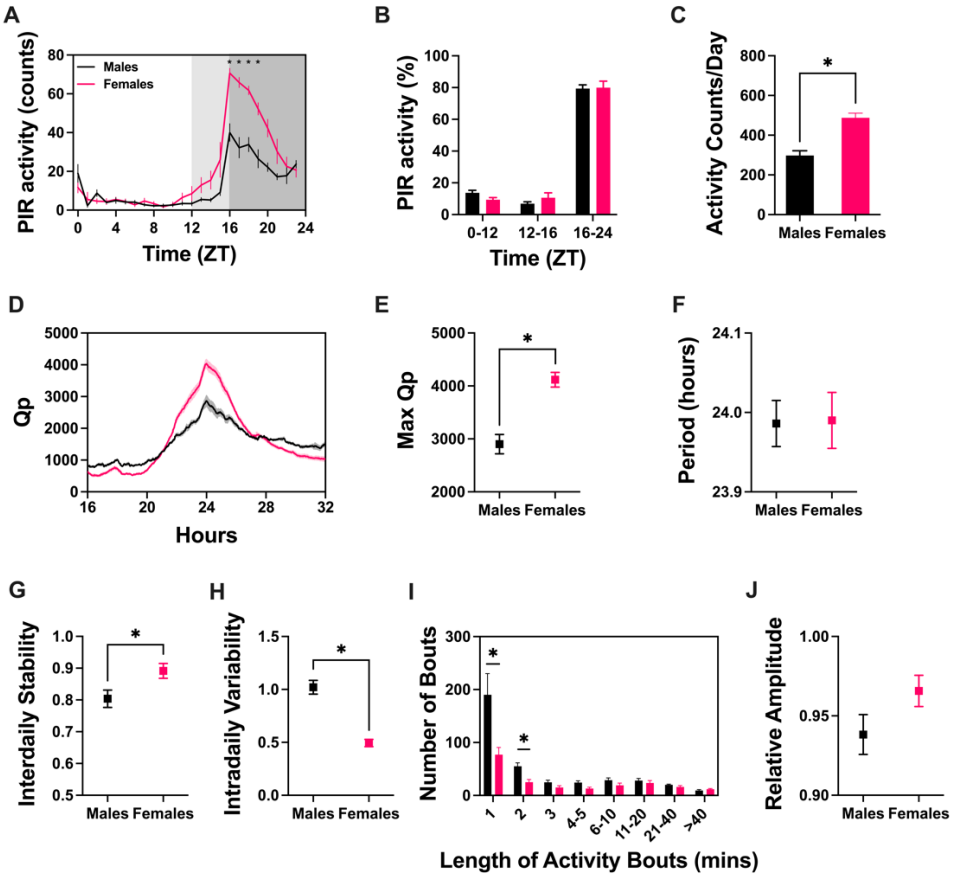

Supplemental Figure 3.4. Analysis of baseline locomotor activity rhythms under acute DLE exposure, disaggregated by sex (N = 6 per group). Data from the DLE and DLE/SD groups were pulled together. **A.** 24-hour activity profile. **B.** Light, dim, and dark-phase activity, as a percentage of total activity per day. **C.** Total activity per day (Mann-Whitney, $U = 0$, $p = 0.0022$). **D.** Chi-square periodogram analysis (Sex, $F_{(1, 10)} = 22.54$, $p = 0.0008$). **E.** Maximum Qp values (Mann-Whitney, $U = 1$, $p = 0.0043$). **F.** Period of activity rhythms. **G.** Inter-daily stability (Mann-Whitney, $U = 5$, $p = 0.0411$). **H.** Intra-daily variability (Mann-Whitney, $U = 0$, $p = 0.0022$). **I.** Distribution of the number and duration of activity bouts (Bout length x Sex, $F_{(7, 70)} = 6.414$, $p < 0.0001$). **J.** Relative amplitude. Mean +/- SEM. Statistically significant multiple comparisons are indicated by an asterisk.

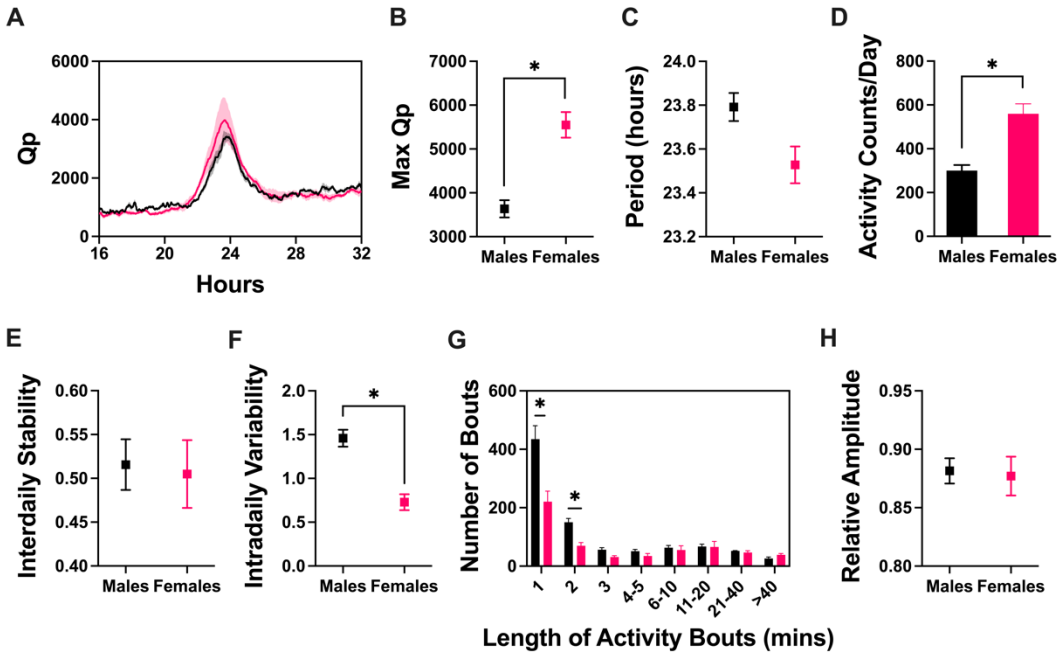

Supplemental Figure 3.5. Analysis of free-running locomotor activity rhythms under DD following acute DLE exposure, disaggregated by sex (N = 6 per group). Data from the DLE and DLE/SD groups were pulled together as no differences were found between groups. **A.** Chi-square periodogram analysis. **B.** Maximum Qp values (Mann-Whitney, $U = 0, p = 0.0022$). **C.** Period of activity rhythms. **D.** Total activity per day (Mann-Whitney, $U = 0, p = 0.0022$). **E.** Inter-daily stability. **F.** Intra-daily variability (Mann-Whitney, $U = 0$, $p = 0.0022$). **G.** Distribution of the number and duration of activity bouts (Bout length x Sex, $F_{(7, 70)} = 10.54$). **H.** Relative amplitude. Mean +/- SEM. Statistically significant multiple comparisons are indicated by an asterisk.

Chapter 4. Interventions to Mitigate the Effects of Dim Light in the Evening

4.1. Introduction

In Chapter 2, we established that DLE exposure leads to significant alterations in circadian rhythms, including delays in activity, sleep, and body temperature rhythms, as well as changes in metabolic parameters and memory performance. In Chapter 3, we demonstrated that these effects are primarily mediated through direct photic entrainment pathways rather than sleep-dependent mechanisms. The circadian system responds to light in nuanced ways, with effects varying based on multiple parameters, including intensity, spectral composition, duration, and timing of the light exposure. Given that DLE directly impacts the circadian system through light-sensitive pathways, mitigation strategies might involve modifying the light environment to attenuate these effects. In this chapter, we investigated three distinct approaches to mitigate the phase-delaying effects of DLE: modifying daytime light intensity, filtering blue wavelengths during the evening, and introducing targeted wavelength stimulation during the dim phase.

While limiting evening light exposure may appear as the most straightforward approach to mitigate DLE effects, this may not always be practical (or a realistic demand) in our modern society. If we cannot change the timing or duration of DLE exposure, and if 20 lux of evening light is the standard in homes, an alternative strategy could involve enhancing the contrast between daytime and evening light levels. As such, in Experiment 1, we examined how varying the intensity of daytime light affects circadian responses to DLE. The circadian system is sensitive to both absolute light levels and the relative contrast between light and dark phases (Kronfeld-Schor et al., 2013). Previous research has shown that the amplitude of the LD cycle plays a crucial role in circadian entrainment, with higher amplitude cycles generally producing stronger rhythms (Aschoff, 1960; Pittendrigh & Daan, 1976b). However, it remains unknown

whether modulating daytime light intensity can reduce the phase-delaying effects of DLE that we observed in our previous experiments. By maintaining a fixed dim light phase (20 lux from ZT12-16) while varying daytime light intensity from 20 to 500 lux, we aimed to determine whether higher daytime light levels could attenuate the phase-delaying effects of DLE. We hypothesized that increased daytime light intensity would strengthen circadian entrainment and reduce the magnitude of evening light-induced phase delays.

If practical constraints prevent modifications to the timing or duration of DLE exposure, and if manipulating daytime brightness proves ineffective, altering the spectral composition of DLE may present a promising alternative. Melanopsin has been proposed as the primary mediator of circadian light responses (Hattar et al., 2002; Panda et al., 2003). Since its peak sensitivity is in the blue light spectrum, blue light has been widely implicated in non-visual responses to light (Brainard et al., 2001; Thapan et al., 2001; Wahl et al., 2019). As such, in Experiment 2, we explored whether filtering short-wavelength light (< 500 nm) during the evening could reduce DLE effects. Using human red cone knock-in mice, which provide enhanced spectral separation between photoreceptor classes, we tested whether blue-blocking filters could prevent or reduce the phase-delaying effects of DLE on activity rhythms. The use of blue-blocking glasses has gained popularity as a potential intervention for evening light exposure in humans. Yet, evidence for their efficacy in preventing sleep and circadian disruption remains limited and inconsistent (Burkhart & Phelps, 2009; Giménez et al., 2014; Hester et al., 2021; Lawrenson et al., 2017; Liset et al., 2022; Shechter et al., 2018; van der Lely et al., 2015). These mixed results suggest that blocking blue light alone may be insufficient to fully counteract evening light effects, possibly due to contributions from other photoreceptors or wavelengths. Therefore, we hypothesized that blue-blocking filters would minimally impact the phase-delaying effects of DLE.

Indeed, previous findings from our lab showed that the acute effects of DLE on activity and sleep persisted in mice lacking melanopsin (Tam et al., 2021). This suggests that the rods and

cones may be driving this response in the absence of melanopsin photoreceptors, or its activation, and that all three photoreceptor classes may be contributing to the effects of DLE in the wild-type retina. Blue-blocking approaches alone may thus be insufficient to prevent the phase-delaying effects of DLE, requiring alternative or complementary intervention strategies. Recent research has revealed that S-cone activation can influence circadian light responses differently from M/L-cones and melanopsin, potentially attenuating phase shifts under certain conditions (Mouland et al., 2019). As such, in Experiment 3, we tested a novel photoreceptor-targeting approach using violet light supplementation during the dim phase. The targeting of S-cones aims to modulate the circadian effects of evening light through their distinct contribution to non-visual responses and opposing signals to that of melanopsin pRGCs (Dacey et al., 2005; Woelders et al., 2018). By supplementing either a constant 5 μW violet light or a 10 Hz flickering violet light during the dim phase while maintaining similar overall illuminance levels, we aimed to investigate whether this photoreceptor-specific approach could reduce the phase-delaying effects observed with standard DLE. The 10 Hz flicker rate was selected to optimize S-cone stimulation while minimizing contributions from other photoreceptors. At this frequency, melanopsin responses are significantly attenuated due to their slow temporal integration characteristics (Dacey et al., 2005; Do & Yau, 2010; McDougal & Gamlin, 2010), while rod contributions are reduced by partial saturation under the 20 lux background illumination. In contrast, cones maintain sufficient temporal resolution to respond effectively to 10 Hz stimulation, allowing for preferential cone pathway activation (Wang & Kefalov, 2011). We hypothesized that S-cone targeted stimulation, particularly with flickering violet light, would reduce the magnitude of DLE-induced phase delays via inhibition of melanopsin pRGC output.

Together, these experiments represent an exploration of potential interventions that could be implemented in human environments to reduce the circadian impact of evening light exposure without requiring significant changes to modern lighting practices. The findings may inform

recommendations for lighting design that could help mitigate the adverse effects of evening light exposure on circadian health.

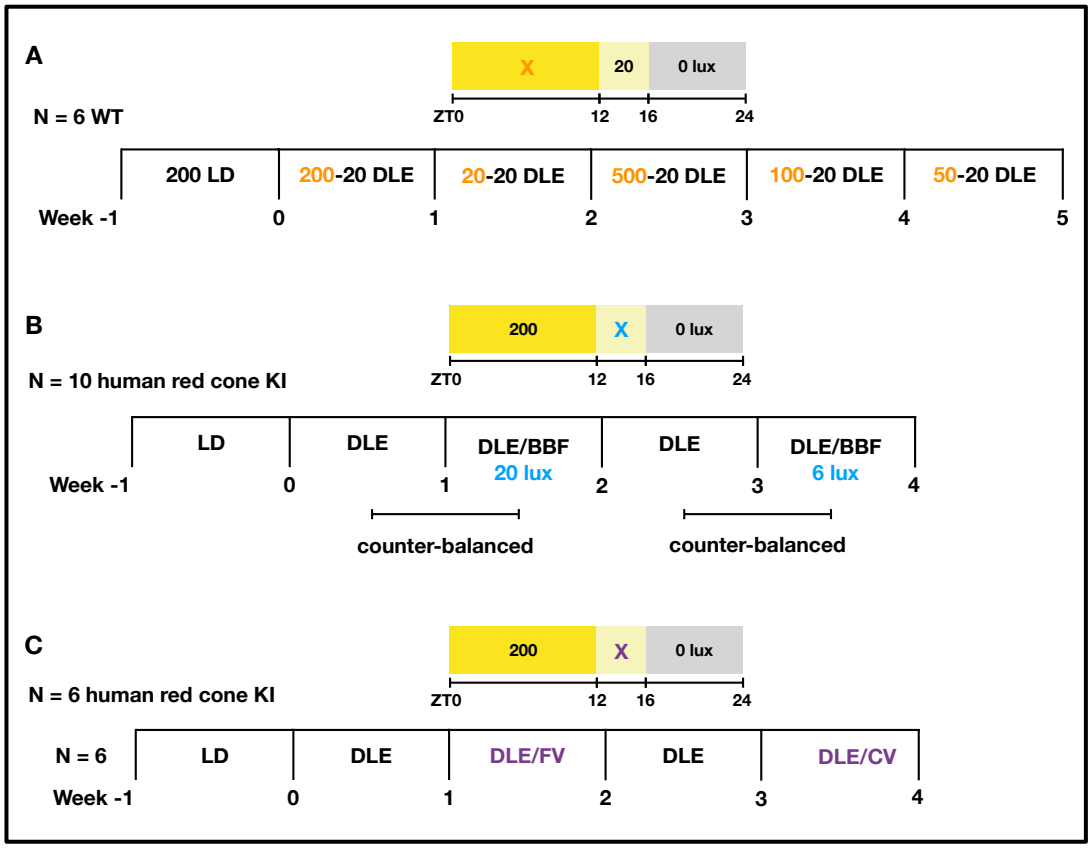

Figure 4.1. Experimental protocol of the interventions to attenuate the phase-delaying effects of DLE. **A.** In Experiment 1, evening light levels were kept at 20 lux, while the light phase intensity varied between 20, 50, 100, 200, and 500 lux. **B.** In Experiment 2, animals were exposed to standard DLE, as well as DLE with the addition of a blue-blocking filter (BBF, blocking wavelengths < 500 nm) at two different dim light intensities (20 lux vs 6 lux). **C.** In Experiment 3, animals were exposed to three conditions: standard DLE, DLE with 5 µW constant violet light (DLE/CV), and DLE with 10 Hz flickering violet light (DLE/FV).

4.2. Methods

Housing Conditions. Animals were singly housed in large MB1 (NKP Isotec) open top cages (45 L x 28 W x 13 H cm) under a 12:12 LD cycle for a minimum of one week prior to the start of experiments. They had no prior history of regulated procedures and experimenters were not blind to the animals' sex or lighting condition. Food (Teklad 2916) and water were provided

ad libitum throughout the study. The temperature and relative humidity of the animal room were maintained at 20–24°C and 45–65%. Pathogen-free conditions were maintained throughout the study by the animal facility. Serology, bacteriology, and parasitology reports (Surrey Diagnostics Ltd., UK) did not note any positive cases.

Lighting. Mice were housed in ventilated LTCs equipped with multiple cool-white LEDs (Luxeon Star LEDs, Quadica Developments Inc., Canada). The spectral power distribution of these LEDs was previously described (See **Chapter 2 section 2.2**, **Supp. Fig. 2.1**, **Supp. Table 2.1**). The control LD condition was set at 12:12 200/0 lux, and the standard DLE at 12:4:8 200/20/0 lux.

Experimental Design. We conducted three separate experiments examining different interventions to mitigate the effects of DLE on activity rhythms (**Fig. 4.1**):

Experiment 1: Daytime Light Intensity Modulation. 6 animals (1:1 male-female ratio) were used as part of a within-subjects design. Wild-type C57BL/6J animals were purchased from Inotiv, Inc. (UK), and were about 8 weeks old at the beginning of the study. After a one-week baseline period under 12:12 LD, animals received DLE from ZT12 to ZT16 for 6 weeks, with a distinct DLE protocol during each week. Evening light levels were kept at 20 lux, while the light phase intensity varied between 20, 50, 100, 200, and 500 lux. The spectral composition remained consistent across all intensity levels. The order of the different DLE exposures was randomized to reduce confounding effects of previous light exposure, as shown in **Figure 4.1A**. At the end of the experiment, mice were euthanized by cervical dislocation.

Experiment 2: Blue-Blocking Filters. 10 male human red cone knock-in mice were used as part of a within-subjects design. These mice were bred in house and were 3-5 months old at the beginning of the study. No females were included as only males were available at the time of the study. Animals were exposed to standard DLE (12:4:8 200/20/0 lux) and DLE with a blue-blocking filter (BBF, blocking wavelengths < 500 nm) at two different dim light intensities (20

lux vs 6 lux). The BBF conditions reduced melanopic EDI by approximately 65% while maintaining similar photopic lux levels. Each condition was maintained for one week with the order counterbalanced across animals (**Fig. 4.1B; Fig. 4.2**).

Experiment 3: Violet Light Supplementation. 6 male human red cone knock-in mice were used as part of a within-subjects design. Animals were exposed to three conditions: standard DLE, DLE with constant violet light (DLE/CV), and DLE with flickering violet light (DLE/FV). For the DLE/CV condition, a 5µW 405 nm violet LED was added to the standard 20 lux white light during the dim phase. For the DLE/FV condition, the violet light was pulsed at 10 Hz (10 ms ON/10 ms OFF) using a USB pulse train generator (Pulser Plus, Prizmatix, Israel). The addition of violet light minimally affected the overall photopic illuminance (increasing from 20 to approximately 20.4-20.8 lux), but significantly increased S-cone activation by approximately 44-fold (from 0.5 to 24 S-cone opic EDI lux). While other photoreceptors experienced a 30-50% increase in activation, the S-cone increase was proportionally much greater (4382%), ensuring that any observed effects would be primarily S-cone mediated. Additionally, the 10 Hz temporal modulation was selected to minimize rod and melanopsin contributions, and the delivery against a 20 lux background helped saturate rod responses. Each condition was maintained for one week (**Fig. 4.1C**).

Experiments 2 and 3 utilized human red cone knock-in mice, in which the mouse medium-wavelength sensitive (M) opsin gene has been replaced with the human long-wavelength sensitive (L) opsin gene (Smallwood et al., 2003). These mice express human L-opsin in a subset of cones, shifting their spectral sensitivity to longer wavelengths compared to wild-type mice. This model provides a valuable tool for studying wavelength-specific photoreception, as it creates a greater spectral separation between cone types, allowing for more precise isolation of S-cone versus M/L-cone contributions to non-image forming responses. This spectral separation is particularly important for experiments involving blue light filtering and violet light stimulation, where specific photoreceptor targeting is essential.

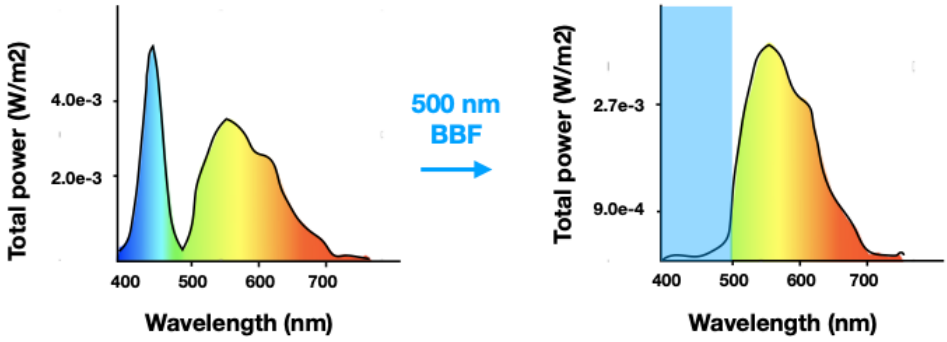

Figure 4.2. Changes in the spectral power distribution of DLE light using blue-blocking filters (BBF).

Compliance. This study is reported in accordance with the ARRIVE 2.0 guidelines. All experimental procedures were carried out at the University of Oxford, UK, in accordance with the University of Oxford Policy on the Use of Animals in Scientific Research and the United Kingdom Animals (Scientific Procedures) Act 1986, under Project License PP0911346 and Personal License I34186130.

Home Cage Activity Monitoring. A passive infrared sensor (PIR, Panasonic AMN32111) was positioned above each cage to monitor locomotor activity, following the validated method described by Brown et al. (2016). To optimize tracking accuracy, gaps beneath the food and water hoppers in MB1 cages were sealed using Perspex blocks, and nesting material (paper-based sizzle-nest or cotton fiber nestlets) was provided in a quantity that did not fully obscure the animal from the sensor. Within each LTC, six PIR sensors were connected to an Arduino (Arduino Uno R3) alongside a light-dependent resistor (Farnell, UK) to monitor the light environment. The Arduinos were interfaced with a Raspberry Pi (Raspberry Pi 3 B) and processed using Node-RED. PIR data were recorded at a 10 s temporal resolution. Data from the last 4 days of LD and each week of DLE exposure were used for analysis. PIR activity counts were averaged in 1 min bins and in 1 h bins to compute the different activity analyses.

Due to equipment malfunction, one animal had missing data during the control LD condition. There were also 9 min of missing data for all animals at ZT9 on the 6th day of 50-20 DLE. As this gap was minimal and occurred during the inactive phase of the animals, data were replaced by zero activity.

Circadian Disruption Measures. Actograms and Chi-square periodogram were computed in ActogramJ (Schmid et al., 2011). Activity onsets were calculated using the median function (without zero activity) and a smoothing gaussian standard deviation of 5 min. Inter-daily stability, intra-daily variability, relative amplitude, light-phase activity, and total activity were calculated in R (Brown et al., 2019; Witting et al., 1990). See equations in **Chapter 2**, **Supplemental Figure 2.2**.

Statistical Analyses. Statistical testing and plotting were conducted in Prism 10. Repeated-measures one-way and two-way ANOVAs, with a Geisser-Greenhouse correction (for lack of sphericity), and Holm-Šídák's multiple comparisons test were computed. The control LD group is represented in the figures, but was not included in the statistical testing in order to focus on the effects of the different DLE protocols. For activity period in Experiment 2, we identified two definite outliers through the ROUT method using Q = 0.1% (two 6 lux DLE/BBF animals with periods of 24.4 and 25.6 hours). As such this data point was removed from the analysis of DLE period. $\alpha = 0.05$ was adopted in all analyses. Mean ± SEM was used for all plots.

4.3. Results

We have already established the differences between standard LD and DLE conditions in previous chapters, so these comparisons will not be analyzed here. However, the LD data is represented on the figures for reference to illustrate the magnitude of phase shifts induced by DLE.

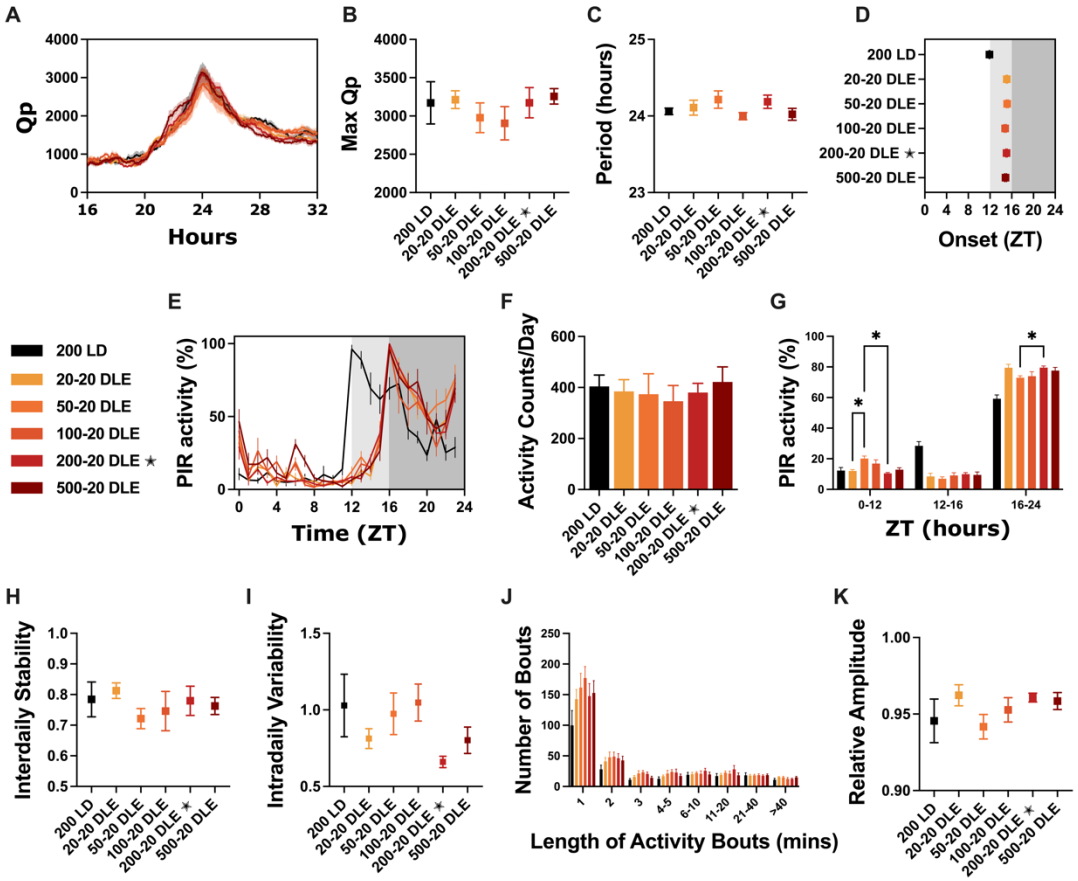

Figure 4.3. Analysis of locomotor activity rhythms under DLE with varying daytime light intensities from 20 to 500 lux in wild-type C57BL/6J animals (N = 6). **A.** Chi-square periodogram analysis. **B.** Maximum Qp values. **C**. Period of activity rhythms. **D.** Activity onsets. **E.** 24-hour activity profile. **F**. Total activity per day. **G.** Light, dim, and dark-phase activity, as a percentage of total activity per day. **H**. Inter-daily stability. **I**. Intra-daily variability. **J**. Distribution of the number and duration of activity bouts. **K**. Relative amplitude. Mean +/- SEM. Statistically significant multiple comparisons are indicated by an asterisk.

Experiment 1: Effects of Daytime Light Intensity. We analyzed how varying daytime light intensity affected activity patterns in mice exposed to DLE, with daytime light varying between 20 and 500 lux. Surprisingly, minimal differences emerged. All five DLE groups exhibited strong rhythms, as measured by periodogram power (Lighting, $F_{(4, 25)} = 0.02177$, $p = 0.9990$; **Fig. 4.3A**), and maximum Qp values (Lighting, $F_{(1.153, 10.76)} = 1.041$, $p = 0.3914$; **Fig. 4.3B**). The period remained at ~ 24 hours (Mean = 24.11 ± 0.22 h; Lighting, $F_{(3.005, 15.02)} = 2.397$, $p = 0.1086$; **Fig. 4.3C**), while a ~ 3 h delay in activity onset was observed across all daytime light intensities (Mean = 14.98 ± 0.72 ZT; Lighting, $F_{(2.991, 65.81)} = 1.328$, $p = 0.2728$; **Fig. 4.3D**). Averaged daily

activity profiles revealed a main effect of Time (Time, $F_{(6.383, 159.6)} = 138.5$, $p < 0.0001$; **Fig. 4.3E**), but no main effect of Lighting (Lighting, $F_{(4, 25)} = 0.8479$, $p = 0.5083$; **Fig. 4.3E**), or interaction (Time x Lighting, $F_{(92, 575)} = 1.113$, $p = 0.2359$; **Fig. 4.3E**). Similarly, there was no effect of Lighting on total daily activity (Lighting, $F_{(2.308, 11.54)} = 0.8781$, $p = 0.4557$; **Fig. 4.3F**). The distribution of activity between the light, dim, and dark phases showed a main effect of Time (Time, $F_{(1.752, 43.81)} = 1567$, $p < 0.0001$; **Fig. 4.3G**), but no effect of Lighting (Lighting, $F_{(4, 25)} = 0.8479$, $p = 0.5083$; **Fig. 4.3G**). However, we found a significant interaction (Time x Lighting, $F_{(8, 50)} = 2.920$, $p = 0.0094$; **Fig. 4.3G**), with post-hoc testing showing that animals exposed to 50-20 DLE were more active during the light phase and less active during the dark phase relative to our standard 200-20 DLE. The 50-20 DLE group was also more active than the 20-20 DLE group during the light phase. Additionally, while there was no effect of Lighting on inter-daily stability (Lighting, $F_{(2.034, 10.17)} = 0.5857$, $p = 0.5771$; **Fig. 4.3H**), we found a main effect of Lighting on intra-daily variability (Lighting, $F_{(2.317, 11.58)} = 4.293$, $p = 0.0361$; **Fig. 4.3I**), but post-hoc testing did not reveal any significant differences between individual lighting conditions. There were no main effects of Lighting on the number and distribution of activity bouts (Lighting, $F_{(4, 25)} = 0.4352$, $p = 0.7819$; **Fig. 4.3J**), or relative amplitude (Lighting, $F_{(1.782, 8.911)} = 1.565$, $p = 0.2596$; **Fig. 4.3K**). Analysis by sex was not conducted as only minimal differences emerged overall.

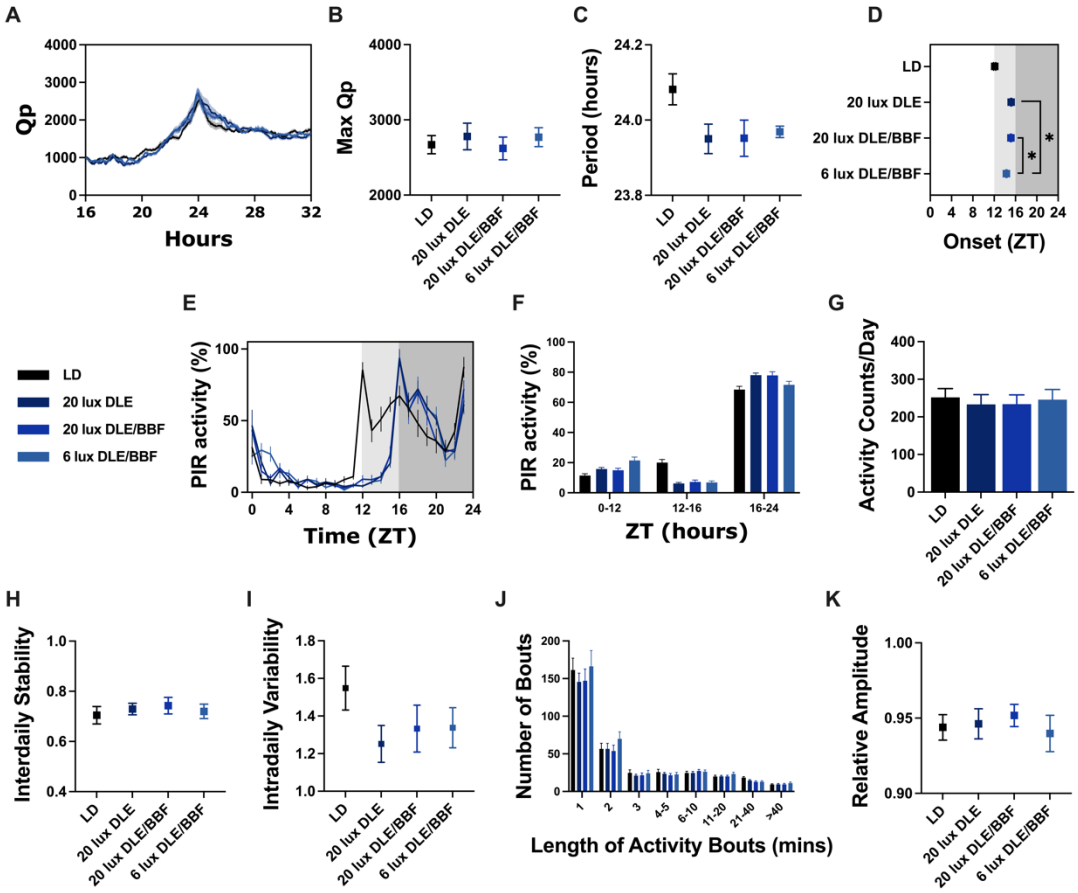

Figure 4.4. Analysis of locomotor activity rhythms under DLE, and DLE with a blue-blocking filter (BBF, < 500 nm) at two different intensities in red cone KI mice (N = 10), which have the same red sensitivity as humans. **A.** Chi-square periodogram analysis. **B.** Maximum Qp values. **C**. Period of activity rhythms. **D.** Activity onsets (Lighting, $F_{(1.980,\ 73.26)} = 21.29$, $p < 0.0001$). **E.** 24-hour activity profile. **F**. Light, dim, and dark-phase activity, as a percentage of total activity per day. **G.** Total activity per day. **H**. Inter-daily stability. **I**. Intra-daily variability. **J**. Distribution of the number and duration of activity bouts. **K**. Relative amplitude. Mean +/- SEM.

Experiment 2: Effects of Blue-Blocking Filters. We examined how filtering short wavelengths of light (< 500 nm) during the dim phase impacted locomotor activity rhythms under acute DLE exposure. All three DLE groups exhibited strong rhythms, as measured by periodogram power (Lighting, $F_{(2,\ 27)} = 0.1853$, $p = 0.8319$; **Fig. 4.4A**), and maximum Qp values (Lighting, $F_{(1.980,\ 17.82)} = 0.4166$, $p = 0.6636$; **Fig. 4.4B**). The period remained at ~ 24 hours for all conditions (Mean = 23.96 ± 0.12 h; Lighting, $F_{(2,\ 25)} = 0.06448$, $p = 0.9377$; **Fig. 4.4C**). Interestingly, there was a main effect of Lighting on activity onsets (Lighting, $F_{(1.980,\ 73.26)} =$

21.29, $p < 0.0001$; **Fig. 4.4D**), with post-hoc testing revealing a significant difference between the 6 lux DLE/BBF group (Mean = 14.31 ± 0.12 ZT) and the standard DLE (Mean = 15.20 ± 0.11 ZT) or 20 lux DLE/BBF condition (Mean = 15.14 ± 0.12 ZT). This suggests that the combination of lower intensity DLE and a blue-blocking filter attenuated the phase delay by ~ 50 min. Averaged daily profiles did not differ (Lighting, $F_{(2, 27)} = 0.09671$, $p = 0.9081$; **Fig. 4.4E**), with a similar distribution between the light, dim, and dark phases (F and p values could not be computed because of the lack of variation; **Fig. 4.4F**), as well as total amount of activity (Lighting, $F_{(1.261, 11.35)} = 0.3090$, $p = 0.6403$; **Fig. 4.4G)**. All animals displayed high inter-daily stability (Lighting, $F_{(1.558, 14.02)} = 0.1917$, $p = 0.7741$; **Fig. 4.4H**), low intra-daily variability (Lighting, $F_{(1.488, 13.39)} = 0.4501$, $p = 0.5904$; **Fig. 4.4I**), consolidated bouts of activity (Lighting, $F_{(2, 27)} = 0.7525$, $p = 0.4808$; **Fig. 4.4J**), and high relative amplitude (Lighting, $F_{(1.859, 16.73)} = 1.298$, $p = 0.2971$; **Fig. 4.4K**). Together, these results revealed a significant attenuation of the phase-delaying effect of DLE when blue light was filtered at lower light intensities, suggesting a complex interaction between light composition, intensity, and circadian entrainment. It also suggests that non-melanopsin photoreceptors play a complex role in mediating circadian responses to evening light.

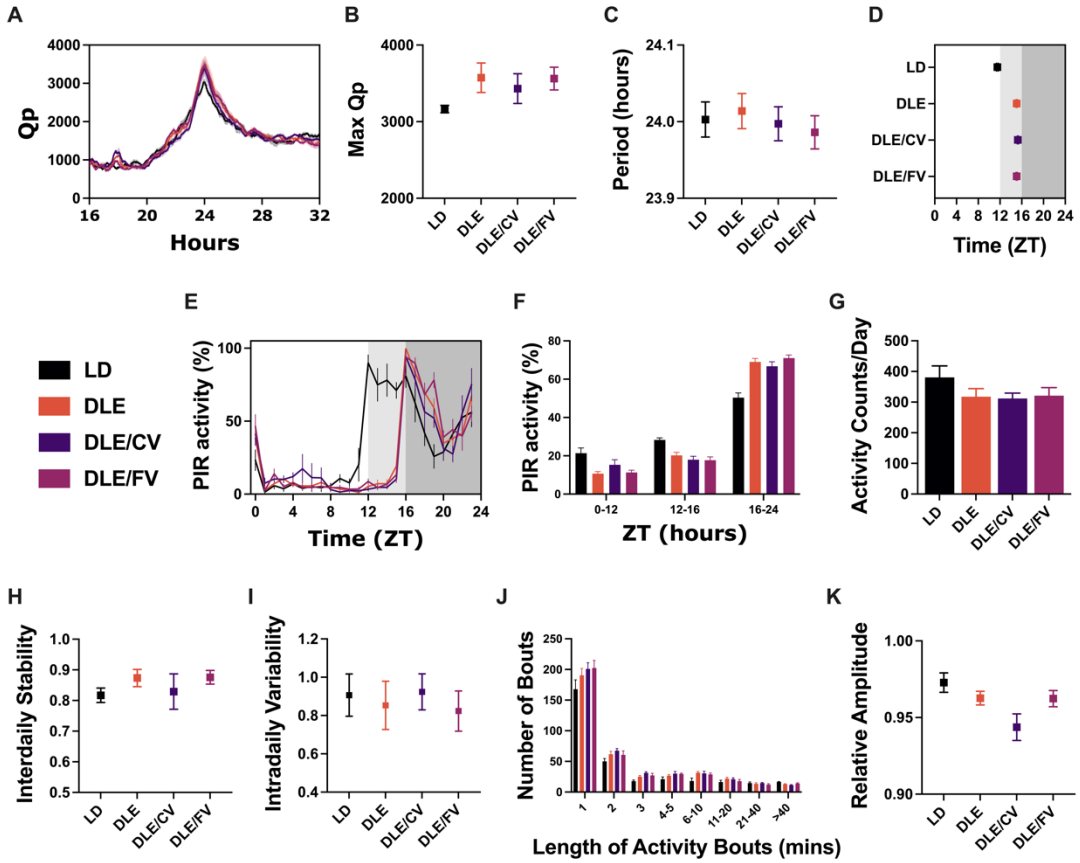

Figure 4.5. Analysis of locomotor activity rhythms under acute DLE, and with the addition of a 5µW constant (DLE/CV) or 10Hz flickering (DLE/FV) violet light in red cone KI mice (N = 6), which have the same red sensitivity as humans. **A.** Chi-square periodogram analysis. **B.** Maximum Qp values. **C**. Period of activity rhythms. **D.** Activity onsets. **E.** 24-hour activity profile. **F**. Light, dim, and dark-phase activity, as a percentage of total activity per day. **G.** Total activity per day. **H**. Inter-daily stability. **I**. Intra-daily variability. **J**. Distribution of the number and duration of activity bouts. **K**. Relative amplitude. Mean +/- SEM.

Experiment 3: Effects of Violet Light Supplementation. We examined how the addition of a constant or flickering violet light during the dim phase impacted locomotor activity rhythms under acute DLE exposure. Overall, we found no effect of our experimental condition, with no statistically significant differences between DLE groups in any of the activity measures. All three DLE groups exhibited strong rhythms, as measured by periodogram power (Lighting, $F_{(2, 15)} = 0.9888$, $p = 0.3950$; **Fig. 4.5A**), and maximum Qp values (Lighting, $F_{(1.673, 8.363)} = 2.241$, $p = 0.1689$; **Fig. 4.5B**). The period remained at ~ 24 hours (Mean = 24.00 ± 0.05 h; Lighting, $F_{(1.721, 8.607)} = 0.3718$, $p = 0.6702$; **Fig. 4.5C**), while a ~ 3.15 h delay in activity onset was

observed across all DLE conditions (Mean = 15.15 ± 0.57 ZT; Lighting, $F_{(1, 23)} = 1.631$, $p = 0.2143$; **Fig. 4.5D)**. Averaged daily profiles did not differ (Lighting, $F_{(2, 15)} = 0.1208$, $p = 0.8871$; **Fig. 4.5E**), with a similar distribution between the light, dim, and dark phases (F and p values could not be computed because of the lack of variation; **Fig. 4.5F**), as well as total amount of activity (Lighting, $F_{(1.497, 7.487)} = 0.1063$, $p = 0.8466$; **Fig. 4.5G)**. All animals displayed high inter-daily stability (Lighting, $F_{(1.144, 5.721)} = 1.458$, $p = 0.2824$; **Fig. 4.5H)**, low intra-daily variability (Lighting, $F_{(1.631, 8.156)} = 2.030$, $p = 0.1938$; **Fig. 4.5I)**, consolidated bouts of activity (Lighting, $F_{(2, 15)} = 0.3998$, $p = 0.6774$; **Fig. 4.5J)**, and high relative amplitude (Lighting, $F_{(1.260, 6.302)} = 3.530$, $p = 0.1033$; **Fig. 4.5K)**. These results indicate that S-cone activation through violet light supplementation, whether constant or flickering, did not counteract the phase-delaying effects of DLE on activity patterns.

4.4. Discussion

In this chapter, we explored three distinct approaches to mitigate the circadian-disrupting effects of DLE exposure: varying the intensity of daytime light, filtering short-wavelength light during the evening, and supplementing evening light with violet wavelengths to increase S-cone inhibition of melanopsin pRGCs. Our results revealed that while most interventions were ineffective, the combination of reduced light intensity and a blue-blocking filter partially attenuated the phase-delaying effects of DLE.

Daytime Light Intensity. Our investigation into whether modulating daytime light intensity could counteract the phase-delaying effects of DLE revealed remarkably minimal differences across a range of daytime light levels (20-500 lux). The delay in activity onset remained remarkably consistent at approximately 3 hours across all conditions. This suggests that a contrast from 1:1 to 25:1 between daytime and evening light intensities is not a critical factor in determining the magnitude of the phase delay. This finding is somewhat surprising given the well-established role of light/dark cycle amplitude in circadian entrainment (Czeisler et al., 1989; Pittendrigh & Daan, 1976b).

Interestingly, we observed a small effect at moderate/low daytime light intensity (50 lux), where animals displayed increased activity during the light phase and decreased activity during the dark phase compared to our standard 200 lux condition. This redistribution of activity occurred without altering the overall phase or period, suggesting an effect of moderate daytime illuminance on the daily pattern of activity. However, this could potentially result from experimental variability or a localized environmental disturbance during this precise experimental week rather than a biological change.

One limitation of Experiment 1 was our inability to test daytime light intensities exceeding 500 lux. In natural and artificial environments, humans can experience much greater light/dark contrasts, with daytime illuminance potentially reaching several thousand lux. It remains possible that more dramatic differences in light intensity might yield different results, as the contrast ratio in our experiments (maximum 25:1) may have been insufficient to significantly impact entrainment mechanisms. Future studies utilizing higher daytime illuminance levels would help address this limitation.

Blue-Blocking Filters. Blue-blocking glasses and filters have been widely promoted as a means to prevent the deleterious effects of evening light exposure on circadian rhythms and sleep. This approach is based on the premise that melanopsin, with its peak sensitivity in the blue light spectrum, is the primary mediator of circadian responses to light (Brainard et al., 2001; Hattar et al., 2002). Our results demonstrated that filtering wavelengths below 500 nm had no effect at standard DLE illuminance (20 lux), but significantly attenuated the phase-delaying effect of DLE when combined with reduced light intensity (6 lux), resulting in an approximately 50-minute advance in activity onset compared to the standard DLE condition.

This finding suggests an interaction between light intensity and spectral composition in mediating responses to DLE. The effectiveness of blue-blocking filters appears to be highly dependent on the overall illuminance level, becoming significant only when the total light intensity is reduced below a certain threshold. This is consistent with previous research

demonstrating different photic thresholds for various non-image forming visual functions (Butler & Silver, 2011). Non-image forming responses like circadian entrainment, masking, and the pupillary light reflex have been shown to have distinct sensitivity thresholds, with entrainment occurring at lower irradiances than other responses. Our results suggest that at standard evening light levels, the contribution of remaining wavelengths above 500 nm are sufficient to maintain robust circadian entrainment even when blue light is filtered. It also suggests that reducing overall illuminance brings the system below a critical threshold where changes in spectral composition becomes more influential.

These findings are particularly noteworthy in light of our previous observation that the phase-delaying effects of DLE on activity and sleep persist in melanopsin-knockout mice (Tam et al., 2021), suggesting that other photoreceptors contribute significantly to this response. Rods and cones, particularly M-cones with peak sensitivity around 510 nm, likely play an important role in mediating the effects of evening light on the circadian system, especially at the relatively low light levels used in our DLE paradigm (Lall et al., 2010; van Diepen et al., 2013). This is consistent with the action spectrum for phase shifting circadian rhythms in wild-type mice, which is shifted to longer wavelengths (Provencio & Foster, 1995; Yoshimura & Ebihara, 1996). The nonuniform distribution and spectral tuning of photosensitive retinal ganglion cells in the mouse retina further complicates this picture, as different subpopulations of pRGCs may have varying roles in circadian entrainment (Berson et al., 2010).

The human literature on blue-blocking interventions presents mixed results, with some studies reporting benefits for sleep and circadian parameters (Burkhart & Phelps, 2009; van der Lely et al., 2015). This inconsistency likely stems from substantial methodological variations across studies, particularly regarding the ambient lighting conditions (Hester et al., 2021). Many studies fail to adequately characterize room lighting in terms of spectral composition and intensity, making it difficult to interpret and compare results. Our findings might help explain this inconsistency by highlighting the importance of absolute light intensity. Based on human

photometry, filtering wavelengths below 500 nm typically reduces melanopic illuminance by approximately three-fold (Lucas et al., 2014), but this reduction may only produce measurable effects when the overall light intensity is relatively low. Indeed, at higher ambient light levels (> 100 lux), which are common in many indoor environments, the contribution of remaining wavelengths may be sufficient to maintain circadian effects even when blue light is filtered. These results have important implications for the application of blue-blocking interventions in real-world settings. They suggest that such approaches may be most effective when combined with overall reductions in light intensity, rather than relying solely on spectral filtering while maintaining typical indoor illuminance levels.

A limitation of our experimental design is the absence of a 6 lux DLE condition without a blue-blocking filter, which would have allowed for a more precise separation of reduced intensity and changes in spectral composition. As a result, we cannot definitively attribute the observed shift in activity onset to either factor or their interaction. However, our aim was specifically to compare their combined effect to the standard 20 lux DLE condition. Future studies should include a full factorial design with both intensity (20 vs 6 lux) and spectral composition (with vs without BBF) to definitively characterize their independent and interactive effects.

Violet Light Supplementation. Our third approach explored whether targeted stimulation of S-cones, which have been shown to influence circadian responses differently from M/L-cones and melanopsin (Mouland et al., 2019), could counteract the phase-delaying effects of DLE. This strategy was based on evidence suggesting that S-cone activation might provide opposing signals that could potentially attenuate the phase-delaying effects of evening light.

Despite our careful design to selectively enhance S-cone activation while minimizing effects on overall illuminance, neither the addition of constant nor flickering violet light produced any significant reduction in DLE-induced phase delays. Activity onsets remained consistently delayed by approximately 3.15 hours across all conditions, similar to standard DLE. This

suggests that S-cone stimulation at the parameters we tested is not sufficient to counteract the phase-delaying effects of broadband white light at 20 lux.

Recent research has highlighted that ultraviolet light provides a major input to non-image-forming light detection in mice (van Oosterhout et al., 2012), primarily through S-opsin expressing cones. While our experiment targeted these same S-cones using violet light (405 nm) that falls within the visible spectrum, it is possible that the specific parameters we employed (intensity or duration) were insufficient to effectively counteract the entraining effects of the broader spectrum white light. The relatively small population of S-cones compared to M-cones in the mouse retina might also contribute to the limited impact of our intervention, despite our efforts to target these cells specifically (Nadal-Nicolás et al., 2020). Moreover, not all S-cones, but only a subset were found to have this inhibitory effect, which could account for the lack of changes (Dacey et al., 2005).

Additionally, the 10 Hz flicker rate we employed was specifically selected to optimize S-cone stimulation while minimizing melanopsin contributions due to its slow temporal integration characteristics, and minimizing rod involvement due to partial saturation under the 20 lux background evening light. However, it appears that even with this targeted approach, the S-cone contribution was insufficient to significantly alter the phase-shifting effects of the broadband light.

4.5. Conclusion

Our investigation of potential interventions to mitigate the phase-delaying effects of DLE has yielded important insights into the complexity of circadian responses to evening light exposure. While varying daytime light intensity and supplementing violet light had no impact on phase delays, we found that blue-blocking filters can attenuate DLE effects, but only when combined with reduced overall light intensity.

This finding has significant implications for developing practical interventions to minimize circadian disruption from evening light exposure. It suggests that comprehensive approaches addressing both spectral composition and absolute light levels may be more effective than interventions targeting only one aspect of the light stimulus. The effectiveness of blue-blocking filters specifically at lower light intensities may explain the mixed results observed in human studies and highlights the importance of considering overall illuminance levels when implementing such interventions.

The consistency of phase delays across different daytime light intensities suggests that the contrast ratio between day and evening light may be less important than previously thought, at least within the range tested in this study. The lack of effect from violet light supplementation, despite significant increases in S-cone activation, indicates that the inhibitory influence of S-cones on circadian responses may be context-dependent or insufficient to override signals from other photoreceptors under typical indoor lighting conditions. Collectively, these results suggest that mitigation strategies to attenuate DLE require more comprehensive approaches than the interventions tested here.

Chapter 5. General Discussion & Conclusion

This thesis investigated the effects of DLE exposure on circadian rhythms and associated physiological and behavioral parameters in mice, and aimed to understand both the underlying mechanisms and potential mitigation strategies. In Chapter 1, we reviewed the disruptions caused by the modern artificial light environment and how these conditions have been studied in laboratory animals so far. We then introduced our DLE paradigm, which parallels more closely the exposure experienced by humans. In Chapter 2, through a comprehensive phenotyping series, we established that chronic DLE exposure induces significant phase delays in activity, sleep and body temperature rhythms, as well as subtle changes in metabolism and memory performance. In Chapter 3, we determined that these effects are primarily mediated through direct photic entrainment pathways rather than negative masking or sleep-dependent mechanisms. Finally, in Chapter 4, we evaluated several intervention approaches to mitigate the phase-delaying effects of DLE.

This general discussion integrates our findings across all experimental chapters, contextualizing them within the broader scientific literature, addressing methodological considerations, and exploring their implications for understanding and addressing the effects of artificial evening light exposure in modern environments.

5.1. Key Findings

Description of the Modern Artificial Light Environment. We established a paradigm for evening light exposure that models the most common pattern of circadian disruption experienced in modern society. Unlike continuous DLAN, which has been extensively studied but does not represent typical human experience, our DLE protocol provides a more ecologically valid model of contemporary artificial lighting conditions. Our comprehensive review of the DLAN literature revealed widespread effects on circadian physiology across multiple rodent models, including altered activity and sleep patterns, impaired metabolic

function, depression-like behaviors, and changes in hippocampal morphology. However, most people are exposed to artificial light primarily during evening hours rather than throughout the night. The DLE paradigm we developed addresses this discrepancy by exposing mice to standard daytime illumination (200 lux) followed by 4 hours of dim light (20 lux) in the evening before complete darkness, paralleling the experience of people who spend evenings under artificial illumination before sleep.

Characterization of Chronic DLE Effects. In Chapter 2, we demonstrated that chronic exposure to DLE (12 weeks) consistently delayed locomotor activity rhythms by approximately 3-4 hours in C57BL/6J mice. This delay was accompanied by parallel shifts in body temperature rhythms and changes in the distribution of sleep, with increased sleep during the dim light phase. Despite these timing changes, the overall quantity of activity and sleep, and the robustness of circadian rhythms remained largely intact, with minimal effects on periodogram power, amplitude, stability or variability measures. Additionally, we observed sex-specific effects on metabolic parameters, with females showing greater vulnerability to DLE-induced alterations in lipid metabolism markers. Building on previous findings, these results indicate that both acute and chronic DLE exposure causes a coordinated realignment of the circadian system rather than rhythm fragmentation or desynchrony.

Mechanisms Underlying DLE Effects. Chapter 3 provided critical insights into the mechanisms mediating DLE effects by examining the contribution of sleep versus circadian rhythms. We demonstrated that the phase-delaying effects of DLE are primarily mediated through direct photic entrainment pathways rather than sleep-dependent mechanisms. By depriving mice of sleep during the dim phase before transitioning to DD, we showed that activity onsets in DD began to free-run from the delayed phase established under DLE (ZT15-16), regardless of prior sleep during the dim phase, indicating a delayed phase of entrainment rather than a masking effect. This finding confirms that DLE directly entrains the circadian clock through photic pathways independent of sleep state.

Interventions to Mitigate DLE Effects. In Chapter 4, we explored three distinct approaches to attenuate the phase-delaying effects of DLE: varying daytime light intensity, filtering short-wavelength light during the evening, and supplementing evening light with specific wavelengths to inhibit melanopsin activation. Surprisingly, varying daytime light intensity from 20 to 500 lux had minimal impact on the phase-delaying effects of DLE. However, we discovered that combining a blue-blocking filter with reduced light intensity (6 lux) significantly attenuated the delay in activity onset by approximately 50 min, while blue-blocking filters at standard intensity (20 lux) or violet light supplementation targeting S-cones activation and melanopsin inhibition proved ineffective. These findings suggest a complex interaction between light intensity and spectral composition in mediating circadian responses to DLE, revealing that blue-blocking interventions are only likely to be effective under reduced light intensity.

5.2. Comprehensive Assessment of DLE Exposure in Mice

Direct Photic Entrainment and Multi-Photoreceptor Contributions. Together, our findings in Chapters 3 and 4 demonstrate that DLE effects are primarily mediated through direct photic entrainment pathways involving multiple photoreceptor classes. The persistence of DLE effects in melanopsin-knockout mice (Tam et al., 2021), and the inability of blue-blocking filters to prevent phase delays at standard light intensities suggest that non-melanopsin photoreceptors (rods and cones) play significant roles in mediating circadian responses to evening light. This aligns with the growing recognition that all retinal photoreceptor classes contribute to non-image forming responses, with their relative contributions varying based on lighting parameters (Lucas et al., 2014; Spitschan et al., 2019). The interaction we observed between light intensity and spectral filtering supports the existence of intensity thresholds for different photoreceptor contributions. The reduction of both the intensity and the short-wavelength content may show mitigation effects by bringing the system below a critical threshold where remaining photoreceptor activation is insufficient to generate a complete phase-delay. This is consistent

with previous research demonstrating different irradiance thresholds for various non-image forming visual functions (Butler & Silver, 2011).

Coordinated Realignment vs. Disruption. A key insight from our work is that DLE induces a coordinated realignment of the circadian system rather than causing fragmentation or internal desynchrony. In Chapter 2, we observed parallel delays in activity, temperature, and sleep patterns while the overall robustness of rhythms remained intact. In Chapter 3, we showed that this realignment represents true entrainment rather than masking effects, as the delayed phase persisted in constant darkness. This coordinated response suggests that the circadian system adapted to the new dark onset, shifting all outputs accordingly.

Molecular Clock and SCN Circuit Mechanisms. The coordinated phase delays we observed across multiple physiological outputs likely reflect systematic changes in molecular clock function within specific SCN neuronal populations. DLE exposure likely induces phase delays through light-activated transcription of *Per1* and *Per2*, particularly in core SCN neurons such as VIP- and GRP-expressing cells, which then propagate phase information to shell neurons and reset the broader SCN network (Shigeyoshi et al., 1997). The magnitude and persistence of the phase delays we observed (~3-4 hours) suggests substantial reorganization of *Per1/Per2* expression patterns, potentially accompanied by changes in other core clock genes including *Clock*, *Bmal1*, and *Cry1/2*. The preservation of rhythm robustness despite these delays implies that the amplitude and synchrony of clock gene cycling remain intact, even as their phase is shifted. The involvement of multiple photoreceptor pathways in DLE effects, as evidenced by the persistence of phase delays in melanopsin-knockout mice, suggests that both the classical rod/cone pathway through the IGL and the direct melanopsin pathway to VIP neurons contribute to entrainment. Indeed, the IGL serves as an integrative node, receiving rod/cone input and projecting neuropeptide Y (NPY) to the SCN, where it can modulate the magnitude of photic phase shifts (Harrington, 1997; Weber & Rea, 1997). This convergence of

photoreceptive input pathways may further explain why spectral filtering alone was insufficient to eliminate DLE-induced phase shifts under standard DLE conditions.

Sex-Specific Vulnerabilities. A consistent finding across our studies was the presence of sex differences in both baseline rhythmicity and responses to DLE. Females were consistently more active and exhibited more robust circadian rhythms than males, with stronger periodogram power, higher amplitude, higher inter-daily stability, and lower intra-daily variability. However, females also showed greater vulnerability to metabolic disruptions from DLE exposure, with significant alterations in lipid metabolism parameters that were absent in males. These findings align with growing evidence for sex differences in circadian biology and emphasize the importance of including both sexes in circadian research. They also have implications for understanding sex differences in susceptibility to circadian-related disorders in humans, where women often show higher prevalence of conditions associated with circadian disruption (Mong et al., 2011). Additionally, our analysis revealed that the estrous cycle-related variations in home cage activity observed with running wheels were not evidenced with PIR data, suggesting that these effects are driven by motivated exploratory behavior rather than baseline home cage activity.

Sex Differences in SCN Neurophysiology and Molecular Clock Function. The sex differences observed in rhythm robustness and metabolic vulnerability to DLE likely reflect underlying differences in SCN structure and function. Female SCN neurons exhibit higher baseline electrical activity and stronger synchrony between cellular oscillators than males, which may explain the more robust rhythms observed in females (Kuljis et al., 2013; Nakamura et al., 2005). This enhanced synchrony is associated with higher amplitude clock gene expression (Chun et al., 2015). However, this enhanced sensitivity may paradoxically increase susceptibility to circadian disruption under certain conditions. The SCN exhibits sex-specific neurochemical organization, including differences in the distribution and connectivity of VIP and AVP neurons, which may alter photic signal processing and contribute to the sex-specific

DLE responses we observed (Thirouin et al., 2023; Yan & Silver, 2016). The greater metabolic disruption seen in females may also reflect differences in coupling between central and peripheral clocks. Estrogen modulates both SCN function and peripheral metabolic gene expression, while reproductive hormones fluctuate across the estrous cycle and can influence circadian light sensitivity and metabolism (Bailey & Silver, 2014).

5.3. Methodological Considerations

Experimental Model. Our use of mice as a model organism for studying evening light exposure offers both advantages and limitations. Mice are a well-established model for circadian research with extensively characterized circadian mechanisms. However, as nocturnal animals, mice have different temporal niche adaptations than humans, potentially limiting direct translational applications. Nevertheless, the fundamental mechanisms of photic entrainment are conserved across mammals, making our findings on photoreceptor contributions and entrainment mechanisms broadly relevant (Tir et al., 2022). Examining the effects of DLE on a diurnal rodent model would be particularly valuable for translational purposes, though such models do not readily allow for genetic modification. The use of human red cone knock-in mice in Chapters 4 provided enhanced spectral separation between photoreceptor classes, enabling more precise manipulations of wavelength-dependent effects. This genetically modified model offers unique advantages for studying the specific contributions of different photoreceptors to circadian responses (Smallwood et al., 2003).

Lighting Parameters. A strength of our approach was the careful characterization and reporting of lighting parameters using the standardized melanopic EDI framework (Lucas et al., 2024; Lucas et al., 2014). This allows for precise comparison with other studies and potential translation to human applications. However, laboratory lighting conditions inevitably differ from naturalistic light exposure patterns, where intensity, spectral composition, and timing vary continuously throughout the day. The relatively low intensity of our daytime light (20-500 lux) compared to natural daylight (typically > 1000 lux outdoors) represents a

limitation that may have affected our intervention outcomes, particularly in the daytime intensity modulation experiment. However, it has been shown that the standard indoor lighting exposure for humans is set around 100-300 lux in typical office environments, with evening home lighting often below 100 lux (Figueiro et al., 2017; Phillips et al., 2019), making our paradigm relatively comparable to modern human indoor environments. Moreover, human circadian responses to light typically saturate above 200 lux (Cajochen et al., 2005; Zeitzer et al., 2000), so further increasing light levels may not significantly increase the magnitude of the effects of evening light. This ecological relevance strengthens the potential translational implications of our findings despite the laboratory setting restrictions. Additionally, studying higher light intensities presents methodological challenges when using nocturnal photophobic rodents such as mice. Our PIR activity monitoring system requires animals to remain visible within their cages, preventing them from exhibiting normal light avoidance behaviors that would occur at higher intensities. This constraint represents an inherent limitation in translational research between diurnal humans and nocturnal animal models when investigating high-intensity lighting effects.

Measurement Approaches. Our use of passive infrared sensors for continuous and non-invasive monitoring of locomotor activity and indirect assessment of sleep represents both a strength and a limitation. This approach enabled long-term monitoring without disrupting natural behavior, but provided less detailed information than electroencephalography would regarding sleep architecture and quality. Similarly, our use of infrared thermography for peripheral body temperature assessment allowed non-invasive monitoring, but may not have captured subtle changes in core body temperature regulation.

5.4. Implications and Applications

Understanding Modern Light Environments. Our findings provide important insights into how modern light environments might affect circadian physiology. The sensitivity of the circadian system to even modest evening illumination (20 lux) highlights how typical indoor

evening lighting could impact circadian timing. The magnitude of the phase delay observed in our studies (~ 3 h) is substantial and would represent a significant shift in the timing of physiological processes if translated to humans. Indeed, such a delay would be equivalent to a delayed sleep phase disorder in human subjects (Micic et al., 2016). This may explain epidemiological associations between evening light exposure and various health conditions, including metabolic disorders and sleep disturbances (Lunn et al., 2017).

Designing Effective Interventions. Our intervention studies have practical implications for developing strategies to mitigate the circadian impact of evening light exposure. The finding that blue-blocking interventions are effective only when combined with reduced overall light intensity suggests that current approaches focusing solely on spectral manipulation may have limited efficacy at typical indoor light levels. This may explain the mixed results observed in human studies of blue-blocking glasses and applications (Hester et al., 2021; Lawrenson et al., 2017). Our results suggest that comprehensive approaches addressing both light intensity and spectral composition would be most effective. Specifically, reducing evening light to below approximately 10 lux while also filtering short wavelengths might provide better protection against circadian phase delays than either intervention alone (Brown et al., 2022). This has implications for the design of both light environments and light-filtering technologies.

Biological Sex as a Modulator of Light Sensitivity. The sex differences observed in our studies, particularly regarding metabolic responses to DLE, have important implications for personalized approaches to managing evening light exposure. The heightened female vulnerability to metabolic disruption suggests that women might benefit from better mitigation of evening light exposure. This aligns with epidemiological evidence suggesting stronger associations between shift work and metabolic disorders in women compared to men (Sun et al., 2018).

5.5. Future Directions

Our findings open several promising avenues for future research that would extend and complement the work presented in this thesis:

Energy Balance and Metabolic Regulation. Despite the lack of significant weight gain differences under DLE, investigating food consumption patterns would provide valuable insights into potential temporal reorganization of feeding behavior. While overall caloric intake might remain unchanged, alterations in the timing of food consumption could affect metabolic health through misalignment with metabolic oscillators. Complementing this with indirect calorimetry measurements would reveal whether DLE alters substrate utilization (carbohydrate vs. fat oxidation) or energy expenditure patterns across the 24-hour cycle. Moreover, examining the interaction between DLE and high-fat diet could provide an insightful model to investigate metabolic vulnerability.

Cardiovascular Function. Metabolic and cardiac dysfunction have often been associated under altered light exposure (West et al., 2017). Examining the effects of DLE on cardiovascular parameters would provide complementary insights into the regulation of peripheral clocks. We expect that the delay in activity and temperature rhythms we observed may extend to cardiovascular parameters.

Affective Responses. While we assessed stress responses and anxiety behaviors, expanding the behavioral phenotyping to include depression phenotypes using tests such as forced swim, tail suspension, or sucrose preference would provide a comprehensive understanding of how DLE affects mood regulation. The use of more refined tests, such as affective bias, would also be informational (Hinchcliffe & Robinson, 2024).

Disease models. Another interesting future direction would be to examine the DLE effects in mouse models of neuropsychiatric disorders where circadian disruption is already implicated, such as depression, anxiety, and schizophrenia (Jagannath et al., 2013). While our findings

suggest that healthy mice maintain robust rhythms despite temporal reorganization under DLE, animals with pre-existing circadian vulnerabilities might show more pronounced adverse consequences. Using DLE exposure in these models could reveal threshold effects where seemingly mild circadian challenges become significantly disruptive in the context of disease models.

Molecular Clock Mechanisms. Examining changes in clock gene expression (*Per1/2*, *Cry1/2*, *Clock*, *Bmal1*) in both the SCN and peripheral tissues would help connect our observed physiological and behavioral changes to underlying molecular mechanisms. Tissue-specific alterations in clock gene rhythms could explain the sex-specific metabolic vulnerabilities we observed and identify potential intervention targets.

Circadian Plasticity and Adaptability. Investigating how DLE affects responses to additional circadian challenges, such as phase-shifting light pulses or simulated jet lag, would be particularly relevant to modern lifestyles. Individuals in artificially lit environments often face additional circadian challenges like travel across time zones or irregular work schedules. Understanding how DLE impacts circadian plasticity could inform strategies for managing multiple sources of circadian disruption.

Spectral Manipulation. Building on our finding that blue-blocking filters were effective only at lower light intensities, investigating whether more comprehensive spectral modulation (beyond just wavelengths < 500 nm) could provide greater protection against DLE effects at standard light intensities. Selective filtering of multiple wavelength bands or modulation of the spectral power might more effectively reduce circadian-disrupting potential while maintaining visual function (Souman et al., 2018).

Recovery. Examining the time course of recovery during re-exposure to LD conditions following chronic DLE exposure would provide insights into the persistence of effects and potential long-term consequences of chronic exposure.

These future directions would collectively provide a more comprehensive understanding of how evening light exposure affects physiology and behavior, as well as the associated mechanisms, ultimately informing more effective strategies for managing light exposure in modern environments.

5.6. Conclusion

This thesis provides the first characterization of the consequences of chronic DLE exposure, the mechanisms mediating these effects, and potential strategies for mitigation in mice. Our findings demonstrate that even modest evening light exposure can significantly delay circadian phase through direct photic entrainment pathways involving multiple photoreceptor classes. While the circadian system maintains internal temporal coherence under DLE conditions, downstream physiological processes, particularly metabolic parameters in females, show vulnerability to disruption. Our intervention studies reveal complex interactions between light intensity and spectral composition in mediating circadian responses, with implications for designing more effective strategies to manage evening light exposure in modern environments. Collectively, this work enhances our understanding of how artificial lighting affects circadian biology and provides a foundation for developing evidence-based recommendations to support circadian health in settings where evening light exposure is unavoidable.

6. Appendix: Evaluation of the Digital Ventilated Cage System for Circadian Phenotyping

The experiments presented in the main body of this thesis relied on robust and reliable methods for measuring circadian rhythms in mice. Throughout Chapters 2-4, PIR sensors were used to continuously monitor locomotor activity as a behavioral output of the circadian system under various lighting conditions. While conducting this research, I also evaluated alternative methodologies for circadian phenotyping, including the Digital Ventilated Cage (DVC) system, which presented potential advantages for high-throughput circadian studies. This appendix presents the validation of the DVC system for circadian phenotyping, demonstrating its effectiveness in detecting the same circadian parameters used throughout this thesis, and highlighting its limitations. This chapter has been published as a scientific article (Tir et al., 2025)[1].

6.1. Introduction

In healthy subjects, consolidated, robust, and stable rhythms are observed. However, circadian rhythms can become misaligned or disrupted with respect to the external LD cycle under conditions that include disease and abnormal exposure to light. Such disruption can be characterized by disturbances in the timing, amplitude, or synchronization of these rhythms, and has been identified as a common comorbidity in various health conditions, including mood disorders and cardiovascular diseases (Brown et al., 2019; Crnko et al., 2019; LeGates et al., 2014; West & Bechtold, 2015). Studying the mechanisms underlying circadian rhythms and their disruption is therefore crucial for understanding disease pathophysiology and for the development of targeted therapeutic interventions.

[1] The content of this chapter was previously published in Tir, S., Foster, R. G., & Peirson, S. N. (2025). Evaluation of the Digital Ventilated Cage® system for circadian phenotyping. *Scientific Reports*, *15*(1), 3674. https://doi.org/10.1038/s41598-025-87530-6 . I produced the material and received permission from my co-authors to include it in my thesis.

The effects of light on the circadian system are complex, contingent upon multiple factors including the intensity, wavelength, duration, and timing of light exposure. Furthermore, light history and age can modify circadian responses to light (Foster, 2021; Peirson et al., 2018; Tir et al., 2022). As a result, different lighting conditions can be used to identify the distinct components contributing to circadian entrainment. Standard LD cycles are typically used to assess the phase of entrainment, period, activity bouts, and the robustness of behavioral rhythms, and provide a baseline for the study of circadian rhythms in response to different environmental conditions. The assessment of circadian rhythmicity can only be determined in the absence of zeitgebers. Constant darkness allows for the measurement of free-running periods and is particularly useful in identifying clock mutants, where the endogenous circadian period may be longer or shorter than normal, or even arrhythmic. Conversely, constant light (LL) leads to period lengthening in a dose-dependent manner, and can even induce arrhythmicity. As such, LL conditions provide valuable insights into the sensitivity of the central pacemaker to light of different intensities and wavelengths (Lall et al., 2010). A LP administered during the subjective night can shift the circadian clock, with the magnitude and direction of the subsequent phase shift dictated by the intensity and timing of the light exposure. A LP administered at the beginning of the night will induce a phase delay, while a LP at the end of the night will prompt a phase advance of activity onsets (Pittendrigh, 1981). Phase shifting responses to light played an important role in the identification of the melanopsin-based pRGCs, particularly via action spectroscopy methods employing different wavelengths and intensities of light (Foster et al., 2007a; Lucas et al., 2001; Peirson et al., 2005). Another approach to studying phase shifting and responses to circadian challenges, is the use of abrupt shifts of the LD cycle, or “jet lag” protocols. In addition, an animal may appear to entrain to a LD cycle, while activity may simply be suppressed during the light phase of the LD cycle (negative masking) (Aschoff, 1960; Mrosovsky, 1999). For example, *Cry1*$^{-/-}$/*Cry2*$^{-/-}$ dKO mice appear to display normal activity under LD conditions, but become arrhythmic under DD, as they lack a functional clock (Horst et al., 1999). Understanding circadian rhythms in mice

therefore requires the study of behavior under a range of lighting conditions, to determine how animals respond under entrained, free-running and shifted LD cycles.

Screening circadian behavior is not straightforward and requires a comprehensive assessment of an animal's locomotor activity as a behavioral output of the underlying clock mechanisms. This approach requires a detailed phenotyping screen to define any underlying disruptions to the clock (Albrecht & Foster, 2002; Hughes et al., 2015; Jud et al., 2005). Typically, this involves the study of home cage activity under specific lighting conditions, including LD cycles, DD, and LL, as well as assessments of phase shifting responses (Eckel-Mahan & Sassone-Corsi, 2015). Standard metrics are then computed to determine circadian period, as well as measurements of circadian rhythm disruption, including measures of the fragmentation, strength, regularity, and day-to-day stability of the rhythms under different lighting conditions (Brown et al., 2019). Wheel-running behavior has historically been the most common methodology for assessing circadian rhythms (Albrecht & Foster, 2002; Bains et al., 2018; Banks & Nolan, 2011; Foster et al., 1991; Siepka & Takahashi, 2005). The pioneering studies of Curt Richter showed that rodents have a natural tendency to engage with running wheels, making it a convenient and efficient method for monitoring voluntary activity patterns over extended periods (Geary, 2007). This method has a high signal to noise ratio, resulting from minimal activity during the rest phase. This facilitates the identification of activity onsets and circadian phase under LD, DD, and LL, or following a brief light exposure in DD (Jud et al., 2005). Wheel-running behavior has been shown to be effective in identifying phenotypic differences based on mouse strains and age (Banks et al., 2015; Kitanaka et al., 2012; Possidente et al., 1995), as well as playing a critical role in the identification of mammalian clock mutants (Vitaterna et al., 1994). However, studies have shown that the introduction of running wheels can alter behavioral responses in rodents, including changes in food intake (Pendergast et al., 2014), depression-like behavior (Solberg et al., 1999), and aggression (Gammie et al., 2003). It can also affect other aspects of circadian or sleep physiology, notably strengthening circadian rhythms in aging mice (Leise, 2013), improving circadian disruption (Power et al., 2010), and

affecting sleep (Fisher et al., 2016; Vyazovskiy et al., 2006; Vyazovskiy & Tobler, 2012). Moreover, wheel-running activity does not capture behaviors such as grooming, feeding, anticipatory behavior preceding the dark phase, or other activity during the light phase. Finally, sleep/wake behavior cannot be inferred using wheel-running. By contrast, mouse immobility has been correlated with sleep bouts using video tracking and passive infrared based systems (Brown et al., 2016; Fisher et al., 2012; Pack et al., 2007).

In recent years, home cage monitoring techniques have undergone substantial improvements, driven primarily by welfare and behavioral research initiatives, facilitating continuous and non-invasive monitoring of animal behavior, and often accompanied by real-time data analysis. In addition to running wheels, these systems include PIR sensors, video tracking, radiofrequency identification (RFID) systems, and capacitive sensors (Voikar & Gaburro, 2020). As a result, researchers can choose the most appropriate monitoring method based upon their specific research questions, experimental design, and laboratory constraints. Home cage activity monitoring presents several challenges and limitations. Technical issues such as sensor malfunction, data loss, and environmental disturbances can affect the reliability and reproducibility of the results. By leveraging capacitive sensor technology and real-time data analytics, the DVC system (Tecniplast SpA, Italy), presents a novel solution to these challenges. The DVC system is based upon widely used individually ventilated cages (IVCs) placed in a rack that continuously records home cage activity (Pernold et al., 2019). It comprises capacitive sensor boards equipped with 12 equally spaced electrodes, which detect the presence of animals based on changes in capacitance across electrodes. This provides an animal locomotion index measuring cage level activity. Clear and red IVCs can be used to entrain animals to the room light cycle, while black IVCs equipped with lighting systems (Leddy) can provide individual LD cycles in every cage. As well as activity inside the cage, the DVC system can record when cages are removed from the rack as well as information regarding environmental room conditions outside the cage, enabling potential sources of disturbance to be monitored. Data are available and stored in real-time on the cloud-based DVC Analytics

platform, which also provides visualization and data analysis algorithms. The DVC system has been used across various fields of mouse biomedical research. The animal locomotion index was used to identify bouts of rest and physical activity in C57BL/6J mice (Pernold et al., 2023), to analyze outcomes in a stroke mouse model (Shenk et al., 2020), and to characterize rest and activity phenotypes in a mouse model of amyotrophic lateral sclerosis (Golini et al., 2020) and myotonic dystrophy type 1 (Golini et al., 2023). The DVC system has also been employed to investigate the effects of cage change (introduction of fresh bedding) (Pernold et al., 2019; Ulfhake et al., 2022) and the position of a cage in a rack on activity rhythms (Steel et al., 2022), as well as the associations between activity and recovery from an Achilles tendon injury (Faydaver et al., 2023). The spatial resolution of the DVC further allowed differences in home-cage behavior preferences to be determined between three mouse strains (Fuochi et al., 2023). However, despite its increasing use, to date, no studies have investigated whether the DVC system is suitable for conducting detailed circadian experiments.

Here we present new data exploring the use of the DVC system for circadian phenotyping. Mouse home cage activity was recorded under 12:12 LD, DD, and LL, as well as a 6-hour phase advance, and DD following exposure to a LP to measure phase shifting responses. Key circadian parameters and measures of circadian disruption were then determined under each lighting condition. To define the effectiveness of the DVC system in detecting phenotypic differences, mice lacking a functional circadian clock (*Cry1*$^{-/-}$, *Cry2*$^{-/-}$) were investigated under 12:12 LD and DD conditions. The DVC provides a novel approach to studying circadian rhythms in mice under IVC husbandry conditions, and combined with black cages and LED lighting can replicate the wide range of lighting conditions used in standard circadian phenotyping screens.

6.2. Methods

Animals. All animals were single housed under a 12:12 LD cycle for a minimum of one week prior to the start of experiments. *Ad libitum* access to food (Envigo 2916) and water was

provided throughout. Wild-type C57BL/6J animals were purchased from Envigo, UK, while Cryptochrome 1 and 2 dKO (*Cry1*$^{-/-}$, *Cry2*$^{-/-}$) animals (Horst et al., 1999) were bred in-house on a C57BL/6J background. This study is reported in accordance with the ARRIVE guidelines. All animals were included and were between 3 and 4 months old at the beginning of the study. Control and experimental groups were subjected to the same conditions at the same time to reduce confounding variables. As such, no randomization or blinding was used. All experimental procedures were carried out at the University of Oxford, UK, in accordance with the University of Oxford Policy on the Use of Animals in Scientific Research and the United Kingdom Animals (Scientific Procedures) Act 1986, under Project License PP0911346 and Personal License I34186130.

Lighting and Housing Conditions. The DVC system (Tecniplast SpA, Italy) allows for the continuous recording of home cage locomotor activity (Pernold et al., 2019). The system comprises 60 or 80 IVCs of type GM500, made of clear, red or black polycarbonate, offering options for both single and group housing (**Fig. 6.1A**). In this study, we utilized black IVCs, which were equipped with individual cool white LED systems known as Leddy. The Leddy lighting system facilitated the entrainment of animals to specific lighting cycles within each cage, eliminating the need for light-tight chambers typically used in circadian and sleep research. Light levels were kept at ~ 100 photopic lux at the center of the cage (Leddy light intensity level 22), giving < 2 S-cone opic lux, 70 melanopic lux, 75 rhodopic lux and 78 M-cone opic lux (Lucas et al., 2024) (**Supp. Fig. 6.1; Supp. Table 6.1**).

Home-cage Locomotor Activity Monitoring. Each IVC was positioned on a capacitive sensor board featuring 12 evenly spaced electrodes (**Fig. 6.1B**). This sensor board detected the presence of an animal by monitoring changes in capacitance across electrodes, primarily due to the animal's physiological composition (70% water) and movement. Subsequently, an Animal Locomotion Index (ALI) was calculated. This is based on the number of electrodes activated, with 0% = no electrodes and 100% = all 12 electrodes simultaneously activated within the time

bin (**Fig. 6.1C**). The DVC Analytics platform provided real-time access to the data for visual inspection and download. The system's default minimum activity binning was set to 1 min, although a resolution of 250 msec is possible. We performed daily welfare checks, with the cages being taken out of the rack for animal inspection for less than 5 min.

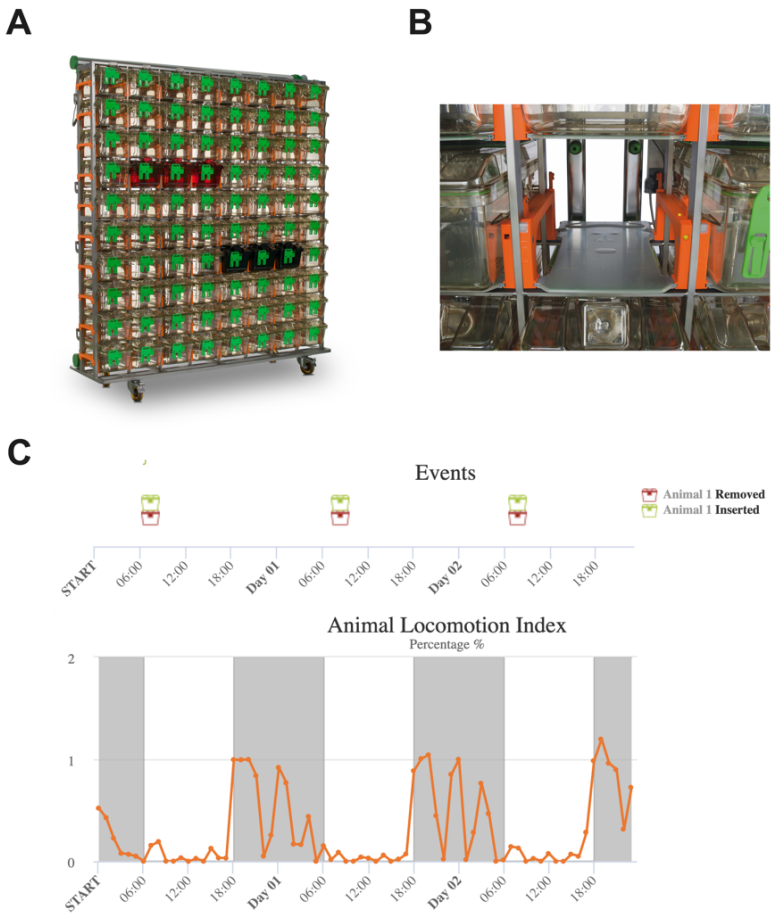

Figure 6.1. The DVC system and the Animal Locomotion Index. **A.** DVC rack equipped with clear, red, and black cages. **B.** Capacitive sensor board. **C.** Animal locomotion index for one WT C57BL/6J mouse, binned by hour, visualized on the cloud-based DVC Analytics platform. Timings of cage insertion and extraction for daily checks are also shown. Dark shading indicates dark phases.

Circadian Phenotyping. A total of 12 WT mice (C57BL/6, 6 males, 6 females) were included in the circadian screen. Home cage locomotor activity was recorded continuously for 10 weeks under various lighting conditions, including 12:12 LD, DD, LL, LD following a 6-hour phase

advance (jet-lag), and DD after exposure to a light pulse (LP) at ZT14-16 to measure phase shifting responses. A cage change was performed after the first period of DD (day 29), and before animals were re-entrained to a 12:12 LD cycle.

Clock-deficient mice. *Cry1*$^{-/-}$*,Cry2*$^{-/-}$ dKO mice (N = 6, 3 males, 3 females, N = 6 C57BL/6J controls) animals were used as a circadian clock deficient model. Cryptochrome-deficient mice are characterized by the deletion of the core clock genes Cryptochrome 1 and 2 (Horst et al., 1999). These mice have no circadian clock and exhibit arrhythmic behavior under constant conditions. This animal model was employed to assess whether the DVC system could effectively detect phenotypic differences based on locomotor activity, particularly under LD and DD conditions (1 week each).

Statistical Analyses. Raw animal locomotion index data were exported from the DVC Analytics platform in 1 min and 1 hour bins. Chi-square periodogram and activity onsets were computed in ActogramJ (Schmid et al., 2011). A 30-min running average was applied in order to account for missing values (daily checks) and to compute actograms. Inter-daily stability, intra-daily variability and relative amplitude were coded in R based on the equations provided in Witting et al. (1990). Light phase activity and total activity were calculated in R. One week of data was used to compute the circadian disruption measures for each lighting condition. Due to a user error, one female mouse is missing the final 17 h of activity recording during the DD period. Statistical testing and plotting were conducted in Prism 10. One-way or two-way repeated-measures ANOVA, with a Geisser-Greenhouse correction (for lack of sphericity) and Holm-Šídák's multiple comparisons test were computed. When comparing two groups, unpaired nonparametric Mann-Whitney tests or Wilcoxon matched-pairs signed rank tests were used, as the distribution of the data was not Gaussian. $\alpha = 0.05$ was adopted in all analyses. Mean ± standard error of the mean (SEM) was used for all plots.

6.3. Results

Circadian Screen. To assess the suitability of the DVC system for circadian phenotyping studies, mice were singly housed in DVCs, and locomotor activity was monitored under LD, DD, LL, a 6-hour phase advance, and DD following a LP. A representative double plotted actogram is shown in **Fig. 6.2** and illustrates entrainment to the various light-dark cycles, with orange dots indicating activity onsets. Home cage locomotor activity rhythms in LD, DD and LL, were further analyzed using standard measures of circadian disruption (Brown et al., 2019).

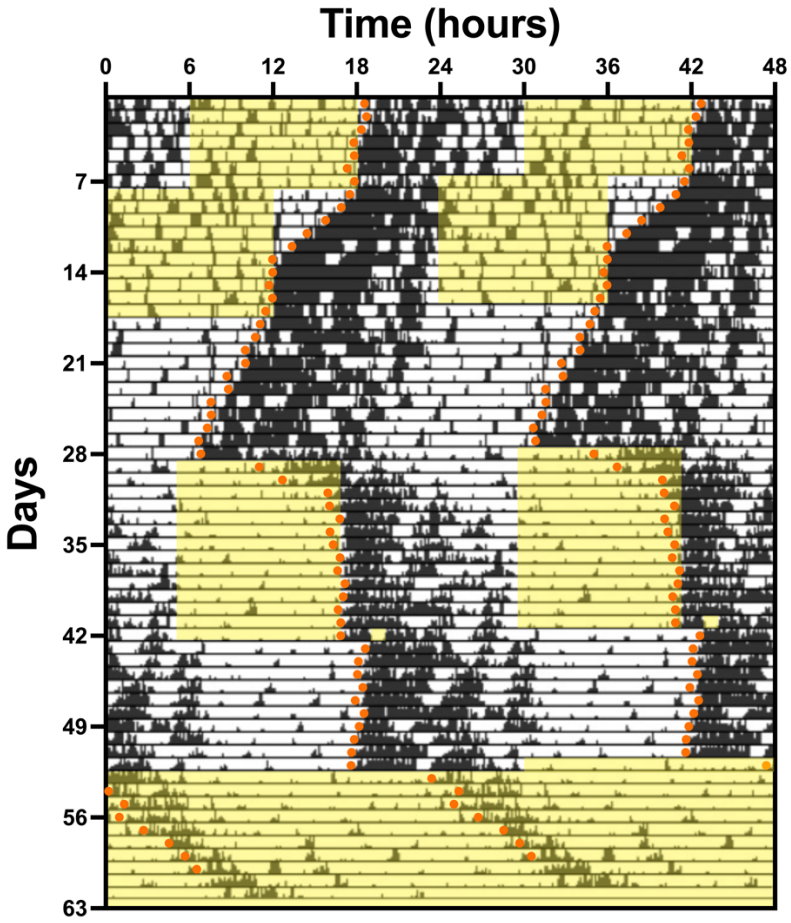

Figure 6.2. Measuring circadian rhythms with the DVC system. Representative double-plotted actogram of locomotor activity for a WT C57BL/6J mouse using the DVC system. The circadian screen included 1 week in 12:12 LD, 10 days in LD following a 6-hour advance, 10 days in DD, 2 weeks in LD to re-entrainment, 10 days in DD following a LP at ZT14-16, and 10 days in LL. Yellow shading indicates light phases, while orange dots depict activity onsets.

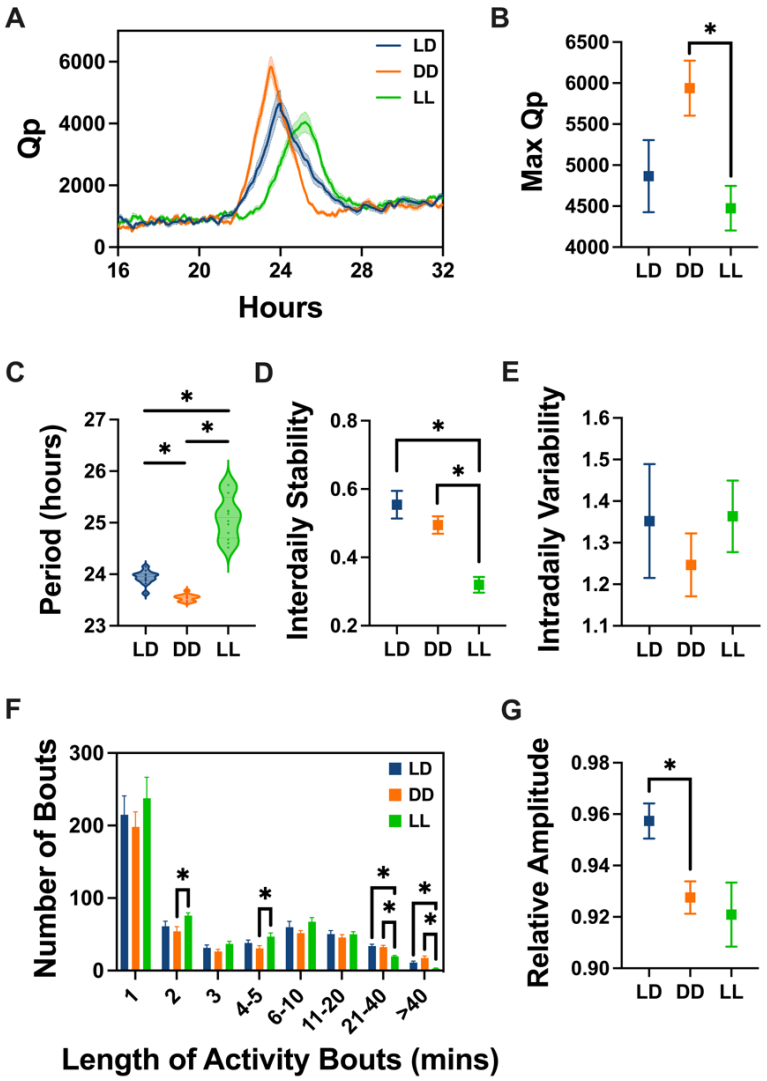

Figure 6.3. Measures of circadian disruption for 12 WT C57BL/6J mice under 12:12 LD, DD and LL. **A.** Chi-square periodogram analysis. **B.** Maximum Qp values (Lighting, $F_{(1.565, 17.22)} = 4.507$, $p = 0.0340$). **C.** Period of activity rhythms (Lighting, $F_{(1.121, 12.34)} = 106.3$, $P < 0.0001$) **D.** Inter-daily stability (Lighting, $F_{(1.437, 15.81)} = 16.71$, $p = 0.0003$). **E.** Intra-daily variability. **F.** Distribution of the number and duration of activity bouts. **G.** Relative amplitude (Lighting, $F_{(1.465, 16.12)} = 4.942$, $p = 0.0295$). Mean +/- SEM. Statistically significant multiple comparisons are indicated by an asterisk.

Periodogram Analysis. The Chi-square periodogram was employed to quantify the strength and regularity of the activity rhythms (**Fig. 6.3A**), expressed through the Qp value (Refinetti, 2004). A significant effect of lighting condition on the periodogram power was observed (Lighting, $F_{(1.565, 17.22)} = 4.507$, $p = 0.0340$), with a higher Max Qp value under DD compared to LL (mean diff = 1464, $p = 0.0047$; **Fig. 6.3B**), indicative of more robust rhythms in DD. Activity patterns under entrained conditions are typically influenced by environmental cues. Under a 24-hour LD cycle, C57BL/6J mice generally display a 24-hour period. However, in DD, the endogenous circadian period is expressed, resulting in a free-running period of approximately 23.5 hours (Valentinuzzi et al., 1997). By contrast, constant light suppresses night-time activity, causing the period of activity to lengthen to more than 24 hours (Aschoff, 1952). Our results showed that the period statistically differed between lighting conditions (Lighting, $F_{(1.121, 12.34)} = 106.3$, $P < 0.0001$), and aligned with the outlined patterns, revealing mean periods of 23.9 hours (SEM = 0.04) under LD, 23.5 hours (SEM = 0.02) under DD, and 25.1 hours (SEM = 0.12) under LL, with higher variability under LL (**Fig. 6.3C**).

Inter-Daily Stability. Under a 12:12 LD cycle, high inter-daily stability values are expected due to the presence of consistent time cues. Under DD, and in the absence of such cues, inter-daily stability is expected to decrease slightly. Under LL, constant light weakens the circadian clock in the SCN, leading to reduced day-to-day reproducibility. Here, inter-daily stability values decreased accordingly from LD, to DD and LL (Lighting, $F_{(1.437, 15.81)} = 16.71$, $p = 0.0003$; **Fig. 6.3D**).

Intra-Daily Variability. Our data showed that activity rhythms remained consolidated, with no significant differences in intra-daily variability between lighting conditions (Lighting, $F_{(1.598, 17.58)} = 0.7966$, $p = 0.4404$; **Fig. 6.3E**).

Activity Bouts. The overall number and distribution of activity bouts did not statistically differ between lighting conditions (Lighting x Bout length, $F_{(14, 231)} = 0.8822$, $p = 0.5789$; **Fig. 6.3F**). This suggests that the structure of activity patterns was consistent across conditions.

Relative Amplitude. Relative amplitude is determined by the difference between the period of maximum and minimum activity levels over the 24-hour cycle. It serves as a simple measure of the contrast between periods of high activity and rest. In the absence of external cues, such as DD, the strength of activity rhythms often declines, leading to a decrease in relative amplitude. This decrease tends to be even more pronounced under LL, where light during the subjective night suppresses mouse activity. Consistent with these patterns, here, the relative amplitude varied between lighting conditions (Lighting, $F_{(1.465, 16.12)} = 4.942$, $p = 0.0295$), with a decrease in both DD and LL conditions when compared to LD (**Fig. 6.3G**).

Jet Lag. We subjected animals to a 6-hour phase advance of the LD cycle and recorded the duration required for them to re-entrain to the new LD cycle. Results showed that it required 6 days for animals to successfully re-entrain to the LD cycle, suggesting that one day of adjustment is required per hour of phase shift (**Fig. 6.4A**).

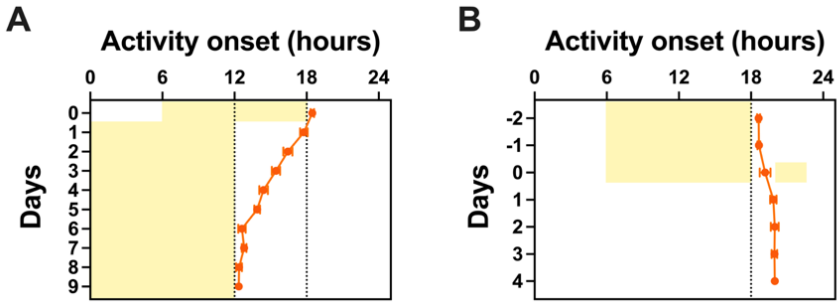

Figure 6.4. Phase shifting responses for 12 WT C57BL/6J mice. **A.** Animals required about 6 days to re-entrain to the LD cycle following a 6-hour phase advance, as illustrated by the shift in activity onset. **B.** Animals' activity onsets were delayed by 1.3 hours in constant darkness following exposure to a light pulse at ZT14-16 (Wilcoxon matched-pairs signed rank test, Day -1 vs Day 4, $z = -1.375$, $p = 0.0005$). Mean +/- SEM.

Phase Shifting Responses. Additionally, we investigated whether a LP administered at the beginning of the night (ZT14-16) could shift the phase of activity (Jud et al., 2005). When comparing the activity onset of animals one day before the LP (Day -1) and four days after

(Day 4), we observed a delay of about 1.3 hours, confirming a shift in the phase of activity consistent with an Aschoff type II protocol (Wilcoxon matched-pairs signed rank test, z = -1.375, p = 0.0005; **Fig. 6.4B**).

Sex differences. Sex differences can manifest in various aspects, including the timing and amplitude of activity patterns, sleep/wake cycles, and responses to environmental cues (Joye & Evans, 2022). Subtle differences between the activity profiles of male and female mice were observed using the DVC system (**Supp. Fig. 6.2**). We found a significant main effect of Sex on IV ($F_{(1, 10)}$ = 14.52, p = 0.0034), and total activity ($F_{(1, 10)}$ = 14.85, p = 0.0032). Overall, females demonstrated more consolidated rhythms and greater activity levels compared to males. Furthermore, a significant Lighting x Sex interaction was found for both period ($F_{(2, 20)}$ = 3.982, p = 0.0350), and RA ($F_{(2, 20)}$ = 4.953, p = 0.0179). Females displayed a shorter period (Mean Diff = -0.095) and higher amplitude (Mean Diff = 0.018) under LD, a longer period (Mean Diff = 0.055) and higher amplitude (Mean Diff = 0.006) under DD, and a longer period (Mean Diff = 0.445) and lower amplitude (Mean Diff = - 0.045) under LL. The number and distribution of activity bouts differed between sexes under LD (Bout length x Sex, $F_{(7, 70)}$ = 4.091, p = 0.0008), and LL (Bout length x Sex, $F_{(7, 70)}$ = 5.040, p = 0.0001), but not under DD (Bout length x Sex, $F_{(7, 70)}$ = 1.451, p = 0.1991). Under LD and LL, females showed more long bouts of activity. Females also exhibited a greater delay in activity onset in the days following a LP (Sex, $F_{(1, 10)}$ = 15.47, p = 0.0028), but did not show significant differences in re-entrainment following a 6-hour jet lag (Sex, $F_{(1, 10)}$ = 0.5986, p = 0.4570; **Supp. Fig. 6.3**). Together, these findings highlight the importance of considering both male and female animals in circadian phenotyping studies.

Clock-deficient mice. In the mammalian circadian clock, CRY1 and CRY2 proteins inhibit the activation of the CLOCK-BMAL1 transcription complex, thereby regulating the expression of clock-controlled genes and ultimately controlling the timing of physiological processes and behaviors (Patton & Hastings, 2023). Deletion of both *Cry1* and *Cry2* results in arrhythmic

behavior under constant conditions such as DD (Horst et al., 1999). Cryptochrome-deficient mice have also been characterized by abnormalities in cognition and habituation behavior, and increases in immobility, restlessness and anxiety-like behavior (De Bundel et al., 2013; Hühne et al., 2020). Here, we investigate whether home cage activity monitoring using the DVC system could detect arrhythmic mouse models.

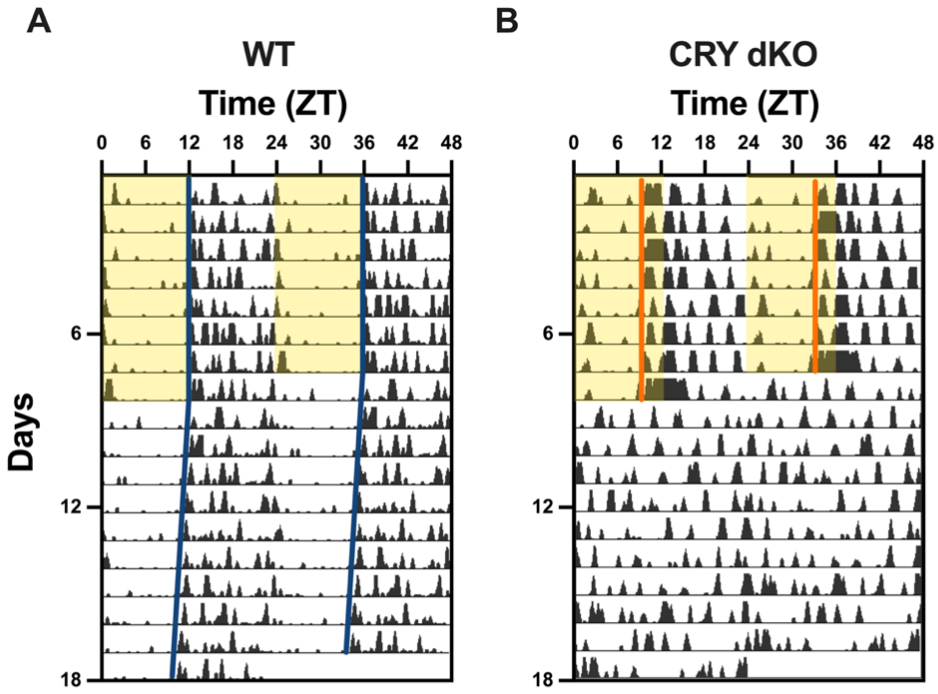

Figure 6.5. Representative double-plotted actogram of locomotor activity for a WT C57BL/6J (WT) and a Cryptochrome-deficient (*Cry1*$^{-/-}$, *Cry2*$^{-/-}$, labelled CRY dKO) mouse using the DVC system. Animals were exposed to one week of 12:12 LD cycle and 10 days of DD. Yellow shading indicates light phases, while blue and orange lines depict activity onsets.

Representative actograms of cryptochrome-deficient mice show apparently normal nocturnal activity under LD conditions, but arrhythmic activity under DD in comparison with free-running activity in C57BL/6J WT mice (**Fig. 6.5**). Chi-square periodogram analysis indicated no significant difference in the period of activity rhythms between WT and Cryptochrome-deficient animals under 12:12 LD cycles (M = 23.99, SEM = 0.009, and M = 24.06, SEM = 0.078, respectively; **Fig. 6.6A**). However, Cryptochrome-deficient animals displayed lower Max Qp values (Genotype, $F_{(1, 10)} = 19.31$, $p = 0.0013$; **Fig. 6.6B**), earlier activity onsets (Genotype, $F_{(1, 10)} = 259.4$, $P < 0.0001$; **Fig. 6.6C**), more light-phase activity (Mann-Whitney, $U = 0$, $p = 0.0022$, **Fig. 6.6D**), and a higher frequency of short bouts of activity compared to WT mice (Genotype x Bout length, $F_{(7, 70)} = 4.211$, $p = 0.0006$; 1 min bout, mean diff = -135.3, $P < 0.0001$; **Fig. 6.6E**). This suggests that Cryptochrome-deficient animals exhibited less robust and more fragmented rhythms under LD, with increased daytime activity. Under DD, Cryptochrome-deficient mice showed a lack of rhythmicity, as anticipated for animals lacking a functional endogenous clock in the absence of zeitgebers (**Fig. 6.5**). Periodogram analysis identified a high variance in their circadian period and lower Max Qp values (Genotype, $F_{(1, 10)} = 19.31$, $p = 0.0013$; **Fig. 6.6B**). However, there was no statistical difference between the distribution of their activity bouts compared to WT animals (Genotype x Bout length, $F_{(7, 70)} = 0.1472$, $p = 0.9938$; **Fig. 6.6F**). Furthermore, standard measures of circadian disruption highlighted lower IS (Genotype, $F_{(1, 10)} = 38.95$, $P < 0.0001$; **Fig. 6.6G**), higher IV (Genotype, $F_{(1, 10)} = 6.571$, $p = 0.0282$; **Fig. 6.6H**), and lower RA values (Genotype, $F_{(1, 10)} = 122.6$, $P < 0.0001$; **Fig. 6.6I**) in Cryptochrome-deficient mice compared to WTs under both LD and DD conditions. These findings suggest less reproducible day-to-day rhythms, increased fragmentation, and weaker amplitude in animals lacking a circadian clock. Although Cryptochrome-deficient animals appeared less active overall, the statistical tests did not reach significance, which is likely due to the WT's high variance (Genotype, $F_{(1, 10)} = 3.969$, $p = 0.0743$; **Fig. 6.6J**). Additionally, sex differences were found for period (Sex, $F_{(1, 4)} = 25.88$, $p = 0.0070$) and Max Qp values (Sex, $F_{(1, 4)} = 12.64$, $p = 0.0237$), but no statistically significant

differences were observed for circadian disruption measures between male and female cryptochrome-deficient mice (**Supp. Fig. 6.4**).

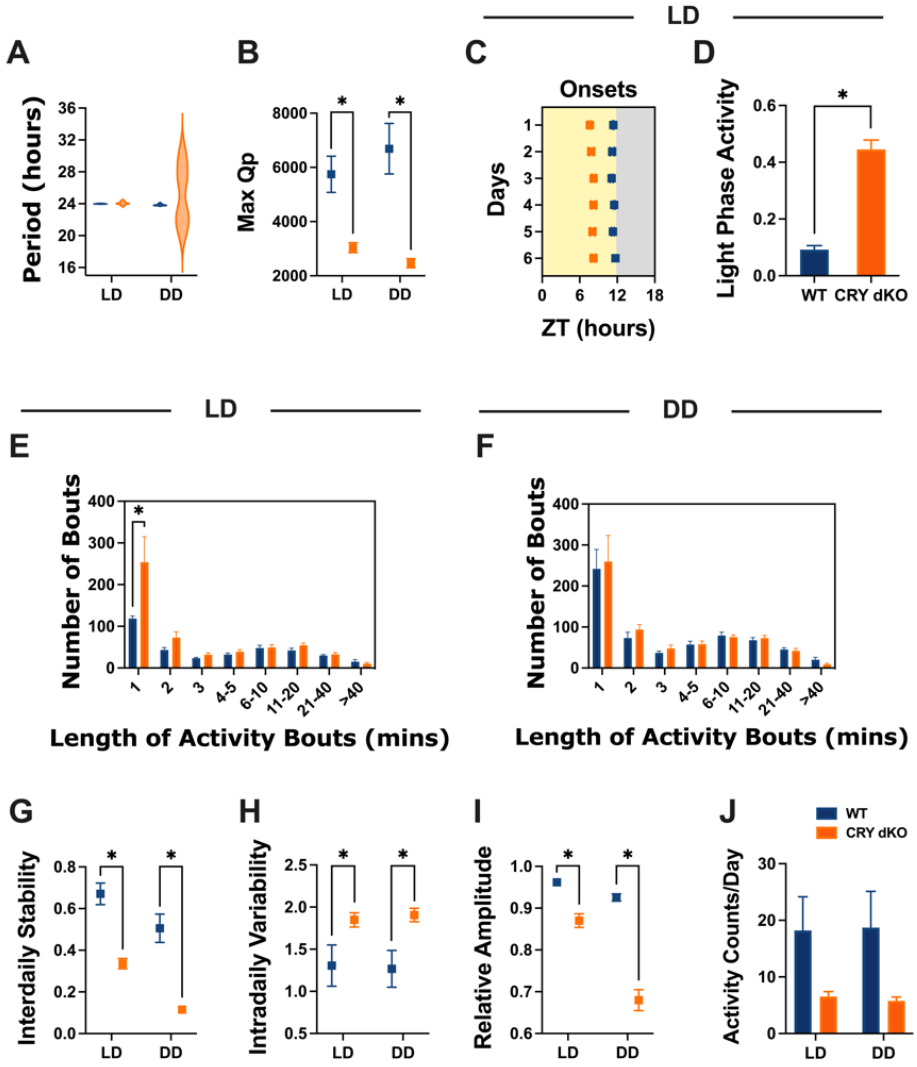

Figure 6.6. Measures of circadian disruption for 6 WT C57BL/6J (WT) and 6 Cryptochrome-deficient (CRY dKO) mice under 12:12 LD and DD. **A.** Period of activity rhythms. **B.** Maximum Qp values (Genotype, $F_{(1, 10)} = 19.31$, $p = 0.0013$). **C.** Activity onsets in LD. **D.** Proportion of light phase activity in LD. **E.** Distribution of the number and duration of activity bouts in LD (Bout length x Genotype, $F_{(7, 70)} = 4.211$, $p = 0.0006$). **F.** Distribution of the number and duration of activity bouts in DD. **G.** Inter-daily stability (Genotype, $F_{(1, 10)} = 38.95$, $p < 0.0001$). **H.** Intra-daily variability (Genotype, $F_{(1, 10)} = 6.571$, $p = 0.0282$). **I.** Relative Amplitude (Genotype, $F_{(1, 10)} = 122.6$, $p < 0.0001$). **J.** Total activity per day (Genotype, $F_{(1, 10)} = 3.969$, $p = 0.0743$). Mean +/- SEM. Statistically significant multiple comparisons are indicated by an asterisk.

6. 4. Discussion

Here we show the feasibility of conducting a comprehensive circadian screen within standard IVCs using the DVC system in combination with black cages with in-built cage lighting. Using well-established circadian parameters commonly employed in circadian phenotyping studies, we observed the repertoire of circadian phenotypes typically measured with standard monitoring techniques. Our results showed that mice housed within the DVC system exhibited a circadian period close to 24 hours when subjected to a 12:12 LD cycle. Mice further demonstrated a free-running period of about 23.5 hours under DD, and a period lengthening under LL, indicative of a robust circadian clock under DD and weaker rhythms under LL. Consistent with previous studies, mice effectively responded to phase shifts induced by interventions such as jet-lag or light pulses. Animals took 6 days to re-entrain to a 6-hour phase advance of the LD cycle, which indicates a rate of 1 day per hour shifted. Following a 2-hour LP at the beginning of the subjective night (ZT 14-16), mice delayed their circadian phase by approximately 1 hour under subsequent DD.

Sex differences in period, amplitude and the stability of rhythms, as well as phase shifting responses, were also observed. Female reproductive cycles can change both activity levels and phase, with an increased activity in proestrus/estrus, which can lead to a distinctive “scalloping” pattern of activity across the days of the estrous cycle in hamsters. However, results on these estrous effects are more varied in mice, potentially reflecting strain, diet, housing conditions and methods of activity monitoring. Here we show subtle sex-dependent differences in home cage activity, with higher activity in females consistent with previous studies (Joye & Evans, 2022). However, as our study primarily focused on responses to changing light conditions, we did not maintain mice under consistent lighting for extended periods nor perform estrous cytology. Future studies are thus needed to relate patterns of home cage locomotor activity to the estrous cycle using the DVC system.

Additionally, the DVC system successfully detected arrhythmic mutants and their expected phenotypic differences. Our results showed that under LD conditions, Cryptochrome-deficient mice exhibited no differences in period compared to WT controls, yet they displayed increased activity during the light phase and earlier activity onsets. Under DD, cryptochrome-deficient animals were arrhythmic, as expected for mice lacking a functional circadian clock. An important issue when adopting a different approach to circadian activity monitoring is its performance against other methods, such as running wheels, particularly when comparing its ability to detect differences between experimental groups. For mutagenesis screens, published data from C57BL/6J mice *tau* are 23.69 h ± 0.06 (Nolan et al., 1997), and 23.7 h ± 0.17 (Takahashi et al., 2008), which is comparable to that observed here in the DVC (23.50 h ± 0.07). This suggests that it should be possible to reliably detect phenodeviants in forward genetic screens (typically defined as 3 standard deviations from the mean). Where comparisons are made between two groups (e.g. WT vs KO), power calculations based on $\alpha = 0.05$ and power $(1-\beta) = 0.80$, show that detecting an effect size (Cohen's d) of 2 requires 6 animals per group. For the DVC data, this would translate to detecting a 0.13 h difference in *tau* between groups with N = 6 per group. This is again comparable to running wheels and sufficient to detect most transgenic lines with all but the most subtle circadian phenotypes.

Collectively, these findings show that the DVC system provides a versatile tool for quantifying circadian disruption, investigating clock gene mutants, and facilitating comprehensive circadian phenotyping. Moreover, this is, to our knowledge, the first example of a comprehensive circadian screen conducted using IVCs.

As with any home cage activity monitoring system, the DVC possesses both strengths and limitations that potential users should consider (**Table 6.1**). These are detailed below.

Table 6.1. Strengths and limitations of the DVC and Leddy systems for circadian rhythm studies.

Strengths	Limitations
High-capacity monitoring	Daily observation logistics
Individual light-dark cycle control	Leddy battery system
Enhanced biosecurity	Leddy configuration
Environmental enrichment compatibility	Absence of light sensor
Environmental monitoring	Additional analytics
Wheel-running integration	Cost
Real-time data accessibility	Research flexibility

6.4.1. Strengths

1) **High-capacity monitoring**. An advantage of the DVC system is its high capacity, allowing for the simultaneous monitoring of up to 80 individual cages. Circadian rhythm studies often utilize light-tight chambers or "coffins", which typically house between 6-10 animals per chamber. The DVC system offers a space-efficient alternative, as one 80 cage DVC rack occupies the space equivalent of a stack of four typical chambers, which would hold between 24-40 cages (2 – 3 times stocking density). By maximizing laboratory space utilization, the DVC system is an advantageous solution for institutions with limited animal facility space.

2) **Individual LD cycle control.** Each cage in the DVC system can be programmed to operate under its own light-dark cycle. The Leddy lighting system allows for adjustable light intensity, duration, dawn-dusk transitions and non-24 h LD cycles, simulating a wide range of lighting conditions. This provides researchers with a high level of experimental flexibility and customization.

3) **Enhanced biosecurity**. The use of IVCs can also help prevent the spread of animal pathogens and reduce staff exposure to laboratory animal allergens, as opposed to open-top

cages. These are key factors in the widespread adoption of IVCs in laboratory animal husbandry.

4) **Environmental enrichment compatibility**. The incorporation of environmental enrichment, such as nesting materials and tubes, does not limit the detection of animal movement by the DVC system, unlike other methods such as PIR recordings and video tracking where the animal must be in view throughout.

5) **Environmental monitoring.** The DVC system can also provide alerts for cage disturbances such as low food or water, water bottle leaks and soiled bedding conditions, as well as deviations from normal activity patterns. This ensures the reliability and accuracy of experimental data by promptly identifying potential disruptions as well as providing a useful welfare check for researcher and animal care staff. The DVC also timestamps any cage removal and replacement in the rack. For example, this can be used to correlate daily welfare checks and other non-photic cues with small sudden changes in behavior. Additionally, the Rack Environmental Monitoring device can monitor environmental parameters outside the rack such as temperature, humidity, noise, light, vibration and human presence. This also enables users to receive alerts and correlate these parameters to activity metrics to determine how facility disturbances may affect data. This environmental monitoring may benefit the reproducibility of circadian and behavioral studies by enabling detection of changes in the environment that may influence animal behavior.

6) **Wheel-running integration**. Running wheels can be integrated into the DVCs, providing additional opportunities for the monitoring of voluntary activity and exercise behavior in a manner comparable with the majority of published circadian studies.

7) **Real-time data accessibility**. The DVC system provides researchers with access to real-time data through its cloud-based DVC Analytics platform. This feature allows for continuous monitoring of animal behavior from any location, facilitating timely intervention, data analysis and storage. The platform offers a range of parameters for data inspection and visualization, including single actograms. The DVC system measures home

cage locomotor activity, distance, and velocity, as well as variables relevant to circadian rhythm studies, such as environmental disturbances and alerts for potential behavioral impacts. This comprehensive data collection may enable researchers to gain insights into the complex interplay between circadian rhythms and laboratory environmental factors. Critically, real-time analytics enable researchers and technicians to respond to changes in activity patterns, for example if animals are sick.

Despite its strengths, the current format of the DVC system does have several potential limitations that circadian researchers should be aware of.

6.4.2. Limitations

1) **Daily observation logistics.** The benefits of using black cages as independent light-tight chambers must be weighed against practical considerations of their use. Black cages require specific protocols for daily animal checks, similar to light-tight chambers, where cages must be opened at appropriate phases of the LD cycle. When room lights match the cages' light cycles, checks can be performed during the light phase. Similarly, if cages are under constant darkness, they can be observed when the room is in darkness using dim red light or infrared goggles. If the room lights and the cages' light cycles cannot be aligned, cages must be removed from the rack and observed in a different room to avoid light exposure. Where complex lighting schedules are required or multiple users require different lighting schedules, this may be a logistical challenge to manage. Researchers should be aware of these limitations when considering using the DVC system.

2) **Leddy battery power**. One drawback of the Leddy lighting system is its requirement to be removed from the cage for charging. The air-tight sealed cages prevent the use of cables and the system cannot operate while charging. This necessitates additional Leddy systems to be switched in to maintain experimental conditions. Under a 12:12 LD cycle at ~ 100 lux, a Leddy battery can last up to three weeks. However, the non-linear battery life

necessitates regular checks and maintenance, which may pose an additional logistical challenge for researchers.

3) **Leddy configuration**. The Leddy lighting system is unable to accommodate complex LD cycles. Its configuration allows for changes between light and dark phases, including dim light ramps, but not consecutive periods of light at different intensities, such as DLE. Moreover, the system only provides cool white LEDs, precluding any adjustments to the light spectrum. Incorporating additional lighting components, such as red LEDs for welfare checks or violet LEDs to help simulate daylight, would further enhance its versatility and functionality (Lucas et al., 2024).

4) **Absence of light sensor**. Individual light sensors are not present within each cage, necessitating careful monitoring to ensure data accuracy and consistency of lighting schedules.

5) **Additional analytics**. The inclusion of double plotted actograms and standard measures of circadian disruptions within the DVC Analytics platform would enhance its utility for circadian researchers. This would allow comprehensive data analysis and interpretation on a single platform. For example, periodogram analysis and activity onset detection, as well as key metrics of circadian disruption such as IS, IV and RA would be particularly beneficial.

6) **Cost**. The initial investment needed to deploy the DVC and Leddy lighting systems represents a substantial capital investment, with additional expenses incurred for ongoing analytics. Consequently, this approach may be better suited for core research facilities that accommodate multiple research groups rather than individual labs. Increasing interest from labs working on mouse behavior may also facilitate such integration within core facilities. Whilst costs are decreasing with increasing uptake, users should be aware of overheads associated with this technology.

7) **Research flexibility**. The standard IVC cage format may not be suitable for researchers requiring greater flexibility in their experimental design. For example, researchers using non-standard caging, complex lighting systems, cameras/sensors, telemetry, tethered recordings, or in-cage behavioral measurements may preclude the use of an IVC.

As can be seen from the above, the DVC system offers many advantages, including high-capacity monitoring, individual LD cycle control, enhanced biosecurity, environmental monitoring features, high resolution, real-time accessibility and user-friendly online analytics. However, new users should consider potential limitations, such as the absence of light sensors and the charging logistics of the Leddy system, that may affect its performance in circadian rhythm studies. Additionally, research flexibility may be key. The DVC system might not work for researchers aiming to perform complex light cycle manipulations or specific types of studies where an IVC format is unsuitable.

6. 5. Conclusion

Here we show that the DVC system provides an alternative tool for circadian phenotyping, providing an opportunity to conduct such assessments in IVC cages. The storage and real-time availability of the data on the cloud-based DVC analytics platform facilitates data analysis, as well as ongoing experimental monitoring and interventions, providing an advantage over existing systems. However, researchers should be aware of the current limitations particularly with regard to cost and research flexibility, which may influence the adoption of an IVC based system. In this regard, the DVC system may be more suited for central phenotyping facilities rather than individual circadian labs.

6. 5. Supplemental Material

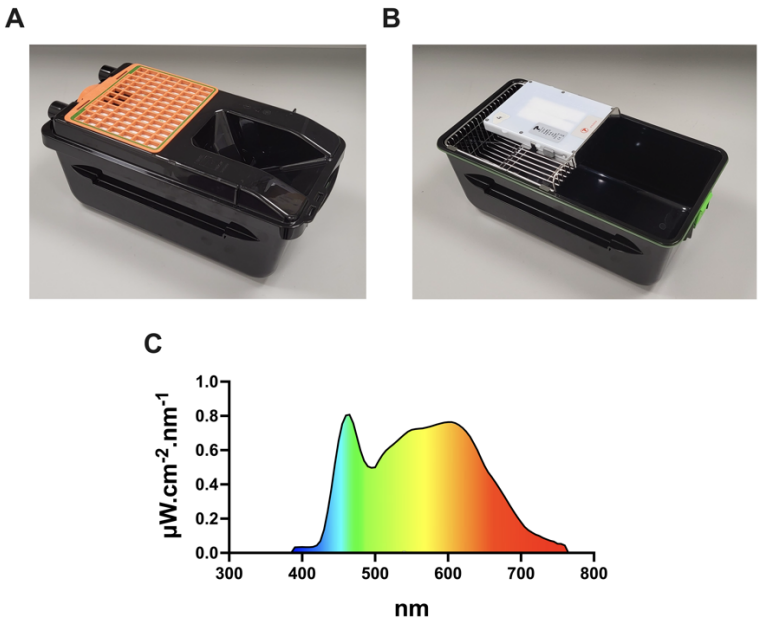

Supplemental Figure 6.1. Black DVC cage and Leddy lighting system. **A.** Closed view and **B.** Open view of a black DVC cage equipped with a Leddy lighting system. **C.** Spectral power distribution of the Leddy at light intensity level 22.

Supplemental Table 6.1. Spectral power distribution of the Leddy lighting system at light intensity level 22.

nm	$\mu W.cm^{-2}.s^{-1}$	nm	$\mu W.cm^{-2}.s^{-1}$
300	0	545	0.707907428
305	0	550	0.718842202
310	0	555	0.722735247
315	0	560	0.725142483
320	0	565	0.727482315
325	0	570	0.73192321
330	0	575	0.737395487
335	0	580	0.743373588
340	0	585	0.750512991
345	0	590	0.756208319
350	0	595	0.761354284
355	0	600	0.763915072
360	0	605	0.763767282
365	0	610	0.757710251
370	0	615	0.746227219
375	0	620	0.729391235
380	0	625	0.707889267
385	0	630	0.679822289
390	0.032529912	635	0.642123981
395	0.033849468	640	0.601247593
400	0.034693374	645	0.554548111
405	0.033590906	650	0.508052821
410	0.033575219	655	0.471222214
415	0.035761695	660	0.442100136
420	0.043843236	665	0.412491179
425	0.069125606	670	0.379144738
430	0.136052666	675	0.345627195
435	0.241369271	680	0.310587784
440	0.373673509	685	0.275717379
445	0.520506524	690	0.241339905
450	0.656460295	695	0.209853461
455	0.752857712	700	0.179711496
460	0.80319366	705	0.152475128
465	0.807369011	710	0.133126363
470	0.757781439	715	0.11938742
475	0.6797518	720	0.106866188
480	0.596800237	725	0.099167912
485	0.537800661	730	0.08790518
490	0.505381555	735	0.079725687
495	0.497358909	740	0.07128311
500	0.499728078	745	0.06588531
505	0.538099965	750	0.053602231
510	0.572088873	755	0.052955424
515	0.598159677	760	0.043976372
520	0.617308833	765	0
525	0.633836375	770	0
530	0.652874762	775	0
535	0.672169495	780	0
540	0.691301073		

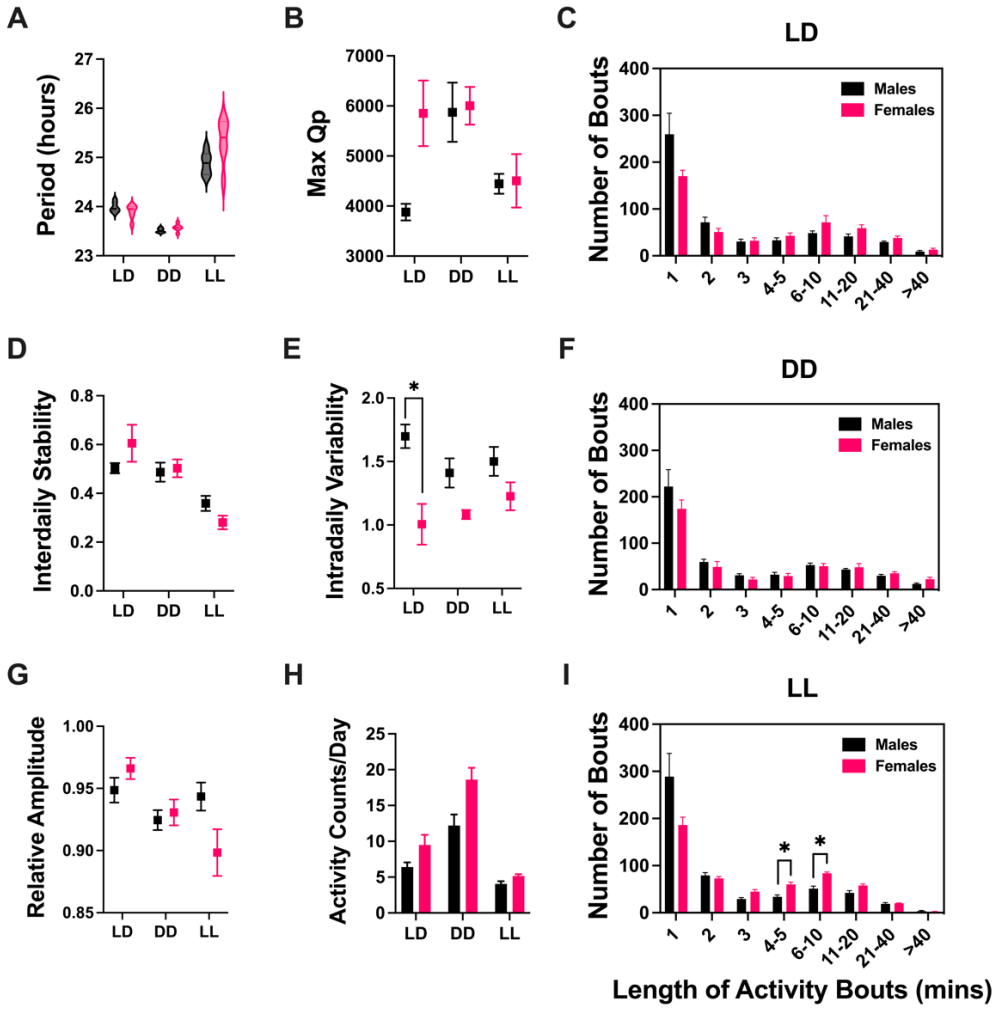

Supplemental Figure 6.2. Disaggregation of circadian disruption measures by sex for 6 male and 6 female WT C57BL/6J mice under 12:12 Light-Dark (LD), constant darkness (DD) and constant light (LL). **A.** Period of activity rhythms (Sex, $F_{(1, 10)} = 4.313$, $p = 0.0645$). **B.** Maximum Qp values (Sex, $F_{(1, 10)} = 4.033$, $p = 0.0724$). **C.** Distribution of the number and duration of activity bouts in LD (Bout length x Sex, $F_{(7, 70)} = 4.091$, $p = 0.0008$). **D.** Inter-daily stability. **E.** Intra-daily variability (Sex, $F_{(1, 10)} = 14.52$, $p = 0.0034$). **F.** Distribution of the number and duration of activity bouts in DD. **G.** Relative Amplitude. **H.** Total activity per day (Sex, $F_{(1, 10)} = 14.85$, $p = 0.0032$). **I.** Distribution of the number and duration of activity bouts in LL (Bout length x Sex, $F_{(7, 70)} = 5.040$, $p = 0.0001$). Mean +/- SEM. Statistically significant multiple comparisons are indicated by an asterisk.

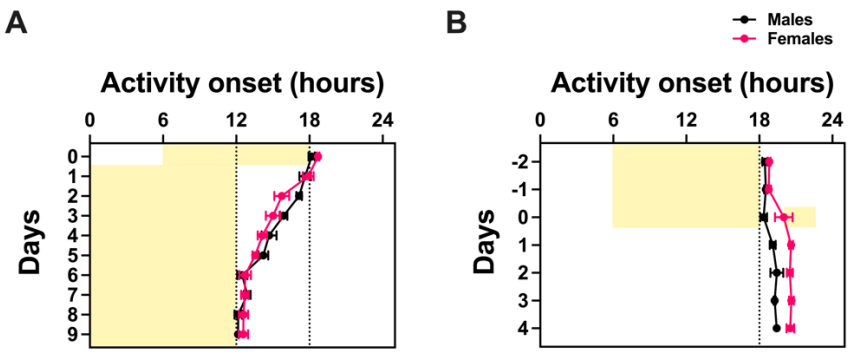

Supplemental Figure 6.3. Disaggregation of phase shifting responses by sex for 6 male and 6 female WT C57BL/6J mice. **A.** Both sexes required about 6 days to re-entrain to the Light-Dark (LD) cycle following a 6-hour phase advance, as illustrated by the shift in activity onset. **B.** Females exhibited a greater delay in activity onset by about 2 fold in constant darkness (DD) following exposure to a light pulse at ZT14-16, as compared to males (Sex, $F_{(1, 10)} = 15.47$, $p = 0.0028$). Mean +/- SEM.

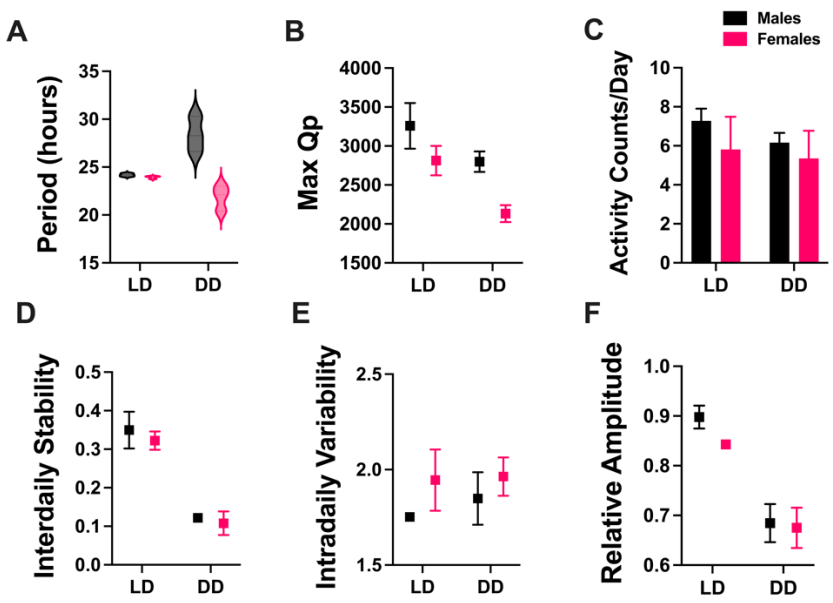

Supplemental Figure 6.4. Disaggregation of circadian disruption measures by sex for 3 male and 3 female Cryptochrome-deficient mice under 12:12 Light-Dark (LD) and constant darkness (DD). **A.** Period of activity rhythms. **B.** Maximum Qp values (Sex, $F_{(1, 4)} = 12.64$, $p = 0.0237$). **C.** Total activity per day. **D.** Inter-daily Stability. **E.** Intra-daily Variability. **F.** Relative Amplitude. Mean +/- SEM.

References

Abrahamson, E. E., & Moore, R. Y. (2001). Suprachiasmatic nucleus in the mouse: retinal innervation, intrinsic organization and efferent projections. *Brain Res*, *916*(1-2), 172-191. https://doi.org/10.1016/s0006-8993(01)02890-6

Albrecht, U., & Foster, R. G. (2002). Placing ocular mutants into a functional context: a chronobiological approach. *Methods*, *28*(4), 465-477. https://doi.org/https://doi.org/10.1016/S1046-2023(02)00266-9

Allen, A. E., Storchi, R., Martial, F. P., Petersen, R. S., Montemurro, M. A., Brown, T. M., & Lucas, R. J. (2014). Melanopsin-driven light adaptation in mouse vision. *Curr Biol*, *24*(21), 2481-2490. https://doi.org/10.1016/j.cub.2014.09.015

Applebury, M. L., Antoch, M. P., Baxter, L. C., Chun, L. L., Falk, J. D., Farhangfar, F., Kage, K., Krzystolik, M. G., Lyass, L. A., & Robbins, J. T. (2000). The murine cone photoreceptor: a single cone type expresses both S and M opsins with retinal spatial patterning. *Neuron*, *27*(3), 513-523. https://doi.org/10.1016/s0896-6273(00)00062-3

Aschoff, J. (1952). Changes of frequency of periods of activity of mice in constant light and lasting darkness. *Pflugers Arch Gesamte Physiol Menschen Tiere*, *255*(3), 197-203. https://doi.org/10.1007/bf00363483 (Frequenzänderungen der Aktivitätsperiodik bei Mäusen im Dauerlicht und Dauerdunkel.)

Aschoff, J. (1960). Exogenous and Endogenous Components in Circadian Rhythms. *Cold Spring Harbor Symposia on Quantitative Biology*, *25*(0). https://doi.org/10.1101/SQB.1960.025.01.004

Aschoff, J. (1965). Circadian Rhythms in Man. *Science*, *148*(3676), 1427-1432. https://doi.org/10.1126/science.148.3676.1427

Atkinson, H. C., & Waddell, B. J. (1997). Circadian Variation in Basal Plasma Corticosterone and Adrenocorticotropin in the Rat: Sexual Dimorphism and Changes across the Estrous Cycle*. *Endocrinology*, *138*(9), 3842-3848. https://doi.org/10.1210/endo.138.9.5395

Aton, S. J., Colwell, C. S., Harmar, A. J., Waschek, J., & Herzog, E. D. (2005). Vasoactive intestinal polypeptide mediates circadian rhythmicity and synchrony in mammalian clock neurons. *Nature neuroscience*, *8*(4), 476-483. https://doi.org/10.1038/nn1419

Aubrecht, T. G., Jenkins, R., & Nelson, R. J. (2015). Dim light at night increases body mass of female mice. *Chronobiology International*, *32*(4), 557-560. https://doi.org/10.3109/07420528.2014.986682

Aubrecht, T. G., Weil, Z. M., Magalang, U. J., & Nelson, R. J. (2013). Dim light at night interacts with intermittent hypoxia to alter cognitive and affective responses. *Am J Physiol Regul Integr Comp Physiol*, *305*(1), R78-86. https://doi.org/10.1152/ajpregu.00100.2013

Bailey, K. R., & Crawley, J. N. (2009). Anxiety-Related Behaviors in Mice. In J. J. Buccafusco (Ed.), *Methods of Behavior Analysis in Neuroscience*. CRC Press/Taylor & Francis Group, LLC.

Bailey, M., & Silver, R. (2014). Sex differences in circadian timing systems: implications for disease. *Front Neuroendocrinol*, *35*(1), 111-139. https://doi.org/10.1016/j.yfrne.2013.11.003

Bains, R. S., Wells, S., Sillito, R. R., Armstrong, J. D., Cater, H. L., Banks, G., & Nolan, P. M. (2018). Assessing mouse behaviour throughout the light/dark cycle using automated in-cage analysis tools. *Journal of Neuroscience Methods*, *300*. https://doi.org/10.1016/j.jneumeth.2017.04.014

Banks, G., Heise, I., Starbuck, B., Osborne, T., Wisby, L., Potter, P., Jackson, I. J., Foster, R. G., Peirson, S. N., & Nolan, P. M. (2015). Genetic background influences age-related decline in visual and nonvisual retinal responses, circadian rhythms, and sleep. *Neurobiology of Aging*, *36*(1). https://doi.org/10.1016/j.neurobiolaging.2014.07.040

Banks, G. T., & Nolan, P. M. (2011). Assessment of Circadian and Light-Entrainable Parameters in Mice Using Wheel-Running Activity. *Current protocols in mouse biology*, *1*(3). https://doi.org/10.1002/9780470942390.mo110123

Baron, K. G., & Reid, K. J. (2014). Circadian misalignment and health. *Int Rev Psychiatry*, *26*(2), 139-154. https://doi.org/10.3109/09540261.2014.911149

Bartling, B., Al-Robaiy, S., Lehnich, H., Binder, L., Hiebl, B., & Simm, A. (2017). Sex-related differences in the wheel-running activity of mice decline with increasing age. *Experimental Gerontology*, *87*, 139-147. https://doi.org/https://doi.org/10.1016/j.exger.2016.04.011

Bass, J., & Takahashi, J. S. (2010). Circadian Integration of Metabolism and Energetics. *Science*, *330*(6009), 1349-1354. https://doi.org/10.1126/science.1195027

Bedrosian, T. A., Fonken, L. K., Walton, J. C., Haim, A., & Nelson, R. J. (2011). Dim light at night provokes depression-like behaviors and reduces CA1 dendritic spine density in female

hamsters. *Psychoneuroendocrinology*, *36*(7), 1062-1069. https://doi.org/10.1016/j.psyneuen.2011.01.004

Bedrosian, T. A., Galan, A., Vaughn, C. A., Weil, Z. M., & Nelson, R. J. (2013). Light at night alters daily patterns of cortisol and clock proteins in female Siberian hamsters. *Journal of Neuroendocrinology*, *25*(6), 590-596. https://doi.org/10.1111/jne.12036

Bedrosian, T. A., Weil, Z. M., & Nelson, R. J. (2013). Chronic dim light at night provokes reversible depression-like phenotype: possible role for TNF. *Molecular Psychiatry*, *18*(8), 930-936. https://doi.org/10.1038/mp.2012.96

Bellet, M. M., & Sassone-Corsi, P. (2010). Mammalian circadian clock and metabolism - the epigenetic link. *Journal of Cell Science*, *123*(22), 3837-3848. https://doi.org/10.1242/jcs.051649

Berson, D. M., Castrucci, A. M., & Provencio, I. (2010). Morphology and mosaics of melanopsin-expressing retinal ganglion cell types in mice. *J Comp Neurol*, *518*(13), 2405-2422. https://doi.org/10.1002/cne.22381

Berson, D. M., Dunn, F. A., & Takao, M. (2002). Phototransduction by retinal ganglion cells that set the circadian clock. *Science*, *295*(5557), 1070-1073. https://doi.org/10.1126/science.1067262

Bierman, A., Figueiro, M., & Rea, M. (2011). Measuring and predicting eyelid spectral transmittance. *Journal of Biomedical Optics*, *16*(6), 067011. https://doi.org/10.1117/1.3593151

Blattner, M. S., & Mahoney, M. M. (2012). Circadian parameters are altered in two strains of mice with transgenic modifications of estrogen receptor subtype 1. *Genes Brain Behav*, *11*(7), 828-836. https://doi.org/10.1111/j.1601-183X.2012.00831.x

Boergers, J., Gable, C. J., & Owens, J. A. (2014). Later school start time is associated with improved sleep and daytime functioning in adolescents. *J Dev Behav Pediatr*, *35*(1), 11-17. https://doi.org/10.1097/dbp.0000000000000018

Boivin, D. B., Boudreau, P., & Kosmadopoulos, A. (2022). Disturbance of the Circadian System in Shift Work and Its Health Impact. *J Biol Rhythms*, *37*(1), 3-28. https://doi.org/10.1177/07487304211064218

Borbély, A. A., Daan, S., Wirz-Justice, A., & Deboer, T. (2016). The two-process model of sleep regulation: a reappraisal. *Journal of Sleep Research*, *25*(2), 131-143. https://doi.org/10.1111/jsr.12371

Borniger, J. C., Maurya, S. K., Periasamy, M., & Nelson, R. J. (2014). Acute dim light at night increases body mass, alters metabolism, and shifts core body temperature circadian rhythms. *Chronobiology International*, *31*(8), 917-925. https://doi.org/10.3109/07420528.2014.926911

Borniger, J. C., Weil, Z. M., Zhang, N., & Nelson, R. J. (2013). Dim light at night does not disrupt timing or quality of sleep in mice. *Chronobiol Int*, *30*(8), 1016-1023. https://doi.org/10.3109/07420528.2013.803196

Bourin, M., & Hascoët, M. (2003). The mouse light/dark box test. *European Journal of Pharmacology*, *463*(1), 55-65. https://doi.org/https://doi.org/10.1016/S0014-2999(03)01274-3

Brainard, G. C., Hanifin, J. P., Greeson, J. M., Byrne, B., Glickman, G., Gerner, E., & Rollag, M. D. (2001). Action spectrum for melatonin regulation in humans: evidence for a novel circadian photoreceptor. *J Neurosci*, *21*(16), 6405-6412. https://doi.org/10.1523/jneurosci.21-16-06405.2001

Bramham, C. R., & Messaoudi, E. (2005). BDNF function in adult synaptic plasticity: The synaptic consolidation hypothesis. *Progress in Neurobiology*, *76*(2), 99-125. https://doi.org/https://doi.org/10.1016/j.pneurobio.2005.06.003

Brown, L. A., Fisk, A. S., Pothecary, C. A., & Peirson, S. N. (2019). Telling the Time with a Broken Clock: Quantifying Circadian Disruption in Animal Models. *Biology*, *8*(1). https://doi.org/10.3390/biology8010018

Brown, L. A., Hasan, S., Foster, R. G., & Peirson, S. N. (2016). COMPASS: Continuous Open Mouse Phenotyping of Activity and Sleep Status. *Wellcome Open Research*, *1*. https://doi.org/10.12688/wellcomeopenres.9892.2

Brown, S. A., & Azzi, A. (2013). Peripheral circadian oscillators in mammals. *Handb Exp Pharmacol*(217), 45-66. https://doi.org/10.1007/978-3-642-25950-0_3

Brown, T. M., Brainard, G. C., Cajochen, C., Czeisler, C. A., Hanifin, J. P., Lockley, S. W., Lucas, R. J., Münch, M., O'Hagan, J. B., Peirson, S. N., Price, L. L. A., Roenneberg, T., Schlangen, L. J. M., Skene, D. J., Spitschan, M., Vetter, C., Zee, P. C., & Wright, K. P., Jr. (2022). Recommendations for daytime, evening, and nighttime indoor light exposure to best support physiology, sleep, and wakefulness in healthy adults. *PLoS Biol*, *20*(3), e3001571. https://doi.org/10.1371/journal.pbio.3001571

Buhr, E. D., & Takahashi, J. S. (2013). Molecular components of the mammalian circadian clock [Article]. *Handbook of Experimental Pharmacology*, *217*, 3-27. https://doi.org/10.1007/978-3-642-25950-0_1

Buijs, R. M., & Kalsbeek, A. (2001). Hypothalamic integration of central and peripheral clocks. *Nature Reviews Neuroscience*, *2*(7), 521-526. https://doi.org/10.1038/35081582

Bumgarner, J. R., Walker, W. H., II, Quintana, D. D., White, R. C., Richmond, A. A., Meléndez-Fernández, O. H., Liu, J. A., Becker-Krail, D. D., Walton, J. C., Simpkins, J. W., DeVries, A. C., & Nelson, R. J. (2023). Acute exposure to artificial light at night alters hippocampal vascular structure in mice. *iScience*, *26*(7). https://doi.org/10.1016/j.isci.2023.106996

Burgess, H. J. (2010). Partial sleep deprivation reduces phase advances to light in humans. *J Biol Rhythms*, *25*(6), 460-468. https://doi.org/10.1177/0748730410385544

Burkhart, K., & Phelps, J. R. (2009). Amber lenses to block blue light and improve sleep: a randomized trial. *Chronobiol Int*, *26*(8), 1602-1612. https://doi.org/10.3109/07420520903523719

Butler, M. P., & Silver, R. (2011). Divergent photic thresholds in the non-image-forming visual system: entrainment, masking and pupillary light reflex. *Proc Biol Sci*, *278*(1706), 745-750. https://doi.org/10.1098/rspb.2010.1509

Byers, S. L., Wiles, M. V., Dunn, S. L., & Taft, R. A. (2012). Mouse estrous cycle identification tool and images. *PLOS ONE*, *7*(4), e35538. https://doi.org/10.1371/journal.pone.0035538

Cailotto, C., La Fleur, S. E., Van Heijningen, C., Wortel, J., Kalsbeek, A., Feenstra, M., Pévet, P., & Buijs, R. M. (2005). The suprachiasmatic nucleus controls the daily variation of plasma glucose via the autonomic output to the liver: are the clock genes involved? *European Journal of Neuroscience*, *22*(10), 2531-2540. https://doi.org/10.1111/j.1460-9568.2005.04439.x

Cain, S. W., McGlashan, E. M., Vidafar, P., Mustafovska, J., Curran, S. P. N., Wang, X., Mohamed, A., Kalavally, V., & Phillips, A. J. K. (2020). Evening home lighting adversely impacts the circadian system and sleep. *Scientific Reports*, *10*(1), 19110. https://doi.org/10.1038/s41598-020-75622-4

Cajochen, C., Frey, S., Anders, D., Späti, J., Bues, M., Pross, A., Mager, R., Wirz-Justice, A., & Stefani, O. (2011). Evening exposure to a light-emitting diodes (LED)-backlit computer screen affects circadian physiology and cognitive performance. *J Appl Physiol (1985)*, *110*(5), 1432-1438. https://doi.org/10.1152/japplphysiol.00165.2011

Cajochen, C., Kräuchi, K., & Wirz-Justice, A. (2003). Role of melatonin in the regulation of human circadian rhythms and sleep. *Journal of Neuroendocrinology*, *15*(4), 432-437. https://doi.org/10.1046/j.1365-2826.2003.00989.x

Cajochen, C., Münch, M., Kobialka, S., Kräuchi, K., Steiner, R., Oelhafen, P., Orgül, S., & Wirz-Justice, A. (2005). High sensitivity of human melatonin, alertness, thermoregulation, and heart rate to short wavelength light. *J Clin Endocrinol Metab*, *90*(3), 1311-1316. https://doi.org/10.1210/jc.2004-0957

Cajochen, C., Zeitzer, J. M., Czeisler, C. A., & Dijk, D. J. (2000). Dose-response relationship for light intensity and ocular and electroencephalographic correlates of human alertness. *Behav Brain Res*, *115*(1), 75-83. https://doi.org/10.1016/s0166-4328(00)00236-9

Carey, M. P., Deterd, C. H., de Koning, J., Helmerhorst, F., & de Kloet, E. R. (1995). The influence of ovarian steroids on hypothalamic-pituitary-adrenal regulation in the female rat. *J Endocrinol*, *144*(2), 311-321. https://doi.org/10.1677/joe.0.1440311

Carter-Dawson, L. D., & LaVail, M. M. (1979). Rods and cones in the mouse retina. I. Structural analysis using light and electron microscopy. *J Comp Neurol*, *188*(2), 245-262. https://doi.org/10.1002/cne.901880204

Challet, E., Turek, F. W., Laute, M., & Van Reeth, O. (2001). Sleep deprivation decreases phase-shift responses of circadian rhythms to light in the mouse: role of serotonergic and metabolic signals. *Brain Res*, *909*(1-2), 81-91. https://doi.org/10.1016/s0006-8993(01)02625-7

Chang, A. M., Aeschbach, D., Duffy, J. F., & Czeisler, C. A. (2015). Evening use of light-emitting eReaders negatively affects sleep, circadian timing, and next-morning alertness. *Proceedings of the National Academy of Sciences of the United States of America*, *112*(4), 1232-1237. https://doi.org/10.1073/pnas.1418490112

Chen, D., Buchanan, G. F., Ding, J. M., Hannibal, J., & Gillette, M. U. (1999). Pituitary adenylyl cyclase-activating peptide: A pivotal modulator of glutamatergic regulation of the suprachiasmatic circadian clock. *Proceedings of the National Academy of Sciences*, *96*(23), 13468-13473. https://doi.org/10.1073/pnas.96.23.13468

Chen, R., Weitzner, A. S., McKennon, L. A., & Fonken, L. K. (2021). Light at night during development in mice has modest effects on adulthood behavior and neuroimmune activation. *Behav Brain Res*, *405*, 113171. https://doi.org/10.1016/j.bbr.2021.113171

Chen, S. K., Badea, T. C., & Hattar, S. (2011). Photoentrainment and pupillary light reflex are mediated by distinct populations of ipRGCs. *Nature*, *476*(7358), 92-95. https://doi.org/10.1038/nature10206

Choi, H. J., Lee, C. J., Schroeder, A., Kim, Y. S., Jung, S. H., Kim, J. S., Kim, D. Y., Son, E. J., Han, H. C., Hong, S. K., Colwell, C. S., & Kim, Y. I. (2008). Excitatory actions of GABA in the suprachiasmatic nucleus. *J Neurosci*, *28*(21), 5450-5459. https://doi.org/10.1523/jneurosci.5750-07.2008

Chun, L. E., Woodruff, E. R., Morton, S., Hinds, L. R., & Spencer, R. L. (2015). Variations in Phase and Amplitude of Rhythmic Clock Gene Expression across Prefrontal Cortex, Hippocampus, Amygdala, and Hypothalamic Paraventricular and Suprachiasmatic Nuclei of Male and Female Rats. *J Biol Rhythms*, *30*(5), 417-436. https://doi.org/10.1177/0748730415598608

Chung, S., Son, G. H., & Kim, K. (2011). Circadian rhythm of adrenal glucocorticoid: Its regulation and clinical implications. *Biochimica et Biophysica Acta (BBA) - Molecular Basis of Disease*, *1812*(5), 581-591. https://doi.org/https://doi.org/10.1016/j.bbadis.2011.02.003

Cinzano, P., Falchi, F., & Elvidge, C. D. (2001). The first World Atlas of the artificial night sky brightness. *Monthly Notices of the Royal Astronomical Society*, *328*(3), 689-707. https://doi.org/10.1046/j.1365-8711.2001.04882.x

Cissé, Y. M., Peng, J., & Nelson, R. J. (2017). Effects of Dim Light at Night on Food Intake and Body Mass in Developing Mice. *Front Neurosci*, *11*, 294. https://doi.org/10.3389/fnins.2017.00294

Cissé, Y. M., Russart, K. L., & Nelson, R. J. (2017). Parental Exposure to Dim Light at Night Prior to Mating Alters Offspring Adaptive Immunity. *Sci Rep*, *7*, 45497. https://doi.org/10.1038/srep45497

Cleary-Gaffney, M., & Coogan, A. N. (2018). Limited evidence for affective and diurnal rhythm responses to dim light-at-night in male and female C57Bl/6 mice. *Physiology & behavior*, *189*, 78-85. https://doi.org/10.1016/j.physbeh.2018.03.010

Clegg, D. J., Brown, L. M., Woods, S. C., & Benoit, S. C. (2006). Gonadal Hormones Determine Sensitivity to Central Leptin and Insulin. *Diabetes*, *55*(4), 978-987. https://doi.org/10.2337/diabetes.55.04.06.db05-1339

Colwell, C. S. (2011). Linking neural activity and molecular oscillations in the SCN. *Nature Reviews Neuroscience*, *12*(10), 553-569. https://doi.org/10.1038/nrn3086

Coogan, A. N., & Wyse, C. A. (2008). Neuroimmunology of the circadian clock. *Brain research*, *1232*, 104-112. https://doi.org/10.1016/j.brainres.2008.07.087

Crawley, J., & Goodwin, F. K. (1980). Preliminary report of a simple animal behavior model for the anxiolytic effects of benzodiazepines. *Pharmacology Biochemistry and Behavior*, *13*(2), 167-170. https://doi.org/https://doi.org/10.1016/0091-3057(80)90067-2

Crnko, S., Du Pré, B. C., Sluijter, J. P. G., Van Laake, L. W., Crnko, S., Du Pré, B. C., Sluijter, J. P. G., & Van Laake, L. W. (2019). Circadian rhythms and the molecular clock in cardiovascular biology and disease. *Nature Reviews Cardiology*, *16*(7). https://doi.org/10.1038/s41569-019-0167-4

Curcio, C. A., Sloan, K. R., Kalina, R. E., & Hendrickson, A. E. (1990). Human photoreceptor topography. *J Comp Neurol*, *292*(4), 497-523. https://doi.org/10.1002/cne.902920402

Czeisler, C. A., Kronauer, R. E., Allan, J. S., Duffy, J. F., Jewett, M. E., Brown, E. N., & Ronda, J. M. (1989). Bright light induction of strong (type 0) resetting of the human circadian pacemaker. *Science*, *244*(4910), 1328-1333. https://doi.org/10.1126/science.2734611

Czeisler, C. A., Shanahan, T. L., Klerman, E. B., Martens, H., Brotman, D. J., Emens, J. S., Klein, T., & Rizzo, J. F., 3rd. (1995). Suppression of melatonin secretion in some blind patients by exposure to bright light. *N Engl J Med*, *332*(1), 6-11. https://doi.org/10.1056/nejm199501053320102

Daan, S., & Aschoff, J. (1982, 1982//). Circadian Contributions to Survival. Vertebrate Circadian Systems, Berlin, Heidelberg.

Dacey, D. M., Liao, H. W., Peterson, B. B., Robinson, F. R., Smith, V. C., Pokorny, J., Yau, K. W., & Gamlin, P. D. (2005). Melanopsin-expressing ganglion cells in primate retina signal colour and irradiance and project to the LGN. *Nature*, *433*(7027), 749-754. https://doi.org/10.1038/nature03387

Dallmann, R., Brown, S. A., & Gachon, F. (2014). Chronopharmacology: new insights and therapeutic implications. *Annu Rev Pharmacol Toxicol*, *54*, 339-361. https://doi.org/10.1146/annurev-pharmtox-011613-135923

Damiola, F., Le Minh, N., Preitner, N., Kornmann, B., Fleury-Olela, F., & Schibler, U. (2000). Restricted feeding uncouples circadian oscillators in peripheral tissues from the central pacemaker in the suprachiasmatic nucleus. *Genes Dev*, *14*(23), 2950-2961. https://doi.org/10.1101/gad.183500

Dantzer, R., O'Connor, J. C., Freund, G. G., Johnson, R. W., & Kelley, K. W. (2008). From inflammation to sickness and depression: when the immune system subjugates the brain. *Nature Reviews Neuroscience*, *9*(1), 46-56. https://doi.org/10.1038/nrn2297

Dartnall, H. J., Bowmaker, J. K., & Mollon, J. D. (1983). Human visual pigments: microspectrophotometric results from the eyes of seven persons. *Proc R Soc Lond B Biol Sci*, *220*(1218), 115-130. https://doi.org/10.1098/rspb.1983.0091

De Bundel, D., Gangarossa, G., Biever, A., Bonnefont, X., & Valjent, E. (2013). Cognitive dysfunction, elevated anxiety, and reduced cocaine response in circadian clock-deficient cryptochrome knockout mice. *Front Behav Neurosci*, *7*, 152. https://doi.org/10.3389/fnbeh.2013.00152

de la Iglesia, H. O., Fernández-Duque, E., Golombek, D. A., Lanza, N., Duffy, J. F., Czeisler, C. A., & Valeggia, C. R. (2015). Access to Electric Light Is Associated with Shorter Sleep Duration in a Traditionally Hunter-Gatherer Community. *J Biol Rhythms*, *30*(4), 342-350. https://doi.org/10.1177/0748730415590702

Debruyne, J. P., Noton, E., Lambert, C. M., Maywood, E. S., Weaver, D. R., & Reppert, S. M. (2006). A clock shock: mouse CLOCK is not required for circadian oscillator function. *Neuron*, *50*(3), 465-477. https://doi.org/10.1016/j.neuron.2006.03.041

Delorme, T. C., Srikanta, S. B., Fisk, A. S., Cloutier, M., Sato, M., Pothecary, C. A., Merz, C., Foster, R. G., Brown, S. A., Peirson, S. N., Cermakian, N., & Banks, G. T. (2022). Chronic Exposure to Dim Light at Night or Irregular Lighting Conditions Impact Circadian Behavior, Motor Coordination, and Neuronal Morphology. *Front Neurosci*, *16*, 855154. https://doi.org/10.3389/fnins.2022.855154

Díaz-Morales, J. F., & Escribano, C. (2015). Social jetlag, academic achievement and cognitive performance: Understanding gender/sex differences. *Chronobiol Int*, *32*(6), 822-831. https://doi.org/10.3109/07420528.2015.1041599

Dibner, C., Schibler, U., & Albrecht, U. (2010). The mammalian circadian timing system: organization and coordination of central and peripheral clocks. *Annu Rev Physiol*, *72*, 517-549. https://doi.org/10.1146/annurev-physiol-021909-135821

Dickmeis, T. (2009). Glucocorticoids and the circadian clock. *J Endocrinol*, *200*(1), 3-22. https://doi.org/10.1677/joe-08-0415

Dijk, D. J., & Czeisler, C. A. (1995). Contribution of the circadian pacemaker and the sleep homeostat to sleep propensity, sleep structure, electroencephalographic slow waves, and sleep spindle activity in humans. *J Neurosci*, *15*(5 Pt 1), 3526-3538. https://doi.org/10.1523/jneurosci.15-05-03526.1995

Do, M. T., & Yau, K. W. (2010). Intrinsically photosensitive retinal ganglion cells. *Physiological reviews*, *90*(4), 1547-1581. https://doi.org/10.1152/physrev.00013.2010

Do, M. T. H. (2019). Melanopsin and the Intrinsically Photosensitive Retinal Ganglion Cells: Biophysics to Behavior. *Neuron*, *104*(2), 205-226. https://doi.org/10.1016/j.neuron.2019.07.016

Duffy, J. F., & Czeisler, C. A. (2009). Effect of Light on Human Circadian Physiology. *Sleep Medicine Clinics*, *4*(2), 165-177. https://doi.org/10.1016/j.jsmc.2009.01.004

Dzirbíková, Z., Stebelová, K., Kováčová, K., Okuliarová, M., Olexová, L., & Zeman, M. (2022). Artificial Dim Light at Night during Pregnancy Can Affect Hormonal and Metabolic Rhythms in Rat Offspring. *Int J Mol Sci*, *23*(23). https://doi.org/10.3390/ijms232314544

Ebling, F. J. P. (1996). The role of glutamate in the photic regulation of the suprachiasmatic nucleus. *Progress in Neurobiology*, *50*(2), 109-132. https://doi.org/https://doi.org/10.1016/S0301-0082(96)00032-9

Eckel-Mahan, K., & Sassone-Corsi, P. (2013). Metabolism and the circadian clock converge. *Physiological reviews*, *93*(1), 107-135. https://doi.org/10.1152/physrev.00016.2012

Eckel-Mahan, K., & Sassone-Corsi, P. (2015). Phenotyping Circadian Rhythms in Mice. *Current protocols in mouse biology*, *5*(3). https://doi.org/10.1002/9780470942390.mo140229

Ecker, J. L., Dumitrescu, O. N., Wong, K. Y., Alam, N. M., Chen, S.-K., LeGates, T., Renna, J. M., Prusky, G. T., Berson, D. M., & Hattar, S. (2010). Melanopsin-Expressing Retinal Ganglion-Cell Photoreceptors: Cellular Diversity and Role in Pattern Vision. *Neuron*, *67*(1), 49-60. https://doi.org/https://doi.org/10.1016/j.neuron.2010.05.023

Eide, E. J., Woolf, M. F., Kang, H., Woolf, P., Hurst, W., Camacho, F., Vielhaber, E. L., Giovanni, A., & Virshup, D. M. (2005). Control of Mammalian Circadian Rhythm by CKIε-Regulated Proteasome-Mediated PER2 Degradation. *Molecular and Cellular Biology*, *25*(7), 2795-2807. https://doi.org/10.1128/MCB.25.7.2795-2807.2005

Emanuel, A. J., & Do, M. T. (2015). Melanopsin tristability for sustained and broadband phototransduction. *Neuron*, *85*(5), 1043-1055. https://doi.org/10.1016/j.neuron.2015.02.011

Falchi, F., Cinzano, P., Duriscoe, D., Kyba, C. C., Elvidge, C. D., Baugh, K., Portnov, B. A., Rybnikova, N. A., & Furgoni, R. (2016). The new world atlas of artificial night sky brightness. *Sci Adv*, *2*(6), e1600377. https://doi.org/10.1126/sciadv.1600377

Faydaver, M., Khatib, M. E., Russo, V., Rigamonti, M., Raspa, M., Giacinto, O. D., Berardinelli, P., Mauro, A., Scavizzi, F., Bonaventura, F., Mastrorilli, V., Valbonetti, L., & Barboni, B. (2023). Unraveling the link: locomotor activity exerts a dual role in predicting Achilles tendon healing and boosting regeneration in mice. *Frontiers in veterinary science*, *10*. https://doi.org/10.3389/fvets.2023.1281040

Ferrannini, E. (1988). The theoretical bases of indirect calorimetry: a review. *Metabolism*, *37*(3), 287-301. https://doi.org/10.1016/0026-0495(88)90110-2

Figueiro, M. G., Bierman, A., & Rea, M. S. (2013). A train of blue light pulses delivered through closed eyelids suppresses melatonin and phase shifts the human circadian system. *Nat Sci Sleep*, *5*, 133-141. https://doi.org/10.2147/nss.S52203

Figueiro, M. G., Steverson, B., Heerwagen, J., Kampschroer, K., Hunter, C. M., Gonzales, K., Plitnick, B., & Rea, M. S. (2017). The impact of daytime light exposures on sleep and mood in office workers. *Sleep Health*, *3*(3), 204-215. https://doi.org/https://doi.org/10.1016/j.sleh.2017.03.005

Fisher, S. P., Cui, N., McKillop, L. E., Gemignani, J., Bannerman, D. M., Oliver, P. L., Peirson, S. N., & Vyazovskiy, V. V. (2016). Stereotypic wheel running decreases cortical activity in mice. *Nature Communications*, *7*, 13138. https://doi.org/10.1038/ncomms13138

Fisher, S. P., Godinho, S. I. H., Pothecary, C. A., Hankins, M. W., Foster, R. G., & Peirson, S. N. (2012). Rapid assessment of sleep/wake behaviour in mice. *Journal of biological rhythms*, *27*(1). https://doi.org/10.1177/0748730411431550

Fonken, L. K., Aubrecht, T. G., Meléndez-Fernández, O. H., Weil, Z. M., & Nelson, R. J. (2013). Dim light at night disrupts molecular circadian rhythms and increases body weight. *J Biol Rhythms*, *28*(4), 262-271. https://doi.org/10.1177/0748730413493862

Fonken, L. K., Bedrosian, T. A., Zhang, N., Weil, Z. M., DeVries, A. C., & Nelson, R. J. (2019). Dim light at night impairs recovery from global cerebral ischemia. *Exp Neurol*, *317*, 100-109. https://doi.org/10.1016/j.expneurol.2019.02.008

Fonken, L. K., Kitsmiller, E., Smale, L., & Nelson, R. J. (2012). Dim nighttime light impairs cognition and provokes depressive-like responses in a diurnal rodent. *J Biol Rhythms*, *27*(4), 319-327. https://doi.org/10.1177/0748730412448324

Fonken, L. K., Lieberman, R. A., Weil, Z. M., & Nelson, R. J. (2013). Dim light at night exaggerates weight gain and inflammation associated with a high-fat diet in male mice. *Endocrinology*, *154*(10), 3817-3825. https://doi.org/10.1210/en.2013-1121

Fonken, L. K., Meléndez-Fernández, O. H., Weil, Z. M., & Nelson, R. J. (2014). Exercise attenuates the metabolic effects of dim light at night. *Physiol Behav*, *124*, 33-36. https://doi.org/10.1016/j.physbeh.2013.10.022

Fonken, L. K., & Nelson, R. J. (2013). Dim light at night increases depressive-like responses in male C3H/HeNHsd mice. *Behav Brain Res*, *243*, 74-78. https://doi.org/10.1016/j.bbr.2012.12.046

Fonken, L. K., Weil, Z. M., & Nelson, R. J. (2013a). Dark nights reverse metabolic disruption caused by dim light at night. *Obesity (Silver Spring)*, *21*(6), 1159-1164. https://doi.org/10.1002/oby.20108

Fonken, L. K., Weil, Z. M., & Nelson, R. J. (2013b). Mice exposed to dim light at night exaggerate inflammatory responses to lipopolysaccharide. *Brain Behav Immun*, *34*, 159-163. https://doi.org/10.1016/j.bbi.2013.08.011

Fonken, L. K., Workman, J. L., Walton, J. C., Weil, Z. M., Morris, J. S., Haim, A., & Nelson, R. J. (2010). Light at night increases body mass by shifting the time of food intake. *Proceedings of the National Academy of Sciences*, *107*(43), 18664-18669. https://doi.org/10.1073/pnas.1008734107

Foster, R. (2021). Fundamentals of circadian entrainment by light. *Lighting Research & Technology*, *53*(5). https://doi.org/10.1177/14771535211014792

Foster, R. G., & Hankins, M. W. (2007). Circadian vision. *Current Biology*, *17*(17), R746-R751. https://doi.org/https://doi.org/10.1016/j.cub.2007.07.007

Foster, R. G., Hankins, M. W., & Peirson, S. N. (2007a). Light, Photoreceptors, and Circadian Clocks. *Methods in Molecular Biology*. https://doi.org/10.1007/978-1-59745-257-1_1

Foster, R. G., Hankins, M. W., & Peirson, S. N. (2007b). Light, Photoreceptors, and Circadian Clocks. In E. Rosato (Ed.), *Circadian Rhythms: Methods and Protocols* (pp. 3-28). Humana Press. https://doi.org/10.1007/978-1-59745-257-1_1

Foster, R. G., & Helfrich-Förster, C. (2001). The regulation of circadian clocks by light in fruitflies and mice. *Philosophical Transactions of the Royal Society B: Biological Sciences*, *356*(1415), 1779-1789. https://doi.org/10.1098/rstb.2001.0962

Foster, R. G., Hughes, S., & Peirson, S. N. (2020). Circadian Photoentrainment in Mice and Humans. *Biology*, *9*(7), 180. https://www.mdpi.com/2079-7737/9/7/180

Foster, R. G., Provencio, I., Hudson, D., Fiske, S., De Grip, W., & Menaker, M. (1991). Circadian photoreception in the retinally degenerate mouse (rd/rd). *J Comp Physiol A*, *169*(1), 39-50. https://doi.org/10.1007/bf00198171

Freedman, M. S., Lucas, R. J., Soni, B., von Schantz, M., Muñoz, M., David-Gray, Z., & Foster, R. (1999). Regulation of mammalian circadian behavior by non-rod, non-cone, ocular photoreceptors. *Science*, *284*(5413), 502-504. https://doi.org/10.1126/science.284.5413.502

Fuochi, S., Rigamonti, M., Raspa, M., Scavizzi, F., de Girolamo, P., D'Angelo, L., Fuochi, S., Rigamonti, M., Raspa, M., Scavizzi, F., de Girolamo, P., & D'Angelo, L. (2023). Data repurposing from digital home cage monitoring enlightens new perspectives on mouse motor behaviour and reduction principle. *Scientific Reports*, *13*(1). https://doi.org/10.1038/s41598-023-37464-8

Gall, G. A. E., & Kyle, W. H. (1968). Growth of the laboratory mouse. *Theoretical and Applied Genetics*, *38*(7), 304-308. https://doi.org/10.1007/BF01297571

Gammie, S. C., Hasen, N. S., Rhodes, J. S., Girard, I., & Garland, T. (2003). Predatory aggression, but not maternal or intermale aggression, is associated with high voluntary wheel-running behavior in mice. *Hormones and behavior*, *44*(3), 209-221. https://doi.org/https://doi.org/10.1016/S0018-506X(03)00140-5

Gargiulo, S., Gramanzini, M., Megna, R., Greco, A., Albanese, S., Manfredi, C., & Brunetti, A. (2014). Evaluation of growth patterns and body composition in C57Bl/6J mice using dual energy X-ray absorptiometry. *Biomed Res Int*, *2014*, 253067. https://doi.org/10.1155/2014/253067

Geary, N. (2007). Curt Richter and the female rat. *Appetite*, *49*(2), 376-387. https://doi.org/https://doi.org/10.1016/j.appet.2007.01.013

Gerstner, J. R., & Yin, J. C. (2010). Circadian rhythms and memory formation. *Nature Reviews Neuroscience*, *11*(8), 577-588. https://doi.org/10.1038/nrn2881

Giménez, M. C., Beersma, D. G., Bollen, P., van der Linden, M. L., & Gordijn, M. C. (2014). Effects of a chronic reduction of short-wavelength light input on melatonin and sleep patterns in humans: evidence for adaptation. *Chronobiol Int*, *31*(5), 690-697. https://doi.org/10.3109/07420528.2014.893242

Golini, E., Rigamonti, M., Iannello, F., Rosa, C. D., Scavizzi, F., Raspa, M., & Mandillo, S. (2020). A Non-invasive Digital Biomarker for the Detection of Rest Disturbances in the SOD1G93A Mouse Model of ALS. *Frontiers in neuroscience*, *14*. https://doi.org/10.3389/fnins.2020.00896

Golini, E., Rigamonti, M., Raspa, M., Scavizzi, F., Falcone, G., Gourdon, G., & Mandillo, S. (2023). Excessive rest time during active phase is reliably detected in a mouse model of myotonic dystrophy type 1 using home cage monitoring. *Frontiers in behavioral neuroscience*, *17*. https://doi.org/10.3389/fnbeh.2023.1130055

Goo, R. H., Moore, J. G., Greenberg, E., & Alazraki, N. P. (1987). Circadian variation in gastric emptying of meals in humans. *Gastroenterology*, *93*(3), 515-518. https://doi.org/10.1016/0016-5085(87)90913-9

Gooley, J. J., Chamberlain, K., Smith, K. A., Khalsa, S. B., Rajaratnam, S. M., Van Reen, E., Zeitzer, J. M., Czeisler, C. A., & Lockley, S. W. (2011). Exposure to room light before bedtime suppresses melatonin onset and shortens melatonin duration in humans. *J Clin Endocrinol Metab*, *96*(3), E463-472. https://doi.org/10.1210/jc.2010-2098

Gooley, J. J., & Chua, E. C. (2014). Diurnal regulation of lipid metabolism and applications of circadian lipidomics. *J Genet Genomics*, *41*(5), 231-250. https://doi.org/10.1016/j.jgg.2014.04.001

Gordon, S. M., Li, H., Zhu, X., Shah, A. S., Lu, L. J., & Davidson, W. S. (2015). A comparison of the mouse and human lipoproteome: suitability of the mouse model for studies of human lipoproteins. *J Proteome Res*, *14*(6), 2686-2695. https://doi.org/10.1021/acs.jproteome.5b00213

Gould, T. D., Dao, D. T., & Kovacsics, C. E. (2009). The Open Field Test. In T. D. Gould (Ed.), *Mood and Anxiety Related Phenotypes in Mice: Characterization Using Behavioral Tests* (pp. 1-20). Humana Press. https://doi.org/10.1007/978-1-60761-303-9_1

Green, A., M., C.-Z., A., H., & and Dagan, Y. (2017). Evening light exposure to computer screens disrupts human sleep, biological rhythms, and attention abilities. *Chronobiology International*, *34*(7), 855-865. https://doi.org/10.1080/07420528.2017.1324878

Guan, Q., Wang, Z., Cao, J., Dong, Y., Tang, S., & Chen, Y. (2024). Melatonin restores hepatic lipid metabolic homeostasis disrupted by blue light at night in high-fat diet-fed mice. *J Pineal Res*, *76*(4), e12963. https://doi.org/10.1111/jpi.12963

Güler, A. D., Ecker, J. L., Lall, G. S., Haq, S., Altimus, C. M., Liao, H. W., Barnard, A. R., Cahill, H., Badea, T. C., Zhao, H., Hankins, M. W., Berson, D. M., Lucas, R. J., Yau, K. W., & Hattar, S. (2008). Melanopsin cells are the principal conduits for rod-cone input to non-image-forming vision. *Nature*, *453*(7191), 102-105. https://doi.org/10.1038/nature06829

Gutiérrez-Pérez, M., González-González, S., Estrada-Rodriguez, K. P., Espítia-Bautista, E., Guzmán-Ruiz, M. A., Escalona, R., Escobar, C., & Guerrero-Vargas, N. N. (2023). Dim Light at Night Promotes Circadian Disruption in Female Rats, at the Metabolic, Reproductive, and Behavioral Level. *Adv Biol (Weinh)*, *7*(11), e2200289. https://doi.org/10.1002/adbi.202200289

Hamada, T., Antle, M. C., & Silver, R. (2004). Temporal and spatial expression patterns of canonical clock genes and clock-controlled genes in the suprachiasmatic nucleus. *European Journal of Neuroscience*, *19*(7), 1741-1748. https://doi.org/10.1111/j.1460-9568.2004.03275.x

Hannibal, J. (2006). Roles of PACAP-Containing Retinal Ganglion Cells in Circadian Timing. In *International Review of Cytology* (Vol. 251, pp. 1-39). Academic Press. https://doi.org/https://doi.org/10.1016/S0074-7696(06)51001-0

Harmar, A. J., Marston, H. M., Shen, S., Spratt, C., West, K. M., Sheward, W. J., Morrison, C. F., Dorin, J. R., Piggins, H. D., Reubi, J. C., Kelly, J. S., Maywood, E. S., & Hastings, M. H. (2002). The VPAC(2) receptor is essential for circadian function in the mouse suprachiasmatic nuclei. *Cell*, *109*(4), 497-508. https://doi.org/10.1016/s0092-8674(02)00736-5

Harrington, M. E. (1997). The ventral lateral geniculate nucleus and the intergeniculate leaflet: interrelated structures in the visual and circadian systems. *Neuroscience and Biobehavioral Reviews*, *21*(5), 705-727. https://doi.org/10.1016/s0149-7634(96)00019-x

Hastings, M. H., Maywood, E. S., & Brancaccio, M. (2018). Generation of circadian rhythms in the suprachiasmatic nucleus. *Nature Reviews Neuroscience*, *19*(8), 453-469. https://doi.org/10.1038/s41583-018-0026-z

Hattar, S., Liao, H. W., Takao, M., Berson, D. M., & Yau, K. W. (2002). Melanopsin-containing retinal ganglion cells: architecture, projections, and intrinsic photosensitivity. *Science*, *295*(5557), 1065-1070. https://doi.org/10.1126/science.1069609

Hattar, S., Lucas, R. J., Mrosovsky, N., Thompson, S., Douglas, R. H., Hankins, M. W., Lem, J., Biel, M., Hofmann, F., Foster, R. G., & Yau, K. W. (2003). Melanopsin and rod-cone photoreceptive systems account for all major accessory visual functions in mice. *Nature*, *424*(6944), 76-81. https://doi.org/10.1038/nature01761

He, C., Shen, W., Chen, C., Wang, Q., Lu, Q., Shao, W., Jiang, Z., & Hu, H. (2021). Circadian Rhythm Disruption Influenced Hepatic Lipid Metabolism, Gut Microbiota and Promoted Cholesterol Gallstone Formation in Mice [Original Research]. *Frontiers in Endocrinology*, *12*. https://doi.org/10.3389/fendo.2021.723918

Henslee, E. A., Crosby, P., Kitcatt, S. J., Parry, J. S. W., Bernardini, A., Abdallat, R. G., Braun, G., Fatoyinbo, H. O., Harrison, E. J., Edgar, R. S., Hoettges, K. F., Reddy, A. B., Jabr, R. I., von Schantz, M., O'Neill, J. S., & Labeed, F. H. (2017). Rhythmic potassium transport regulates the circadian clock in human red blood cells. *Nature Communications*, *8*(1), 1978. https://doi.org/10.1038/s41467-017-02161-4

Herman, J. P., McKlveen, J. M., Ghosal, S., Kopp, B., Wulsin, A., Makinson, R., Scheimann, J., & Myers, B. (2016). Regulation of the Hypothalamic-Pituitary-Adrenocortical Stress Response. *Compr Physiol*, *6*(2), 603-621. https://doi.org/10.1002/cphy.c150015

Herzog, E. D., Hermanstyne, T., Smyllie, N. J., & Hastings, M. H. (2017). Regulating the Suprachiasmatic Nucleus (SCN) Circadian Clockwork: Interplay between Cell-Autonomous and Circuit-Level Mechanisms. *Cold Spring Harbor Perspectives in Biology*, *9*(1). https://doi.org/10.1101/cshperspect.a027706

Hester, L., Dang, D., Barker, C. J., Heath, M., Mesiya, S., Tienabeso, T., & Watson, K. (2021). Evening wear of blue-blocking glasses for sleep and mood disorders: a systematic review. *Chronobiol Int*, *38*(10), 1375-1383. https://doi.org/10.1080/07420528.2021.1930029

Hinchcliffe, J. K., & Robinson, E. S. J. (2024). The Affective Bias Test and Reward Learning Assay: Neuropsychological Models for Depression Research and Investigating Antidepressant Treatments in Rodents. *Curr Protoc*, *4*(6), e1057. https://doi.org/10.1002/cpz1.1057

Hogan, M. K., Kovalycsik, T., Sun, Q., Rajagopalan, S., & Nelson, R. J. (2015). Combined effects of exposure to dim light at night and fine particulate matter on C3H/HeNHsd mice. *Behav Brain Res*, *294*, 81-88. https://doi.org/10.1016/j.bbr.2015.07.033

Horst, G. T. J. v. d., Muijtjens, M., Kobayashi, K., Takano, R., Kanno, S.-i., Takao, M., Wit, J. d., Verkerk, A., Eker, A. P. M., Leenen, D. v., Buijs, R., Bootsma, D., Hoeijmakers, J. H. J., Yasui, A., Horst, G. T. J. v. d., Muijtjens, M., Kobayashi, K., Takano, R., Kanno, S.-i., . . . Yasui, A.

(1999). Mammalian Cry1 and Cry2 are essential for maintenance of circadian rhythms. *Nature*, *398*(6728). https://doi.org/10.1038/19323

Hughes, S., Jagannath, A., Hankins, M. W., Foster, R. G., & Peirson, S. N. (2015). Chapter Six - Photic Regulation of Clock Systems. In A. Sehgal (Ed.), *Methods in enzymology* (Vol. 552, pp. 125-143). Academic Press. https://doi.org/https://doi.org/10.1016/bs.mie.2014.10.018

Hughes, S., Jagannath, A., Rodgers, J., Hankins, M. W., Peirson, S. N., & Foster, R. G. (2016). Signalling by melanopsin (OPN4) expressing photosensitive retinal ganglion cells. *Eye*, *30*(2). https://doi.org/10.1038/eye.2015.264

Hühne, A., Volkmann, P., Stephan, M., Rossner, M., & Landgraf, D. (2020). An in-depth neurobehavioral characterization shows anxiety-like traits, impaired habituation behavior, and restlessness in male Cryptochrome-deficient mice. *Genes Brain Behav*, *19*(8), e12661. https://doi.org/10.1111/gbb.12661

Hussey, K. D. (2023). Timeless spaces: Field experiments in the physiological study of circadian rhythms, 1938–1963. *History and Philosophy of the Life Sciences*, *45*(2), 17. https://doi.org/10.1007/s40656-023-00571-w

Impey, S., Obrietan, K., Wong, S. T., Poser, S., Yano, S., Wayman, G., Deloulme, J. C., Chan, G., & Storm, D. R. (1998). Cross talk between ERK and PKA is required for Ca2+ stimulation of CREB-dependent transcription and ERK nuclear translocation. *Neuron*, *21*(4), 869-883. https://doi.org/10.1016/s0896-6273(00)80602-9

Jagannath, A., Peirson, S. N., & Foster, R. G. (2013). Sleep and circadian rhythm disruption in neuropsychiatric illness. *Curr Opin Neurobiol*, *23*(5), 888-894. https://doi.org/10.1016/j.conb.2013.03.008

Jagannath, A., Varga, N., Dallmann, R., Rando, G., Gosselin, P., Ebrahimjee, F., Taylor, L., Mosneagu, D., Stefaniak, J., Walsh, S., Palumaa, T., Di Pretoro, S., Sanghani, H., Wakaf, Z., Churchill, G. C., Galione, A., Peirson, S. N., Boison, D., Brown, S. A., . . . Vasudevan, S. R. (2021). Adenosine integrates light and sleep signalling for the regulation of circadian timing in mice. *Nature Communications*, *12*(1), 2113. https://doi.org/10.1038/s41467-021-22179-z

James, S. M., Honn, K. A., Gaddameedhi, S., & Van Dongen, H. P. A. (2017). Shift Work: Disrupted Circadian Rhythms and Sleep-Implications for Health and Well-Being. *Curr Sleep Med Rep*, *3*(2), 104-112. https://doi.org/10.1007/s40675-017-0071-6

Jerigova, V., Zeman, M., & Okuliarova, M. (2023). Chronodisruption of the acute inflammatory response by night lighting in rats. *Sci Rep*, *13*(1), 14109. https://doi.org/10.1038/s41598-023-41266-3

Johnston, J. D., Ebling, F. J., & Hazlerigg, D. G. (2005). Photoperiod regulates multiple gene expression in the suprachiasmatic nuclei and pars tuberalis of the Siberian hamster (Phodopus sungorus). *European Journal of Neuroscience*, *21*(11), 2967-2974. https://doi.org/10.1111/j.1460-9568.2005.04148.x

Johnston, J. D., Ordovás, J. M., Scheer, F. A., & Turek, F. W. (2016). Circadian Rhythms, Metabolism, and Chrononutrition in Rodents and Humans. *Adv Nutr*, *7*(2), 399-406. https://doi.org/10.3945/an.115.010777

Joye, D. A. M., & Evans, J. A. (2022). Sex differences in daily timekeeping and circadian clock circuits. *Seminars in cell & developmental biology*, *126*, 45-55. https://doi.org/https://doi.org/10.1016/j.semcdb.2021.04.026

Jud, C., Schmutz, I., Hampp, G., Oster, H., & Albrecht, U. (2005). A guideline for analyzing circadian wheel-running behavior in rodents under different lighting conditions. *Biological procedures online*, *7*(1). https://doi.org/10.1251/bpo109

Kalsbeek, A., la Fleur, S., & Fliers, E. (2014). Circadian control of glucose metabolism. *Mol Metab*, *3*(4), 372-383. https://doi.org/10.1016/j.molmet.2014.03.002

Kitanaka, N., Kitanaka, J., Hall, F. S., Uhl, G. R., Watabe, K., Kubo, H., Takahashi, H., Tatsuta, T., Morita, Y., & Takemura, M. (2012). A single administration of methamphetamine to mice early in the light period decreases running wheel activity observed during the dark period. *Brain research*, *1429*. https://doi.org/10.1016/j.brainres.2011.10.037

Ko, C. H., & Takahashi, J. S. (2006). Molecular components of the mammalian circadian clock. *Hum Mol Genet*, *15 Spec No 2*, R271-277. https://doi.org/10.1093/hmg/ddl207

Komada, M., Takao, K., & Miyakawa, T. (2008). Elevated plus maze for mice. *J Vis Exp*(22). https://doi.org/10.3791/1088

Konopka, R. J., & Benzer, S. (1971). Clock mutants of Drosophila melanogaster. *Proceedings of the National Academy of Sciences of the United States of America*, *68*(9), 2112-2116. https://doi.org/10.1073/pnas.68.9.2112

Konturek, P. C., Brzozowski, T., & Konturek, S. J. (2011). Gut clock: implication of circadian rhythms in the gastrointestinal tract. *J Physiol Pharmacol*, *62*(2), 139-150.

Kowalski, G. M., & Bruce, C. R. (2014). The regulation of glucose metabolism: implications and considerations for the assessment of glucose homeostasis in rodents. *American Journal of Physiology-Endocrinology and Metabolism*, *307*(10), E859-E871. https://doi.org/10.1152/ajpendo.00165.2014

Kraeuter, A. K., Guest, P. C., & Sarnyai, Z. (2019). The Open Field Test for Measuring Locomotor Activity and Anxiety-Like Behavior. *Methods Mol Biol*, *1916*, 99-103. https://doi.org/10.1007/978-1-4939-8994-2_9

Krizo, J. A., & Mintz, E. M. (2014). Sex differences in behavioral circadian rhythms in laboratory rodents. *Front Endocrinol (Lausanne)*, *5*, 234. https://doi.org/10.3389/fendo.2014.00234

Kronfeld-Schor, N., Bloch, G., & Schwartz, W. J. (2013). Animal clocks: when science meets nature. *Proc Biol Sci*, *280*(1765), 20131354. https://doi.org/10.1098/rspb.2013.1354

Krude, H., & Grüters, A. (2000). Implications of proopiomelanocortin (POMC) mutations in humans: the POMC deficiency syndrome. *Trends Endocrinol Metab*, *11*(1), 15-22. https://doi.org/10.1016/s1043-2760(99)00213-1

Kuljis, D. A., Loh, D. H., Truong, D., Vosko, A. M., Ong, M. L., McClusky, R., Arnold, A. P., & Colwell, C. S. (2013). Gonadal- and sex-chromosome-dependent sex differences in the circadian system. *Endocrinology*, *154*(4), 1501-1512. https://doi.org/10.1210/en.2012-1921

la Fleur, S. E., Kalsbeek, A., Wortel, J., Fekkes, M. L., & Buijs, R. M. (2001). A daily rhythm in glucose tolerance: a role for the suprachiasmatic nucleus. *Diabetes*, *50*(6), 1237-1243. https://doi.org/10.2337/diabetes.50.6.1237

Lall, G. S., Revell, V. L., Momiji, H., Al Enezi, J., Altimus, C. M., Güler, A. D., Aguilar, C., Cameron, M. A., Allender, S., Hankins, M. W., & Lucas, R. J. (2010). Distinct contributions of rod, cone, and melanopsin photoreceptors to encoding irradiance. *Neuron*, *66*(3), 417-428. https://doi.org/10.1016/j.neuron.2010.04.037

Lamia, K. A., Storch, K. F., & Weitz, C. J. (2008). Physiological significance of a peripheral tissue circadian clock. *Proceedings of the National Academy of Sciences of the United States of America*, *105*(39), 15172-15177. https://doi.org/10.1073/pnas.0806717105

Lawrenson, J. G., Hull, C. C., & Downie, L. E. (2017). The effect of blue-light blocking spectacle lenses on visual performance, macular health and the sleep-wake cycle: a systematic review of the literature. *Ophthalmic Physiol Opt*, *37*(6), 644-654. https://doi.org/10.1111/opo.12406

Lazzerini Ospri, L., Prusky, G., & Hattar, S. (2017). Mood, the Circadian System, and Melanopsin Retinal Ganglion Cells. *Annu Rev Neurosci*, *40*, 539-556. https://doi.org/10.1146/annurev-neuro-072116-031324

Lee, I. T., Chang, A. S., Manandhar, M., Shan, Y., Fan, J., Izumo, M., Ikeda, Y., Motoike, T., Dixon, S., Seinfeld, J. E., Takahashi, J. S., & Yanagisawa, M. (2015). Neuromedin s-producing neurons act as essential pacemakers in the suprachiasmatic nucleus to couple clock neurons and dictate circadian rhythms. *Neuron*, *85*(5), 1086-1102. https://doi.org/10.1016/j.neuron.2015.02.006

Lee-Rueckert, M., Escola-Gil, J. C., & Kovanen, P. T. (2016). HDL functionality in reverse cholesterol transport — Challenges in translating data emerging from mouse models to human disease. *Biochimica et Biophysica Acta (BBA) - Molecular and Cell Biology of Lipids*, *1861*(7), 566-583. https://doi.org/https://doi.org/10.1016/j.bbalip.2016.03.004

LeGates, T. A., Fernandez, D. C., & Hattar, S. (2014). Light as a central modulator of circadian rhythms, sleep and affect. *Nature reviews. Neuroscience*, *15*(7). https://doi.org/10.1038/nrn3743

Lehman, M. N., Silver, R., Gladstone, W. R., Kahn, R. M., Gibson, M., & Bittman, E. L. (1987). Circadian Rhythmicity Restored by Neural Transplant. lmmunocytochemical Characterization of the Graft and Its Integration with the Host Brain. *The Journal of Neuroscience*, *7*(6), 1626-1638.

Leise, T. L. (2013). Wavelet analysis of circadian and ultradian behavioral rhythms. *Journal of Circadian Rhythms*, *11*(0), 5. https://doi.org/10.1186/1740-3391-11-5

Liset, R., Grønli, J., Henriksen, R. E., Henriksen, T. E. G., Nilsen, R. M., & Pallesen, S. (2022). A randomized controlled trial on the effect of blue-blocking glasses compared to partial blue-blockers on melatonin profile among nulliparous women in third trimester of the pregnancy. *Neurobiol Sleep Circadian Rhythms*, *12*, 100074. https://doi.org/10.1016/j.nbscr.2021.100074

Liu, Walton, J. C., Bumgarner, J. R., Walker, W. H., 2nd, Meléndez-Fernández, O. H., DeVries, A. C., & Nelson, R. J. (2022). Chronic exposure to dim light at night disrupts cell-mediated immune response and decreases longevity in aged female mice. *Chronobiol Int*, *39*(12), 1674-1683. https://doi.org/10.1080/07420528.2022.2135442

Liu, J., Walker, W., Meléndez-Fernández, H., Bumgarner, J., Walton, J., Zhang, N., Courtney DeVries, A., & Nelson, R. (2022). Exposure to dim lighting increases infarct size and alters neuroimmune

activation. *Brain, Behavior, and Immunity*, *106*, 18. https://doi.org/https://doi.org/10.1016/j.bbi.2022.07.067

Liu, J. A., Walker, W. H., 2nd, Meléndez-Fernández, O. H., Bumgarner, J. R., Zhang, N., Walton, J. C., Meares, G. P., DeVries, A. C., & Nelson, R. J. (2024). Dim light at night shifts microglia to a pro-inflammatory state after cerebral ischemia, altering stroke outcome in mice. *Exp Neurol*, *377*, 114796. https://doi.org/10.1016/j.expneurol.2024.114796

Liu, Q., Wang, Z., Cao, J., Dong, Y., & Chen, Y. (2023). Insulin ameliorates dim blue light at night-induced apoptosis in hippocampal neurons via the IR/IRS1/AKT/GSK3β/β-catenin signaling pathway. *Ecotoxicol Environ Saf*, *250*, 114488. https://doi.org/10.1016/j.ecoenv.2022.114488

Lovejoy, J. C., & Sainsbury, A. (2009). Sex differences in obesity and the regulation of energy homeostasis. *Obes Rev*, *10*(2), 154-167. https://doi.org/10.1111/j.1467-789X.2008.00529.x

Lowrey, P. L., & Takahashi, J. S. (2011). Genetics of Circadian Rhythms in Mammalian Model Organisms. *Advances in Genetics*, 175-230. https://doi.org/10.1016/B978-0-12-387690-4.00006-4

Lucas, R. J., Allen, A. E., Brainard, G. C., Brown, T. M., Dauchy, R. T., Didikoglu, A., Do, M. T. H., Gaskill, B. N., Hattar, S., Hawkins, P., Hut, R. A., McDowell, R. J., Nelson, R. J., Prins, J. B., Schmidt, T. M., Takahashi, J. S., Verma, V., Voikar, V., Wells, S., & Peirson, S. N. (2024). Recommendations for measuring and standardizing light for laboratory mammals to improve welfare and reproducibility in animal research. *PLoS Biol*, *22*(3), e3002535. https://doi.org/10.1371/journal.pbio.3002535

Lucas, R. J., Douglas, R. H., & Foster, R. G. (2001). Characterization of an ocular photopigment capable of driving pupillary constriction in mice. *Nature neuroscience*, *4*(6), 621-626. https://doi.org/10.1038/88443

Lucas, R. J., Freedman, M. S., Muñoz, M., Garcia-Fernández, J. M., & Foster, R. G. (1999). Regulation of the mammalian pineal by non-rod, non-cone, ocular photoreceptors. *Science*, *284*(5413), 505-507. https://doi.org/10.1126/science.284.5413.505

Lucas, R. J., Lall, G. S., Allen, A. E., & Brown, T. M. (2012). How rod, cone, and melanopsin photoreceptors come together to enlighten the mammalian circadian clock. *Prog Brain Res*, *199*, 1-18. https://doi.org/10.1016/b978-0-444-59427-3.00001-0

Lucas, R. J., Peirson, S. N., Berson, D. M., Brown, T. M., Cooper, H. M., Czeisler, C. A., Figueiro, M. G., Gamlin, P. D., Lockley, S. W., O'Hagan, J. B., Price, L. L., Provencio, I., Skene, D. J., & Brainard, G. C. (2014). Measuring and using light in the melanopsin age. *Trends Neurosci*, *37*(1), 1-9. https://doi.org/10.1016/j.tins.2013.10.004

Lunn, R. M., Blask, D. E., Coogan, A. N., Figueiro, M. G., Gorman, M. R., Hall, J. E., Hansen, J., Nelson, R. J., Panda, S., Smolensky, M. H., Stevens, R. G., Turek, F. W., Vermeulen, R., Carreón, T., Caruso, C. C., Lawson, C. C., Thayer, K. A., Twery, M. J., Ewens, A. D., . . . Boyd, W. A. (2017). Health consequences of electric lighting practices in the modern world: A report on the National Toxicology Program's workshop on shift work at night, artificial light at night, and circadian disruption. *Sci Total Environ*, *607-608*, 1073-1084. https://doi.org/10.1016/j.scitotenv.2017.07.056

Marcheva, B., Ramsey, K. M., Peek, C. B., Affinati, A., Maury, E., & Bass, J. (2013). Circadian clocks and metabolism. *Handb Exp Pharmacol*(217), 127-155. https://doi.org/10.1007/978-3-642-25950-0_6

Mason, I. C., Boubekri, M., Figueiro, M. G., Hasler, B. P., Hattar, S., Hill, S. M., Nelson, R. J., Sharkey, K. M., Wright, K. P., Boyd, W. A., Brown, M. K., Laposky, A. D., Twery, M. J., & Zee, P. C. (2018). Circadian Health and Light: A Report on the National Heart, Lung, and Blood Institute's Workshop. *J Biol Rhythms*, *33*(5), 451-457. https://doi.org/10.1177/0748730418789506

McClintock, M. K. (1983). Synchronizing Ovarian and Birth Cycles by Female Pheromones. In D. Müller-Schwarze & R. M. Silverstein (Eds.), *Chemical Signals in Vertebrates 3* (pp. 159-178). Springer US. https://doi.org/10.1007/978-1-4757-9652-0_10

McDougal, D. H., & Gamlin, P. D. (2010). The influence of intrinsically-photosensitive retinal ganglion cells on the spectral sensitivity and response dynamics of the human pupillary light reflex. *Vision Res*, *50*(1), 72-87. https://doi.org/10.1016/j.visres.2009.10.012

McEwen, B. S., Nasca, C., & Gray, J. D. (2016). Stress Effects on Neuronal Structure: Hippocampus, Amygdala, and Prefrontal Cortex. *Neuropsychopharmacology*, *41*(1), 3-23. https://doi.org/10.1038/npp.2015.171

McGlynn, N., Kirsh, V. A., Cotterchio, M., Harris, M. A., Nadalin, V., & Kreiger, N. (2015). Shift Work and Obesity among Canadian Women: A Cross-Sectional Study Using a Novel Exposure Assessment Tool. *PLOS ONE*, *10*(9), e0137561. https://doi.org/10.1371/journal.pone.0137561

Medrikova, D., Jilkova, Z. M., Bardova, K., Janovska, P., Rossmeisl, M., & Kopecky, J. (2012). Sex differences during the course of diet-induced obesity in mice: adipose tissue expandability and glycemic control. *International Journal of Obesity*, *36*(2), 262-272. https://doi.org/10.1038/ijo.2011.87

Messager, S., Ross, A. W., Barrett, P., & Morgan, P. J. (1999). Decoding photoperiodic time through Per1 and ICER gene amplitude. *Proceedings of the National Academy of Sciences of the United States of America*, *96*(17), 9938-9943. https://doi.org/10.1073/pnas.96.17.9938

Micic, G., Lovato, N., Gradisar, M., Ferguson, S. A., Burgess, H. J., & Lack, L. C. (2016). The etiology of delayed sleep phase disorder. *Sleep Medicine Reviews*, *27*, 29-38. https://doi.org/https://doi.org/10.1016/j.smrv.2015.06.004

Mieda, M., Ono, D., Hasegawa, E., Okamoto, H., Honma, K.-i., Honma, S., & Sakurai, T. (2015). Cellular Clocks in AVP Neurons of the SCN Are Critical for Interneuronal Coupling Regulating Circadian Behavior Rhythm. *Neuron*, *85*(5), 1103-1116. https://doi.org/https://doi.org/10.1016/j.neuron.2015.02.005

Miller, B. H., & Takahashi, J. S. (2014). Central Circadian Control of Female Reproductive Function [Review]. *Frontiers in Endocrinology*, *4*. https://doi.org/10.3389/fendo.2013.00195

Mistlberger, R. E. (2005). Circadian regulation of sleep in mammals: Role of the suprachiasmatic nucleus. *Brain Research Reviews*, *49*(3), 429-454. https://doi.org/https://doi.org/10.1016/j.brainresrev.2005.01.005

Mistlberger, R. E., Landry, G. J., & Marchant, E. G. (1997). Sleep deprivation can attenuate light-induced phase shifts of circadian rhythms in hamsters. *Neuroscience Letters*, *238*(1), 5-8. https://doi.org/https://doi.org/10.1016/S0304-3940(97)00815-X

Mohawk, J. A., Green, C. B., & Takahashi, J. S. (2012). Central and peripheral circadian clocks in mammals. *Annu Rev Neurosci*, *35*, 445-462. https://doi.org/10.1146/annurev-neuro-060909-153128

Molcan, L., Babarikova, K., Cvikova, D., Kincelova, N., Kubincova, L., & Mauer Sutovska, H. (2024). Artificial light at night suppresses the day-night cardiovascular variability: evidence from humans and rats. *Pflügers Archiv - European Journal of Physiology*, *476*(3), 295-306. https://doi.org/10.1007/s00424-023-02901-0

Molcan, L., Sutovska, H., Okuliarova, M., Senko, T., Krskova, L., & Zeman, M. (2019). Dim light at night attenuates circadian rhythms in the cardiovascular system and suppresses melatonin in rats. *Life Sci*, *231*, 116568. https://doi.org/10.1016/j.lfs.2019.116568

Mong, J. A., Baker, F. C., Mahoney, M. M., Paul, K. N., Schwartz, M. D., Semba, K., & Silver, R. (2011). Sleep, rhythms, and the endocrine brain: influence of sex and gonadal hormones. *J Neurosci*, *31*(45), 16107-16116. https://doi.org/10.1523/jneurosci.4175-11.2011

Moore, R. Y., & Eichler, V. B. (1972). Loss of a circadian adrenal corticosterone rhythm following suprachiasmatic lesions in the rat. *Brain Res*, *42*(1), 201-206. https://doi.org/10.1016/0006-8993(72)90054-6

Morgan, K. N., & Tromborg, C. T. (2007). Sources of stress in captivity. *Applied Animal Behaviour Science*, *102*(3), 262-302. https://doi.org/https://doi.org/10.1016/j.applanim.2006.05.032

Morgenthaler, T. I., Hashmi, S., Croft, J. B., Dort, L., Heald, J. L., & Mullington, J. (2016). High School Start Times and the Impact on High School Students: What We Know, and What We Hope to Learn. *J Clin Sleep Med*, *12*(12), 1681-1689. https://doi.org/10.5664/jcsm.6358

Morin, L. P. (2007). SCN organization reconsidered. *J Biol Rhythms*, *22*(1), 3-13. https://doi.org/10.1177/0748730406296749

Mosendane, T., Mosendane, T., & Raal, F. J. (2008). Shift work and its effects on the cardiovascular system. *Cardiovasc J Afr*, *19*(4), 210-215.

Mouland, J. W., Martial, F., Watson, A., Lucas, R. J., & Brown, T. M. (2019). Cones Support Alignment to an Inconsistent World by Suppressing Mouse Circadian Responses to the Blue Colors Associated with Twilight. *Curr Biol*, *29*(24), 4260-4267.e4264. https://doi.org/10.1016/j.cub.2019.10.028

Mrosovsky, N. (1999). Masking: history, definitions, and measurement. *Chronobiol Int*, *16*(4), 415-429. https://doi.org/10.3109/07420529908998717

Mure, L. S., Rieux, C., Hattar, S., & Cooper, H. M. (2007). Melanopsin-dependent nonvisual responses: evidence for photopigment bistability in vivo. *J Biol Rhythms*, *22*(5), 411-424. https://doi.org/10.1177/0748730407306043

Nadal-Nicolás, F. M., Kunze, V. P., Ball, J. M., Peng, B. T., Krishnan, A., Zhou, G., Dong, L., & Li, W. (2020). True S-cones are concentrated in the ventral mouse retina and wired for color detection in the upper visual field. *eLife*, *9*. https://doi.org/10.7554/eLife.56840

Nakamura, T. J., Moriya, T., Inoue, S., Shimazoe, T., Watanabe, S., Ebihara, S., & Shinohara, K. (2005). Estrogen differentially regulates expression of Per1 and Per2 genes between central and peripheral clocks and between reproductive and nonreproductive tissues in female rats. *Journal of neuroscience research*, *82*(5), 622-630. https://doi.org/10.1002/jnr.20677

Naylor, E., Aillon, D. V., Barrett, B. S., Wilson, G. S., Johnson, D. A., Johnson, D. A., Harmon, H. P., Gabbert, S., & Petillo, P. A. (2012). Lactate as a Biomarker for Sleep. *Sleep*, *35*(9), 1209-1222. https://doi.org/10.5665/sleep.2072

Nelson, D. E., & Takahashi, J. S. (1991). Sensitivity and integration in a visual pathway for circadian entrainment in the hamster (Mesocricetus auratus). *J Physiol*, *439*, 115-145. https://doi.org/10.1113/jphysiol.1991.sp018660

Nolan, P. M., Kapfhamer, D., & Bućan, M. (1997). Random mutagenesis screen for dominant behavioral mutations in mice. *Methods*, *13*(4), 379-395. https://doi.org/10.1006/meth.1997.0545

O'Neill, J. S., & Reddy, A. B. (2011). Circadian clocks in human red blood cells. *Nature*, *469*(7331), 498-503. https://doi.org/10.1038/nature09702

Obayashi, K., Saeki, K., Iwamoto, J., Okamoto, N., Tomioka, K., Nezu, S., Ikada, Y., & Kurumatani, N. (2013). Exposure to light at night, nocturnal urinary melatonin excretion, and obesity/dyslipidemia in the elderly: a cross-sectional analysis of the HEIJO-KYO study. *J Clin Endocrinol Metab*, *98*(1), 337-344. https://doi.org/10.1210/jc.2012-2874

Ogawa, S., Chan, J., Gustafsson, J. A., Korach, K. S., & Pfaff, D. W. (2003). Estrogen increases locomotor activity in mice through estrogen receptor alpha: specificity for the type of activity. *Endocrinology*, *144*(1), 230-239. https://doi.org/10.1210/en.2002-220519

Okuliarova, M., Rumanova, V. S., Stebelova, K., & Zeman, M. (2020). Dim Light at Night Disturbs Molecular Pathways of Lipid Metabolism. *Int J Mol Sci*, *21*(18). https://doi.org/10.3390/ijms21186919

Ono, D., Honma, K. I., & Honma, S. (2021). Roles of Neuropeptides, VIP and AVP, in the Mammalian Central Circadian Clock. *Front Neurosci*, *15*, 650154. https://doi.org/10.3389/fnins.2021.650154

Ono, D., Honma, K. I., Yanagawa, Y., Yamanaka, A., & Honma, S. (2018). Role of GABA in the regulation of the central circadian clock of the suprachiasmatic nucleus. *J Physiol Sci*, *68*(4), 333-343. https://doi.org/10.1007/s12576-018-0604-x

Pack, A. I., Galante, R. J., Maislin, G., Cater, J., Metaxas, D., Lu, S., Zhang, L., Von Smith, R., Kay, T., Lian, J., Svenson, K., & Peters, L. L. (2007). Novel method for high-throughput phenotyping of sleep in mice. *Physiol Genomics*, *28*(2), 232-238. https://doi.org/10.1152/physiolgenomics.00139.2006

Panagiotou, M., & Deboer, T. (2020). Effects of Chronic Dim-light-at-night Exposure on Sleep in Young and Aged Mice. *Neuroscience*, *426*, 154-167. https://doi.org/10.1016/j.neuroscience.2019.11.033

Panda, S. (2016). Circadian physiology of metabolism. *Science*, *354*(6315), 1008-1015. https://doi.org/10.1126/science.aah4967

Panda, S., Hogenesch, J. B., & Kay, S. A. (2002). Circadian rhythms from flies to human. *Nature*, *417*(6886), 329-335. https://doi.org/10.1038/417329a

Panda, S., Provencio, I., Tu, D. C., Pires, S. S., Rollag, M. D., Castrucci, A. M., Pletcher, M. T., Sato, T. K., Wiltshire, T., Andahazy, M., Kay, S. A., Van Gelder, R. N., & Hogenesch, J. B. (2003). Melanopsin is required for non-image-forming photic responses in blind mice. *Science*, *301*(5632), 525-527. https://doi.org/10.1126/science.1086179

Parihar, V. K., Hattiangady, B., Kuruba, R., Shuai, B., & Shetty, A. K. (2011). Predictable chronic mild stress improves mood, hippocampal neurogenesis and memory. *Molecular Psychiatry*, *16*(2), 171-183. https://doi.org/10.1038/mp.2009.130

Partch, C. L., Green, C. B., & Takahashi, J. S. (2014). Molecular architecture of the mammalian circadian clock. *Trends in Cell Biology*, *24*(2), 90-99. https://doi.org/10.1016/j.tcb.2013.07.002

Patke, A., Young, M. W., & Axelrod, S. (2020). Molecular mechanisms and physiological importance of circadian rhythms. *Nature Reviews Molecular Cell Biology*, *21*(2), 67-84. https://doi.org/10.1038/s41580-019-0179-2

Patton, A. P., & Hastings, M. H. (2023). The Mammalian Circadian Time-Keeping System. *J Huntingtons Dis*, *12*(2), 91-104. https://doi.org/10.3233/jhd-230571

Peirson, S. N., Brown, L. A., Pothecary, C. A., Benson, L. A., & Fisk, A. S. (2018). Light and the laboratory mouse. *Journal of Neuroscience Methods*, *300*, 26-36. https://doi.org/10.1016/j.jneumeth.2017.04.007

Peirson, S. N., Thompson, S., Hankins, M. W., & Foster, R. G. (2005). Mammalian Photoentrainment: Results, Methods, and Approaches. In M. W. Young (Ed.), *Methods in enzymology* (Vol. 393, pp. 697-726). Academic Press. https://doi.org/https://doi.org/10.1016/S0076-6879(05)93037-1

Pellow, S., Chopin, P., File, S. E., & Briley, M. (1985). Validation of open:closed arm entries in an elevated plus-maze as a measure of anxiety in the rat. *J Neurosci Methods*, *14*(3), 149-167. https://doi.org/10.1016/0165-0270(85)90031-7

Pendergast, J. S., Branecky, K. L., Huang, R., Niswender, K. D., & Yamazaki, S. (2014). Wheel-running activity modulates circadian organization and the daily rhythm of eating behavior. *Frontiers in Psychology*, *5*. https://doi.org/10.3389/fpsyg.2014.00177

Pernold, K., Iannello, F., Low, B. E., Rigamonti, M., Rosati, G., Scavizzi, F., Wang, J., Raspa, M., Wiles, M. V., & Ulfhake, B. (2019). Towards large scale automated cage monitoring – Diurnal rhythm and impact of interventions on in-cage activity of C57BL/6J mice recorded 24/7 with a non-disrupting capacitive-based technique. *PLOS ONE*, *14*(2). https://doi.org/10.1371/journal.pone.0211063

Pernold, K., Rullman, E., & Ulfhake, B. (2023). Bouts of rest and physical activity in C57BL/6J mice. *PLOS ONE*, *18*(6). https://doi.org/10.1371/journal.pone.0280416

Phillips, A. J. K., Vidafar, P., Burns, A. C., McGlashan, E. M., Anderson, C., Rajaratnam, S. M. W., Lockley, S. W., & Cain, S. W. (2019). High sensitivity and interindividual variability in the response of the human circadian system to evening light. *Proceedings of the National Academy of Sciences*, *116*(24), 12019-12024. https://doi.org/10.1073/pnas.1901824116

Pittendrigh, C. S. (1981). Circadian Systems: Entrainment. https://doi.org/10.1007/978-1-4615-6552-9_7

Pittendrigh, C. S., & Daan, S. (1976a). A functional analysis of circadian pacemakers in nocturnal rodents. *Journal of Comparative Physiology*, *106*, 30.

Pittendrigh, C. S., & Daan, S. (1976b). A functional analysis of circadian pacemakers in nocturnal rodents: I. The stability and lability of spontaneous frequency. *Journal of Comparative Physiology ? A*, *106*(3), 223-252. https://doi.org/10.1007/BF01417856

Porcu, A., Riddle, M., Dulcis, D., & Welsh, D. K. (2018). Photoperiod-Induced Neuroplasticity in the Circadian System. *Neural Plast*, *2018*, 5147585. https://doi.org/10.1155/2018/5147585

Possidente, B., McEldowney, S., & Pabon, A. (1995). Aging lengthens circadian period for wheel-running activity in C57BL mice. *Physiology & behavior*, *57*(3), 575-579. https://doi.org/https://doi.org/10.1016/0031-9384(94)00298-J

Power, A., Hughes, A. T., Samuels, R. E., & Piggins, H. D. (2010). Rhythm-promoting actions of exercise in mice with deficient neuropeptide signaling. *J Biol Rhythms*, *25*(4), 235-246. https://doi.org/10.1177/0748730410374446

Provencio, I., & Foster, R. G. (1995). Circadian rhythms in mice can be regulated by photoreceptors with cone-like characteristics. *Brain Res*, *694*(1-2), 183-190. https://doi.org/10.1016/0006-8993(95)00694-1

Provencio, I., Rodriguez, I. R., Jiang, G., Hayes, W. P., Moreira, E. F., & Rollag, M. D. (2000). A novel human opsin in the inner retina. *J Neurosci*, *20*(2), 600-605. https://doi.org/10.1523/jneurosci.20-02-00600.2000

Qian, J., & Scheer, F. (2016). Circadian System and Glucose Metabolism: Implications for Physiology and Disease. *Trends Endocrinol Metab*, *27*(5), 282-293. https://doi.org/10.1016/j.tem.2016.03.005

Rahman, S. A., St Hilaire, M. A., Chang, A. M., Santhi, N., Duffy, J. F., Kronauer, R. E., Czeisler, C. A., Lockley, S. W., & Klerman, E. B. (2017). Circadian phase resetting by a single short-duration light exposure. *JCI Insight*, *2*(7), e89494. https://doi.org/10.1172/jci.insight.89494

Ralph, M., Foster, R., Davis, F., & Menaker, M. (1990). Transplanted suprachiasmatic nucleus determines circadian period. *Science*, *247*(4945), 975-978. https://doi.org/10.1126/science.2305266

Ramkisoensing, A., Gu, C., van Engeldorp Gastelaars, H. M., Michel, S., Deboer, T., Rohling, J. H., & Meijer, J. H. (2014). Enhanced phase resetting in the synchronized suprachiasmatic nucleus network. *J Biol Rhythms*, *29*(1), 4-15. https://doi.org/10.1177/0748730413516750

Ramos, A. (2008). Animal models of anxiety: do I need multiple tests? *Trends Pharmacol Sci*, *29*(10), 493-498. https://doi.org/10.1016/j.tips.2008.07.005

Rea, M. S., Figueiro, M. G., Bierman, A., & Bullough, J. D. (2010). Circadian light. *Journal of Circadian Rhythms*, *8*(1), 2. https://doi.org/10.1186/1740-3391-8-2

Redlin, U. (2001). Neural basis and biological function of masking by light in mammals: suppression of melatonin and locomotor activity. *Chronobiol Int*, *18*(5), 737-758. https://doi.org/10.1081/cbi-100107511

Refinetti, R. (2004). Non-stationary time series and the robustness of circadian rhythms. *J Theor Biol*, *227*(4), 571-581. https://doi.org/10.1016/j.jtbi.2003.11.032
Refinetti, R. (2010). Entrainment of circadian rhythm by ambient temperature cycles in mice. *J Biol Rhythms*, *25*(4), 247-256. https://doi.org/10.1177/0748730410372074
Refinetti, R., & Menaker, M. (1992). The circadian rhythm of body temperature. *Physiol Behav*, *51*(3), 613-637. https://doi.org/10.1016/0031-9384(92)90188-8
Ren, W., Wang, Z., Dong, Y., Cao, J., Gao, T., Guo, Q., & Chen, Y. (2025). Dim blue light at night worsens high-fat diet-induced kidney damage via increasing corticosterone levels and modulating the expression of circadian clock genes. *Ecotoxicol Environ Saf*, *289*, 117636. https://doi.org/10.1016/j.ecoenv.2024.117636
Reppert, S. M., & Weaver, D. R. (2001). Molecular Analysis of Mammalian Circadian Rhythms. *Annual Review of Physiology*, *63*(Volume 63, 2001), 647-676. https://doi.org/https://doi.org/10.1146/annurev.physiol.63.1.647
Reppert, S. M., & Weaver, D. R. (2002). Coordination of circadian timing in mammals. *Nature*, *418*(6901), 935-941. https://doi.org/10.1038/nature00965
Richter, C. P. (1922). A Behavioristic Study of the Activity of the Rat. *Comparative Psychology Monographs*, *1, 2*, 56-56.
Richter, C. P. (1971). Inborn nature of the rat's 24-hour clock. *J Comp Physiol Psychol*, *75*(1), 1-4. https://doi.org/10.1037/h0030681
Rodgers, R. J., & Dalvi, A. (1997). Anxiety, defence and the elevated plus-maze. *Neuroscience and Biobehavioral Reviews*, *21*(6), 801-810. https://doi.org/10.1016/s0149-7634(96)00058-9
Roenneberg, T., Allebrandt, K. V., Merrow, M., & Vetter, C. (2012). Social jetlag and obesity. *Curr Biol*, *22*(10), 939-943. https://doi.org/10.1016/j.cub.2012.03.038
Roenneberg, T., Daan, S., & Merrow, M. (2003). The art of entrainment [Review]. *Journal of biological rhythms*, *18*(3), 183-194. https://doi.org/10.1177/0748730403018003001
Rosenfeld, C. S. (2017). Sex-dependent differences in voluntary physical activity. *Journal of neuroscience research*, *95*(1-2), 279-290. https://doi.org/10.1002/jnr.23896
Rudic, R. D., McNamara, P., Curtis, A. M., Boston, R. C., Panda, S., Hogenesch, J. B., & Fitzgerald, G. A. (2004). BMAL1 and CLOCK, two essential components of the circadian clock, are involved in glucose homeostasis. *PLoS Biol*, *2*(11), e377. https://doi.org/10.1371/journal.pbio.0020377
Rumanova, V. S., Foppen, E., Okuliarova, M., Zeman, M., & Kalsbeek, A. (2025). Time-restricted feeding does not improve daily rhythms in locomotion and drinking disrupted by artificial light at night. *Physiol Behav*, *290*, 114780. https://doi.org/10.1016/j.physbeh.2024.114780
Russart, K. L. G., Chbeir, S. A., Nelson, R. J., & Magalang, U. J. (2019). Light at night exacerbates metabolic dysfunction in a polygenic mouse model of type 2 diabetes mellitus. *Life Sci*, *231*, 116574. https://doi.org/10.1016/j.lfs.2019.116574
Sahar, S., & Sassone-Corsi, P. (2009). Metabolism and cancer: the circadian clock connection. *Nature Reviews Cancer*, *9*(12), 886-896. https://doi.org/10.1038/nrc2747
Saini, C., Liani, A., Curie, T., Gos, P., Kreppel, F., Emmenegger, Y., Bonacina, L., Wolf, J. P., Poget, Y. A., Franken, P., & Schibler, U. (2013). Real-time recording of circadian liver gene expression in freely moving mice reveals the phase-setting behavior of hepatocyte clocks. *Genes Dev*, *27*(13), 1526-1536. https://doi.org/10.1101/gad.221374.113
Sanchez-Alavez, M., Alboni, S., & Conti, B. (2011). Sex- and age-specific differences in core body temperature of C57Bl/6 mice. *Age (Dordr)*, *33*(1), 89-99. https://doi.org/10.1007/s11357-010-9164-6
Santhi, N., Thorne, H. C., van der Veen, D. R., Johnsen, S., Mills, S. L., Hommes, V., Schlangen, L. J., Archer, S. N., & Dijk, D. J. (2012). The spectral composition of evening light and individual differences in the suppression of melatonin and delay of sleep in humans. *J Pineal Res*, *53*(1), 47-59. https://doi.org/10.1111/j.1600-079X.2011.00970.x
Saper, C. B., Cano, G., & Scammell, T. E. (2005). Homeostatic, circadian, and emotional regulation of sleep. *J Comp Neurol*, *493*(1), 92-98. https://doi.org/10.1002/cne.20770
Sarmiento, J., Pulgar, R., Mandakovic, D., Porras, O., Flores, C. A., Luco, D., Trujillo, C. A., Díaz-Esquivel, B., Alvarez, C., Acevedo, A., & Catalán, M. A. (2022). Nocturnal Light Pollution Induces Weight Gain in Mice and Reshapes the Structure, Functions, and Interactions of Their Colonic Microbiota. *Int J Mol Sci*, *23*(3). https://doi.org/10.3390/ijms23031673
Schernhammer, E. S., Kroenke, C. H., Laden, F., & Hankinson, S. E. (2006). Night Work and Risk of Breast Cancer. *Epidemiology*, *17*(1), 108-111. https://doi.org/10.1097/01.ede.0000190539.03500.c1
Schibler, U., Gotic, I., Saini, C., Gos, P., Curie, T., Emmenegger, Y., Sinturel, F., Gosselin, P., Gerber, A., Fleury-Olela, F., Rando, G., Demarque, M., & Franken, P. (2015). Clock-Talk: Interactions

between Central and Peripheral Circadian Oscillators in Mammals. *Cold Spring Harb Symp Quant Biol*, *80*, 223-232. https://doi.org/10.1101/sqb.2015.80.027490

Schmid, B., Helfrich-Förster, C., & Yoshii, T. (2011). A new ImageJ plug-in "ActogramJ" for chronobiological analyses. *J Biol Rhythms*, *26*(5), 464-467. https://doi.org/10.1177/0748730411414264

Schmidt, C., Collette, F., Cajochen, C., & Peigneux, P. (2007). A time to think: circadian rhythms in human cognition. *Cogn Neuropsychol*, *24*(7), 755-789. https://doi.org/10.1080/02643290701754158

Schmidt, T. M., Chen, S. K., & Hattar, S. (2011). Intrinsically photosensitive retinal ganglion cells: many subtypes, diverse functions. *Trends Neurosci*, *34*(11), 572-580. https://doi.org/10.1016/j.tins.2011.07.001

Schwartz, W. J., & Zimmerman, P. (1990). Circadian timekeeping in BALB/c and C57BL/6 inbred mouse strains. *J Neurosci*, *10*(11), 3685-3694. https://doi.org/10.1523/jneurosci.10-11-03685.1990

Seibenhener, M. L., & Wooten, M. C. (2015). Use of the Open Field Maze to measure locomotor and anxiety-like behavior in mice. *J Vis Exp*(96), e52434. https://doi.org/10.3791/52434

Sekaran, S., Foster, R. G., Lucas, R. J., & Hankins, M. W. (2003). Calcium imaging reveals a network of intrinsically light-sensitive inner-retinal neurons. *Curr Biol*, *13*(15), 1290-1298. https://doi.org/10.1016/s0960-9822(03)00510-4

Serin, Y., & Acar Tek, N. (2019). Effect of Circadian Rhythm on Metabolic Processes and the Regulation of Energy Balance. *Annals of Nutrition and Metabolism*, *74*(4), 322-330. https://doi.org/10.1159/000500071

Shechter, A., Kim, E. W., St-Onge, M. P., & Westwood, A. J. (2018). Blocking nocturnal blue light for insomnia: A randomized controlled trial. *J Psychiatr Res*, *96*, 196-202. https://doi.org/10.1016/j.jpsychires.2017.10.015

Shenk, J., Lohkamp, K. J., Wiesmann, M., & Kiliaan, A. J. (2020). Automated Analysis of Stroke Mouse Trajectory Data With Traja. *Frontiers in neuroscience*, *14*. https://doi.org/10.3389/fnins.2020.00518

Shi, H., Seeley, R. J., & Clegg, D. J. (2009). Sexual differences in the control of energy homeostasis. *Front Neuroendocrinol*, *30*(3), 396-404. https://doi.org/10.1016/j.yfrne.2009.03.004

Shigeyoshi, Y., Taguchi, K., Yamamoto, S., Takekida, S., Yan, L., Tei, H., Moriya, T., Shibata, S., Loros, J. J., Dunlap, J. C., & Okamura, H. (1997). Light-induced resetting of a mammalian circadian clock is associated with rapid induction of the mPer1 transcript. *Cell*, *91*(7), 1043-1053. https://doi.org/10.1016/s0092-8674(00)80494-8

Shostak, A., Meyer-Kovac, J., & Oster, H. (2013). Circadian regulation of lipid mobilization in white adipose tissues. *Diabetes*, *62*(7), 2195-2203. https://doi.org/10.2337/db12-1449

Shuboni, D., & Yan, L. (2010). Nighttime dim light exposure alters the responses of the circadian system. *Neuroscience*, *170*(4), 1172-1178. https://doi.org/10.1016/j.neuroscience.2010.08.009

Siepka, S. M., & Takahashi, J. S. (2005). Methods to Record Circadian Rhythm Wheel Running Activity in Mice. *Methods in enzymology*, *393*. https://doi.org/10.1016/S0076-6879(05)93008-5

Skeldon, A. C., Phillips, A. J., & Dijk, D. J. (2017). The effects of self-selected light-dark cycles and social constraints on human sleep and circadian timing: a modeling approach. *Sci Rep*, *7*, 45158. https://doi.org/10.1038/srep45158

Smallwood, P. M., Olveczky, B. P., Williams, G. L., Jacobs, G. H., Reese, B. E., Meister, M., & Nathans, J. (2003). Genetically engineered mice with an additional class of cone photoreceptors: implications for the evolution of color vision. *Proceedings of the National Academy of Sciences of the United States of America*, *100*(20), 11706-11711. https://doi.org/10.1073/pnas.1934712100

Smolensky, M. H., Hermida, R. C., Reinberg, A., Sackett-Lundeen, L., & Portaluppi, F. (2016). Circadian disruption: New clinical perspective of disease pathology and basis for chronotherapeutic intervention. *Chronobiol Int*, *33*(8), 1101-1119. https://doi.org/10.1080/07420528.2016.1184678

Sokolove, P. G., & Bushell, W. N. (1978). The chi square periodogram: its utility for analysis of circadian rhythms. *J Theor Biol*, *72*(1), 131-160. https://doi.org/10.1016/0022-5193(78)90022-x

Solberg, L. C., Horton, T. H., & Turek, F. W. (1999). Circadian rhythms and depression: effects of exercise in an animal model. *American Journal of Physiology-Regulatory, Integrative and Comparative Physiology*, *276*(1), R152-R161. https://doi.org/10.1152/ajpregu.1999.276.1.R152

Sonoda, T., & Schmidt, T. M. (2016). Re-evaluating the Role of Intrinsically Photosensitive Retinal Ganglion Cells: New Roles in Image-Forming Functions. *Integr Comp Biol*, *56*(5), 834-841. https://doi.org/10.1093/icb/icw066

Souman, J. L., Borra, T., de Goijer, I., Schlangen, L. J. M., Vlaskamp, B. N. S., & Lucassen, M. P. (2018). Spectral Tuning of White Light Allows for Strong Reduction in Melatonin Suppression without Changing Illumination Level or Color Temperature. *J Biol Rhythms*, *33*(4), 420-431. https://doi.org/10.1177/0748730418784041

Spitschan, M., Kervezee, L., Lok, R., McGlashan, E., & Najjar, R. P. (2023). ENLIGHT: A consensus checklist for reporting laboratory-based studies on the non-visual effects of light in humans. *EBioMedicine*, *98*, 104889. https://doi.org/10.1016/j.ebiom.2023.104889

Spitschan, M., Mead, J., Roos, C., Lowis, C., Griffiths, B., Mucur, P., Herf, M., Nam, S., & Veitch, J. A. (2021). luox: validated reference open-access and open-source web platform for calculating and sharing physiologically relevant quantities for light and lighting. *Wellcome Open Res*, *6*, 69. https://doi.org/10.12688/wellcomeopenres.16595.3

Spitschan, M., Stefani, O., Blattner, P., Gronfier, C., Lockley, S. W., & Lucas, R. J. (2019). How to Report Light Exposure in Human Chronobiology and Sleep Research Experiments. *Clocks & Sleep*, *1*(3), 280-289. https://www.mdpi.com/2624-5175/1/3/24

Stapleton, S., Welch, G., DiBerardo, L., & Freeman, L. R. (2024). Sex differences in a mouse model of diet-induced obesity: the role of the gut microbiome. *Biology of Sex Differences*, *15*(1), 5. https://doi.org/10.1186/s13293-023-00580-1

Steel, L. C. E., Tir, S., Spitschan, M., Foster, R. G., & Peirson, S. N. (2022). Frontiers | Effects of Cage Position and Light Transmission on Home Cage Activity and Circadian Entrainment in Mice. *Frontiers in neuroscience*, *15*. https://doi.org/10.3389/fnins.2021.832535

Stenvers, D. J., van Dorp, R., Foppen, E., Mendoza, J., Opperhuizen, A.-L., Fliers, E., Bisschop, P. H., Meijer, J. H., Kalsbeek, A., & Deboer, T. (2016). Dim light at night disturbs the daily sleep-wake cycle in the rat. *Scientific Reports*, *6*(1), 35662. https://doi.org/10.1038/srep35662

Stephan, F. K., & Zucker, I. (1972). Circadian rhythms in drinking behavior and locomotor activity of rats are eliminated by hypothalamic lesions. *Proceedings of the National Academy of Sciences of the United States of America*, *69*(6), 1583-1586. https://doi.org/10.1073/pnas.69.6.1583

Stevens, R. G., & Zhu, Y. (2015). Electric light, particularly at night, disrupts human circadian rhythmicity: is that a problem? *Philosophical Transactions of the Royal Society B: Biological Sciences*, *370*(1667). https://doi.org/10.1098/rstb.2014.0120

Stokkan, K. A., Yamazaki, S., Tei, H., Sakaki, Y., & Menaker, M. (2001). Entrainment of the circadian clock in the liver by feeding. *Science*, *291*(5503), 490-493. https://doi.org/10.1126/science.291.5503.490

Stothard, E. R., McHill, A. W., Depner, C. M., Birks, B. R., Moehlman, T. M., Ritchie, H. K., Guzzetti, J. R., Chinoy, E. D., LeBourgeois, M. K., Axelsson, J., & Wright, K. P., Jr. (2017). Circadian Entrainment to the Natural Light-Dark Cycle across Seasons and the Weekend. *Curr Biol*, *27*(4), 508-513. https://doi.org/10.1016/j.cub.2016.12.041

Straif, K., Baan, R., Grosse, Y., Secretan, B., El Ghissassi, F., Bouvard, V., Altieri, A., Benbrahim-Tallaa, L., & Cogliano, V. (2007). Carcinogenicity of shift-work, painting, and fire-fighting. *Lancet Oncol*, *8*(12), 1065-1066. https://doi.org/10.1016/s1470-2045(07)70373-x

Sun, M., Feng, W., Wang, F., Li, P., Li, Z., Li, M., Tse, G., Vlaanderen, J., Vermeulen, R., & Tse, L. A. (2018). Meta-analysis on shift work and risks of specific obesity types. *Obes Rev*, *19*(1), 28-40. https://doi.org/10.1111/obr.12621

Tahara, Y., Aoyama, S., & Shibata, S. (2017). The mammalian circadian clock and its entrainment by stress and exercise. *The Journal of Physiological Sciences*, *67*(1), 1-10. https://doi.org/10.1007/s12576-016-0450-7

Takahashi, J. S. (2017). Transcriptional architecture of the mammalian circadian clock. *Nature Reviews Genetics*, *18*(3), 164-179. https://doi.org/10.1038/nrg.2016.150

Takahashi, J. S., DeCoursey, P. J., Bauman, L., & Menaker, M. (1984). Spectral sensitivity of a novel photoreceptive system mediating entrainment of mammalian circadian rhythms. *Nature*, *308*(5955), 186-188. https://doi.org/10.1038/308186a0

Takahashi, J. S., Shimomura, K., & Kumar, V. (2008). Searching for genes underlying behavior: lessons from circadian rhythms. *Science*, *322*(5903), 909-912. https://doi.org/10.1126/science.1158822

Tam, S. K. E., Brown, L. A., Wilson, T. S., Tir, S., Fisk, A. S., Pothecary, C. A., Vinne, V. v. d., Foster, R. G., Vyazovskiy, V. V., Bannerman, D. M., Harrington, M. E., Peirson, S. N., Tam, S. K. E., Brown, L. A., Wilson, T. S., Tir, S., Fisk, A. S., Pothecary, C. A., van der Vinne, V., . . . Peirson, S. N. (2021). Dim light in the evening causes coordinated realignment of circadian rhythms,

sleep, and short-term memory. *Proceedings of the National Academy of Sciences*, *118*(39). https://doi.org/10.1073/pnas.2101591118

Thapan, K., Arendt, J., & Skene, D. J. (2001). An action spectrum for melatonin suppression: evidence for a novel non-rod, non-cone photoreceptor system in humans. *J Physiol*, *535*(Pt 1), 261-267. https://doi.org/10.1111/j.1469-7793.2001.t01-1-00261.x

Thirouin, Z. S., Gizowski, C., Murtaz, A., & Bourque, C. W. (2023). Sex-specific differences in the circadian pattern of action potential firing by rat suprachiasmatic nucleus vasopressin neurons. *Journal of Neuroendocrinology*, *35*(9), e13273. https://doi.org/10.1111/jne.13273

Thosar, S. S., Butler, M. P., & Shea, S. A. (2018). Role of the circadian system in cardiovascular disease. *J Clin Invest*, *128*(6), 2157-2167. https://doi.org/10.1172/jci80590

Tir, S., Foster, R. G., & Peirson, S. N. (2025). Evaluation of the Digital Ventilated Cage® system for circadian phenotyping. *Scientific Reports*, *15*(1), 3674. https://doi.org/10.1038/s41598-025-87530-6

Tir, S., Steel, L. C. E., Tam, S. K. E., Semo, M. a., Pothecary, C. A., Vyazovskiy, V. V., Foster, R. G., & Peirson, S. N. (2022). Chapter 6 - Rodent models in translational circadian photobiology. In N. Santhi & M. Spitschan (Eds.), *Progress in Brain Research* (Vol. 273, pp. 97-116). Elsevier. https://doi.org/https://doi.org/10.1016/bs.pbr.2022.02.015

Ulfhake, B., Lerat, H., Honetschlager, J., Pernold, K., Rynekrová, M., Escot, K., Recordati, C., Kuiper, R. V., Rosati, G., Rigamonti, M., Zordan, S., & Prins, J.-B. (2022). A multicentre study on spontaneous in-cage activity and micro-environmental conditions of IVC housed C57BL/6J mice during consecutive cycles of bi-weekly cage-change. *PLOS ONE*, *17*(5). https://doi.org/10.1371/journal.pone.0267281

Valentinuzzi, V. S., Scarbrough, K., Takahashi, J. S., & Turek, F. W. (1997). Effects of aging on the circadian rhythm of wheel-running activity in C57BL/6 mice. *American Journal of Physiology-Regulatory, Integrative and Comparative Physiology*, *273*(6). https://doi.org/10.1152/ajpregu.1997.273.6.R1957

Van Den Pol, A. N., Cao, V., & Heller, H. C. (1998). Circadian system of mice integrates brief light stimuli. *Am J Physiol*, *275*(2), R654-657. https://doi.org/10.1152/ajpregu.1998.275.2.R654

van der Lely, S., Frey, S., Garbazza, C., Wirz-Justice, A., Jenni, O. G., Steiner, R., Wolf, S., Cajochen, C., Bromundt, V., & Schmidt, C. (2015). Blue blocker glasses as a countermeasure for alerting effects of evening light-emitting diode screen exposure in male teenagers. *J Adolesc Health*, *56*(1), 113-119. https://doi.org/10.1016/j.jadohealth.2014.08.002

van der Vinne, V., Pothecary, C. A., Wilcox, S. L., McKillop, L. E., Benson, L. A., Kolpakova, J., Tam, S. K. E., Krone, L. B., Fisk, A. S., Wilson, T. S., Yamagata, T., Cantley, J., Vyazovskiy, V. V., & Peirson, S. N. (2020). Continuous and non-invasive thermography of mouse skin accurately describes core body temperature patterns, but not absolute core temperature. *Sci Rep*, *10*(1), 20680. https://doi.org/10.1038/s41598-020-77786-5

van Diepen, H. C., Ramkisoensing, A., Peirson, S. N., Foster, R. G., & Meijer, J. H. (2013). Irradiance encoding in the suprachiasmatic nuclei by rod and cone photoreceptors. *Faseb j*, *27*(10), 4204-4212. https://doi.org/10.1096/fj.13-233098

van Oosterhout, F., Fisher, S. P., van Diepen, H. C., Watson, T. S., Houben, T., VanderLeest, H. T., Thompson, S., Peirson, S. N., Foster, R. G., & Meijer, J. H. (2012). Ultraviolet light provides a major input to non-image-forming light detection in mice. *Curr Biol*, *22*(15), 1397-1402. https://doi.org/10.1016/j.cub.2012.05.032

VanderLeest, H. T., Houben, T., Michel, S., Deboer, T., Albus, H., Vansteensel, M. J., Block, G. D., & Meijer, J. H. (2007). Seasonal encoding by the circadian pacemaker of the SCN. *Curr Biol*, *17*(5), 468-473. https://doi.org/10.1016/j.cub.2007.01.048

Vetter, C., Fischer, D., Matera, J. L., & Roenneberg, T. (2015). Aligning work and circadian time in shift workers improves sleep and reduces circadian disruption. *Curr Biol*, *25*(7), 907-911. https://doi.org/10.1016/j.cub.2015.01.064

Vitaterna, M. H., King, D. P., Chang, A.-M., Kornhauser, J. M., Lowrey, P. L., McDonald, J. D., Dove, W. F., Pinto, L. H., Turek, F. W., & Takahashi, J. S. (1994). Mutagenesis and Mapping of a Mouse Gene, Clock, Essential for Circadian Behavior. *Science (New York, N.Y.)*, *264*(5159). https://doi.org/10.1126/science.8171325

Voikar, V., & Gaburro, S. (2020). Three Pillars of Automated Home-Cage Phenotyping of Mice: Novel Findings, Refinement, and Reproducibility Based on Literature and Experience. *Frontiers in behavioral neuroscience*, *14*. https://doi.org/10.3389/fnbeh.2020.575434

Vyazovskiy, V. V., Ruijgrok, G., Deboer, T., & Tobler, I. (2006). Running wheel accessibility affects the regional electroencephalogram during sleep in mice. *Cereb Cortex*, *16*(3), 328-336. https://doi.org/10.1093/cercor/bhi110

Vyazovskiy, V. V., & Tobler, I. (2012). The temporal structure of behaviour and sleep homeostasis. *PLOS ONE*, *7*(12), e50677. https://doi.org/10.1371/journal.pone.0050677
Wahl, S., Engelhardt, M., Schaupp, P., Lappe, C., & Ivanov, I. V. (2019). The inner clock-Blue light sets the human rhythm. *J Biophotonics*, *12*(12), e201900102. https://doi.org/10.1002/jbio.201900102
Walf, A. A., & Frye, C. A. (2007). The use of the elevated plus maze as an assay of anxiety-related behavior in rodents. *Nat Protoc*, *2*(2), 322-328. https://doi.org/10.1038/nprot.2007.44
Walker, W. H., 2nd, Meléndez-Fernández, O. H., & Nelson, R. J. (2019). Prior exposure to dim light at night impairs dermal wound healing in female C57BL/6 mice. *Archives of Dermatological Research*, *311*(7), 573-576. https://doi.org/10.1007/s00403-019-01935-8
Walsh, R. N., & Cummins, R. A. (1976). The Open-Field Test: a critical review. *Psychol Bull*, *83*(3), 482-504.
Wang, J. S., & Kefalov, V. J. (2011). The cone-specific visual cycle. *Prog Retin Eye Res*, *30*(2), 115-128. https://doi.org/10.1016/j.preteyeres.2010.11.001
Weber, E. T., & Rea, M. A. (1997). Neuropeptide Y blocks light-induced phase advances but not delays of the circadian activity rhythm in hamsters. *Neuroscience Letters*, *231*(3), 159-162. https://doi.org/https://doi.org/10.1016/S0304-3940(97)00559-4
Weil, Z. M., Fonken, L. K., Walker, W. H., 2nd, Bumgarner, J. R., Liu, J. A., Melendez-Fernandez, O. H., Zhang, N., DeVries, A. C., & Nelson, R. J. (2020). Dim light at night exacerbates stroke outcome. *European Journal of Neuroscience*, *52*(9), 4139-4146. https://doi.org/10.1111/ejn.14915
Weitzman, E. D., Fukushima, D., Nogeire, C., Roffwarg, H., Gallagher, T. F., & Hellman, L. (1971). Twenty-four hour pattern of the episodic secretion of cortisol in normal subjects. *J Clin Endocrinol Metab*, *33*(1), 14-22. https://doi.org/10.1210/jcem-33-1-14
Welsh, D. K., Logothetis, D. E., Meister, M., & Reppert, S. M. (1995). Individual neurons dissociated from rat suprachiasmatic nucleus express independently phased circadian firing rhythms. *Neuron*, *14*(4), 697-706. https://doi.org/10.1016/0896-6273(95)90214-7
Wen, S. a., Ma, D., Zhao, M., Xie, L., Wu, Q., Gou, L., Zhu, C., Fan, Y., Wang, H., & Yan, J. (2020). Spatiotemporal single-cell analysis of gene expression in the mouse suprachiasmatic nucleus. *Nature Neuroscience*, *23*(3), 456-467. https://doi.org/10.1038/s41593-020-0586-x
West, & Bechtold. (2015). The cost of circadian desynchrony: Evidence, insights and open questions. *BioEssays*, *37*(7), 777-788. https://doi.org/10.1002/bies.201400173
West, A. C., Smith, L., Ray, D. W., Loudon, A. S. I., Brown, T. M., & Bechtold, D. A. (2017). Misalignment with the external light environment drives metabolic and cardiac dysfunction. *Nature Communications*, *8*(1), 417. https://doi.org/10.1038/s41467-017-00462-2
Witting, W., Kwa, I. H., Eikelenboom, P., Mirmiran, M., & Swaab, D. F. (1990). Alterations in the circadian rest-activity rhythm in aging and Alzheimer's disease. *Biological Psychiatry*, *27*(6), 563-572. https://doi.org/https://doi.org/10.1016/0006-3223(90)90523-5
Wittmann, M., Dinich, J., Merrow, M., & Roenneberg, T. (2006). Social jetlag: misalignment of biological and social time. *Chronobiol Int*, *23*(1-2), 497-509. https://doi.org/10.1080/07420520500545979
Woelders, T., Leenheers, T., Gordijn, M. C. M., Hut, R. A., Beersma, D. G. M., & Wams, E. J. (2018). Melanopsin- and L-cone-induced pupil constriction is inhibited by S- and M-cones in humans. *Proceedings of the National Academy of Sciences of the United States of America*, *115*(4), 792-797. https://doi.org/10.1073/pnas.1716281115
Wolf, S. A., Boddeke, H. W., & Kettenmann, H. (2017). Microglia in Physiology and Disease. *Annu Rev Physiol*, *79*, 619-643. https://doi.org/10.1146/annurev-physiol-022516-034406
Wong, K. Y., Dunn, F. A., & Berson, D. M. (2005). Photoreceptor adaptation in intrinsically photosensitive retinal ganglion cells. *Neuron*, *48*(6), 1001-1010. https://doi.org/10.1016/j.neuron.2005.11.016
Wong, K. Y., Dunn, F. A., Graham, D. M., & Berson, D. M. (2007). Synaptic influences on rat ganglion-cell photoreceptors. *J Physiol*, *582*(Pt 1), 279-296. https://doi.org/10.1113/jphysiol.2007.133751
Wright, K. P., Jr., McHill, A. W., Birks, B. R., Griffin, B. R., Rusterholz, T., & Chinoy, E. D. (2013). Entrainment of the human circadian clock to the natural light-dark cycle. *Curr Biol*, *23*(16), 1554-1558. https://doi.org/10.1016/j.cub.2013.06.039
Yamamoto, T., Nakahata, Y., Soma, H., Akashi, M., Mamine, T., & Takumi, T. (2004). Transcriptional oscillation of canonical clock genes in mouse peripheral tissues. *BMC Mol Biol*, *5*, 18. https://doi.org/10.1186/1471-2199-5-18

Yan, L., & Silver, R. (2016). Neuroendocrine underpinnings of sex differences in circadian timing systems. *J Steroid Biochem Mol Biol*, *160*, 118-126. https://doi.org/10.1016/j.jsbmb.2015.10.007

Yang, J. N., Tiselius, C., Daré, E., Johansson, B., Valen, G., & Fredholm, B. B. (2007). Sex differences in mouse heart rate and body temperature and in their regulation by adenosine A1 receptors. *Acta physiologica (Oxford, England)*, *190*(1), 63-75. https://doi.org/10.1111/j.1365-201X.2007.01690.x

Yoshimura, T., & Ebihara, S. (1996). Spectral sensitivity of photoreceptors mediating phase-shifts of circadian rhythms in retinally degenerate CBA/J (rd/rd) and normal CBA/N (+/+) mice. *Journal of Comparative Physiology A*, *178*(6), 797-802. https://doi.org/10.1007/BF00225828

Young, M. E., & Bray, M. S. (2007). Potential role for peripheral circadian clock dyssynchrony in the pathogenesis of cardiovascular dysfunction. *Sleep Medicine*, *8*(6), 656-667. https://doi.org/10.1016/j.sleep.2006.12.010

Zeitzer, J. M., Dijk, D. J., Kronauer, R., Brown, E., & Czeisler, C. (2000). Sensitivity of the human circadian pacemaker to nocturnal light: melatonin phase resetting and suppression. *J Physiol*, *526 Pt 3*(Pt 3), 695-702. https://doi.org/10.1111/j.1469-7793.2000.00695.x

Zeitzer, J. M., Fisicaro, R. A., Ruby, N. F., & Heller, H. C. (2014). Millisecond flashes of light phase delay the human circadian clock during sleep. *J Biol Rhythms*, *29*(5), 370-376. https://doi.org/10.1177/0748730414546532

Zeitzer, J. M., Ruby, N. F., Fisicaro, R. A., & Heller, H. C. (2011). Response of the human circadian system to millisecond flashes of light. *PLOS ONE*, *6*(7), e22078. https://doi.org/10.1371/journal.pone.0022078

Zhang, R., Lahens, N. F., Ballance, H. I., Hughes, M. E., & Hogenesch, J. B. (2014). A circadian gene expression atlas in mammals: Implications for biology and medicine. *Proceedings of the National Academy of Sciences*, *111*(45), 16219-16224. https://doi.org/10.1073/pnas.1408886111